THE
PHYSICAL REVIEW
A Journal of Experimental and Theoretical Physics Established by E. L. Nichols in 1893
VOL. 53, NO. 12 JUNE 15, 1938 SECOND SERIES

The Multiplicative Theory of Showers as Applied to Large Bursts of Cosmic-Ray Ionization *

C. G. MONTGOMERY AND D. D. MONTGOMERY
Bartol Research Foundation of the Franklin Institute, Swarthmore, Pennsylvania
(Received March 30, 1938)

In order to decide whether the multiplicative theory of showers offers an adequate explanation of the experimental data on large showers, or whether it is necessary to suppose that they are produced by some other process, such as has been outlined by Heisenberg, the following calculations are undertaken. The energy spectrum of the electrons and photons incident upon a small thickness of material is calculated from the observed frequency distribution in size of bursts of ionization produced by large showers, the effect of fluctuations being taken into account. The energy distribution obtained is of the form $E^{-\alpha}$, where α is 2.6 for energies of the order of 10^9 volts, and decreases slowly with increasing energy, in agreement with the energy distribution calculated by Heitler to explain the variation of cosmic-ray intensity with altitude. The maximum number of electrons necessary to give the observed frequency of bursts is less than 0.5 percent of the total number of particles observed in a cloud chamber at sea level in the energy range between 10^9 and 10^{10} volts, which is in good accord with the cloud chamber observations. This calculated incident energy spectrum is utilized to calculate the number and frequency distribution of large bursts for large thicknesses of material. These calculated values differ considerably from the experimental ones, but this difference is probably to be ascribed to the effect of the penetrating cosmic rays, and is not to be regarded as evidence of a breakdown of the cascade theory. The experiments on the absorption of a shower are also shown to be in harmony with the theoretical estimates. It is concluded that no mechanism involving the production of many shower particles in a single act need be invoked to explain the occurrence of large showers, but that the ordinary multiplicative processes are entirely adequate when proper account is taken of the fluctuations.

INTRODUCTION

THE theory of the growth and decay of the secondary radiations which accompany a high energy electron in its passage through matter has been worked out in some detail by Carlson and Oppenheimer[1] and by Bhabha and Heitler.[2] This theory has been applied, with considerable success, to explain the variation of cosmic radiation with latitude and altitude by Heitler[3] and Nordheim.[4] The properties of small showers of rays are also well accounted for in this way. It remains to show whether the large showers, such as produce bursts of ionization, or Hoffmann Stösse, are consistent with this mechanism of production or not. It has been realized for some time that the formation of a large shower is not the result of a single act, but that some sort of a multiplicative process must be involved.[5] To what extent this "production of

* A preliminary report of this paper was presented at the New York meeting of the American Physical Society, February, 1938.

[1] J. F. Carlson and J. R. Oppenheimer, Phys. Rev. **51**, 220 (1937).

[2] H. J. Bhabha and W. Heitler, Proc. Roy. Soc. **A159**, 432 (1937).

[3] W. Heitler, Proc. Roy. Soc. **A161**, 261 (1937).

[4] L. W. Nordheim, Phys. Rev. **51**, 1110 (1937).

[5] C. G. Montgomery, Phys. Rev. **45**, 62 (1934); G. L. Locher, Phys. Rev. **44**, 779 (1933); C. G. Montgomery, D. D. Montgomery and W. F. G. Swann, Phys. Rev. **47**, 512 (1935).

one shower by another" is important has not been clear. On the other hand, Heisenberg[6] has suggested a mechanism whereby a large number of electrons would be produced in the interaction with a single nucleus. It is the purpose of this paper to inquire whether some such mechanism as is postulated by Heisenberg is necessary to explain the experimental properties of large showers, or whether successive pair formation by the radiations resulting from the slowing down of high energy electrons is sufficient.

Calculation of the Energy Distribution of Incident Rays

Suppose we have a piece of heavy material, say lead, placed above an ionization chamber, and we make observations of the rates of occurrence of the bursts of ionization as a function of the size of the burst. We suppose that the ionization produced is proportional to the number of electrons which make up the shower. Then it has been pointed out[7] that the frequency of showers, $R(N)dN$, containing numbers of rays between N and $N+dN$ can be well represented by the empirical expression

$$R(N)=A/N^3.$$

This expression is valid over quite a large range of N, and its form is almost independent of the thickness of the shower producing material. The value of the exponent necessary to obtain a best fit of the data varies somewhat with the observations considered, but we may take it as integral for simplicity.

The cascade theory of showers is given in the most convenient form for calculation by Bhabha and Heitler. They give, in graphical form, the expected number, ϵ, of electrons, positive and negative, of energy greater than a critical value, E_c, ($E_c=10^7$ volts for lead) which emerge from a plate of a given thickness when an incident electron of energy E falls upon the plate. Let us first consider the case of a lead plate 1.2 cm thick. The actual number of rays, N, which emerge from the plate will not, of course, in general be equal to this expected number, ϵ. Furry[8] has shown that, for thin pieces of material,

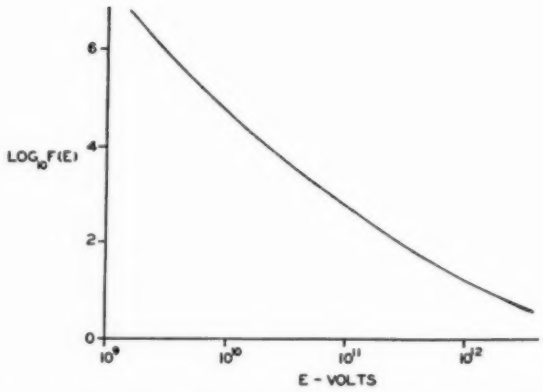

Fig 1. The energy distribution of electrons and photons necessary to produce the observed distribution in size of large showers.

the probability of finding N rays when ϵ rays are expected is given by the expression $(1-1/\epsilon)^{N-1}/\epsilon$. Let us suppose that the number of ion pairs observed in our chamber is proportional to the number of rays above the critical energy. Then if we have a number of electrons $F(E)dE$ of energy between E and $E+dE$ falling upon the lead plate, the number of showers containing N rays will be given by

$$R(N)=A/N^3=\int_{E_c}^{\infty}\epsilon^{-1}(1-\epsilon^{-1})^{N-1}F(E)dE.$$

We thus have an integral equation which can be solved for $F(E)$. An approximate solution of this can easily be obtained. We note that, for a given thickness, ϵ is a function of E only, so that a change of variable gives us

$$R(N)=\int_1^{\infty}\epsilon^{-1}(1-\epsilon^{-1})^{N-1}f(\epsilon)d\epsilon.$$

If we assume $f(\epsilon)$ is of the form B/ϵ^s, the integral may be evaluated directly, and we have

$$R(N)=B\Gamma(s)\Gamma(N)/\Gamma(s+N).$$

Now if we equate $B\Gamma(s)=A$ and $s=3$, we obtain

$$R(N)=A/N(N+1)(N+2),$$

which, for large N, is indistinguishable from the experimental A/N^3, and hence $f(\epsilon)=A/2\epsilon^3$ is the desired solution.

We may then immediately apply Bhabha and Heitler's calculations, and find which $F(E)$ corresponds to $f(\epsilon)=A/2\epsilon^3$. Fig. 1 gives the

[6] W. Heisenberg, Zeits. f. Physik **101**, 533 (1936).
[7] C. G. Montgomery and D. D. Montgomery, Phys. Rev. **48**, 786, 969 (1935).
[8] W. H. Furry, Phys. Rev. **52**, 569 (1937).

values of $F(E)$ so calculated. This energy distribution may be considered to be proportional to $E^{-\alpha}$ where α is 2.6 for $E=10^9$ volts, and α decreases with increasing E to a value of 2.1 for $E=10^{11}$ volts. This decrease in α cannot continue indefinitely, of course, since the total energy of the distribution would diverge. It may be shown, however, that if the function $R=A/N^3$ is a good representation of the experimental data from $N=10$ to $N=1000$, then the function $F(E)$ is determined as above from 10^9 to 10^{12} volts. The $F(E)$ calculated here has been spoken of as if it were a distribution of electrons which produced the observed showers. If, on the other hand, we had carried through the calculations assuming that all the observed showers were produced by photons, we would have been led to the same $F(E)$, which, however, would then represent an energy distribution of photons, since the behavior of a high energy photon is almost identical with that of an electron. Actually we know that both electrons and photons produce the showers, and we must regard $F(E)$ as made up of both entities in amounts of comparable importance. Since the shower producing effects are independent of the proportion of electrons and photons, we cannot utilize the shower phenomena to give us any information regarding this proportion.

We may compare our calculated form of $F(E)$ with the energy distribution of electrons at sea level obtained in another way. Heitler,[3] in order to explain the variation of the soft component of the cosmic radiation with elevation, assumes a distribution of electrons entering the earth's atmosphere. This results in an energy distribution of electrons at sea level which is of the form $E^{-2.5}$ approximately.[9] Thus there is good agreement between the two methods of calculation, which are based on quite independent data.

We have determined the form of the energy distribution of the shower producing rays; let us now determine the number of them necessary to produce the observed number of showers. The quantity measured as the size of a shower is the number of ion pairs produced. Since N is the number of rays above the critical energy, E_c, and since there are roughly an equal number of rays above and below the critical energy,[10] we should choose an "effective specific ionization" approximately twice the specific ionization of a single electron. Now there is considerable uncertainty in this quantity, but the maximum value of the constant A will be given by the minimum value of the specific ionization. We shall take this to be 30 ion pairs per cm. We choose for illustration the rate of occurrence of bursts greater than 1.5×10^6 ion pairs produced in a magnesium chamber containing about 15 atmospheres of nitrogen and covered by one centimeter of lead.[11] We are thus dealing with showers containing of the order of 100 rays. These data result in an upper limit for A of 9.8×10^{-3} cm^{-2} sec.$^{-1}$. If we now consider the region of the energy spectrum from 10^9 to 10^{10} volts, we should need only 4.0×10^{-5} electrons and photons per sq. cm per second to account for all the showers produced. The total number of charged particles observed in a cloud chamber in this energy range may be taken from the observations of Blackett,[12] and is 950×10^{-5} cm^{-2} sec^{-1}. Thus at most only 0.5 percent of the particles in this energy range observed in a cloud chamber need be electrons. That there are some electrons is shown by the fact that showers have been observed, in cloud chamber photographs, whose total energies are greater than 10^9 volts[13]. Thus we have good consistency with cloud chamber observations. Similarly even the largest bursts which have been reported can be produced electrons or photons whose number is a negligibly

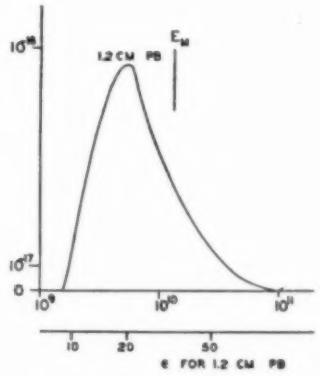

FIG. 2. The contribution to the number of 100 ray showers by the rays of various energies. The vertical line, E_M, marks the median energy.

[9] Reference 3, page 276.
[10] H. J. Bhabha, Proc. Roy. Soc. **A164**, 257 (1938).
[11] C. G. Montgomery and D. D. Montgomery, Phys. Rev. **48**, 786 (1935).
[12] P. M. S. Blackett, Proc. Roy. Soc. **A159**, 1 (1937).
[13] C. D. Anderson and S. H. Neddermeyer, Phys. Rev. **50**, 263 (1936).

small proportion of the total number of particles. We see that it is unnecessary to invoke any special mechanism for the production of large showers such as suggested by Heisenberg.

It is interesting to see what energies are effective in producing showers of a given size. Fig. 2 gives the contribution of each energy to the total number of showers for $N=100$. The lower scale of abscissae gives the expected number of rays, ϵ, for each energy. We note the striking fact that the rays which are most effective in producing 100 ray showers would only be expected to produce about 20 rays, and that the rays for which we expect 100 shower particles give a wholly negligible contribution. Table I shows some characteristics of this distribution. Thus all the observed showers of 100 rays are fluctuations from expectation.

It might seem from a cursory examination of the problem that since $f(\epsilon)$ and $R(N)$ are the same functions of their respective variables, the effect of the fluctuations is only to introduce a small constant factor. However, this is quite illusory since, in the absence of the fluctuation phenomena, the rays which would be effective in producing 100 ray showers would not lie in the energy range between 10^9 and 10^{10} volts, but would have considerably higher energies in the neighborhood of 5×10^{11} volts. Thus in the absence of fluctuations we should need, in order to account for the observed number of bursts, considerably more electrons of energy around 10^9 volts than all the particles of this energy observed. It is the neglect of the fluctuations which has led many investigators,[14] ourselves included,[15] to the view that it is necessary to have some mechanism whereby many shower particles are produced in a single act to account for the large showers from small thicknesses. However, when the fluctuations are properly taken into account, the ordinary cascade picture is entirely adequate.

TABLE I. *Characteristics of distribution in Fig. 2.*

	ENERGY	ϵ
Most probable	5.0×10^9 volts	20
Median	1.2×10^{10}	35
Mean	4.3×10^{10}	51

[14] Reference 10, page 265; H. Euler, Physik. Zeits. **38**, 943 (1937).

[15] C. G. Montgomery and D. D. Montgomery, Phys. Rev. **50**, 490 (1936).

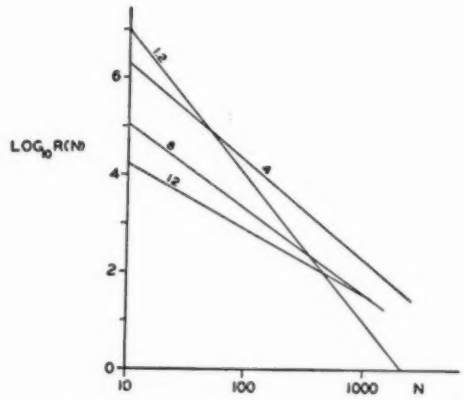

FIG. 3. The variation of frequency distribution in size of showers with thickness of the producing material. The numbers indicate the thickness of lead in centimeters.

THE VARIATION OF THE PRODUCTION OF LARGE SHOWERS WITH THICKNESS OF THE MATERIAL

We may use the energy spectrum of the incident rays derived above to calculate how many showers would be expected at large thicknesses of material. However, we enter here on more uncertain ground. Although the effect of the fluctuations is all important at small thicknesses, its importance should become less and less as the thickness increases. In the absence of a more accurate knowledge of the effect of fluctuations, the best approximation possible at the present time would appear to be to neglect the fluctuations entirely for large thicknesses. The calculation of the number of showers is then quite straightforward, and we give only the results. Fig. 3 shows the distributions in shower sizes to be expected at several thicknesses of lead. The lines in the figure have been drawn as straight, although they have a slight curvature concave upward.

These results differ considerably from experiment.[16] This disagreement may be expressed in this way: for showers of a given size, the predicted decrease at large thicknesses is much too large, and the shapes of the distribution in size curves, that is, the slopes of the lines in Fig. 3, change too much with thickness. The experimental data do show some decrease in slope, but not nearly as large a one as is indicated here. This is usually expressed as a shift of the maxi-

[16] E.g., R. T. Young, Phys. Rev. **52**, 559 (1937); J. K. Bøggild, Diss. Copenhagen, 1937.

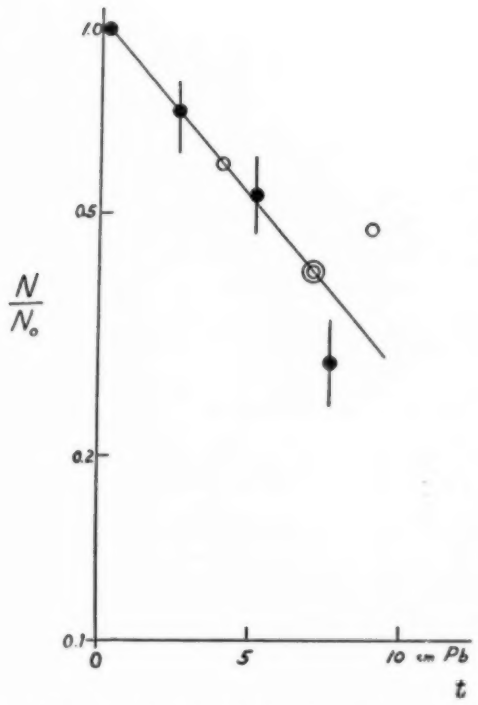

FIG. 4. Observations on the absorption of showers. Open circles: data of H. Nie recalculated by the authors; double circle: authors' measurements, first method; filled circles: authors' measurements, second method.

mum to larger thicknesses in the relation between the number of showers and the thickness of the material, as the size of the showers under consideration increases. These points of disagreement are probably the result of neglecting the effects of the penetrating cosmic radiation, and probably do not represent any fault in the theory of showers produced by electrons or photons. As this point of view has been much discussed previously,[10, 17] we merely wish to emphasize that there need be no discrepancy in the cascade theory of showers here.

THE ABSORPTION OF A SHOWER

Another means of testing the multiplicative theory of showers is to utilize the experiments on the passage of a shower through lead. Such experiments have been performed by Nie[18] and the authors,[19] and lead to results substantially in agreement. Fig. 4 shows the results of these experiments. Again the showers dealt with contain approximately 100 rays. Now, on account of the importance of the fluctuations, we cannot expect to be able to treat this question exactly, but can only obtain a rough estimate of the absorption from the theory. We may represent the experimental points by the equation $N=N_0e^{-\mu t}$, where N is the number of rays in the shower after it has passed through t cm of lead, N_0 the original number of rays ($N_0=100$), and $\mu=\frac{1}{8}$ cm^{-1} of lead. Nordheim[4] has shown that a particular solution of the diffusion equations of Carlson and Oppenheimer is given by

$$P(t, E)=e^{-\mu t}E^{-n},$$

for energies above the critical energy, E_c, with the relation between n and μ:

$$0.4\mu=4/3-1/n-[(\tfrac{2}{3}-1/n)^2+4/3n(n-1)]^{\frac{1}{2}}$$

when μ is measured in cm^{-1} of lead. Now if we suppose that the N_0 rays in the "average" shower have an energy distribution of the form E^{-n}, we can compute what the value of n must be in order that the shower will be absorbed exponentially with the observed coefficient. This leads to the value $n=2.07$. The total energy of the shower is easily seen to be $E=N_0E_c(n-1)/(n-2)$, or for this case, $E=1.5\times10^{10}$ volts. This "average" energy of the shower is equal to the energy of the incident ray, and may be compared with the energies listed in Table I for 100 ray showers. It is seen to be of the correct order of magnitude. Thus, although these calculations are only approximate, here again we obtain agreement with the cascade theory, and find no evidence that any other mechanism is necessary to account for the observed behavior of large showers.

The authors wish to thank Professor W. F. G. Swann for much valuable discussion of these matters.

[17] R. H. Woodward, Phys. Rev. **49**, 711 (1936); H. Euler, ref. 14; R. T. Young and J. C. Street, Phys. Rev. **52**, 552 (1937).

[18] H. Nie, Zeits. f. Physik **99**, 776 (1936).

[19] C. G. Montgomery and D. D. Montgomery, Phys. Rev. **49**, 705 (1936); Zeits. f. Physik **102**, 534 (1936).

Transition Effects of Cosmic Rays in the Atmosphere

H. SNYDER
University of California, Berkeley, California
(Received April 22, 1938)

In this paper we give an improved treatment of the multiplication and absorption of cosmic-ray electrons and gamma-rays in the atmosphere. After a brief recapitulation, in I, of the principal processes involved in the cascade theory of showers and the resulting diffusion equations, we give, in II and III, a solution of these diffusion equations, making no further approximations. In IV, an expression for the probable number of charged particles is given; the values of the functions necessary for numerical calculations are given in a tabular form. In V, it is shown how the Bhabha-Heitler cut-off energy method for estimating the effect of ionization losses may be consistently used. In VI, a comparison is made with the Carlson-Oppenheimer calculations. The differences near the top of the atmosphere are small and in a direction to improve the agreement with observations. At sea level the new calculations give an intensity roughly ⅔ of the Carlson-Oppenheimer results.

RECENT experiments with ionization chambers and vertical coincidence counters have extended the study of cosmic-ray intensities nearly to the top of the atmosphere. In this paper we shall return to the question of a theoretical estimate of the intensity to be expected on the assumption that cosmic rays consist only of electrons, positrons, and gamma-rays. It is known that this assumption fails to give an adequate description of the observations, and that other phenomena, which have to do with the production and absorption of the "penetrating" component, must be essentially involved. We want here to improve the theoretical treatment of the multiplication and absorption of the "soft" radiation, in the hope that this will help, when further experimental results are available, to throw light on the behavior of the penetrating component.

Carlson and Oppenheimer[1] have given an expression for the average number of charged particles that would be expected at a given depth below the top of the atmosphere, provided only that this distance is not too small. In their calculations they made two types of approximations: (a) Analytic forms for the probabilities of pair production and gamma-radiation which closely approximate the quantum theoretical expressions in the high energy region were used; (b) Whereas, in calculating the energy distribution of emitted gamma-rays, the theoretical spectrum with constant intensities was used, a distribution corresponding to constant probability for various quanta was used to estimate the direct effect of radiation on the energy distribution of the charged particles. We have found it possible to calculate the probable number of charged particles at a given depth without making the second approximation, and to extend the calculation to the case of small thicknesses. The approximations (a) are very good, and these have been retained.

[1] Carlson and Oppenheimer, Phys. Rev. **51**, 220 (1937). Referred to as C.O.

I

For convenience, a brief resume of the principal processes will be given. The three essential processes which will be considered are: (1) production of gamma-rays by charged particles, (2) pair production by gamma-rays, (3) ionization losses of the electrons and positrons. The Compton recoil of electrons under impact by photons was not explicitly introduced, because *in air* at the low energies for which pair production gives too few particles, the recoil electrons absorb enough gamma-radiation to keep the gamma-ray absorption coefficient nearly constant. The Compton effect produces one particle per photon, whereas pair production gives two. Either process contributes the same quota to the ionization, since such charged particles have energies so low that they are stopped by ionization losses so quickly that they radiate very little. No consideration will be given to other processes, as production of high energy secondaries or pairs in the nuclear fields by charged particles, because they are relatively much rarer, and because the

resultant particles would be nearly as penetrating as the incident one.

The analytically amenable expressions for the probabilities of pair production, emission of gamma-radiation, and ionization losses, which were chosen by Carlson and Oppenheimer will be used for these calculations.

The probability that an electron or positron of energy greater than E shall radiate a photon of energy between E and $E+\Delta E$, while passing through matter a distance Δx, will be taken to be

$$P\Delta E\Delta x=(K/E)\Delta E\Delta x. \tag{1}$$

If the atomic number of the matter is Z and the density of atoms is N,

$$K=\frac{4Z^2e^6N}{\hbar m^2c^5}\ln(200/Z^{\frac{1}{3}}).$$

The probability that a gamma-ray of energy E shall produce a pair having energies between E' and $E'+\Delta E'$, and $E-E'$ and $E-E'-\Delta E'$, will be taken to be

$$P'\Delta E'\Delta x=(K'/E)\Delta E'\Delta x' \tag{2}$$

with $E'<E$, and for which

$$K'/K=\sigma\sim\tfrac{2}{3}.$$

The ionization losses will be assumed to be independent of the energy and will be evaluated at energies for which they are important. If one regauges the measure of distance by the transformation $t=Kx$, the energy loss by ionization per unit distance becomes

$$\beta=(4\pi NZe^4/Kmc^2)\ln(\beta/ZRh). \tag{3}$$

Let $N(t, E)$ be the probable number of charged particles of energy greater than E to be found at a thickness t. Further, take $\gamma(t, E)\Delta E$ to be the probable number of photons having energies between E and $E+\Delta E$ at t. Then, in accordance with (1), (2) and (3), diffusion equations take the form

$$\partial\gamma/\partial t=-\sigma\gamma+N/E, \tag{4}$$

$$\frac{\partial N}{\partial t}=\beta\frac{\partial N}{\partial E}+2\sigma\int_E^\infty dE'\int_{E'}^\infty\frac{\gamma(E'')}{E''}dE''+\int_0^E\frac{N(E+E')-N(E)}{E'}dE'+\int_E^\infty\frac{N(E+E')-N(E')}{E'}dE'. \tag{5}$$

If one supposes that the incoming radiation is a charged particle of energy E_0, the boundary conditions which the solution to (4) and (5) must satisfy are

$$\gamma(t=0, E)=0;\quad N(t=0, E)=\begin{matrix}1 & E<E_0\\ 0 & E>E_0.\end{matrix} \tag{6}$$

II

An exact solution of Eqs. (4) and (5) with the boundary conditions (6) may be found for $\beta=0$. If one writes

$$\gamma_0=e^{-\sigma t}z_0/\dot{E}, \tag{7}$$

then it follows that

$$N_0=e^{-\sigma t}\dot{z}_0. \tag{8}$$

In Eq. (8) and succeeding equations a dot will represent differentiation with respect to t. The substitution of (7) and (8) in (5) gives rise to the integral-differential equation

$$K(z_0)=\ddot{z}_0-\sigma\dot{z}_0-2\sigma\int_E^\infty dE'\int_{E'}^\infty\frac{z_0(E'')}{(E'')^2}dE''-\int_0^E\frac{\dot{z}_0(E+E')-\dot{z}_0(E)}{E'}dE'-\int_E^\infty\frac{\dot{z}_0(E+E')-\dot{z}_0(E')}{E'}dE'=0. \tag{9}$$

Simple solutions of the form $z_0=e^{\mu t}E^{-\nu}$ exist, provided μ is one of the roots of the quadratic equation

$$\mu^2-(\sigma+L(y))\mu-2\sigma/y(y+1)=0, \tag{10}$$

in which

$$L(y)=\int_0^1\frac{(1+x)^{-\nu}-1}{x}dx+\int_1^\infty\frac{(1+x)^{-\nu}-x^{-\nu}}{x}dx=-[\psi(y)+\gamma] \tag{11}$$

$$\psi(y)=(d/dy)\ln\Gamma(y+1);\quad \gamma=0.577\cdots.$$

The roots of (10) are

$$\begin{matrix}\mu\\ \nu\end{matrix}=\frac{\sigma+L(y)}{2}\pm\left[\left(\frac{\sigma+L(y)}{2}\right)^2+\frac{2\sigma}{y(y+1)}\right]^{\frac{1}{2}};\quad \mu>\nu. \tag{12}$$

The general solution of (9) is now given by

$$z_0=\frac{1}{2\pi i}\int_C \frac{dy}{y}\left(\frac{E}{E_0}\right)^{-y}[A(y)e^{\mu t}+B(y)e^{\nu t}] \quad (13)$$

if the contour C and $A(y)$ and $B(y)$ are determined so that this integral exists.

To satisfy the boundary conditions (6) one must have

$$z_0(t=0, E)=0; \quad \dot{z}_0(t=0, E)=\begin{matrix}1 & E<E_0\\ 0 & E>E_0.\end{matrix}$$

The contour for the integration with respect to y was chosen to be a straight line parallel to the imaginary axis, at a distance δ to the right, and from $-i\infty+\delta$ to $i\infty+\delta$.

Equation (13) may then be written

$$z_0=\frac{1}{2\pi i}\int_C \frac{dy}{y}e^{\lambda y}[A(y)e^{\mu t}+B(y)e^{\nu t}]$$

$$\text{with} \quad \lambda=\ln(E_0/E).$$

From $z(t=0, E)=0$, it must be true that

$$B(y)=-A(y). \quad (14)$$

The second boundary condition leads to

$$\frac{1}{2\pi i}\int_C \frac{dy}{y}e^{\lambda y}A(y)[\mu-\nu]=\begin{matrix}1 & \lambda>0\\ 0 & \lambda<0.\end{matrix} \quad (15)$$

Multiplying (15) by $e^{-y_0\lambda}$ and integrating with respect to λ from 0 to ∞, one gets

$$\frac{1}{2\pi i}\int_C \frac{dy}{y}A(y)\frac{\mu-\nu}{y-y_0}=-\frac{1}{y_0} \quad \text{for} \quad R(y_0)>0. \quad (16)$$

The integral in (16) may be evaluated by taking the residue at $y=y_0$, from which one obtains

$$A(y)=1/(\mu-\nu). \quad (17)$$

The solution satisfying the boundary conditions (6) is:

$$z_0=\frac{1}{2\pi i}\int_C \frac{dy}{y}e^{\lambda y}\frac{e^{\mu t}-e^{\nu t}}{\mu-\nu}. \quad (18)$$

Equation (18) is an analytic expression of the solution of the cosmic-ray problem considered by Bhabha and Heitler.[2]

[2] Bhabha and Heitler, Proc. Roy. Soc. **A159**, 432 (1937).

III

If one takes as before

$$\gamma=e^{-\sigma t}z/E; \quad N=e^{-\sigma t}\dot{z}, \quad (19)$$

a solution of (4) and (5) with $\beta\neq 0$ which satisfies the boundary conditions (6) to terms of order β/E_0 may be found. The equation which z must satisfy is:

$$K(z)=\beta\partial\dot{z}/\partial E \quad (20)$$

with the operator K defined in Eq. (9).

In analogy with the work of Carlson and Oppenheimer, we look for simple solutions of (20) which depend upon a parameter, say y, and which may be combined to satisfy the boundary conditions. We set

$$z(y)=\frac{e^{\mu t}}{2\pi i}\int_s ds\left(\frac{E}{E_0}\right)^{-y}\left(\frac{E}{\beta}\right)^{-s}$$

$$\times C(y, s)\frac{\Gamma(-s)\Gamma(y+s)}{\Gamma(y)}. \quad (21)$$

The contour for the integration with respect to s is from $-i\infty$ to $i\infty$. The contour is kept to the left of the poles at 0, 1, 2, etc. and to the right of the poles at $-y$, $-y-1$, $-y-2$, etc. We look for a $C(y, s)$ which for $R(y)>0$ is free of singularities in the strip $0\leq R(s)\leq 1$, since one can see that this condition is necessary to make the total number of particles in the shower finite. Substituting (21) into (20), one obtains:

$$\int_s ds\left(\frac{E}{E_0}\right)^{-y}\left(\frac{E}{\beta}\right)^{-s}C(y, s)\frac{\Gamma(-s)\Gamma(y+s)}{\Gamma(y)}$$

$$\times\{\mu^2-(\sigma+L(y+s))\mu-2\sigma/(y+s)(y+s+1)\}$$

$$=-\int_s ds\left(\frac{E}{E_0}\right)^{-y}\left(\frac{E}{\beta}\right)^{-s-1}C(y, s)\frac{\Gamma(-s)\Gamma(y+s)}{\Gamma(y)}$$

$$\times\mu(y+s). \quad (22)$$

In order that the integrals over E obtained by this substitution converge, it is necessary that $R(y+s)>0$, although the expressions thus obtained may be analytically extended into the left half-plane. One may now note that the coefficient of $C(y, s)$ in the left-hand side of (22) differs from that of the right side by a first power in E. If one

then takes the $C(y, s)$ to satisfy the functional relation

$$\{\mu^2-(\sigma+L(y+s))\mu-2\sigma/(y+s)(y+s+1)\}\times C(y, s)=\frac{s(y+s-1)\mu C(y, s-1)}{(y+s)}. \quad (23)$$

(21) is at least a formal solution of (20). To insure that (21) be a solution of (20), y will be restricted to $R(y)>0$, and μ will be taken to satisfy (10). When these conditions are satisfied, one may deform the contour for the integration with respect to s for the last term in (22) and show that (21) is a solution of (20).

If μ^2 is eliminated from (23) by means of (10), it may be written:

$$\{\mu[\psi(y+s)-\psi(y)]+2\sigma[1/y(y+1)-1/(y+s)(y+s+1)]\}C(y, s)=\frac{s(y+s-1)\mu}{(y+s)}C(y, s-1). \quad (24)$$

Thus for $R(y)>0$, $C(y, s)$ is free of singularities for $-1-R(y)<R(s)$.

As there are two roots to (10), there are two linearly independent solutions of (20) for each value of y. The $C(y, s)$ corresponding to the two roots μ and ν will be denoted by $C_\mu(y, s)$ and $C_\nu(y, s)$. In addition, the C's will be chosen so that $C_\mu(y, 0)=C_\nu(y, 0)=1$. A solution satisfying the boundary conditions (6) to terms of order β/E_0 may now be written:

$$z=-\frac{1}{4\pi^2}\int_C\frac{dy}{y}e^{\lambda y}\int_s ds\left(\frac{E}{\beta}\right)^{-s}\frac{\Gamma(-s)\Gamma(y+s)}{\Gamma(y)}\times\left\{\frac{C_\mu(y, s)e^{\mu t}-C_\nu(y, s)e^{\nu t}}{\mu-\nu}\right\} \quad (25)$$

for evaluating the integral over s in terms of the residues of the poles at 0, 1, 2, etc., we find

$$z=\frac{1}{2\pi i}\int_C\frac{dy}{y}e^{\lambda y}\frac{e^{\mu t}-e^{\nu t}}{\mu-\nu}-\frac{1}{2\pi i}\int_C dy e^{\lambda y}\left(\frac{\beta}{E}\right)\times\left\{\frac{C_\mu(y, 1)e^{\mu t}-C_\nu(y, 1)e^{\nu t}}{\mu-\nu}\right\}+0(\beta/E)^2+\cdots. \quad (26)$$

From (26) it follows that (25) satisfies the boundary conditions (6) for $E\gg\beta$, at least to order β/E; this suggests that the total energy of the shower is E_0 to terms of order β. This is shown to be true in Eq. (41). Further, the total number of particles of energy greater than zero at $t=0$ determined from (25) is $1+0(\beta/E_0)$, as $\beta/E_0\to 0$, which follows from Eqs. (28) and (34). It is only for large E_0/β that (25) satisfies the boundary conditions, and it is only for this case that we shall calculate the total number of particles.

IV

For the purpose of calculating the number of charged particles in the shower, deform the contour to the left. There are no singularities between $s=0$ and $-y$. In the limit $E=0$, the only contribution to the integral comes from the simple pole at $s=-y$. One then has

$$z(E=0)=\frac{1}{2\pi i}\int_C\frac{dy}{y}e^{\epsilon y}\left\{\frac{C_\mu(y, -y)e^{\mu t}-C_\nu(y, -y)e^{\nu t}}{\mu-\nu}\right\};\quad \epsilon=\ln(E_0/\beta). \quad (27)$$

From Eqs. (19) and (27), one can easily obtain

$$N=\frac{e^{-\sigma t}}{2\pi i}\int_C\frac{dy}{y}e^{\epsilon y}\times\left\{\frac{C_\mu(y, -y)\mu e^{\mu t}-C_\nu(y, -y)\nu e^{\nu t}}{\mu-\nu}\right\}. \quad (28)$$

It is convenient to divide (28) into two parts,

$$N_\mu=\frac{1}{2\pi i}\int_C\frac{dy}{y}\left[\frac{\mu C_\mu(y, -y)}{\mu-\nu}\right]\cdot e^{\epsilon y+(\mu-\sigma)t} \quad (29)$$

and

$$N_\nu=-\frac{1}{2\pi i}\int_C\frac{dy}{y}\left[\frac{\nu C_\nu(y, -y)}{\mu-\nu}\right]e^{\epsilon y+(\nu-\sigma)t}. \quad (30)$$

The first part, (29), gives the principal contribution to the shower. In the second, ν is less than zero for all y on the contour, so (30) falls off exponentially with increasing t.

For large values of t and ϵ, (29) may be calculated by the saddle point method. The quantity

$$\mu C_\mu(y, -y)/(\mu-\nu) \quad (31)$$

is a slowly varying function of y, and may be

taken from under the integral sign and evaluated at the saddle point. One then obtains

$$N_\mu=\frac{C_{\mu_s}(y_s,\,-y_s)\mu_s e^{\epsilon y_s+(\mu_s-\sigma)t}}{[2\pi(\mu_s''y_s^2t+1)]^{\frac{1}{2}}(\mu_s-\nu_s)} \tag{32}$$

with the saddle point determined by

$$\mu_s't+\epsilon-1/y_s=0, \tag{33}$$

in which $\mu'=d\mu/dy$; $\mu''=d\mu'/dy$.

In fact, (32) gives satisfactory results even for small t. For small values of t and large values of ϵ the saddle point determined by (33) is at y very near zero, so it is possible to approximate μ by $(2\sigma/y)^{\frac{1}{2}}$. When this is effected, (29) may be evaluated in a rapidly converging series, and one obtains

$$N_\mu=\frac{C_{\mu_s}(y_s,\,-y_s)\mu_s}{(\mu_s-\nu_s)}e^{-\sigma t}\sum_{n=0}^{\infty}\frac{[(2\sigma\epsilon)^{\frac{1}{2}}t]^n}{\Gamma(\frac{1}{2}n+1)\Gamma(n+1)}. \tag{34}$$

Numerical calculation of (34) shows that even for $t=0$ the corrections to be applied to (32) are small; for $t=0$, they amount to a decrease of eight percent.

The function $C_\mu(y,\,-y)$ is a very complicated but slowly varying analytic function of y for all y near the saddle points determined from (33). It is, however, easily calculated from (24) for integral values of y. Its values for these points were plotted, and a smooth interpolating curve drawn through them.

If the substitutions

$$H(y)=(2\pi)^{-\frac{1}{2}}C_\mu(y,\,-y)\mu/(\mu-\nu), \tag{35}$$
$$k=\mu-\sigma,\quad a=-\mu'y,\quad b=\mu''y^2$$

are made in Eqs. (32) and (33), they may be written in the simple forms

$$N_\mu=(1+bt)^{-\frac{1}{2}}He^{kt+\epsilon y} \tag{36}$$

and

$$t=(\epsilon y-1)/a. \tag{37}$$

TABLE I.

y	k	a	b	H
0.2	1.8876	1.485	2.06	0.286
0.4	0.9538	1.207	1.51	0.330
0.6	0.4944	1.063	1.41	0.351
0.8	0.2026	0.957	1.37	0.352
1.0	0.0000	0.857	1.35	0.342
1.2	−0.1479	0.762	1.33	0.320
1.4	−0.2588	0.669	1.30	0.294
1.6	−0.3418	0.581	1.26	0.267
1.8	−0.4055	0.504	1.18	0.243
2.0	−0.4542	0.428	1.08	0.221
2.2	−0.4920	0.366	0.99	0.201
2.4	−0.5215	0.313	0.91	0.185

In Table I, the values of a, b, k, and H are given over a range of values sufficiently large to cover showers from the top of the atmosphere to sea level. The value of t given by (37) increases uniformly as a function of y.

For air the value of β is about 90 Mev. t is in units of 0.4 m water equivalent.

N_ν is completely negligible for values of t greater than 0.5. For values of t less than this, it is easy to estimate its contribution to the size of the shower: (a) $N_\mu=\frac{1}{2}$, $N_\nu=\frac{1}{2}$ at $t=0$; (b) at $t=0$ the slope of N_ν is equal and opposite to that of N_μ; (c) N_ν falls exponentially to a half-value of $\frac{1}{4}$ at about $t=0.2$.

V

We will now look at Eq. (18) and see if we can find a rational way in which to introduce a low energy cut-off by means of which we can estimate the total size of the shower. This is the procedure suggested by Bhabha and Heitler.[2] We introduce E_c, supposed independent of t, and assume that the energy distribution of particles of energy greater than E_c is not disturbed by the ionization losses, and that because of the ionization losses there are no particles of energy lower than this. Since the initial energy of the shower E_0 must be absorbed by ionization, we must have

$$\int_0^\infty N_0(E_c)dt=E_0/\beta$$
$$=\frac{1}{2\pi i}\int_0^\infty dt\int_c\frac{dy}{y}\frac{\mu e^{(\mu-\sigma)t+\lambda_c y}}{\mu-\nu} \tag{38}$$

with $\lambda_c=\ln(E_0/E_c)$.

These integrals are easy to evaluate if we neglect terms of order β/E_0; then (38) gives

$$E_c=\left[\frac{\mu(1)(-1)}{[\mu(1)-\nu(1)]\mu'(1)}\right]\beta$$
$$=\frac{1}{C_\mu(1,\,-1)}\beta=0.467\beta. \tag{39}$$

In accordance with (39), the number of particles in the shower becomes

$$N_0=\frac{(0.467)^{-\nu_s}\mu_s e^{\epsilon\nu_s+(\mu_s-\sigma)t}}{[2\pi(\mu_s''y_s^2t+1)]^{\frac{1}{2}}(\mu_s-\nu_s)} \qquad (40)$$

with the saddle point determined as before by Eq. (37). This equation, (40), is of the same form as (32) with $C(y, -y)$ replaced by

$$\left[-\frac{\mu'(1)(\mu(1)-\nu(1))}{\mu(1)}\right]^y=\left(\frac{1}{0.467}\right)^y.$$

For $y=0$ and 1, these give identical results, and for $y=2$ they give 3.28 and 4.58, respectively. It should be observed that the proper "cut-off energy" is less than half β.

Calculating the total energy of the shower, as given by (29), and again neglecting terms of order β/E_0, we get for this energy

$$-\frac{C_\mu(1, -1)\mu(1)}{[\mu(1)-\nu(1)]\mu'(1)}E_0=E_0. \qquad (41)$$

VI

In their work, Carlson and Oppenheimer replace the last two terms of Eq. (5) by an approximate expression which enabled them to find a differential equation for z. The approximation was made in such a manner that the number of particles lost in one energy range appeared in some other, and so that the average energy lost by radiation by the charged particles was gained by the gamma-rays. The approximation distorts the energy distribution among the charged particles so that there are too many very high energy particles, too many low energy particles, and too few of intermediate energy ($\sim\beta$). In Fig. 1 the effect of this distortion on the results for the average number of particles is shown for $E_0=100\beta$. The curve marked *I* was obtained from the C. O. calculations, and the other, marked *II*, from Eqs. (36) and (37). Their approximation: (a) slightly lowers the height of the maximum, (b) moves the maximum about 0.2 m to greater thicknesses, (c) considerably overestimates the size of the shower at great depths. At ten meters depth, near sea level, the C. O. formula gives $N=7.5\times10^{-3}$, and we find $N=4.5\times10^{-3}$, for a 9×10^3 Mev particle with vertical incidence.

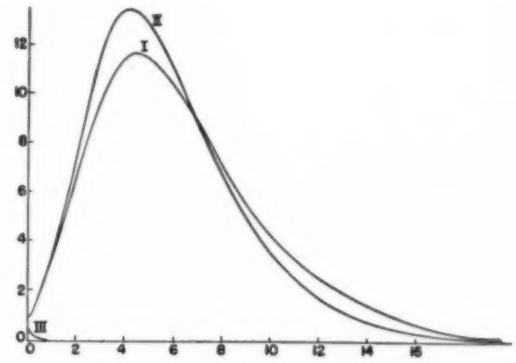

FIG. 1. *I* is a plot of the number of particles against t as determined from the C. O. calculations. *II* is a plot of the same as given by Eqs. (36) and (37). *III* shows the contribution to the shower by N_ν. The calculations were made for $E_0=100\beta$. One unit of t is about 0.4 m water equivalent.

The changes in the theoretical curve near the top of the atmosphere help to remove some of the discrepancies found in this region by Bowen, Millikan and Neher[3] between their experimental results, and the calculation of C. O. applied to an isotropic incident distribution. So detailed a comparison can hardly be significant, however, unless it takes into account the large deviations from isotropy to be expected from the effects of the earth's field. Near sea level, on the other hand, our results are about half those of C. O. and thus accentuate still further the discrepancies with the experimental curves, discrepancies clearly associated with the penetrating component.

The author wishes to thank Professor J. R. Oppenheimer and Dr. R. Serber for many valuable suggestions that have furthered the writing of this paper.

[3] Bowen, Millikan and Neher, Phys. Rev. **52**, 80 (1937).

The Atomic Vibrations of a Zn-Cu Alloy

ROBERT A. HOWARD
Washington University, St. Louis, Missouri
(Received April 18, 1938)

Measurements of x-ray reflection intensities at two temperatures have been made on the $21\bar{3}1$ and $10\bar{1}5$ lines from an alloy of copper and zinc. The idea is put forward that the atomic vibrations should be greatest along the c axis of the crystal in case the axial ratio is greater than 1.633, least when the axial ratio is less than 1.633. The values obtained for the relative amplitudes of vibration along and perpendicular to the c axis confirm this idea. The relative atomic structure factors are also found and show a surprising dependence on the angle which the normal to the reflecting plane makes with the c axis.

1. INTRODUCTION

SEVERAL workers[1] have shown that the atomic vibrations in zinc crystals are anisotropic. Brindley's[2] work on cadmium crystals indicates that its atomic vibrations are also anisotropic. Now zinc and cadmium both crystallize in the so-called "hexagonal close-packed system," and have axial ratios of 1.86 and 1.89 respectively, whereas a system of close-packed geometrical spheres would have an axial ratio of 1.633, so that Zn and Cd both have an abnormal separation of the atoms along the direction of the c axis of the crystal. The interesting thing is that the atomic vibrations are greatest along the direction in which the atoms are furthest apart. Brindley and Ridley,[3] in fact, believe that the asymmetry of these crystals is due wholly or in part to these asymmetric atomic vibrations. However, it has been repeatedly observed in this laboratory that the axial ratio changes by only a very small amount when the crystals are cooled to the temperature of liquid air, at which temperature the atomic vibrations are only about $\frac{1}{2}$ as large as they are at room temperature, so that the atomic vibrations may be said to have very little to do with the anisotropy of the crystal. It would seem that the asymmetry of the atomic vibrations is an effect rather than the cause of the lattice asymmetry.

We may picture (rather crudely) the potential function along a given direction, such as the c axis, which would exist if the atom under consideration were removed from the crystal without altering the position of any of the other atoms, as being a U shaped curve (see Fig. 1*a*) with the bottom of the U at the normal rest position of the atom that has been removed. The last requirement is necessary in order that the crystal be stable. If now, the crystal is stretched out in the direction of the c axis, as it is in Zn and Cd, the whole curve would be stretched horizontally (see Fig. 1*b*), the bottom of the U would become more nearly flat and for a given thermal energy the atom would execute larger vibrations than before. In the case of close-packed geometrical spheres (axial ratio $c/a=1.633$) the distance from any atom to each of its nearest neighbors is the same, and thus one would expect the atomic vibrations to be the same in all directions. According to Brindley[4] this seems to be very nearly true for Mg ($c/a=1.624$).

The purpose of the present research was to see if this idea could be extended to crystals having an axial ratio less than 1.633. The elements beryllium, titanium, zirconium, hafnium, yttrium, ruthenium, and osmium have axial ratios between 1.58 and 1.59. In addition, certain alloys have low axial ratios, and in particular the alloy of Zn and Cu which contains 15 atomic percent of Cu has an axial ratio[5] of 1.556. This alloy has the advantage that it differs only slightly from pure Zn since the 15 percent of Zn atoms (atomic No. 30) are replaced

[1] G. W. Brindley, Phil. Mag. **21**, 790 (1936); G. E. M. Jauncey and W. A. Bruce, Phys. Rev. **50**, 408 (1936); E. O. Wollan and G. G. Harvey, Phys. Rev. **51**, 1054 (1937).
[2] G. W. Brindley, Proc. Leeds Phil. Soc. **3**, 200 (1936).
[3] G. W. Brindley and P. Ridley, Nature **140**, 461 (1936).
[4] G. W. Brindley, Nature **138**, 290 (1936).
[5] E. A. Owen and L. Pickup, Proc. Roy. Soc. **140**, 179 (1933).

by Cu atoms of atomic No. 29. Thus we have a crystal which is essentially a zinc crystal compressed along the c axis, and if our hypothesis is correct, the atomic vibrations should be greatest in a direction normal to the c axis.

For an isotropic crystal (in which case the amplitudes of atomic vibrations are equal in all directions) one gets a smooth curve when the atomic structure factors, f_T, are plotted against $(\sin\theta)/\lambda$, where θ is the Bragg angle for radiation of wave-length λ. Since the f_T are proportional to the square roots of the reflection intensities, and since the reflection intensities decrease as the amplitudes of atomic vibration normal to the reflecting plane increase, it appears possible to detect the relative amplitudes of vibration along and perpendicular to the c axis of the crystal by finding the f_T values. Thus, if our hypothesis is correct, we should expect the f_T values for reflections from planes making a small angle with the c axis to give lower values than those from planes making a large angle with the c axis. It will be seen in Fig. 2 that this is true, and hence the question of the relative amplitudes of atomic vibration might seem to have been answered. The theory of the temperature effect on reflection intensities (see Eqs. (1), (3.0), (6)) shows, however, that the temperature effect should decrease with $(\sin\theta)/\lambda$. It will be noticed in Fig. 2 that just the reverse is true. This means that another effect is coming into play. What this effect is will be left for later discussion, but in any event f_T values do not prove conclusively whether an asymmetry in the atomic vibrations exists or not.

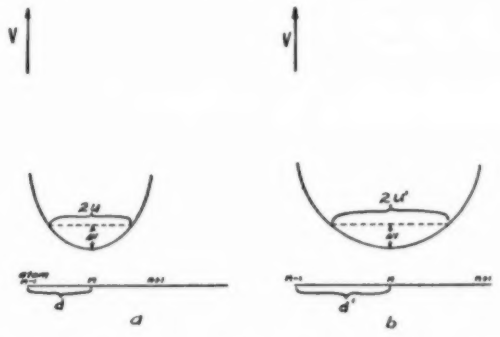

FIG. 1. V is the potential of the nth atom along a given line of atoms in a crystal. ΔV represents the thermal energy of the atom due to vibrations along this line, and u, u' the amplitudes of vibration. d and d' are the distances between atoms for crystals a and b, respectively.

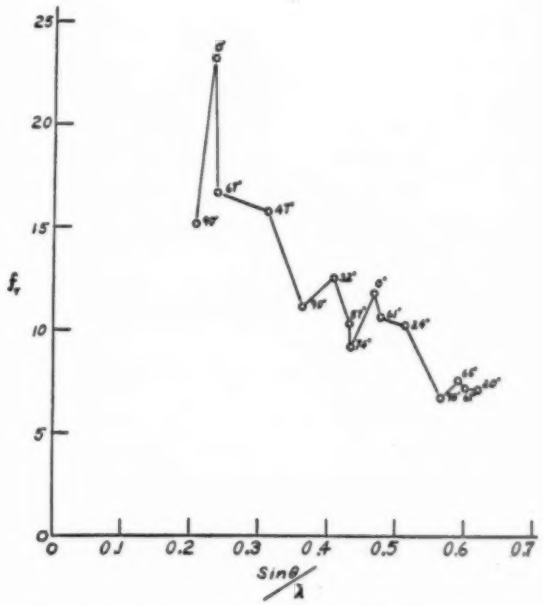

FIG. 2. Atomic structure factor of Zn 85 percent, Cu 15 percent (atomic percent) *vs.* $(\sin\theta)/\lambda$.

Since the f_T values gave inconclusive evidence of atomic vibration asymmetry, it was decided to try the method used by Wollan and Harvey[1] to find the vibration asymmetry in zinc. This method consists in comparing the reflection intensities at two different temperatures. If it is assumed that whatever other causes may make the reflection intensities greater or smaller, their temperature dependence still follows the theories of Debye-Waller, and Zener, then it is possible to determine the quantities a_T and b_T in Eq. (6.0). Since a_T and b_T are proportional to the mean squares of the atomic vibrations along and perpendicular to the c axis, respectively, it is possible to test the atomic vibration asymmetry hypothesis independent of other effects.

2. Description of Apparatus

In determining the atomic structure factors, a metal, self-rectifying, x-ray tube designed by Dr. E. O. Wollan and the author was used in conjunction with a zinc crystal monochromator. Cu $K\alpha$ rays were selected and allowed to fall on the powdered alloy at the center of a circular camera of radius 4.5 cm. The total length of the path of the x-rays from target to film was about 14 cm. With this arrangement it was possible to get good photographs in from three to five

hours, and the use of a crystal monochromator has the advantage that there is almost no divergence of the incident x-rays and hence no focusing, which means that the lines are all of comparable width. This makes it possible to microphotometer all the lines on one film instead of having to microphotometer different sets of Debye-Scherrer lines on different films and then match the overlapped portions. The monochromatic rays from a crystal also give much less background fogging on the film, and the background is far more uniform than it is when filtered radiation is used. This latter fact makes it possible to determine the background with considerably more precision than is possible when filtered radiation is used.

The apparatus used for the temperature effect work has been described in a paper by Wollan and Harvey.[1] In this case two nickel filters were used to get the Cu $K\alpha$ rays. It was found advisable in all cases to clean the surface of the target frequently as this improves the relative amount of characteristic radiation given out by the tube. The background on the film is reduced and the exposure time is shortened. The x-ray outfit was supplied with current from a "constant voltage generator" and the high voltage and emission current were manually adjusted to a set value every five minutes during the exposure in order to get constant radiation output. In half of the cases, the low temperature exposure was made first so that any diminution in x-ray intensity due to progressive coating of the target would average out when several films were used. The microphotometer used in measuring the line intensities on all films consisted of a caesium cell and a DuBridge balanced-bridge d.c. amplifier to operate a short period Moll galvanometer, together with a mechanical system for scanning the film and moving the sensitized paper by proportionate amounts.

3. Experimental Procedure

The alloy was prepared by mixing powdered pure Cu and Zn in proper proportions to give an alloy containing fifteen atomic percent of Cu. The mixed filings were sealed in a quartz tube and heated to 600°C for a period of eleven hours, and then quenched from the molten state in cold water. This gives an alloy in the ϵ phase of the Zn-Cu system with a melting point of 500°C.[6] After quenching, the alloy was annealed for twenty-four hours, gradually heated to 400°C, slowly cooled to 200°C, and then allowed to cool in air. Filings made by a fine file were sealed in an evacuated Pyrex tube and annealed for thirteen hours at 300°C. The Debye-Scherrer lines obtained with this powder had too many spots on them for intensity measurements, so the filings were ground in an agate mortar with a small amount of powdered KCl. After one and a quarter hours of grinding the KCl was dissolved away with water and the alloy powder dried but not reannealed. The average particle size was about 2×10^{-3} cm after grinding, which is only slightly smaller than before grinding. The chief function of the grinding seemed to be to cold-work the metal particles, as the spots on the Debye-Scherrer lines were now small enough that they did not interfere with intensity measurements. Owen and Pickup[5] give the value 1.556 as the axial ratio of this alloy. By plotting the experimentally determined values of $(\lambda/\sin\theta)$ for the alloy used here on Hull and Davey's[7] logarithmic scale and then using their chart, it was confirmed that the crystal belonged to the hexagonal close-packed system and had an axial ratio of 1.56 as nearly as it could be determined.

In finding the atomic structure factors, several Debye-Scherrer photographs were made. Each film had a set of intensity steps made on it so that any difference in the film or its development would not affect the determination of the relative intensities of the lines. The intensity steps were made by placing the film, held in a lead cassette with a rectangular aluminum window at one end, behind a rotating, step-cut wheel and allowing nickel filtered x-rays from a copper target to fall on it. The wheel was so cut that each successive strip on the film received the same increment of radiation energy. The relative intensities were measured by microphotometering the films and measuring the areas under the curves obtained for the various lines. After the intensities had been corrected for absorption in

[6] *International Critical Tables*, Vol. 2, p. 435.
[7] A. W. Hull and W. P. Davey, Phys. Rev. **17**, 549 (1921).

the briquet from Brindley's[8] curve, the values obtained were multiplied by a suitable constant so that the corrected relative intensities from each film were on the same basis. The relative atomic structure factors, f_T, were then calculated from the formula

$$I/A = \text{const.} \times pS^2 f_T^2 \phi(\theta), \tag{1}$$

where p is the multiplicity factor, S the crystal structure factor ($=1$, 2 or $(3)^{\frac{1}{2}}$ for hexagonal close-packed lattices), and

$$\phi(\theta) = \frac{1+\cos^2 2\beta \cos^2 2\theta}{\sin\theta \sin 2\theta}, \tag{2}$$

where θ is the Bragg angle for the reflection and β is the angle which the incident radiation makes with the monochromator crystal face. In this case $\cos^2 2\beta = 0.649$.

In the temperature effect work, two exposures were made on the same film, one at room temperature and one at the temperature of liquid air. Intensity marks were made on each film as before. Nothing was changed between the two exposures except the position of the film. The angle θ changes so little because of lattice contraction, that changes in the absorption factor, A, may be neglected. Only the $21\bar{3}1$ and $10\bar{1}5$ lines were used in this part of the work. The ratio of the intensity at liquid-air temperature to that at room temperature was determined for each line, in some cases by measuring the areas under the microphotometer traces, sometimes by comparing the heights of the two curves, and occasionally by both methods. The sums of the ratios obtained by the area method and the height method were 23.52 and 23.04, respectively, for the sixteen cases where measurements were made by both methods. Each line was microphotometered from one to nine times and the average value used. The mean values of the ratios for these two lines were then substituted in the Debye-Waller and Zener formulas (Eqs. (3.0) and (4)) and the values of a_T and b_T calculated.

[8] G. W. Brindley and F. W. Spiers, Proc. Phys. Soc. **46**, 841 (1934), give a set of curves for the quantity $A = \frac{\sin(2\theta-\alpha)}{\sin(2\theta-\alpha)+\sin\alpha}$ (which is the fraction by which the intensity is reduced by absorption in the briquet) as a function of the Bragg angle θ for several values of α, the angle which the incident radiation makes with the face of the briquet.

4. Results

Table I shows the relative atomic structure factors obtained, and Fig. 2 is a plot of these values against $(\sin\theta)/\lambda$.

Debye has shown that for a given reflection,

$$I_T = I_0 e^{-2M_T}, \tag{3.0}$$

where I_T is the intensity of the reflection, I_0 is the intensity which one would get if the crystal were at the absolute zero of temperature, and M_T is a function of the temperature. Let I_{LA} = intensity

Table I. *Atomic structure factors.*

Line	$\sin\theta/\lambda$	Ψ	Relative Intensities Corrected for Absorption (I/A)									$pS^2\phi(\theta)$	f_T	f_0
			A-19	A-29	A-39	A-40	A-41	A-46	A-48	A-49	A-50			
$10\bar{1}0$	0.207	90°		9.10	8.50							43.9	15.2 ±1.73	16.5
0002	.234	0°	21.0	22.6	19.5							44.9	23.2 ±0.32	25.2
$10\bar{1}1$	.238	60° 55′	46.7		47.0							194.	16.8 ±0.16	18.6
$10\bar{1}2$	.312	41° 55′	6.12	6.08	6.62			7.00		8.74	10.6	35.1	15.7 ±0.50	18.5
$11\bar{2}0$	.363	90°	5.73	4.84	5.73	5.00		5.36	5.73	5.53	5.90	50.7	11.2 ±0.10	14.3
$10\bar{1}3$	.408	31° 41′	8.68	8.56	7.83	7.51		10.2	7.98	7.30	7.97	59.7	12.6 ±0.16	16.7
$20\bar{2}0$	.417	90°									1.44(?)	9.66		
$11\bar{2}2$	.432	57° 19′			8.01			7.18	6.93	6.06	6.11	73.4	10.3 ±0.18	14.3
$20\bar{2}1$	.434	74° 31′			3.98			4.08	3.56	4.22	4.40	54.7	9.23±0.11	13.1
0004	.468	0°			1.47			1.22	1.40	1.37	1.26	11.2	11.8 ±0.14	16.5
$20\bar{2}2$	.478	60° 55′			1.45				1.62	1.76	1.70	16.4	10.6 ±0.16	16.0
$10\bar{1}4$	.512	24° 5′			1.43			1.50	1.73	1.62	1.28	16.3	10.4±0.19	15.8
$20\bar{2}3$	.547	50° 8′	}									52.5		
$21\bar{3}0$	.546	90°			3.13		3.14		3.07	3.37	3.06	17.4		
$21\bar{3}1$	.566	78° 7′			4.92	4.79	4.46	4.51	4.50	4.33	4.13	114.	6.75±0.05	12.2
$11\bar{2}4$	.592	66° 40′			4.51	4.99	4.44	4.29	4.77	4.17	4.32	90.7	7.57±0.06	14.3
$21\bar{3}2$	.601	67° 10′			1.98	2.24	2.25	2.41	2.15	2.11	2.37	49.2	7.22±0.06	14.0
$10\bar{1}5$	.621	19° 37′					4.32	4.19	4.27	4.25	4.48	96.8	7.18±0.03	13.2

of reflection when crystal is at temperature of liquid air, and I_{RT} = intensity at room temperature. Then

$$I_{LA}=I_0e^{-2M_{LA}}, \tag{3.1}$$

$$I_{RT}=I_0e^{-2M_{RT}}, \tag{3.2}$$

$$R=I_{LA}/I_{RT}=e^{2(M_{RT}-M_{LA})}, \tag{4}$$

and

$$\log R=2(M_{RT}-M_{LA}). \tag{5}$$

From the equations derived by Zener,[9]

$$M_T=(a_T\cos^2\psi+b_T\sin^2\psi)(\sin\theta/\lambda)^2Q(x), \tag{6.0}$$

where ψ is the angle which the normal to the reflecting plane makes with the C axis of the crystal, $Q(x)$ is the quantization factor and is nearly equal to unity, $x=\Theta/T$, Θ is the characteristic temperature of the metal, T is the absolute temperature, and a_T and b_T are functions of the temperature only.

For a cubic crystal of atoms of one kind, Debye and Waller have shown that

$$M_T=\frac{6h^2T}{mk\Theta^2}Q(x)\left(\frac{\sin\theta}{\lambda}\right)^2. \tag{7}$$

Since M_T is a linear function of T for cubic crystals, we shall assume that it is also a linear function of T for anisotropic crystals. Letting $a_T=a\cdot T$, and $b_T=b\cdot T$, we get

$$M_T=Q(x)T(\sin\theta/\lambda)^2(a\cos^2\psi+b\sin^2\psi). \tag{6.1}$$

Actually Θ is a function of both ψ and T, but this has such a small effect on the value of Q that Θ is assumed to be constant. Moreover, Θ is not known for this alloy, but it can be taken equal to that of pure zinc to a sufficiently good approximation. Combining Eqs. (5) and (6.1), we get

$$\frac{\log R}{(\sin\theta/\lambda)^2}=2(Q_{RT}T_{RT}-Q_{LA}T_{LA})(a\cos^2\psi$$

$$+b\sin^2\psi)=2\Delta(QT)(a\cos^2\psi+b\sin^2\psi). \tag{8.0}$$

For the $21\bar{3}1$ line,

$$a_T\cos^2\psi_1+b_T\sin^2\psi_1=\frac{T_{RT}\log R_1}{2\Delta(QT)(\sin\theta_1/\lambda)^2}, \tag{8.1}$$

[9] C. Zener, Phys. Rev. **49**, 122 (1936).

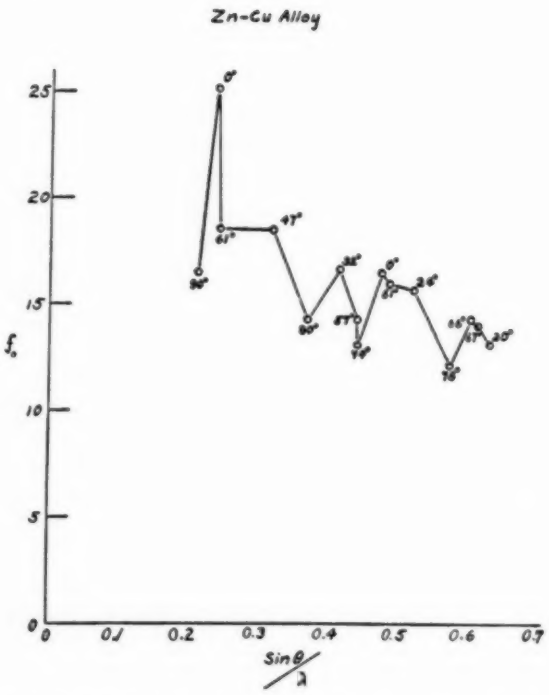

FIG. 3. Relative structure factor for an atom at $T=0$.

and for the $10\bar{1}5$ line,

$$a_T\cos^2\psi_2+b_T\sin^2\psi_2=\frac{T_{RT}\log R_2}{2\Delta(QT)(\sin\theta_2/\lambda)^2}. \tag{8.2}$$

The results of fifteen films and seventy-four microphotometer traces are used in obtaining solutions for a_T and b_T. We get

$$a_T=1.51\pm0.118\text{A}^2$$

and

$$b_T=1.84\pm0.098\text{A}^2.$$

5. Discussion

The individual values of R_1 and R_2 vary over a considerable range, so that the values obtained for a_T and b_T can have no high accuracy. Two facts are to be noted, however. In the first place, the probable errors are sufficiently small that the limiting values of a_T and b_T do not overlap. Secondly, if one uses (a_T-b_T) as a measure of the anisotropy as Jauncey[1] prefers to do, he gets

$$(a_T-b_T)=-0.33\pm0.155\text{A}^2,$$

so that the limiting values of the anisotropy are always negative. Therefore, while the results cannot be said to prove absolutely that b_T is

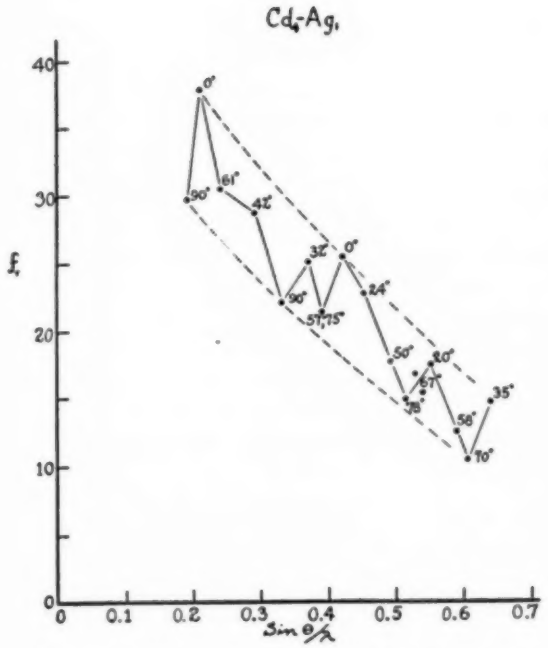

FIG. 4. Atomic structure factor of Cd 80 percent, Ag 20 percent (atomic percent) *vs.* (sin θ)/λ.

greater than a_T, it seems extremely probable that this is the case, and our hypothesis about the vibrations being greater in a direction normal to the c axis of the crystal than along it is apparently confirmed.

If we now use a_T and b_T to calculate the relative structure factors reduced to an atom at absolute zero temperature (no correction for dispersion) we get the results shown in Fig. 3. It will be noticed that the results are not essentially different from those for f_T, and the question immediately comes up, "What causes the f values to vary so violently as a function of the orientation angle, ψ?"

The thing which suggests itself first is distortion caused by grinding the crystals. Elastic distortion we can rule out immediately because the effect of elastic distortion is to broaden the lines, and the lines are no broader than those obtained from annealed filings of the alloy or from pure sublimated zinc. Barrett,[10] and Hengstenberg and Mark[11] have also found that cold working a metal has very little effect on the line width. Plastic deformation, in which slipping takes place along certain planes in the crystal, could give rise to highly strained surface layers at points along the slip planes or at fractures, and possibly even to a layer of amorphous material between the slip planes. Amorphous material along the slip planes would introduce an additional absorption factor which would be a function of both θ and ψ. It is also possible that some part of the scattering of the f values is due to electron asymmetry in the atom. Such an idea is consistent with the fact that the spread of the points *decreases* with increasing (sin θ)/λ, which is just what is to be expected if the electron distribution in the atom is asymmetric. If the whole effect is due to electron distribution asymmetry, the effect must necessarily reach down into the inner electron shells, as an asymmetric distribution of the outer two electrons of zinc is insufficient to give the observed change between the f values for $\psi=90°$ and $\psi=0°$.

Figure 4 shows some unpublished f_T values obtained by Dr. E. O. Wollan[12] for a Cd-Ag alloy containing approximately twenty atomic percent silver. This alloy also has an axial ratio of 1.56. The situation is almost exactly parallel to that of the Zn-Cu alloy, in that we replace part of the atoms of an element whose crystals have a high axial ratio (1.89) by an element whose atomic number is one less. The alloys were both prepared in the same manner, and the powders treated in the same way. It will be noticed that here again the spread of the points increases as (sin θ)/λ decreases, although the percentage change is somewhat less. Whatever the explanation of this large change is, it is evident that it will suffice for both alloys.

6. ACKNOWLEDGMENTS

The author wishes to express his thanks for the many hours of help and discussion given by Dr. E. O. Wollan in the beginning phases of this problem, and for his aid in designing the equipment used. The author is also indebted to Dr. G. E. M. Jauncey for his advice and suggestions relative to the latter phase of this research.

[10] Barrett, Phys. Rev. **47**, 333 (1935).
[11] Hengstenberg and Mark, Zeits. f. Physik **61**, 435 (1930).
[12] E. O. Wollan, Phys. Rev. **53**, 203(A) (1938).

The Determination of the Characteristic Temperature of MgO from X-Ray Measurements

H. S. RIBNER AND E. O. WOLLAN
Washington University, St. Louis, Missouri

(Received April 25, 1938)

The characteristic temperature for MgO has been directly measured by the x-ray method and a value of $\Theta = 743°K$ for the range between room temperature and the temperature of liquid air obtained. A value of Θ was also obtained with the aid of theoretical f_0 values and the result so obtained was found to be in qualitative accord with the above value. In this connection it was noticed that the theoretical f_0 values for MgO are considerably in error. The characteristic temperature determined by the usual method from specific heat data shows a considerable dependence on temperature but the mean of these values over the range under consideration is in good accord with the x-ray value.

INTRODUCTION

THE theory of the effect of temperature on the intensity of reflection of x-rays from crystals which was developed by Debye and later corrected by Waller involves a quantity which is referred to as the characteristic temperature of the crystal. This quantity was introduced in connection with the theory of specific heats, and in the Debye form of this theory the characteristic temperature is defined by the relation $\Theta = h\nu_m/k$ where ν_m is the limiting frequency of the atomic vibrations considered propagated as elastic waves. Some uncertainty still exists, however, as to the conditions under which a value of the characteristic temperature calculated from specific heat data can be used in the Debye-Waller theory for the determination of the effect of temperature on the intensity of x-ray reflection. Measurements which bear on this point have been made by James and Firth [1] on NaCl, by James and Brindley [2] on KCl, by James, Brindley and Wood [3] on Al and by Shonka [4] on NaF. The theory of the temperature effect is strictly valid only for simple cubic crystals containing atoms of one kind and one sees that the above examples represent varying degrees of departure from these conditions. The experiments to be described in this paper deal with measurements of the effect of temperature on the reflection of x-rays from MgO and a comparison of the characteristic temperature so obtained with that which one gets from specific heat data.

[1] R. W. James and E. Firth, Proc. Roy. Soc. **A117**, 62 (1927).
[2] R. W. James and G. W. Brindley, Proc. Roy. Soc. **A121**, 155 (1928).
[3] R. W. James, G. W. Brindley and R. G. Wood, Proc. Roy. Soc. **A125**, 401 (1929).
[4] J. J. Shonka, Phys. Rev. **43**, 947 (1933).

THEORY

Although the Debye-Waller theory is strictly valid only for crystals consisting of atoms of one kind, we shall assume for the present that it can be applied to the case of MgO and later we shall discuss the limitations of this assumption. According to this theory the atomic scattering factor at a temperature T is related to the scattering factor f_0 for the atom at rest by the equation

$$f_T = f_0 \exp(-K \sin^2\theta/\lambda^2) \tag{1}$$

where

$$K = 6h^2TQ(x)/mk\Theta^2 \tag{2}$$

and

$$Q(x) \equiv \left[\frac{1}{x}\int_0^x \frac{\xi d\xi}{e^\xi - 1} + \frac{x}{4}\right] \tag{3}$$

is sometimes referred to as the quantization factor. $Q(x)$ can be obtained from tables [5] for all desired values of $x \equiv \Theta/T$. It is a quantity which departs appreciably from unity only for low temperatures (i.e., $T < \Theta$). The exponent $K \sin^2\theta/\lambda^2$ is commonly denoted by the symbol M, and the expression e^{-M} is known as the Debye-Waller temperature factor.

From Eq. (1) it is seen that K, and hence Θ, may be evaluated from a knowledge of corresponding values of f_T and f_0. If theoretical values

[5] R. W. James and G. W. Brindley, Phil. Mag. **12**, 81 (1931); p. 107. Note correction p. 729.

of f_0 have been calculated from the wave mechanics, experimental values of f_T at one temperature will suffice to determine K.

Let us first consider the more directly experimental determination of M from measurements of f_T at two different temperatures. Since the intensity of reflection from powdered crystals is proportional to the square of the atomic scattering factor we can write Eq. (1) in the form

$$f_{T_1}^2/f_{T_2}^2=\rho_1/\rho_2=e^{2(M_2-M_1)}=e^{2\Delta M}, \qquad (4)$$

where ΔM is written for (M_2-M_1) and ρ_1 and ρ_2 represent the integrated intensities at the two temperatures. Taking logarithms of both sides we obtain

$$\log(\rho_1/\rho_2)=2\Delta M=2\Delta K \sin^2\theta/\lambda^2 \qquad (5)$$

or

$$(\lambda^2/\sin^2\theta)\log(\rho_1/\rho_2)=2\Delta K, \qquad (6)$$

where

$$2\Delta K\equiv 2(K_2-K_1)$$
$$=(12h^2/mk\Theta^2)\{T_2Q(x_2)-T_1Q(x_1)\}. \qquad (5.1)$$

Experimental values of the left-hand side of Eq. (6) afford values of $2\Delta K$ from which Θ may be calculated. Alternatively, if in Eq. (5) we consider $\log(\rho_1/\rho_2)$ to be plotted *vs.* $\sin^2\theta/\lambda^2$ we may regard the quantity $2\Delta K$ as the slope of the resulting straight line.

From this same equation it is seen that the quantity which must be determined experimentally is the ratio ρ_1/ρ_2 of the intensities at two temperatures as a function of the scattering angle. In order to obtain an absolute value of this ratio it is necessary that the measurements at each temperature be made under identical conditions and that the total energy falling on the crystals in each case be the same. In the photographic method of recording intensities this might be accomplished by taking identical exposures in the two cases. This method was used successfully

TABLE I. *Temperature effect* (*see also Fig. 1*).

PLANE	ρ_1'/ρ_2'	$\log_e(\rho_1'/\rho_2')$	$\sin^2\theta/\lambda^2$
200	1.024	0.024	0.057
220	1.050	0.050	0.114
222	1.030	0.030	0.171
420	1.109	0.104	0.284
422	1.070	0.068	0.341
440	1.167	0.156	0.453

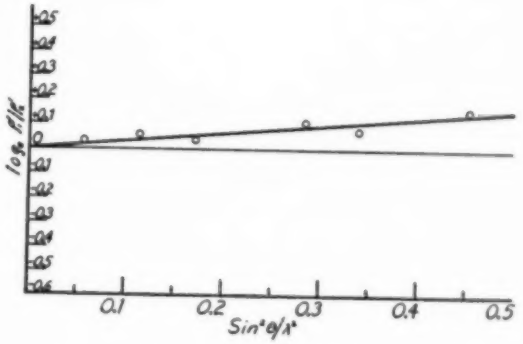

FIG. 1. Weighted mean of ρ_1'/ρ_2' as a function of $\sin^2\theta/\lambda^2$.

by Shonka [4] in his measurements on NaF. The following consideration will however show that a knowledge of the absolute ratio ρ_1/ρ_2 is unnecessary. If the exposure of a film at temperature T_1 is some unknown constant c times as great as the exposure of another film at temperature T_2 then the correct ratio of the intensities for equal exposures is $\rho_1'/c\rho_2'$ where ρ_1' and ρ_2' are the observed integrated intensities for the lines considered. If we now substitute this correct ratio into Eq. (5) it can be written in the form

$$\log(\rho_1'/\rho_2')=2\Delta K \sin^2\theta/\lambda^2+\log c \qquad (7)$$

and we see that the unknown constant c enters as an intercept and the slope $2\Delta K$ of the line has not been affected.

EXPERIMENTAL PROCEDURE

The apparatus used in this research was the same as that used previously by one of us [6] in connection with another problem. It consisted of a cylindrical camera the top of which formed a metal Dewar flask. The sample of powdered MgO in the form of a flat briquet was held against the inner copper wall of the Dewar so that the face of the briquet was always in the center of the camera. Copper $K\alpha$ radiation was used and pictures were taken with the sample held at room temperature and at the temperature of liquid air. Seven pairs of films at the two temperatures were chosen for analysis and for each pair of films values of ρ_1'/ρ_2' were obtained as a function of $\sin^2\theta/\lambda^2$ for all lines of even order ($h+k+l$=even number). The odd order lines ($h+k+l$=odd

[6] E. O. Wollan and G. G. Harvey, Phys. Rev. **51**, 1054 (1937).

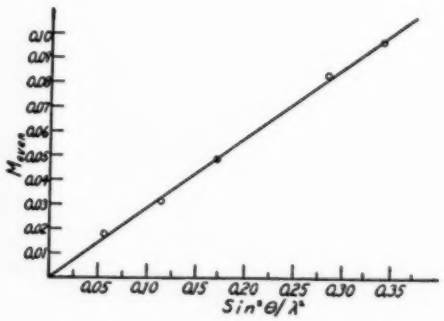

FIG. 2. Values of M_{even} *vs.* $\sin^2\theta/\lambda^2$.

number) were not used for reasons to be discussed below. The data from each pair of films were then combined in such a way as effectively to reduce all the measurements to a common value of the unknown constant c.

The results are shown in Fig. 1, where the weighted mean of the seven values of ρ_1'/ρ_2' have been plotted. The slope of the line, which is a measure of the temperature effect, is seen to be very small. ρ_1' (for liquid-air temperature) is only sixteen percent greater than ρ_2' (for room temperature) for the largest value of $\sin\theta/\lambda$ at which a line was obtained. The slope was determined by the method of least squares to be 0.299.

THE CHARACTERISTIC TEMPERATURE

From direct x-ray measurement

On the basis of the simple theory we can now calculate the characteristic temperature of the crystal by substituting the slope which we have obtained experimentally into Eq. (5.1). Since we are dealing with a crystal containing two kinds of atoms we use an average value of the mass of these atoms. By this method we obtain the value $\Theta=743°\text{K}$ for the characteristic temperature.

Since, however, MgO does not consist of atoms of one kind as the simple theory requires, let us consider what modifications we must make in the treatment. Waller has shown that in the case of such a crystal each kind of atom should be assigned its own temperature factor. For this reason, we must consider separately the even order spectra (reflections from planes containing both kinds of atoms in equal numbers) and the odd order spectra (reflections from alternate planes of each kind of atom). For even order reflections we thus have that

$$F_{\text{even}}=F_1+F_2=f_1e^{-M_1}+f_2e^{-M_2} \tag{8}$$

and for odd order reflections

$$F_{\text{odd}}=F_1-F_2=f_1e^{-M_1}-f_2e^{-M_2}, \tag{9}$$

where the small f's refer to the atoms at rest and the subscripts 1 and 2 refer to Mg and O, respectively. We may then define an effective temperature factor for the purposes of the simple theory by writing for the even reflections

$$f_1e^{-M_1}+f_2e^{-M_2}\equiv(f_1+f_2)e^{-M_{\text{even}}} \tag{10}$$

and for the odd reflections

$$f_1e^{-M_1}-f_2e^{-M_2}\equiv(f_1-f_2)e^{-M_{\text{odd}}}. \tag{11}$$

Since the M's are small quantities we can replace e^{-M} by $1-M$, obtaining

$$M_{\text{even}}=(f_1M_1+f_2M_2)/(f_1+f_2), \tag{12}$$

$$M_{\text{odd}}=(f_1M_1-f_2M_2)/(f_1-f_2) \tag{13}$$

from (10) and (11), respectively.

We see from this that M_{even} is an average of M_1 and M_2 weighted according to the relative scattering powers of atoms 1 and 2, while M_{odd} is nothing like an average. Hence M_{even} may legitimately be used for the unsubscripted M in the simple theory and $e^{-M_{\text{even}}}$ considered as an

TABLE II. *Room temperature values of f for magnesium oxide (even orders only).*

PLANE	$\sin\theta/\lambda$	f			
		WOLLAN	FROMAN	R. AND W.	MEAN
200	0.238	13.40	13.25		13.32
220	0.337	10.15	10.15	10.15	10.15
222	0.413	8.20	8.19	8.29	8.23
400	0.476	6.94	6.41	6.99	6.78
420	0.533	5.92	5.83	6.19	5.98
422	0.583	5.35	4.99	5.57	5.30
440	0.673	4.00	3.68		3.84
442+600	0.714	3.78	3.66		3.72
620	0.752	3.22	3.07		3.14
622	0.790	3.00	3.03		3.01
444	0.825	2.90	3.22		3.06
640	0.858	2.60	2.85		2.72
642	0.891	2.52	2.77		2.64
800	0.952	2.21	2.71		2.46
820+644	0.982	2.05	2.31		2.18
822+660	1.010	1.86	2.26		2.06
662	1.049		2.11		2.11
840	1.063		2.03		2.03
842	1.088		1.80		1.80
664	1.117		1.80		1.80

average temperature factor for the two kinds of atoms. M_{odd} is definitely not suitable and hence we have excluded data from odd order reflections in calculating M. It should be, however, possible from separate values of M_{even} and M_{odd} to obtain M_1 and M_2 separately by the use of equations (12) and (13). We have not done this because the odd order reflections were too weak for sufficient accuracy.

Our method of determining M_{even} for MgO is based on the assumption that this quantity is of the form (const.)$\times\sin^2\theta/\lambda^2$ as is the M of the simple theory. To test this point we have put room temperature values for the f's in Eq. (10) since this introduces a negligible error and these f's are available in the literature (see Table II). For M_1 and M_2 we have taken Brindley's estimates[7] of $0.33\sin^2\theta/\lambda^2$ and $0.20\sin^2\theta/\lambda^2$, respectively. Plotting M_{even} *vs.* $\sin^2\theta/\lambda^2$ gives the very good straight line through the origin shown in Fig. 2, establishing that M_{even} is of the required functional form.

From theoretical f_0 values

As was mentioned above the characteristic temperature can also be determined with the aid of Eq. (1) from measurements of f_T at one temperature if theoretical values of f_0 are available. Various values of the structure factor for even orders of reflection from MgO at room temperature are listed in Table II. The first column gives the absolute measurements of Wollan[8] who used an ionization method, the second gives the data of Froman[9] obtained by a photographic method and the third column gives the data which we have obtained in connection with this investigation. The values in the last two columns, being relative, have been fitted to those in the first column at the 220 reflection. The average of these data is plotted in the lower curve of Fig. 3.

Values of the structure factor for the atoms at rest can be obtained from the work of James and Brindley.[5] These values were obtained by a method of interpolation in connection with solutions by Hartree's method of self-consistent fields for neighboring atoms in the periodic table.

[7] G. W. Brindley, Phil. Mag. **9**, 1081 (1930).
[8] E. O. Wollan, Phys. Rev. **35**, 1019 (1930).
[9] D. K. Froman, Phys. Rev. **36**, 1330 (1930).

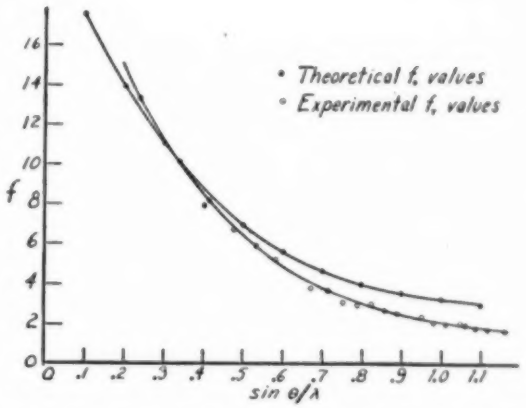

FIG. 3. Upper curve, theoretical f_0 values. Lower curve, experimental f_T values.

The upper curve in Fig. 3 represents the even order structure factor for the atoms at rest as obtained from the James and Brindley paper. One is immediately struck by the fact that the two curves cross at about $\sin\theta/\lambda=0.3$. This means that either the theoretical or the experimental results, or both, are in error. An inspection of the results of Table II shows such good agreement between the various observers that it would seem unlikely that a large error could exist in the f_T curve. On the other hand there are reasons to believe that the f_0 values as determined for atoms not having closed shells may be considerably in error. It is known that measurements on the scattering of x-rays from oxygen and nitrogen in the gaseous form are also not in accord with the calculated f_0 values.[10]

In view of these facts this method of obtaining the temperature factor would seem to be rather unreliable. It seems likely, however, that the errors in f_0 should tend to become smaller as $\sin\theta/\lambda$ increases because the outer electrons contribute very little to the curve at large angles. In accord with this is the curve of Fig. 4 in which K, defined by the relation

$$f_T=f_0\exp(-K\sin^2\theta/\lambda^2),$$

is plotted against $\sin^2\theta/\lambda^2$. The trend of the data make it seem reasonable to suppose that at large angles the curve will approximately asymptote to the solid line, which represents the characteristic temperature $\Theta=743°K$ which we ob-

[10] A. H. Compton and S. K. Allison, *X-Rays in Theory and Experiment* (Van Nostrand, 1936), pp. 161–4.

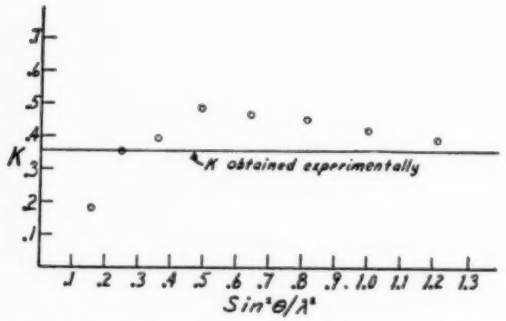

FIG. 4. K from theoretical f_0 values and experimental f_T values.

tained from measurements of f_T at two temperatures.

From specific heat data

The usual method of obtaining the characteristic temperature from specific heat data is to find that value of Θ for a given temperature which makes the observed value of C_v equal that given by the Debye theory. Using experimental data for C_v obtained from tables[11] we have calculated Θ for various temperatures. The results are shown in Fig. 5, the crosses and the circles representing data taken from two different sources. The agreement between the data is seen to be far from satisfactory. One notices also a considerable variation of Θ with temperature. In our determination of Θ from the x-ray data we have assumed that it does not vary appreciably with temperature over the range which we have used, and it can be shown that the x-ray results are inconsistent with a large variation of Θ with T. It is, however, interesting to note that the mean of the specific heat values over the range of temperature used gives a value of $\Theta = 744°K$ which is in surprisingly good agreement with the value obtained from the x-ray measurements. Too much significance should not be attached to this fact, however, since both the x-ray and the specific heat values carry a rather large probable error.

It should be mentioned that Zener and

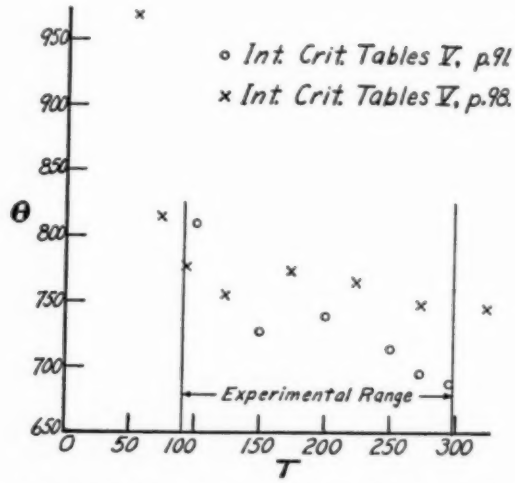

FIG. 5. Values of θ from the experimental data for C_v are calculated for various temperatures.

Bilinsky[12] have given a theoretical justification for a certain amount of variation of Θ with T due to the expansion of the lattice. In the case of MgO this turns out to be of the order of only 3°K which is negligible to our degree of accuracy.

CONCLUSION

A value of the characteristic temperature equal to 743°K obtained by the x-ray method for MgO agrees well with the mean of the specific heat values over the range from room temperature to the temperature of liquid air. It seems to vary inappreciably with the temperature.

The difference between the amount of the temperature variation of the specific-heat Θ given by the Zener-Bilinsky method and that given by the usual method implies that MgO fits the simple Debye model badly, since the former method arises from the application of straightforward thermodynamics to the Debye model of a solid.

The wave mechanical f_0 values available at present for Mg and O are not satisfactory, especially at small angles. The values become more reliable at the larger angles.

[11] *International Critical Tables V*, pp. 91, 98.

[12] C. Zener and S. Bilinsky, Phys. Rev. **50**, 101 (1936).

Intensity Relations in the Low Voltage Helium Arc

JOHN J. HEILEMANN
Randal Morgan Laboratory of Physics, University of Pennsylvania, Philadelphia, Pennsylvania
(Received April 14, 1938)

The linear amplifier photo-cell unit from a Razek-Mulder spectrophotometer is used with a high speed monochromator to measure the relative intensity of helium spectrum lines under various conditions of excitation; the discharge is developed in a copper ball 10.5 cm in diameter. A linear relation is found between arc current and line intensity for a series of voltages between the excitation potential and 100 volts, and from this family of curves a family of excitation functions is drawn for a range of currents up to thirty milliamperes. The voltage intensity relation for eight helium lines (4388, 4438, 4471, 4713, 4922, 5016, 5876, 6678) was determined directly. The results check those of Razek up to 50 volts and those of Elenbaas over the entire range, although secondary maxima are indicated in the region between the ionization potential and 45 volts. Additional experiments show that the cathode surface plays a part in determining the character of the discharge, and that the rise in Razek's curves was caused by the discharge changing to the self-maintaining form; the hysteresis observed by him is eliminated by the use of a two-grid electron source.

THE function which describes the relation between the intensity of a spectral line and the accelerating voltage of the exciting electrons is called the "optical excitation function" of the line. This function in helium has been the subject of considerable investigation.[1–8] If the results of these investigations are to be interpreted in the light of the usual microscopic theories it is necessary to insure that (1) the electrons are homogeneous as to velocity, (2) each electron produces a single photon emission, (3) the number of electrons projected into the gas can be obtained from the measured current, and (4) the energy of the electrons is truly indicated by the voltage measuring device. These conditions will not be met if (1) the mean free path of the electrons is too short, (2) if large space charge effects are present, (3) if the atoms are excited by more than one collision, or by the combined absorption of energy from electrons and photons, (4) if the structures in the tube alter the character of the discharge, (5) if there is self-absorption of the radiation by the gas, or (6) if secondary electrons are present. A linear relation between intensity and both current and pressure is usually accepted as evidence that the conditions enumerated above have been met.

The photographic method of intensity measurement has been used by all previous investigators except Razek.[8] The greatest accuracy claimed for a photographic determination of intensity is 5 percent.[9] However, Hanle[4] reports that variations on the plates used in his work were between 10 and 20 percent, consequently irregularities in the functions he investigated which are of an order of magnitude less than 10 or 20 percent cannot be considered significant. Furthermore, the inherent slowness of the photographic method detracts from its usefulness in excitation function determinations where the "fine structure" of the phenomenon is being studied, since it is difficult to keep constant the discharge tube currents and voltages for a sufficient length of time. Most of the curves in the literature for which data are given indicate a lack of smoothness, but the limited accuracy of the photographic photometry does not justify the drawing of anything but a smooth curve through the points. Furthermore, the number of voltages used is usually insufficient to make the curves which are drawn really indicative of the detailed character of the function.

The spectrum tubes used by other workers[2, 4–7] were usually of small dimensions and were furnished with nonequipotential cathodes, the inequality ranging from 0.3 volts to 5 volts. The envelopes were of glass and the electrodes and shields were large and placed unsymmetrically with respect to the discharge. It is well

[1] Elenbaas, Zeits. f. Physik **59**, 289 (1929).
[2] Hughes and Lowe, Proc. Roy. Soc. **A104**, 480 (1923).
[3] Bazzoni and Lay, Phys. Rev. **23**, 327 (1924).
[4] Hanle, Zeits. f. Physik **56**, 94 (1929).
[5] Michels, Phys. Rev. **36**, 1362 (1929).
[6] Thieme, Zeits. f. Physik **78**, 412 (1932).
[7] Lees, Proc. Roy. Soc. **137**, 173 (1932).
[8] Razek, Phys. Rev. **37**, 1252 (1931).
[9] Lay and Cornog, J. Opt. Soc. Am. **24**, 149 (1934).

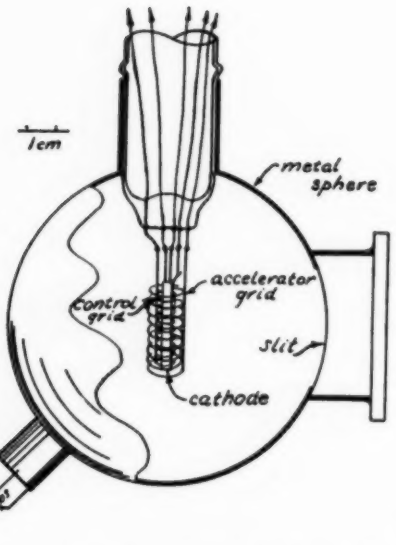

FIG. 1. Diagram of discharge tube for low voltage helium excitation.

known in vacuum tube practice that the disposition of the electrodes plays an important part in determining the tube characteristics, owing to the accumulation of surface charges and similar effects, consequently it might be expected that the behavior of a small discharge in a relatively large system of electrodes would be strongly influenced by the geometry of the system.

Razek used a photoelectric spectrophotometer[10, 11] the response of which was shown to be linear with intensity; this instrument, with which the inherent slowness of the photographic method may be overcome, was shown by him to be applicable to the problem in hand. The linear amplifier from Razek's spectrophotometer and a spectrum tube similar to his were used in the work here reported. From the description of this tube it will be seen that the discharge takes place in a "hohlraum" relatively free from electrodes. The present work was undertaken with the idea of using this kind of tube to determine in greater detail the character of the excitation function, as well as to demonstrate that the sources of error listed above were not present at the relatively high pressures used in this type of equipment. The pressure of the helium was 0.27 mm of mercury.

[10] Mulder and Razek, J. O. S. A. and R. S. I. **18**, 466 (1929).
[11] Razek and Mulder, J. O. S. A. and R. S. I. **19**, 390 (1929).

DESCRIPTION OF THE DISCHARGE TUBE

The discharge takes place in a spun copper ball 10.4 cm in diameter, the inside surface of which is silvered and polished. A slit, over which is placed a tube and a glass plate, allows observation of the discharge. The electron source (Fig. 1) was mounted on the press from a commercial vacuum tube by spot welding to the leads a heater-type oxide coated cathode (diameter 1.7 mm) such as is used in the type '27 tube, a grid from the same type tube (diameter 4 mm) and a second grid from a type '24 tube (diameter 7 mm). The grid nearer the cathode is the "control-grid" and the other is the "accelerator-grid." The wiring is shown in Fig. 2.

The electrons are emitted by the cathode, and the number which is admitted into the space between G_1 and G_2 is determined by the potential difference between G_1 and C; the sense of this potential difference may be changed by means of the reversing switch. Thus the number of electrons available for acceleration by the field between G_1 and G_2 may be regulated without changing the temperature of the cathode; the cathode temperature is maintained by the usual insulated filament heated by a storage battery. A radio B battery supplies the potential difference between G_1 and C, which potential controls the arc current; a bank of storage batteries is used to supply the accelerating potential between G_1 and G_2. The discharge takes place in the equipotential space between the ball and G_2, and the current in the arc is measured by the milli-

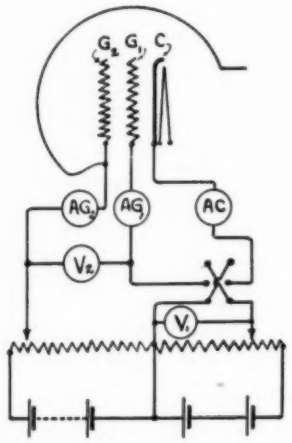

FIG. 2. Wiring diagram of discharge tube for low voltage helium excitation.

ammeter AG_2. For each observation in the course of the experiment a reading of each meter was taken so as to follow the behavior of the discharge tube as closely as possible. It was thought that a study of the relations between the various currents and voltages might yield information as to the function of the parts of the electron gun; as a matter of fact data were obtained (to be mentioned later) which apparently shed light upon the action of the control grid G_1.

Description of Experimental Set-Up

The discharge tube was permanently connected to the vacuum system through a stopcock; between this stopcock and the ball was a charcoal trap which was immersed in liquid air. The initial pumping was continued for several hours, during which time the cathode material was activated. The presence of waxed joints prevented degassing, and the system was considered clean when the electron current between the elements showed no luminosity and when the characteristics of the tube remained constant. Helium was admitted by the conventional arrangement of bulb and stopcocks, having been allowed to stand in two liquid-air traps for a half-hour before admission to the ball. Examination of the discharge by means of a direct vision spectroscope showed no trace of impurity such as mercury or hydrogen.

The large aperture ($f:1.4$) double prism monochromator was designed by Dr. Joseph Razek and was constructed in this laboratory with funds provided by the Faculty Research Committee of the University of Pennsylvania. The entrance slit of this monochromator was placed as close as possible to the slit in the discharge tube, leaving just enough room for the sliding shutter S_1 (Fig. 3). The spectrum is formed on the exit slit I, which may be moved laterally to admit any desired line to the photocell which, with its amplifier, is attached to the monochromator. The photoelectric current is amplified, and the amplified current is indicated by a galvanometer. A 6–8 volt headlight lamp provided a standard of intensity; its brightness was kept constant by the Richardson's bridge arrangement indicated in Fig. 3 and described in detail by Razek.[8] A piece of plate glass P

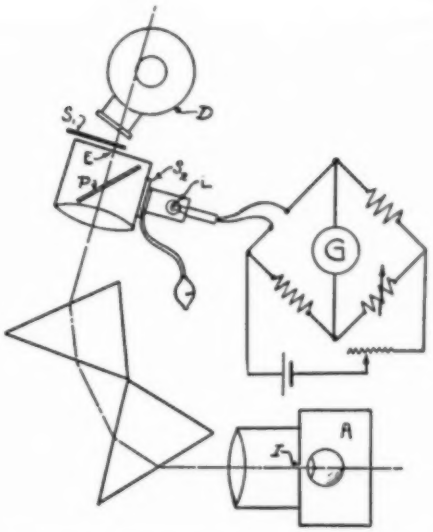

Fig. 3. Optical arrangement for comparison of helium line intensities with standard source.

reflected a portion of the light into the system so that the lamp was virtually in the same position with respect to the collimator lens as the entrance slit E. Opening the shutter S_2 resulted in the formation of an image at I of the filament of the same color as the line whose intensity was being measured.

The experimental procedure was simply to open shutter S_1 and to note the galvanometer current in the photo-cell amplifier, then having closed S_1, to open S_2 and to make a similar reading for the standard intensity. The relative intensity plotted in the results is the ratio between these two galvanometer currents. Such intensity determinations were made (1) for constant voltage and varying arc current and (2) for constant arc current and varying accelerating voltage. The constant voltage determinations were made to test the assumption that the arc current was a reliable measure of the number of collisions occurring in the field-free space and to test the reliability of the photometry. The constant current determinations gave the optical excitation functions of the lines under the conditions of the experiment.

Previous workers have controlled the arc current by varying the temperature of the cathode, but in this work the distribution of the potentials on the grids was used as the controlling agent. This method was deemed ad-

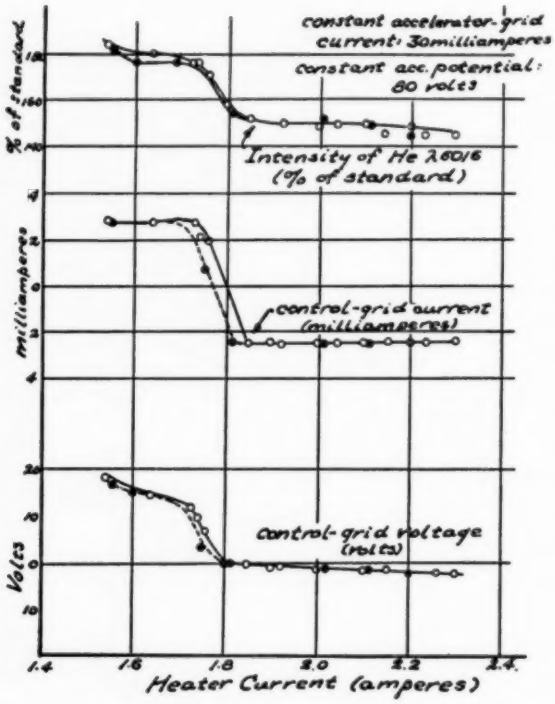

FIG. 4. Behavior of helium discharge tube with changing cathode temperature.

visable since it seemed that the form of the discharge changed with cathode temperature; "hot-spots" formed on the cathode as the result of operating at low temperatures and high accelerating voltages. Improved technique in the matter of applying and forming the cathodes resulted in such active coatings that above certain accelerating voltages the arc became self-sustaining and continued to operate with the cathode cold. This tendency to become self-sustaining began to show itself in most cases when the accelerating voltage was in the neighborhood of sixty volts.

Introduction of the control grid made it necessary to conduct a series of experiments to show that the intensity was not a function of the distribution of the potentials on the grids, but depended solely upon the current to the accelerator grid. Although the temperature of the cathode was varied it was possible to keep the current and voltage between G_1 and G_2 constant by changing the control voltage between G_1 and C. Having decided upon a constant current and voltage, the heater current was varied so as to change the initial supply of electrons; the intensity of a line was measured as a function of cathode temperature. The results are shown in Fig. 4. The curves show that as long as the cathode was kept at a moderately high temperature, the intensity remained constant, regardless of the control grid voltage or the initial supply of electrons, but an increase in intensity was noted when the cathode temperature decreased to the point where a self-sustaining arc began as evidenced by instability in the arc current. In the subsequent work, the cathode was always heated to a temperature well above that at which instability became evident.

By making the control grid positive, the

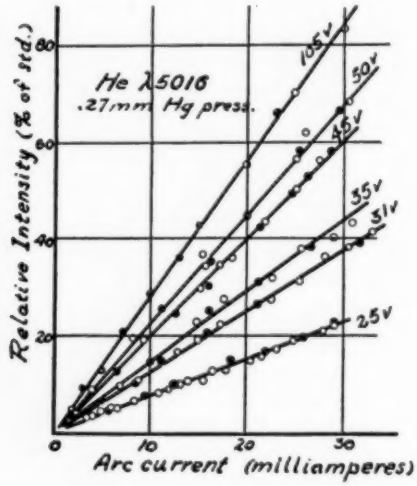

FIG. 5. Current intensity relations in the low voltage helium discharge.

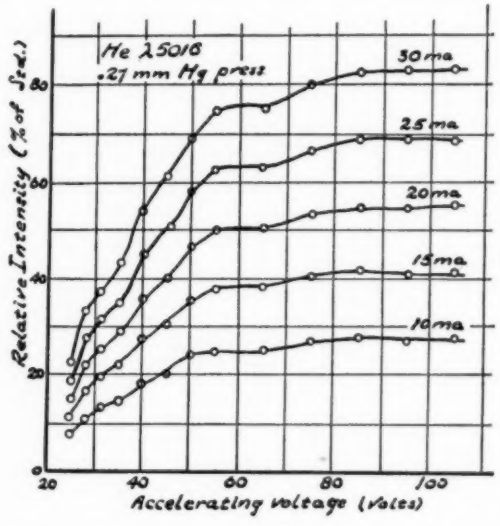

FIG. 6. Family of voltage intensity relations derived from current intensity curves.

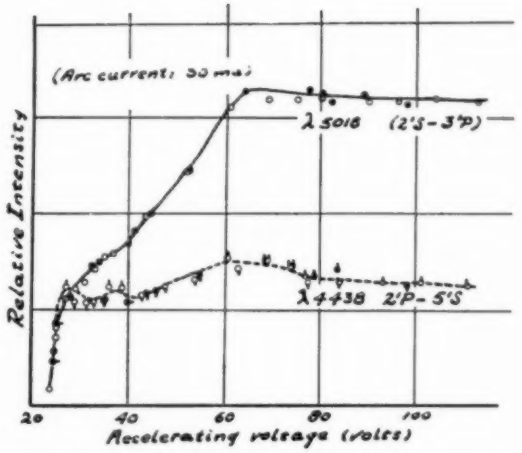

FIG. 7. Voltage-intensity relations in the low voltage helium discharge: lines 5016 (2^1S-3^1P) and 4438 (2^1P-5^1S).

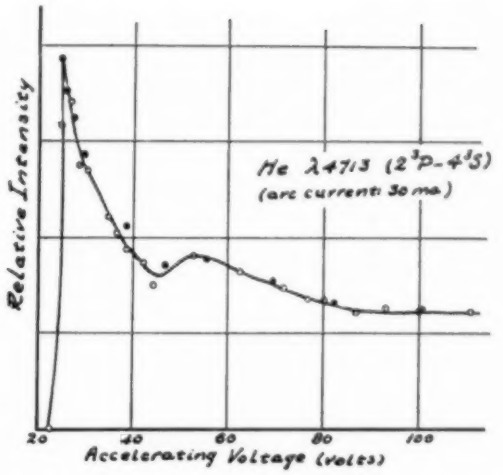

FIG. 8. Voltage intensity relations in the low voltage helium discharge: line 4713 (2^3P-4^3S).

electrons arrived in the field-free space with the energy corresponding to the sum of the potential drops between the two grids, and the full spectrum always appeared when these two voltages added to 24.5, the ionization potential of helium. Characteristic curves were plotted in which the "breaks" were found to occur very close to the ionization potential, regardless of the distribution of the potentials on the grids. These experiments were considered as indicating that the voltages read on the meters were the voltages applied to the electrodes and that the introduction of the control grid gave rise to no significant complication. The drop across the milliammeters was read by the voltmeters, but this was less than the least count of the meters and could be neglected. The absence of contact potentials of notable magnitude was indicated by the agreement between the accepted value of the first ionization potential and the voltage at which the full spectrum appeared. The absence of voltages due to oscillations was ascertained by checking the readings of the voltmeters against a vacuum tube voltmeter; the check was within the precision of the instruments.

RESULTS

The linear relation between current and intensity is demonstrated by the curves in Fig. 5; the open circles represent data taken with increasing current and the solid circles with decreasing current. This linearity shows, as has

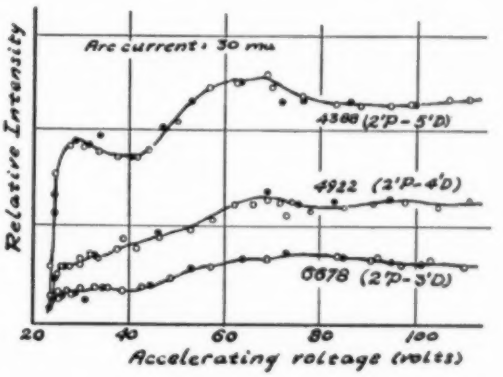

FIG. 9. Voltage intensity relations in the low voltage helium discharge: lines 4922 (2^1P-4^1D), 4388 (2^1P-5^1D), 6678 (2^1P-3^1D).

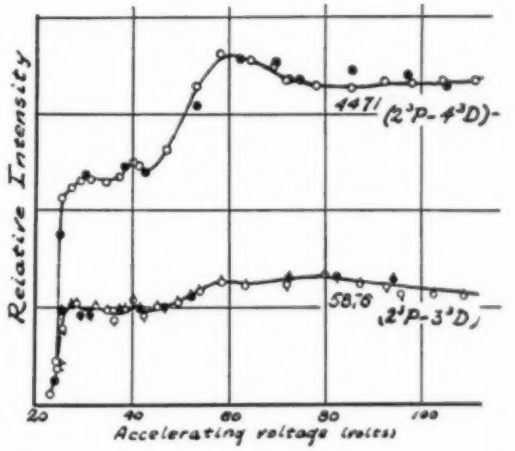

FIG. 10. Voltage intensity relations in the low voltage helium discharge: lines 4471 (2^3P-4^3D) and 5876 (2^3P-3^3D).

been mentioned, that the current to the accelerator grid is a measure of the number of electron collisions and that the photometry is reliable. By making the measurements at a number of voltages, the fact that the linear relation holds for all voltages between the ionization potential and 100 volts is demonstrated. A family of curves such as is shown in part in Fig. 5 may be used to plot a similar family of voltage intensity curves by simply using the ordinates corresponding to the constant current value of the excitation function. The curves shown in Fig. 6 were drawn from the data supplied by the curves in Fig. 5.

Although the linearity is demonstrated to well within the limits of precision of the measurements, the greatest deviations occur in the vicinity of 55 volts, where peak intensities of considerable magnitude have been reported by Cornog.[12] The curves indicate good linearity up to current values of thirty milliamperes, beyond which a slight tendency to saturation is noticed, as might be expected; this would indicate that currents as great as 30 ma may be used without changing the character of the excitation function.

The excitation functions (Figs. 7–10) check the work of Razek as far as 60 volts; where Razek's curves show an increase in intensity, the present results show either a decrease or a flattening. The increase in Razek's functions is probably related to the effect noted above, *viz.*, that at low cathode temperatures the arc tends to change its character; as a result of this change the intensity increases. The collisions which produce the light whose intensity is being measured are presumably in the positive column of the discharge, and should be caused solely by electron-atom encounters, but when the arc tends to become self-sustaining, other light producing mechanisms are involved, as is evidenced by the so-called "negative glow" in the cold discharge. In the present arrangement, in which a dense cloud of electrons is maintained around the cathode, the positive ion bombardment of the cathode is minimized, consequently the negative glow should not be observed. The unusually long life of the cathodes in the two-grid electron source as compared to the one-grid type also indicates that destructive positive ion bombardment has been considerably reduced. The "hysteresis" effect observed by Razek has also been eliminated; this is indicated in the curves, where the solid circles represent intensities measured during a run of decreasing voltages, while the open ones represent increasing voltages. It was in the hope of eliminating this hysteresis effect that the two-grid electron gun was developed, since it would then be possible to carry the tube through a voltage cycle without changing the cathode temperature and consequently without disturbing the condition of the cathode surface. That the cathode surface has something to do with the character of the discharge is evidenced by the fact that there was no hysteresis as long as the cathode was unchanged during a measurement.

The action of the control-grid may be visualized by reference to the curves in Fig. 4. In this experiment the grid was used to keep the supply of electrons in the accelerating field constant; it will be noticed that the current to this grid is constant and that the grid serves to regulate the concentration-gradient between itself and the cathode so as to keep constant the electron density in the acceleration space.

The voltage intensity curves are in good agreement with those of Elenbaas which show maxima in the vicinity of sixty volts as well as a dip around forty volts. This sixty volt maximum was attributed by Lees[7] to a change in the shape of the beam, and the inability of Elenbaas' apparatus to integrate the intensity. The present apparatus is not open to this objection since the silvered sphere does accomplish the integration, so that the sixty volt maximum seems to be real. Some significance may attach to the fact that Elenbaas' apparatus is in general similar to that used in the present work; the cylindrical anode with a slit for observation constitutes a kind of "hohlraum" as does the sphere in the present work, and the entire current to the anode is also measured by Elenbaas. Although the results given here are only in general agreement with the results of the other workers,[4, 5, 7] it will be noticed that a tendency toward an inflection at forty volts is exhibited by the data; the curves are drawn smoothly however, since the precision of the photographic method is not great enough to warrant attaching significance to the indicated irregularities. There

[12] Cornog, Phys. Rev. **32**, 746 (1928).

is also in the present results a marked indication of secondary maxima between the ionization potential and about 45 volts; this is most noticeable in the lines 4471 (2^3P-4^3D) and 5876 (2^3P-3^3D) (Fig. 10). A somewhat similar effect has been reported for mercury by Siebertz;[13] there is a possibility, however, that this effect in mercury is of a different order of magnitude from the effect reported here.

The sudden changes which occur in the neighborhood of the ionization potential make it rather difficult to set the currents and voltages simultaneously, consequently no attempt was made to set the current at the indicated constant value, but intensities corresponding to the indicated value could be calculated on the basis of the experimentally proved linear relation between current and intensity. Beyond about 35 volts these corrections amounted to less than the precision of the measurements.

Conclusions

From these results it may be concluded that the discharge tube used by Razek, modified so as to control the supply of electrons without changing the cathode temperature, gives excitation functions which check with those determined by other workers who used the photographic method. The hypothesis that the "hysteresis" effect noticed by Razek is associated with changes in the condition of the cathode surface is substantiated, since keeping the cathode at a constant temperature and protecting it from positive ion bombardment eliminated the effect.

The linear relation between current and intensity shows that pressures as high as those used do not lead to complications in the large, high intensity source used in this work.

In addition to checking the form of the excitation functions determined by Elenbaas, the present work indicates secondary maxima in the region between the ionization potential and forty-five volts.

The writer wishes to express his thanks to Professor C. B. Bazzoni, under whose guidance the work reported here was done; to Mr. F. R. Banks, who assisted in taking the readings, and to Dr. Joseph Razek for valuable aid and suggestions.

[13] Siebertz, Physik. Zeits. **31**, 141 (1930).

JUNE 15, 1938 PHYSICAL REVIEW VOLUME 53

The Infra-Red Absorption by $C^{13}O_2^{16}$ at 4.375 μ

Alvin H. Nielsen*
Mendenhall Laboratory of Physics, Ohio State University, Columbus, Ohio
(Received April 22, 1938)

The fundamental vibration-rotation band ν_3 of $C^{13}O_2^{16}$ has been found with its center at a wave-length of 4.375μ or 2284.5 cm^{-1}. The individual lines in the band have been fitted by the formula $\nu_3 = 2284.5 + 0.780\,N - 0.0027\,N^2$ where N takes the values -2, -4, -6, $\cdots$, etc. for the P branch and $+1$, $+3$, $+5$, $+\cdots$, etc. for the R branch. On applying the appropriate mass correction to ν_3 and to the anharmonic constant x_{33} given by Adel and Dennison, these constants take values of 2295.8 cm^{-1} and -11.4 cm^{-1}, respectively. Together these constants give the position of the center of the band as 2284.4 cm^{-1}, which is virtually in perfect agreement with observation.

I. Introduction

MEASUREMENTS in the infra-red region near 4.37μ in the atmosphere made by earlier investigators in this laboratory have shown the existence of a weak absorption maximum with resolvable rotation lines on the low frequency side of the very intense fundamental vibration ν_3 of the CO_2 molecule. Since part of this absorption region overlaps with the P branch in ν_3 of CO_2 and the lines appear to

* Assistant Professor of Physics, University of Tennessee, Knoxville.

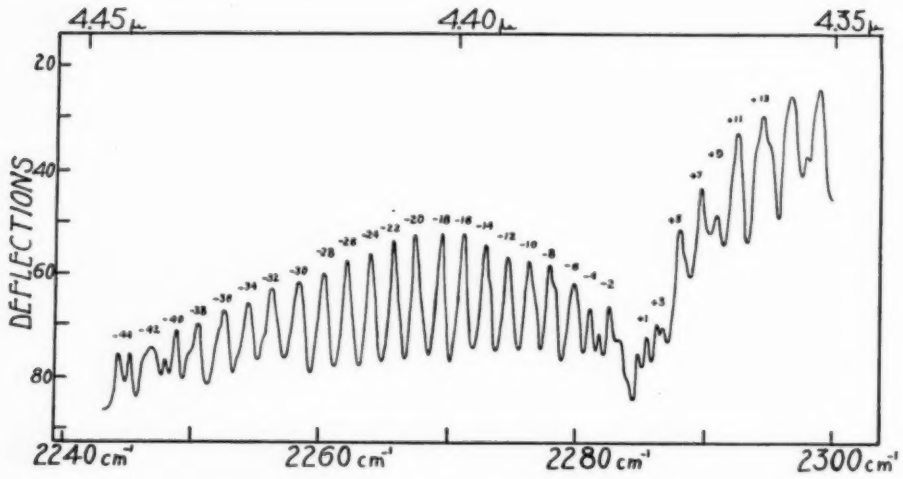

FIG. 1. The fundamental vibration-rotation band ν_3 of $C^{13}O_2^{16}$.

have the same frequency separation[1] it seemed plausible that it might be attributed to an upper stage transition in the energy of the CO_2 molecule. The existence of this band was therefore considered sufficiently interesting to warrant a thorough study of this region.

II. EXPERIMENTAL

The region of the infra-red near 4.37μ has been very carefully mapped with the aid of a prism-grating spectrometer equipped with an echelette grating of 3600 lines per inch ruled for this region by R. W. Wood, and described in previous reports from this laboratory. The slits were narrowed down to include a spectral interval of about 0.4 cm^{-1}, and deflections of the galvanometer were read at intervals of 0.35 cm^{-1}. Fig. 1 shows the P branch, the center, and a few lines in the R branch of the band. The number of lines in the R branch is limited because of overlapping with the P branch of the CO_2 fundamental ν_3. It may be seen that these lines are all resolved very well and the intensities in the P branch follow the usual regular envelope for such bands. The lines are numbered from the center outward. Every other line is missing because of the zero spin of the oxygen nucleus.

[1] P. Martin and E. F. Barker, Phys. Rev. **41**, 291 (1932); Donald Cameron and Harald H. Nielsen, Phys. Rev. **53**, 246 (1938).

III. DISCUSSION

It was possible to write a formula which would predict the frequencies of the lines in this band almost perfectly. Table I gives a list of the lines with the appropriate ordinal numbers, the observed positions in cm^{-1}, and the calculated positions in cm^{-1} as obtained from the formula

$$\nu_3 = 2284.5 + 0.780N - 0.0027N^2;$$

in which N takes the values of -2, -4, -6, -8, $-\cdots$, etc. for the P branch and $+1$, $+3$, $+5$, $+9$, $+\cdots$, etc. for the R branch. It may be seen from Table I that in only one case in the P branch is the disagreement between the observed position and calculated position more than 0.2 cm^{-1}. It may also be seen from Table I that the separation of the lines measured in cm^{-1} is the same as that in ν_3 for CO_2 which makes it almost certain that the band belongs to the CO_2 band system. Although the population of the upper energy levels is small, it was first thought possible that the band was the result of an energy transition from $V_3=2$ to $V_3=3$. The center of this band may be predicted by the use of the constants $\nu_3=2362.8$ cm^{-1} and $x_{33}=-12.7$ cm^{-1} derived by Adel and Dennison[2] and lies at 2299.2 cm^{-1}. Since the observed center of the band is at 2284.5 cm^{-1} the differ-

[2] A. Adel, and D. M. Dennison, Phys. Rev. **43**, 716 (1933) and Phys. Rev. **44**, 99 (1933).

ence between the observed position and this calculated position is 14.7 cm^{-1}.

It was felt that both the measurements and the theory were much more exact than this discrepancy indicates in view of the beautiful positional agreement of all the CO_2 bands following the theory of Adel and Dennison. Because of this belief the identification of the band as an upper stage transition was abandoned in favor of its assignment as ν_3 of the isotopic molecule $C^{13}O_2^{16}$. Following this assumption the individual terms in the expressions for ν_3 and x_{33} in Adel's and Dennison's paper were investigated for their dependence on the reduced mass of the molecule. On applying the appropriate mass correction for the isotopic molecule to the individual terms these expressions become:

$$\nu_3' = \omega_3\left(\frac{\mu}{\mu'}\right)^{\frac{1}{2}} + \frac{3}{2}f\frac{\mu}{\mu'} + \frac{h}{2}\left(\frac{\mu}{\mu'}\right)^{\frac{1}{2}} + i\frac{\mu}{\mu'}$$

$$-\frac{c}{4\omega_1}\left(\frac{\mu}{\mu'}\right)^{\frac{1}{2}}\left[c\left(\frac{\mu}{\mu'}\right)^{\frac{1}{2}} + 6a + 4b\left(\frac{\mu}{\mu'}\right)^{\frac{1}{2}}\right]$$

$$-\frac{3c^2(\mu/\mu')}{8[\omega_1 + 2\omega_3(\mu/\mu')^{\frac{1}{2}}]} + \frac{c^2(\mu/\mu')}{8[\omega_1 - 2\omega_3(\mu/\mu')^{\frac{1}{2}}]} + \frac{h\omega_3}{8\pi^2\omega_2 I};$$

and

$$x_{33}' = \frac{3}{2}f\frac{\mu}{\mu'} - \frac{c^2}{2\omega_1}\frac{\mu}{\mu'} - \frac{c^2}{4}\frac{\mu}{\mu'}\left[\frac{\omega_1}{\omega_1^2 - 4\omega_3^2(\mu/\mu')}\right];$$

where μ and μ' are the reduced masses with $C=12$, and $C=13$, respectively. Substitution of Adel's and Dennison's constants $\omega_1, \omega_2, \omega_3, a, b, c, \cdots$ etc. in the above expressions gives ν_3' and x_{33}' the values 2295.8 cm^{-1} and -11.4 cm^{-1}. These together give the position of the band as 2284.4 cm^{-1} and since the observed position is 2284.5 cm^{-1} the agreement is perfect. The evidence is considered conclusive enough to permit identification of this band as the frequency ν_3 of the molecule $C^{13}O_2^{16}$. Since carbon is the central atom in CO_2, replacement by a heavier atom should not alter the moment of inertia, and this is verified by the fact that the observed spacing is the same as in the corresponding band for $C^{12}O_2^{16}$.

TABLE I. *Frequency positions of the lines in* ν_3 *of* $C^{13}O_2^{16}$.

N	Observed ν	Calculated ν	$\Delta\nu$
−44	2245.1 cm^{-1}	2244.9 cm^{-1}	+0.2 cm^{-1}
−42	2247.1	2246.9	+0.2
−40	2249.0	2248.9	+0.1
−38	2250.8	2250.9	−0.1
−36	2252.8	2252.9	−0.1
−34	2254.8	2254.8	0.0
−32	2256.6	2256.7	−0.1
−30	2258.6	2258.6	0.0
−28	2260.6	2260.5	+0.1
−26	2262.4	2262.4	0.0
−24	2264.2	2264.2	0.0
−22	2266.0	2266.0	0.0
−20	2267.8	2267.1	+0.7
−18	2269.7	2269.5	+0.2
−16	2271.5	2271.3	+0.2
−14	2273.2	2273.0	+0.2
−12	2274.9	2274.7	+0.2
−10	2276.5	2276.4	+0.1
− 8	2278.2	2278.1	+0.1
− 6	2279.7	2279.7	0.0
− 4	2281.3	2281.3	0.0
− 2	2282.7	2282.9	−0.2
0	2284.5	2284.5	
+ 1	2285.5	2285.2	+0.3
+ 3	2286.5	2286.8	−0.3
+ 5	2288.1	2288.3	−0.2
+ 7	2289.5	2289.8	−0.3
+ 9	2290.9	2291.3	−0.4
+11	2292.4	2292.7	−0.3
+13	2294.1	2294.2	−0.1

In conclusion the author expresses his gratitude to Professor David M. Dennison of the University of Michigan who very kindly considered this problem and suggested the identity of the band reported here. The author also acknowledges his indebtedness to Professor Alpheus W. Smith, and to Professor Harald H. Nielsen who suggested the problem and without whose cooperation these measurements could not have been made.

The Energy Loss of Positive Electrons in Passing Through Aluminum*

B. R. CURTIS
University of Michigan, Ann Arbor, Michigan

(Received April 23, 1938)

The energy loss of positive electrons between the energies of 0.3 and 1.5 Mev has been determined in a hydrogen-filled cloud chamber for three thicknesses of aluminum. The positive electrons, which were obtained by bombarding iron with deuterons, were passed through aluminum absorbers of 0.0275, 0.053, and 0.114 cm thickness, and the values of the average energy loss were compared with the values predicted by the theoretical formula of Bloch. The value of the average energy loss for the 0.0275 cm thickness was 0.123 Mev, which is roughly 20 percent greater than the theoretical value; whereas for the 0.053 cm thickness, the loss was 0.274 Mev, an increase in difference to 40 percent. A direct comparison of the energy lost by the negative electron with that lost by the positive electron was made using electrons obtained from radioactive phosphorus. The results show that there is no essential difference in the amount of energy lost by the two particles.

INTRODUCTION

WHEN iron is bombarded with deuterons[1] a radioactive isotope attributed to cobalt is formed. This emits positive electrons of energies up to 1.6 Mev. The problem in this study is to determine the amount of energy lost by these particles in passing through various thicknesses of aluminum. At the same time a direct comparison is made with negative electrons to ascertain whether or not there is any difference in the amount of energy lost by the two particles.

Within the past few years a great deal of work has been done with negative electrons. The experiments show good agreement with theory for substances of low atomic number; whereas for high atomic numbers the experimental values are much higher than theory would predict.[2–4] Absorption measurements with positive electrons of low energy indicate that they lose energy in much the same manner as the negative electrons.[5] In the case of the high energy positrons found in cosmic radiation, the evidence seems to indicate that the amount of energy lost by the positive and negative electrons is the same,[6] although one experiment has seemed to indicate a difference.[7]

APPARATUS

The cloud chamber used in these experiments has been described by Crane.[8] It was 15 cm in diameter and 4 cm deep, filled with hydrogen and ethyl alcohol vapor at a pressure of 100 cm of mercury. The magnetic field was obtained from a pair of air core solenoid coils. In the earlier experimental work, the current through the coils was turned on and off, but in the later experiments, the current was allowed to flow continuously. This removed the possibility of any errors due to the contacts of the circuit breaker or to misreading the swing of the ammeter needle. A collimated beam of parallel light, obtained from a carbon arc, illuminated the center 1.5 cm section of the chamber. A diagram of the experimental arrangement is shown in Fig. 1. By locating the source S at the correct position, it was possible to obtain a partial magnetic separation of the positrons so that particles of only a certain definite energy range entered through the thin window in the wall of the chamber. This prevented the appearance in the pictures of too many extraneous tracks which did not strike the absorber at approximately normal incidence.

The aluminum absorbers were coated with paraffin and lamp black and were placed across the center of the chamber parallel to the light beam. By measuring the radii of curvature of the incident and emergent tracks, the amount of energy lost by the particles in traversing the absorber could be determined.

The method used for determining the curva-

* A preliminary report of this investigation was given at the Chicago meeting of the American Physical Society in November, 1937.

[1] B. T. Darling, B. R. Curtis and J. M. Cork, Phys. Rev. **51**, 1010 (1937).
[2] J. J. Turin and H. R. Crane, Phys. Rev. **52**, 63, 610 (1937).
[3] A. J. Ruhlig and H. R. Crane, Phys. Rev. **53**, 618 (1938).
[4] J. Laslett and D. Hurst, Phys. Rev. **52**, 1035 (1937).
[5] J. Thibaud, Phys. Rev. **45**, 781 (1934).
[6] P. M. S. Blackett and J. G. Wilson, Proc. Roy. Soc. **A160**, 304 (1937).
[7] J. Crussard and L. Leprince-Ringuet, J. de phys. et rad. **8**, 213 (1937).
[8] H. R. Crane, Rev. Sci. Inst. **8**, 440 (1937).

ture of the tracks was to project the full-sized image upon a white card and then to measure the radii of the tracks by means of a celluloid or cardboard template upon which circles of radii varying by 0.5 cm had been drawn. In order to be included in the data actually used, a track was required to satisfy the following conditions:

(1) It must come from the window in the side of the chamber and must strike the absorber at approximately normal incidence (within 10°). Of course this criterion does not exclude the chance that an electron may be ejected from the absorber by a gamma-quantum and come back toward the window.

(2) The track must be of sufficient length to make possible an accurate measurement of its curvature. Since only half of the 15 cm of the chamber is being considered, at least 6 cm of track must be measured.

(3) The track must emerge from the absorber within 15° of the normal and must not make an angle greater than 10° with the plane of the chamber. Any track which satisfies condition (2) will satisfy this condition.

(4) A track must not be visibly scattered. When working with particles of energy as low as

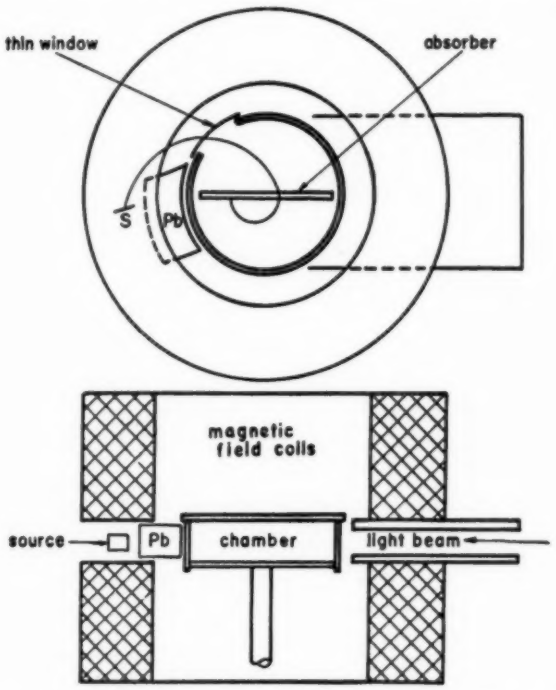

FIG. 1. Experimental arrangement of cloud chamber and electron source.

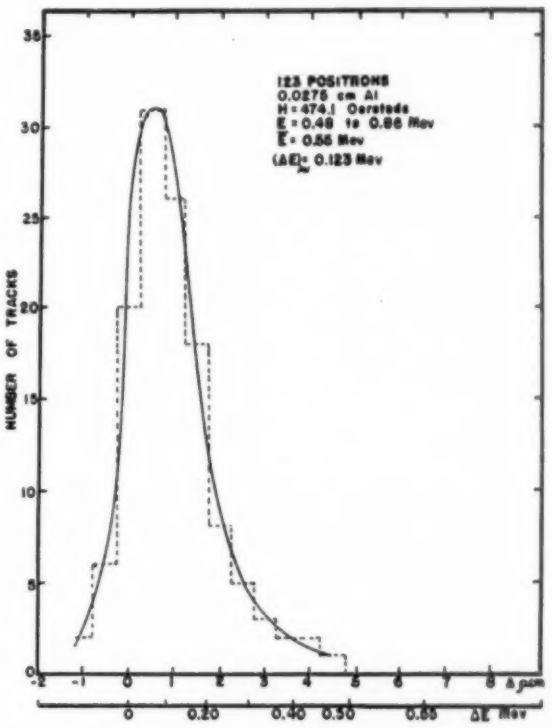

FIG. 2. Energy losses plotted against the number of positive electrons, for 0.0275 cm aluminum and initial energies of 0.48 to 0.86 Mev.

0.5 to 1.0 Mev, it is necessary to fill the chamber with hydrogen in order to keep down scattering to a minimum. The probability for scattering is inversely proportional to the square of the kinetic energy of the particle and directly proportional to the square of the atomic number of the scattering material. Thus if hydrogen is used, the scattering for these energies is very small.

RESULTS

Positive electrons

The principal source of positive electrons was iron bombarded in the cyclotron with deuterons. These electrons have an upper limit in energy of 1.6 Mev and a half-life of 18 hours.

For the 0.0275 cm aluminum, approximately 200 positrons were obtained which satisfied the necessary criteria. In Fig. 2 the momentum loss curve is shown for positrons ranging in initial energy from 0.48 to 0.86 Mev. The curve contains a total of 123 positrons. For convenience, the scale of energy loss is plotted below the $\Delta\rho$ (change in radius of curvature) scale. To obtain

the change in momentum, the latter may be multiplied by the value of the magnetic intensity, H. The following values are recorded in the figure: number of positrons observed, thickness of aluminum used, intensity of the magnetic field, H, interval of initial energies, average value of the initial energies, $\bar{E}$, and the average loss of energy in Mev, $(\Delta E)_{Av.}$.

It will be noted that the curve is roughly symmetrical and fairly sharp. A large number of tracks appear to have passed through the absorber with no change in momentum, and a few appear to have acquired actual gains in momentum. This can be attributed to several factors: (1) Coincident effects. (a) Occasionally a gamma-quantum may eject, from the wall of the cloud chamber, an electron which hits the absorber at a point opposite that at which a positron has entered. If this electron has an energy equal to, or greater than, the initial energy of the positron, it will seem that the positron has actually gained energy. (b) Another positron which is at first out of the light beam may be scattered into view on the far side of the absorber in such a way as to appear to be the emergence of a first particle. (2) Small angle scattering. When working with particles of such low energies as those used in this experiment, scattering is certain to occur. For every large angle scattering which can be easily observed, there is a considerable amount of small angle scattering which cannot be noticed. (3) Errors in measurement.

Of these three factors, the last two are by far the most important. Only one case was observed in the 800 tracks obtained in which a positron appeared to gain so much energy that it was definitely a coincident effect with an electron emitted from the wall. Since it was required that the tracks appear to within 0.5 cm of the absorber on both sides, then from the geometry of the apparatus, it would be impossible for any track to have sufficient path length in the light beam to pass either over or under the absorber. It is still possible, of course, that a particle might be scattered in such a way as to appear to be the continuation of a track which has been stopped by the absorber. Small angle scattering is a factor which is always a great difficulty in this type of experimental work. Its effect is to broaden the general curve.

Undoubtedly the errors in measurement are the chief cause of the large number of tracks which appear to have lost no energy. Since the accuracy of measurement is not high enough to distinguish any loss of energy less than 0.05 Mev, a large number of tracks will be obtained for thin absorbers which seem to have lost no energy.

The number of tracks which have definitely appeared to gain energy is not very large, constituting less than 5 percent of the total number. These cases are probably due to a combination of the two factors, small angle scattering and errors in measurement, although a few of the cases may be due to coincident effects.

The most probable loss of energy may be found by inspection of the curve to be approximately 0.09 Mev. The average energy loss may be found by two different procedures: (1) by determining the energy loss for each particle separately and then averaging; (2) by determining the average $\Delta\bar{\rho}$ and, from the value of $\Delta H\bar{\rho}$ and the initial energy, finding the corresponding $(\Delta E)_{Av.}$.

In order to test these two methods of considering the data, 200 tracks were chosen having energies between 0.50 and 1.00 Mev. The first method gives an average energy loss of 0.128 Mev. It is undoubtedly fortuitous, but the value determined by the second method was again 0.128 Mev.

All of the data were treated by both methods. For energies above 0.5 Mev, the two values were

TABLE I. *Energy loss. (−) indicates a negative electron. An asterisk indicates that tracks have already been included in the data and that the initial energy of all the particles was the same. (?) This low value is attributed to the fact that the initial energies of the particles are so low that large energy losses are discriminated against in measurement.*

Thickness (cm)	Number of Tracks	Initial Energy (Mev)	Most Probable Loss	Average Loss (Mev)	
				Exp.	Theor.
0.0275	123	0.48 to 0.86	0.09	0.123	0.098
	77	0.80 to 1.0	0.10	0.123	0.105
	96(−)	0.48 to 0.86	0.08	0.121	0.098
0.053	209	0.48 to 0.86	0.19	0.266	0.205
	101	0.30 to 0.55	0.21	0.230?	0.214
	52*	0.60		0.270	0.204
	73*	0.74		0.278	0.204
	161	0.67 to 0.93	0.21	0.265	0.205
	114	0.90 to 1.40	0.22	0.285	0.206
0.114	30	0.8 to 1.40		0.480	0.434

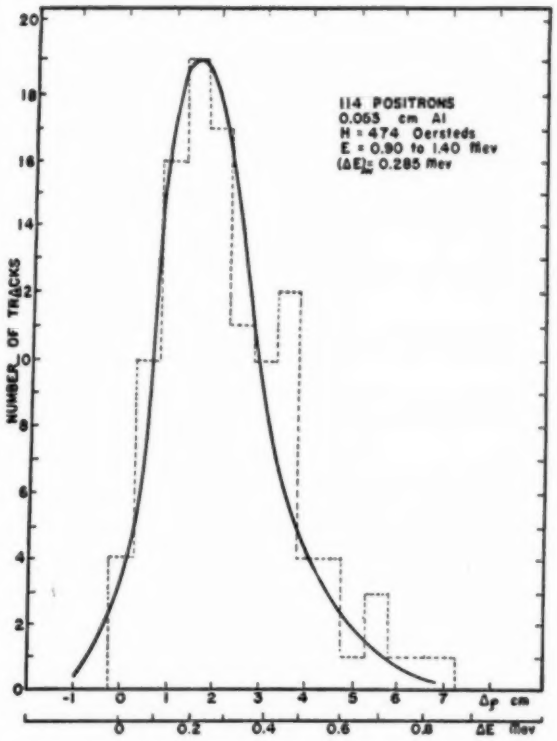

FIG. 3. Energy losses plotted against the number of positive electrons, for 0.053 cm aluminum and initial energies of 0.90 to 1.40 Mev.

usually the same; when any difference occurred the value obtained from the loss of energy of the individual particles was considered to be the final result. Method (1) was found to be advantageous, for there is no necessity in this case for determining the average initial energy of the particles.

The apparent gains in momentum are attributed to instrumental error. They should therefore be regarded as the accuracy of the measurement, and a corresponding error allowed for the values of the large energy losses. If the data are regarded in this way, then the average energy loss for the 0.0275 cm thickness of aluminum is 0.123 Mev. (See Fig. 2.)

The 0.053 cm aluminum was used in obtaining the greater part of the data because it proved to be sufficiently thick to prevent cases of apparent gain in energy without being thick enough to stop an excessive number of particles.

The particles have been grouped into intervals of initial energy, which are kept as small as possible and yet have a sufficient number of tracks so that statistical variations are not too important. Some of the groups overlap slightly, but they have been kept as nearly as possible within 0.2 Mev intervals from 0.3 to 1.5 Mev. These are tabulated in Table I.

The general shape of the curve (see Fig. 3) obtained from this thickness of aluminum illustrates two points: first, that the curve is not quite so symmetrical as those for lesser thicknesses but extends farther to the right; and second, that the width of the curve is in general greater. Theoretically, the half-width of the curve is dependent upon the thickness of the material traversed and the incident energy of the particle considered. Since this thickness is double that first used, the width of the curve will be more pronounced, due to the increased scattering.

The unsymmetrical character of the curve may be attributed to several processes which cannot be distinguished from one another: (1) scattering, which tends to increase the straggling in the energy loss values since the particle actually traverses a greater thickness of material; (2) electron collisions, in which a large fraction of the initial energy has been lost; (3) radiative collisions. The last two of these have very little effect, for the probability of radiative collisions is very small at the energies considered in this work, and electron collisions in which a particle suffers a head-on impact are relatively rare, making the contribution from this process small.

In Fig. 3 the distribution for 114 positrons is shown for particles whose initial energy ranges from 0.90 to 1.40 Mev. The most probable energy loss occurs at an energy of approximately 0.20 Mev. The average energy loss is equal to 0.28 Mev. This illustrates the nature of the curves obtained when sufficient numbers of particles are used so that statistical variations are not large. The other curves for this thickness are similar in nature, the results of which appear in Table I.

The amount of data obtained for the 0.114 cm aluminum is too meager to make any very accurate estimate of the energy loss, but from the results available, the most probable energy loss has been found to be approximately 0.35 Mev, and the average energy loss, 0.48 Mev.

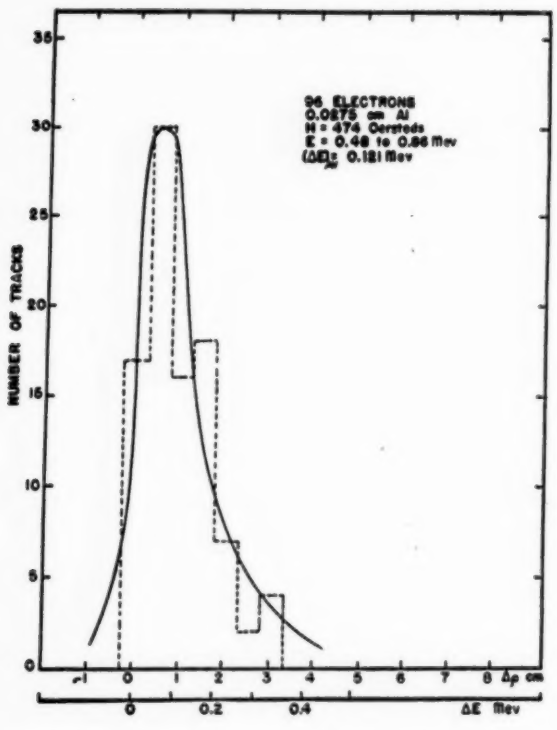

FIG. 4. Energy losses plotted against the number of negative electrons, for 0.0275 cm aluminum and initial energies of 0.48 to 0.86 Mev.

Negative electrons

To compare the energy loss of positrons directly with the energy loss of electrons, radioactive phosphorus was used as a source of particles. The upper limit of the energy obtainable is 1.5 Mev as compared with the limit of 1.6 Mev for the cobalt (55) positrons, so that a direct comparison is possible without changing the experimental arrangement. There was a sufficient number of tracks obtained to show that there is no essential difference between the energy lost by the positive electrons and that lost by the negative electrons. The results procured from 96 particles are shown in Fig. 4. The value of the energy loss is 0.121 Mev, in good agreement with the energy loss of the positrons. It can be definitely stated that, within the accuracy of these experiments, the energy lost by the positive electron is the same as that lost by the negative electron, at least for the energies of the particles considered here.

DISCUSSION

The theoretical values of the average energy loss have been calculated from Bloch's formula.[9] The energy used in this formula has been taken as the energy which the particle possessed at the center of the absorber. These values are compared with the experimental ones in Table I.

Theoretically, there is no difference between the phenomena of energy loss of the positive and the negative electron, except for the fact that the positive electron may be annihilated somewhere along its path and thus decrease its effective range. It can be seen from the values given in Table I that the average energy loss determined by the experiment is about 20 percent higher than the theoretical value for the 0.0275 cm aluminum and that this difference increases to nearly 40 percent when the thickness of the absorber is doubled (0.053 cm aluminum). This fact is interesting, for it would seem to indicate that the discrepancy is increasing with the thickness, and that some process must be taking place which causes this. One explanation might be multiple scattering within the absorber, which would tend to make the actual path traversed by the particle greater than the actual thickness of the absorber. Whether this is the case or not cannot be determined until further data are obtained.

It must be remembered that none of the tracks which are stopped by the absorber are included in the calculation of the average energy loss. These are excluded on the assumption that the particles have been scattered out of the light beam as well as stopped by the absorber. If these tracks were included in the calculation, the value of the energy loss would be much greater.

From the results of this investigation, it may be stated that the experimental value of the energy loss of the positive electron in passing through aluminum seems to be greater than the theoretical formula of Bloch would predict. The direct comparison with the negative electron shows that there is no difference between the amounts of energy lost by the two particles. This is in agreement with the conclusions of Anderson,

[9] Heitler, *The Quantum Theory of Radiation* (Oxford Press, 1936), p. 218.

Blackett and J. G. Wilson, and Ruhlig and Crane, but is in disagreement with the results of Crussard and Leprince-Ringuet for cosmic-ray electrons.

The author wishes to express his sincere gratitude to Professor J. M. Cork and Dr. R. L. Thornton for the privilege of working under their guidance with the University of Michigan cyclotron, and for many helpful suggestions which have facilitated the progress of this work. He is deeply indebted to Dr. H. R. Crane for the original discussion which led to the undertaking of this particular problem and for his constant encouragement. The financial support which made possible the carrying out of this investigation came through the courtesy of the Horace H. Rackham Endowment Fund, which the author gratefully acknowledges.

JUNE 15, 1938 PHYSICAL REVIEW VOLUME 53

Calculations on a New Neutron-Proton Interaction Potential

R. G. SACHS AND M. GOEPPERT-MAYER
Johns Hopkins University, Baltimore, Maryland

(Received April 16, 1938)

On the basis of a neutron-proton interaction potential of the form $Ce^{-r/\alpha}/r$ numerical calculations for the deuteron and for the scattering of neutrons by protons have been made.

INTRODUCTION

THERE has recently been suggested,[1] on theoretical grounds, a new neutron-proton interaction potential of the form $J(r) = -(C/r)\exp(-r/\alpha)$, where $\alpha = \hbar/M_0 c$, M_0 being the mass of the heavy electron. Of the two unknown constants, α determines the range, $A = C\cdot\alpha$ the strength of the interaction. If this potential is to give the correct energy[2] for the ground state of the deuteron ($E_0 = 2.17$ Mev) a relation between A and α must be fulfilled. For other two-constant potentials, namely the spherical well, inverse fifth power, exponential, and Gaussian type interaction, the dependence of the magnitude of the forces on the range of the forces and the neutron-proton scattering cross sections have previously been calculated.[3] In this paper the same calculations are made for the new potential.

[1] H. Yukawa, Proc. Phys-Math Soc. Japan **17**, 48 (1935); **19**, 1084 (1937). N. Kemmer, Nature **141**, 116 (1938). H. J. Bhabha, Nature **141**, 117 (1938).
[2] H. A. Bethe, Phys. Rev. **53**, 313 (1938).
[3] H. S. W. Massey and R. A. Buckingham, Proc. Roy. Soc. **163**, 281 (1937). Morse, Fisk and Schiff, Phys. Rev. **50**, 748 (1936); **51**, 706 (1937).

1. THE GROUND STATE OF THE DEUTERON

The differential equation for the eigenfunction, ψ_0, of the ground state of the deuteron is[4]

$$\frac{\hbar^2}{M}\frac{d^2u_0}{dr^2} + (-E_0)u_0 = -A\frac{e^{-r/\alpha}}{r/\alpha}u_0; \quad u_0 = r\psi_0,$$

where E_0 is taken positive.

The transformation $r = \alpha x$ yields

$$u'' + a(e^{-x}/x - \epsilon_0)u = 0, \tag{1}$$

where $$a = A\alpha^2 M/\hbar^2, \quad \epsilon_0 = E_0/A; \tag{2}$$

$u(x) = u_0(r)$, and primes indicate differentiation with respect to x. The problem is now to determine, for given values of a, the constant ϵ_0 which yields a wave function u satisfying the boundary condition.

In the range between $x = 0$ and $x = \frac{1}{2}$ (the value $\frac{1}{2}$ is chosen for convenience) the integration of (1) is made by using the first six terms of a power series development of $u(x)$. The boundary condition that u be zero (ψ_0 be finite) at $x = 0$ is

[4] H. A. Bethe and R. F. Bacher, Rev. Mod. Phys. **8**, 82 (1936).

TABLE I. *Values of ϵ_0, α and A for various values of a. Values in parentheses are extrapolated.*

a	1.683	2.00	2.30	2.50	2.70	(2.78)
ϵ_0	0	0.010	0.032	0.050	0.073	(0.108)
α ($\times 10^{13}$)		0.62	1.18	1.54	1.93	(2.39)
A (Mev)		217	67.8	43.4	29.7	(20)

then automatically satisfied. For the range beyond $x=\frac{1}{2}$ Eq. (1) may be put in the form

$$p'+p^2+a(e^{-x}/x-\epsilon_0)=0, \quad \text{where} \quad p=u'/u. \quad (3)$$

This equation was integrated numerically from large distances in to $x=\frac{1}{2}$ by the method of Runge-Kutta.[5] The value of p for large x must approach $-(a\epsilon_0)^{\frac{1}{2}}$ in order that the wave function decrease exponentially at large distances. This was used as the boundary condition at $x=7.5$, where e^{-x}/x is 10^{-4} and can be neglected. Values of ϵ_0 were tried for a given value of a, until a value was found that would make the numerical solution join smoothly with the power series solution at $x=\frac{1}{2}$. The values of ϵ_0 for given values of a are listed in Table I. By using the known energy[2] of the ground state of the deuteron, $E_0=2.17$ Mev, the corresponding values of A and α have been calculated and are also listed in Table I. The values in parentheses are interpolated or extrapolated.

The equation for the singlet state is: $u''+a(e^{-x}/x)u=0$. This is obtained from (1) by setting $\epsilon_0=0$ since the binding energy for the singlet state is approximately zero. Eq. (3) is replaced by:

$$p'+p^2+a(e^{-x}/x)=0.$$

Different values of a were tried until one was found that made the two solutions join smoothly at $x=\frac{1}{2}$. This value of a gives a fixed relation between α and A for the singlet state. Its value is $a=1.683$.

2. SCATTERING

In order to calculate the scattering for neutrons on protons, the wave equation is written for positive energy:

$$u''+a(e^{-x}/x)+\epsilon)u=0; \quad a=A\alpha^2M/\hbar^2, \quad \epsilon=E/A, \quad (4)$$

[5] C. Runge and H. König, *Numerisches Rechnen* (J. Springer, 1924) p. 286.

TABLE II. *Values of δ_0 calculated for the triplet and singlet states.*

E_n (Mev)	$\alpha\times 10^{13}$ (cm)	δ_{0t}	δ_{0s}
2.2	0.62	2.382	1.418
	1.93	2.304	1.243
	(2.39)	(2.277)	—
	(2.24)	(2.286)	—
5.4	2.39	1.877	—
	2.24	1.849	—
13.7	2.39	1.520	—
	2.24	1.525	—
21.5	0.62	1.688	1.248
	1.93	1.487	0.862
	(2.39)	(1.417)	—
	(2.24)	(1.439)	—

E being the energy of the neutrons in a coordinate system fixed with respect to the center of gravity. (If E_n be the energy of the neutrons in a system fixed relative to the protons,[4] $E_n=2E$.) The solution[6, 4] of Eq. (4) for large values of x is asymptotically $u=c\sin[(a\epsilon)^{\frac{1}{2}}x+\delta]$; and the total scattering cross section[4] is $\sigma=4\pi(\hbar^2/ME)\sin^2\delta$.

The phases, δ, were calculated for different values of E_n, by using the same type of series solution as before, out to $x=\frac{1}{2}$, and integrating numerically from there out to $x=6.5$ by the Runge-Kutta[7] method for second-order differential equations. The values of α and A were obtained from Table I for the triplet state; and, for the singlet state, A was calculated for those same values of α from $a=1.683$. Table II gives the results. The subscripts "t" and "s" refer to triplet and singlet scattering, respectively.

Table III gives a comparison of the results with the results of Massey and Buckingham[3] for the exponential and spherical well potentials. By

TABLE III. *Comparison of the present results for the phases δ with the results of Massey and Buckingham for the exponential and spherical well potentials.*

$J(r)$	$\alpha\times 10^{13}$ cm	$E_n=2.2$	5.4	13.7	21.5 Mev
$J=C \quad r<\alpha$	(3.107)	(2.277)	(1.914)	(1.461)	(1.226)
$J=0 \quad r<\alpha$					
$(C/r)e^{-r/a}$	2.39	(2.277)	1.877	1.520	(1.417)
$Ce^{-2r/a}$	2.4	2.277	1.930	1.532	1.330

[6] Mott and Massey, *The Theory of Atomic Collisions* (Oxford, 1933) Ch. II.

[7] See reference 5, p. 311.

interpolation, the values of α for the e^{-x}/x and spherical well potentials were adjusted to give the same phase and therefore scattering cross section as the exponential interaction for 2.2 Mev neutrons. The phases for higher energies were then calculated for these values of α. Only the triplet phases were considered since the effect of the singlet state can be neglected[4] above $E_n=2$ Mev. According to the table the values of the phases for the spherical well and exponential potentials diverge slightly but run almost parallel for different values of E_n. However, the phases for the e^{-x}/x interaction first go below and then cross over to go above the phases of the other two potentials.

The observed[8] cross sections for the scattering of neutrons by protons are considerably smaller than those calculated with the usually accepted range of about 2×10^{-13} cm. Ranges as small as 0.5×10^{-13} cm would give agreement, but the experiments are at present too uncertain to draw conclusions.

[8] J. Chadwick, Proc. Roy. Soc. **A142**, 1 (1933). W. H. Zinn, S. Seely and V. W. Cohen, Bull. Am. Phys. Soc. **13**, 14 (1938). R. Ladenburg and M. H. Kanner, Phys. Rev. **51**, 1022 (1937). E. T. Booth and C. Hurst, Proc. Roy. Soc. **A161**, 248 (1937).

Conclusion

It appears that there is little possibility of distinguishing between this and other potentials even by means of scattering experiments over a large range of neutron energies. With the cross sections for the exponential and e^{-x}/x potentials adjusted to be approximately equal for 21.5 Mev neutrons, the total cross sections differ by only 6 percent for 2.2 Mev neutrons.

The ranges of force considered correspond to heavy electron masses ranging from about $700m_e(\alpha=0.5\times10^{-13}$ cm) to $150m_e(\alpha=2.4\times10^{-13}$ cm). Since it is generally accepted[4] that the range of the interaction in any case cannot be much larger than 2×10^{-13} cm, it appears that a lower limit to the mass of the heavy electron would be about 100 electron masses, on the assumption that this potential is the correct one.

The authors wish to thank Professor E. Teller for the suggestion of the problem and the interest taken in it.

JUNE 15, 1938 PHYSICAL REVIEW VOLUME 53

The Scattering of Fast Electrons in Gases *

J. B. Horner Kuper†
Palmer Physical Laboratory, Princeton University, Princeton, New Jersey
(Received January 27, 1938)

The angular distribution of elastically scattered electrons of energies between 49.5 and 87.7 Kev has been measured in argon, neon, and helium over the range 0.3° to 6°. Comparison of the results with the theoretical curves calculated from the Hartree functions with the "Born approximation" shows good agreement in the case of argon, and in neon except at the smallest angles, but there is no agreement at all in the case of helium. The discrepancies are very similar to those found at the smallest angles in studies of scattering of electrons of a few hundred volts energy, and it is felt that the explanation in terms of polarization of the atomic field by the passing electron may be accepted here also.

SINCE the pioneer work of Lenard[1] carried out more than forty years ago, various problems in connection with the passage of electrons through matter have attracted the attention of physicists down to the present time. The scattering of electrons (elastic and inelastic)

* The work here reported forms part of a dissertation presented to the faculty of Princeton University in candidacy for the degree of Doctor of Philosophy. The complete dissertation is on file in the Princeton University library. A preliminary report was given at the Washington meeting of the American Physical Society, 1937; Kuper, Phys. Rev. **51**, 1024A (1937).

† Now at Washington Biophysical Institute, c/o Industrial Hygiene Division, National Institute of Health, Washington, D. C.

[1] Lenard, Wied. Ann. **51**, 225 (1894); **56**, 255 (1895).

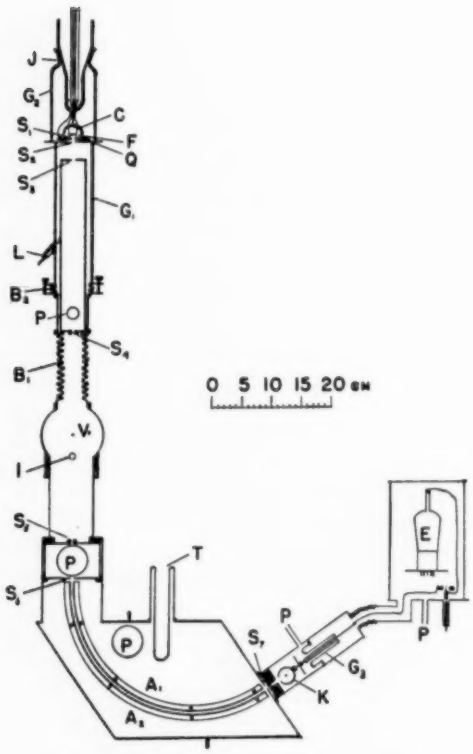

FIG. 1. Sketch of scattering apparatus.

in gases has been studied very thoroughly up to energies of the order of 2000 volts or so, but at higher energies (up to 100 Kev) interest has been concentrated instead on diffraction effects and on scattering in metal foils. While experimental difficulties (mostly attributable to the very small cross sections) prevented the completion of the full program originally planned it was found possible to study the elastic scattering in argon, neon, and helium over a small angular range. Comparison of the experimental results with the theoretical curves calculated with the aid of the "Born approximation" from the Hartree functions reveals agreements and discrepancies that are strikingly similar to those found at very small angles with electrons of a few hundred volts energy. Although various other possible explanations of the discrepancies must receive consideration, it seems likely that the effects are due to polarization of the atomic field by the passing electron[2] as in the low voltage experiments.

The apparatus was similar in general design to that used by S. N. Van Voorhis[3] but built on a larger scale and modified where necessary to permit the application of higher voltages. In this type of apparatus an electron "gun" furnishing a well-collimated beam of electrons of the desired energy is mounted so as to pivot about an axis in the center of a region in which the scattering is to take place. The gas under investigation is admitted to this region and differential pumping is employed. A pair of slits defines the scattered beam selected, which then passes through an electrostatic energy analyzer[4] before reaching the collector.

Electrons from the thin oxide-coated platinum ribbon filament F (see diagram, Fig. 1) are concentrated on the first slit, S_1, by the "reflector" electrode C, which is held about 25 volts negative with respect to the filament. The latter was about 160 volts negative with respect to S_1. The accelerating slit system, S_1 to S_3, was designed to act as an electron lens, producing an approximately parallel beam. All three slits were 0.5 mm wide, the first two being 7 mm long and the third 5 mm. A ring shaped insulator of quartz Q served to maintain a separation of about 3 mm for the first gap, and S_3 was 25 mm below S_2. S_3 and S_4 are mounted on the ends of a brass tube, 292 mm long, which is insulated from the rest of the apparatus. A compromise had to be made in the design of slits S_4 and S_5 in order to obtain sufficient pumping resistance and still have a reasonable beam with which to work. The dimensions finally chosen were: length, 5 mm; width, 0.1 mm; and depth, 5 mm, with the distance between them 343 mm. A pressure ratio of about 1000 could be maintained between the scattering volume and the analyzer. The entire electron gun could be rotated about an axis perpendicular to the plane of the drawing through the center of V. S_6, located 71 mm below S_5, was of the knife-edge type, 12.3 mm long and 0.2 mm wide. The deflecting plates for the energy analyzer A_1 and A_2 are arcs of circles of radii 20.4 and 20.9 cm, respectively, subtending an angle such that the electrons are

[2] Mott and Massey, *The Theory of Atomic Collisions*, (Oxford, 1933). Chap. IX; Chap. X, Sec. 10.

[3] S. N. Van Voorhis, Phys. Rev. **46**, 480 (1934).

[4] Hughes and Rojansky, Phys. Rev. **34**, 284 (1929).

swung through 127° as required for refocusing.[4] The exit slit S_7 was 0.5 mm wide and 12 mm long. Beyond it was another fixed slit 1 mm wide, covered by an aluminium foil 0.01 mm thick which shielded the collector from stray fields. The collector was mounted on a reentrant glass insulator G_3 which was carefully shielded to prevent building up of surface charges.

The electrical connections are indicated schematically in the diagram, Fig. 2. The high voltage was obtained from a Keleket transformer-rectifier outfit provided with an extra filter consisting of two, 50 kv, 0.25 mf Pyranol condensers charged through 0.1 megohm resistors. The divider made of one hundred 0.1 megohm, 50 watt, vitrified wire-wound radio resistors furnished the intermediate potential for the electron lens and potentials for the analyzer. Between 9 and 10 percent of the accelerating voltage was applied between S_1 and S_2. The system of condensers across the portion $n-p$ of the divider and from the midpoint of the high voltage apparatus to ground was necessary to bypass a small alternating current flowing from the main transformer through stray capacity to ground. Residual fluctuations in analyzer voltage limited the resolving power to 1 in 580, in contrast to a resolving power of 1 in 700 expected from the geometry.

The electrometer tube used was a Western Electric D-96475, operated in the modified Barth circuit as described by Penick.[5] Unusual care had to be taken with the shielding on account of the surges from the high voltage, and radiofrequency filters in the galvanometer and battery leads were indispensable. The sensitivity, which remained remarkably constant over a period of months, was 37,600 mm/volt.

Leads to the pumps were connected at the various points marked P, a separate pump being used for the analyzer. The gas under investigation was admitted to the apparatus at I after passing through an adjustable capillary leak and a liquid-air trap. The purity was checked spectroscopically, and on completion of the experiments the helium sample was analyzed with the mass spectrograph by Dr. L. G. Smith, who reported that no heavy impurity was present to as much as 1 part in 7000.

Under the conditions of focus and slit alignment finally chosen more than 90 percent of the electrons were concentrated into a beam less than 0.5° wide, but there was a rather large "wing" present on one side of the main beam.[6] Occasional check tests were made and as no difference in the net scattered currents on the two sides of the beam could be found all readings were taken on the clean side of the beam. Although the currents obtained at scattering angles as small as 0.6° were of the order of 10^{-4} times the direct beam or less the possibility of multiple scattering was carefully checked and excluded. Readings were taken with argon at various pressures, up to a limit considerably in excess of any ever used. Over a range greater than 5 to 1 the scattered current was very accurately proportional to the pressure.

Before taking any readings the apparatus was always thoroughly outgassed by operation at a voltage well above that to be used. The background current was measured over the range of angles to be studied then gas was admitted to the scattering chamber and readings were again taken at the same set of angles. In almost all cases the readings were taken by the rate of drift method (with 1 mm/sec. equal to 7.2×10^{-16} amp.). After the background had been subtracted and allowance made where needed for differences in pressure or filament emission

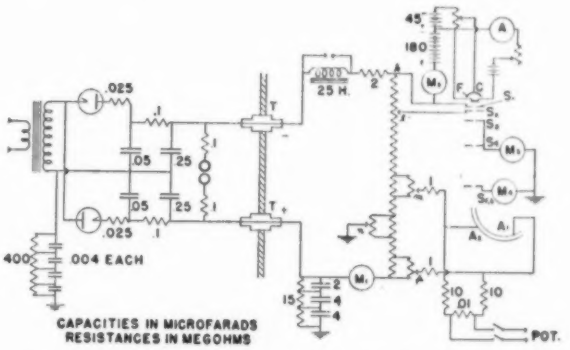

FIG. 2. Schematic diagram of electrical connections.

[5] Penick, Rev. Sci. Inst. **6**, 115 (1935).

[6] It was possible to obtain a beam with the "wings" symmetrically arranged, but as the scattered currents to be measured were exceedingly small it was thought best to use the distorted beam and have a smaller background current to allow for.

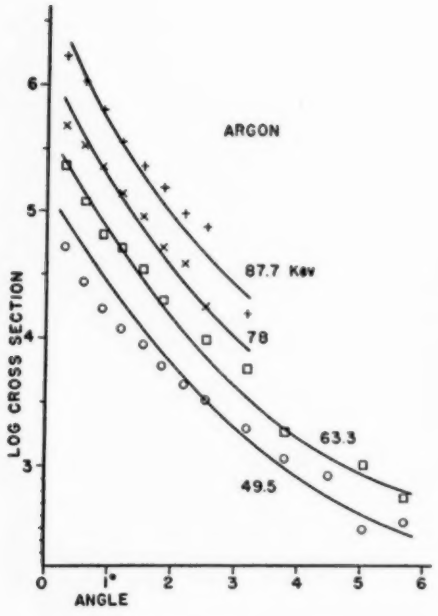

FIG. 3. Cross sections for scattering in argon for electron energies from 49.5 to 87.7 Kev. The ordinates are as shown for the 49.5 Kev curve. The curves for higher voltages are successively displaced upward through 0.5 units.

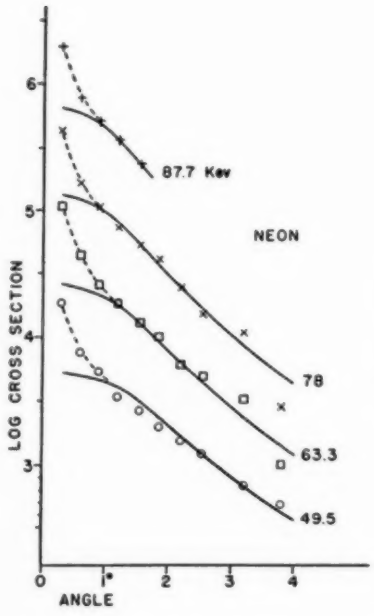

FIG. 4. Cross sections for scattering in neon, for electron energies from 49.5 to 87.7 Kev. The ordinates for the 49.5 Kev curve are as shown. The curves for higher voltages are successively displaced upward through 0.7 units.

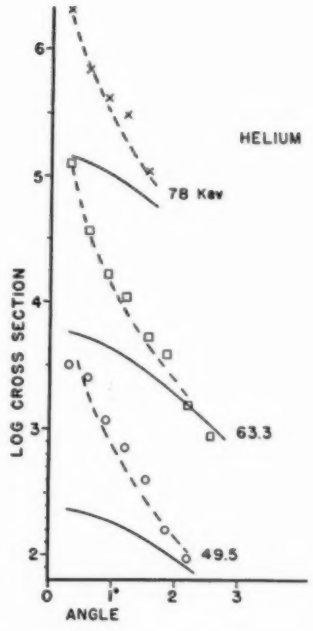

FIG. 5. Cross sections for scattering in helium, for electron energies from 49.5 to 78 Kev. The ordinates for the 49.5 Kev curve are as shown. The curves for higher voltages are successively displaced upward through 1.4 units.

the results of various runs were averaged. Different runs (made usually several days apart) always agreed with each other within the expected errors of the individual points, about 3 percent in the most favorable part of the angular range. A correction for the change in effective scattering volume with angle had to be applied. Although this type of apparatus is not suitable for determining absolute scattering cross sections, it is legitimate to assume that, provided the slits above and below the scattering chamber are parallel, the effective volume varies inversely as the sine of the angle of scattering. Accordingly the results were multiplied by a factor $1000 \sin \theta$, which gave numbers of a convenient size. Finally the points were fitted to the theoretical curves using an empirically determined multiplier. In the case of helium the experimental curves departed so widely from theory that it was necessary to use the average value of the multiplier found for argon and neon to locate the curves with respect to each other. Determination of this factor is practically equivalent to a measurement of the scattering volume, and confidence in the experimental results was increased by the fact that it remained nearly constant during the course of the work. Under standard conditions (pressure in scattering chamber 4×10^{-2} mm and current at 0° equivalent to a drift of 2×10^{6} mm/sec.) the average value of the multiplier was 21 to give numerical agreement with the cross sections given by Mott and Massey in units of 5.66×10^{-20} cm^2.

The results plotted on a logarithmic ordinate scale are shown in Figs. 3 to 5 where the solid lines are the theoretical curves. For clarity the curves have been separated from each other vertically and the order reversed. Actually, of course, the curves for the higher voltages should lie slightly below the low voltage ones. The curves for argon were successively displaced by 0.5 units on the logarithmic ordinate scale, for neon 0.7, and for helium 1.4 units. The scale is correct in each case for the 49.5 Kev curve. The theoretical curves were obtained by graphical interpolation from the tables of cross sections

published by Mott and Massey.[7] It is interesting to note that the measurements in argon at lower voltages, although extending over less than 6 degrees, cover a range greater than that tabulated; the curves of Mott and Massey were extrapolated a small amount at each end.

It is difficult to make a reliable estimate of the probable errors in this work, especially as they varied so much along a single curve. The uncertainties in the pressure measurements could hardly exceed 4 or 5 percent, and in any case would only affect the constancy of the empirical multiplier mentioned above. At the smallest angles the possible error of about 0.05° in the angle could account for an error of 16 percent, but this would of course diminish on going to larger angles. Because of unsteadiness in the high voltage and other factors affecting the grid current of the electrometer tube an uncertainty in the natural rate of drift of 0.3 mm/sec. was not impossible, and as the curves were often followed down to currents that small the points at the largest angles cannot be trusted very much.

In general it may be said that as long as the theoretical curves are concave upward (as in argon or in neon except at the smallest angles) reasonably good agreement is found, but as soon as the theory predicts a bending over of the curve towards the axis (as it must in all cases if followed to small enough angles) the agreement disappears. The results for helium bear a strong resemblance to those for neon at small angles, but unfortunately it was impossible to follow them further to see if the curves would merge. Numerous attempts to obtain curves for hydrogen were all unsuccessful, but it was observed that the variation of cross section with angle was even more rapid than in helium, so the agreement with theory would have been poorer. The discrepancy found in this work seems to be exactly the same as that observed in helium at small angles with medium energy electrons.[8] It must be conceded that because of the limited resolving power of the energy analyzer some inelastically scattered electrons could have been recorded, and that they would tend to give rise to an excess of scattering at very small angles, but it is hard to understand why they would not be at least as abundant in argon as in the other gases, if not more so. It seems best to accept tentatively the qualitative explanation in terms of the polarization of the atomic field as applicable here also.[9]

In conclusion the author wishes to express his great appreciation to his colleagues and the staff of the Palmer Physical Laboratory for many helpful discussions and for technical assistance. In particular it is a pleasure to thank Professor G. P. Harnwell, who originally suggested the problem, for his continued interest and support.

[7] Reference 2, p. 124, for argon and neon, p. 120, for helium. I have corrected four obvious errors in the second column of this table, and also expressed the cross sections in the same units.

[8] Reference 2, p. 122.

[9] An attempt was made to apply the calculations of Massey and Mohr (Proc. Roy. Soc. **A146**, 880 (1934)) to the curves for helium although their results are not given in a convenient form for this purpose. They predict a departure from the Born approximation curves at angles smaller than about 2.2° as observed, but the experimental increase of scattering at smaller angles appears to be much more rapid than expected; in the neighborhood of 0.6° the scattering is about six times the Born approximation value instead of twice.

The Saturation Requirements for Nuclear Forces

G. Breit and E. Wigner
University of Wisconsin, Madison, Wisconsin

(Received April 20, 1938)

The inequalities between the coefficients M, H, B, V, representing the proportions of Majorana, Heisenberg, Bartlett and ordinary interactions in the symmetric Hamiltonian, arising through considerations of saturation and of the instability of odd-odd nuclei heavier than N^{14} are represented graphically (Fig. 1). The allowed values of M, H, B, V correspond to a part of a plane bounded by three straight lines. These inequalities are sufficient for saturation at infinitely high density of nuclear particles and all conditions derivable from the necessity of saturation for the potential energy in the high density condition are derivable from those listed. The limits set on the interactions in the ^3P and ^1P states by the inequalities are discussed. The results are summarized in Table I, Eqs. (7) and (8) and in the adjoining section. The sufficiency of the conditions is discussed in Section 2. The physical limitations are gone into in Section 3.

IT is customary at present to use in nuclear theory a symmetric Hamiltonian consisting of interactions between pairs of nuclear particles represented by potentials of the following types: Majorana exchange (exchange of space coordinates), Heisenberg exchange (exchange of space and spin coordinates), Bartlett exchange (exchange of spin coordinates), ordinary non-exchange potential. It is, of course, not certain that the actual forces are of this type and that the saturation of the nuclear forces owes its origin to a preponderance of exchange forces rather than to saturation phenomena of other types.[1] It appears to be, nevertheless, of interest to systematize the available information[2] regarding the possible proportions of the different types of exchange forces as obtainable from considerations of stability of heavy nuclei (saturation) and the instability of nuclei heavier than N^{14} with an odd number of neutrons N and an odd number of protons Z. A brief elementary discussion is given below of the inequalities that must exist between the four kinds of potentials together with a diagrammatic representation of the values that are possible according to present evidence. A proof is then given by means of group character formulas that the elementary method contains all of the information derivable from requirements of saturation.

[1] G. Gamow and E. Teller, Phys. Rev. **51**, 289 (1937).
[2] G. Breit and E. Feenberg, Phys. Rev. **50**, 850 (1936); D. Inglis and L. A. Young, Phys. Rev. **51**, 525 (1937); E. Wigner, Phys. Rev. **51**, 947 (1937); N. Kemmer, Nature **140**, 192 (1937); E. Feenberg, Phys. Rev. **52**, 667 (1937); cf. also related discussion by H. Volz, Zeits. f. Physik **105**, 537 (1937).

1. Necessary Conditions

The potential energy between a pair of nuclear particles will be represented by

$$[MP^M+HP^H+BP^B+V\cdot 1]J(r);\quad J(0)<0, \tag{1}$$

where M, H, B, V are ordinary dimensionless numbers and P^M, P^H, P^B are, respectively, the Majorana, Heisenberg and Bartlett exchange operators. The function $J(r)$ is taken to be negative in the vicinity of $r=0$. The coefficients M, H, B, V will be supposed to be connected by

$$M+H+B+V=1. \tag{2}$$

The potential energy in the stable ^3S state of the deuteron is $J(r)$. In the ^1S state scattering experiments indicate a smaller degree of attraction represented by the potential $qJ(r)$ with $q\sim 1/2$. Thus

$$M-H-B+V=q<1. \tag{3}$$

If a definite value of q, say $q=3/5$ is assumed, the above relations restrict the four quantities M, H, B, V so that only two of them are independent. The quantities M and H will be used as independent variables and a diagram using M and H as coordinates will be employed. The interactions in the ^3P and ^1P states will be written as $(^3P)J(r)$, $(^1P)J(r)$. Positive values of (^3P) and (^1P) correspond to attractions in these states. These quantities are given by

$$(^3P)=-M-H+B+V=-2M-2H+1, \tag{3.1}$$

$$(^1P)=-M+H-B+V=-2M+2H+q. \tag{3.2}$$

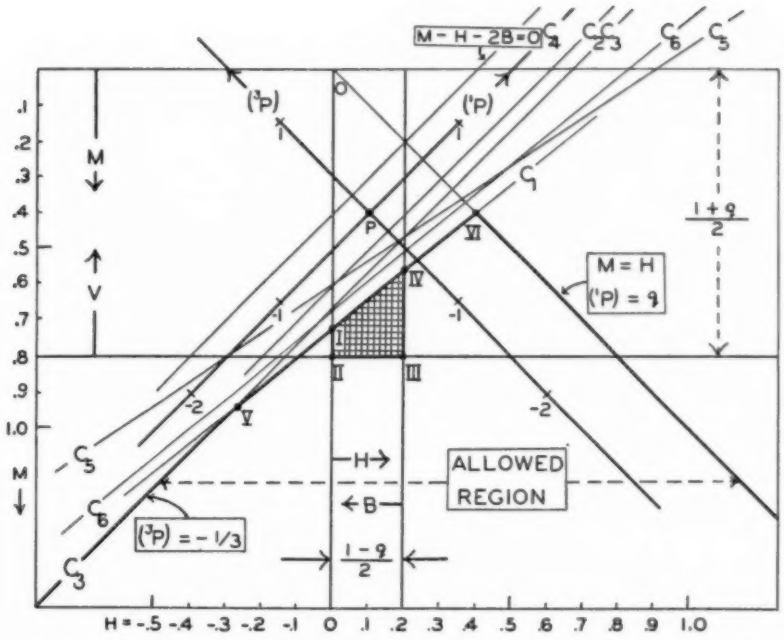

FIG. 1. Graphical representation of inequalities. Origin of M, H coordinate system is at 0. Origin of B, V coordinate system is at III. Origin of (^3P), (^1P) coordinate system is at P. To any point in the plane there correspond the values of M, H, B, V, in these coordinate systems. The inequalities $c_n \leqq 0$, $H+2B-M \leqq 0$, $H-M \leqq 0$ exclude all points above the lines $c_n=0$, $H+2B-M=0$, $H-M=0$. The lines $c_n=0$ are marked by c_n in the figure. The region allowed by all the inequalities considered here lies below the lines c_3, c_1 and $M=H$. The shaded area I, II, III, IV is that part of the allowed region for which M, H, B, V are positive. The scale of (^3P), (^1P) differs from that of M, H, B, V and is marked in the coordinate system (^3P), (^1P). Diagram is drawn for $q=3/5$.

One can express also M, H, B, V in terms of (^3P) and (^1P) as independent variables:

$$M=\tfrac{1}{4}[1+q-(^3P)-(^1P)], \tag{3.3}$$

$$H=\tfrac{1}{4}[1-q-(^3P)+(^1P)], \tag{3.4}$$

$$B=\tfrac{1}{4}[1-q+(^3P)-(^1P)], \tag{3.5}$$

$$V=\tfrac{1}{4}[1+q+(^3P)+(^1P)]. \tag{3.6}$$

Denoting the projection of total spin along an arbitrary axis by $\sigma\hbar/2$ and distinguishing between protons and neutrons by suffixes π and ν one has the following inequalities

$$c_1=4V-M-2H+2B=-5M-4H+3+q\leqq 0; \quad \sigma_\nu=\sigma_\pi=0; \quad Z=N \tag{4.1}$$

$$c_2=2V-M-2H+B=-3M-3H+\tfrac{1}{2}(3+q)\leqq 0; \quad \sigma_\nu=\sigma_\pi=0; \quad Z=0 \tag{4.2}$$

$$c_3=2V-M-H+2B=-3M-3H+2 =c_2+\tfrac{1}{2}(1-q)\leqq 0; \quad \sigma_\nu=N; \quad \sigma_\pi=Z; \quad Z=N \tag{4.3}$$

$$c_4=V-M-H+B=-2M-2H+1 =\tfrac{1}{3}(-1+2c_3)\leqq 0; \quad \sigma_\nu=N; \quad Z=0 \tag{4.4}$$

$$c_5=2V-M-H+B=-3M-2H+\tfrac{1}{2}(3+q)\leqq 0; \quad \sigma_\nu=N; \quad \sigma_\pi=-Z; \quad Z=N \tag{4.5}$$

$$c_6=8V-3M-4H+5B =-11M-9H+\tfrac{1}{2}(13+3q)\leqq 0; \quad \sigma_\nu=N; \quad \sigma_\pi=0; \quad Z=N. \tag{4.6}$$

The first four inequalities are not new[2] and some additional conditions are known as well.[2] It will be shown below that with the value of q indicated by present experimental data all the inequalities are consequences of (4.1), (4.3) and (5.2). If one assumes the inequalities (5), conditions (4.2), (4.4), (4.5) and (4.6) do not give any additional information. On the other hand, if the inequalities (5) are not used then (4.5) gives new information inasmuch as it is sufficient for the validity of (4.1) and (4.3) in the region of small M and large H.

The above six inequalities may be obtained by using trial wave functions contained in a volume that is sufficiently small to make $J(r)$ equal to $J(0)$. The trial wave functions give an expectation value for the energy which is higher than that corresponding to an accurate solution of the wave equation. The numbers of neutrons and protons, N and Z, are contained in this expression as N^2 and Z^2 as well as in lower powers of N and Z. The sum of all terms in N^2 and Z^2 must, therefore, be positive or zero. Otherwise the energy in the most stable condition will go to $-\infty$ as $-N^2$ or $-Z^2$. The conditions (4.1) to (4.6) are obtained in this manner and by neglecting the Coulomb energy which is justifiable[2] in view of its relatively small value. In addition the nonexistence of stable odd-odd nuclei heavier than N^{14} gives[2]

$$H-M+2B=-M-H+1-q\leqq 0 \quad \text{(parallel spin of } \nu \text{ and } \pi \text{ in unstable nucleus)} \quad (5.1)$$

$$H-M\leqq 0 \quad \text{(antiparallel spin of } \nu \text{ and } \pi \text{ in unstable nucleus)} \quad (5.2)$$

The variables H, M are used in Fig. 1 as Cartesian coordinates of a point in a plane. Any one of the inequalities $c\leqq 0$ has the geometrical significance of dividing the H, M plane into an allowed part below the line $c=0$ and a forbidden part above that line. Only the part of the plane below the six lines given by the inequalities (4.1)$\cdots$(4.6) and the two lines corresponding to (5.1) and (5.2) can represent a satisfactory set of M, H, B, V. The six lines corresponding to $c_n=0$ are marked as c_n in the figure. The two lines corresponding to Eqs. (5.1) and (5.2) are labeled by these equations. It is seen that for $q=3/5$ the permissible region of the plane is bounded by the three lines

$$c_3=0, \qquad c_1=0, \qquad H=M. \qquad (6)$$

The axis of H is also the negative of the axis of B with $B=0$ which comes at $H=\frac{1}{2}(1-q)$. Similarly the values of V increase upwards along the M axis with $V=0$ coming at $M=\frac{1}{2}(1+q)$. In the same figure a rotation through $\pi/4$ gives lines of constant (^3P) and (^1P). The values of (^3P) increase as one moves up and to the left, those of (^1P) as one moves up and to the right. The scales for (^3P) and (^1P) are shown on these axes. Unity is seen to be represented by a smaller length in these coordinates than in the $M-H$ system. As has been noticed by Feenberg,[2] the inequality $c_3\leqq 0$ determines an upper limit of $-1/3$ for (^3P) which is of interest for the scattering of protons by protons. According to this the repulsion between protons in the ^3P state should be greater than that corresponding to a potential $-J(r)/3$. The condition is apparent in the diagram. The line $c_3=0$ is one of the bounding lines of the allowed region and for it $(^3P)=-1/3$.

An upper limit is set for (^1P) by the condition $H=M$. For this line $(^1P)=q$ and only smaller values of (^1P) are allowed. If it is supposed that, in addition, the interaction is such[3] that $c_1=0$ then (^1P) must be greater than that corresponding to the intersection of $c_1=0$ with $c_3=0$, which is $-3q$. The latter condition $[(^1P)\geqq -3q]$ was first given by Feenberg. If one similarly restricts the allowed region for (^3P) by the requirement $c_1=0$, then $H<M$ imposes the additional condition $(^3P)\geqq -\frac{1}{9}(4q+3)$. Thus for $c_1=0$

$$-1/3\geqq(^3P)\geqq-(4q+3)/9, \qquad (7)$$

$$q\geqq(^1P)\geqq-3q. \qquad (8)$$

Still closer limits on (^3P) are set by requiring that V, M, H, B should all be positive. The corresponding region is shaded in Fig. 1 and is seen to be a trapezoid. Its vertices are the points I, II, III, IV and the points at the intersection of $c_1=0$ with $c_3=0$ and $H=M$ are

TABLE I. *Values of* (^3P), (^1P), V, M, H, B *for points* (I), (II), (III), (IV), (V), (VI).

Point	Intersecting Lines	(^3P)	(^1P)	V	M	H	B
(I)	$c_1=0$ $H=0$	$\frac{-2q-1}{5}$	$\frac{3q-6}{5}$	$\frac{3q-1}{10}$	$\frac{q+3}{5}$	0	$\frac{1-q}{2}$
(II)	$H=0$ $V=0$	$-q$	-1	0	$\frac{1+q}{2}$	0	$\frac{1-q}{2}$
(III)	$V=0$ $B=0$	-1	$-q$	0	$\frac{1+q}{2}$	$\frac{1-q}{2}$	0
(IV)	$B=0$ $c_1=0$	$\frac{-2-q}{5}$	$\frac{3-6q}{5}$	$\frac{3-q}{10}$	$\frac{1+3q}{5}$	$\frac{1-q}{2}$	0
(V)	$c_1=0$ $c_3=0$	$-\frac{1}{3}$	$-3q$	$\frac{1-3q}{6}$	$\frac{1+3q}{3}$	$\frac{1-3q}{3}$	$\frac{1+3q}{6}$
(VI)	$c_1=0$ $H=M$	$\frac{-4q-3}{9}$	q	$\frac{7q+3}{18}$	$\frac{q+3}{9}$	$\frac{q+3}{9}$	$\frac{3-11q}{18}$

[3] D. Inglis, Phys. Rev. **51**, 531 (1937); E. Feenberg, Phys. Rev. **51**, 777 (1937).

designated by V and VI respectively. In Table I are given the values of (^3P), (^1P), V, M, H, B for these six points. The values of V, M, H, B are very much restricted if one excludes negative values of these quantities. The simultaneous requirements of V, M, H, $B \geqq 0$ and $c_1=0$ determine (^3P) particularly well and place it between the values for the points I and IV. For $q=3/5$ these limits give $-11/25>(^3P)>-13/25$ and for $q=1/2$ they are $-2/5>(^3P)>-1/2$. If one removes the requirement $c_1=0$ but keeps $V, \cdots, B \geqq 0$, then the points I and III set the limits on (^3P) which give for $q=3/5$, $-11/25>(^3P)>-1$. Similarly removing the requirement $c_1=0$ but keeping $V, \cdots, B \geqq 0$ the value of (^1P) is seen to lie between the limits set by points II and IV. Thus $-1<(^1P)<\frac{1}{5}(3-6q)$ which for $q=3/5$ becomes $-1<(^1P)<-3/25$. The requirement of positiveness of M, H, B, V is seen to restrict (^3P) within a narrower region than (^1P).

2. Sufficient Conditions

The inequalities (4.1)$\cdots$(4.6) have been obtained by considering states with special spin orientations that have been listed. It is not obvious that they correspond to the most stringent conditions on V, M, H, B because by a suitable change of the wave function it may be possible to lower the expectation value of the energy. It will be shown in this section that the requirement of the absence of terms in the expectation value of the potential energy, that go to $-\infty$ as $-N^2$ and $-Z^2$, in the approximation of long range forces, gives conditions on V, M, H, B that follow from the inequalities (4.1), (4.3), (5.2). This means that these inequalities are sufficient for saturation of the potential energy at high particle densities where by saturation is meant the impossibility of finding a trial wave function which gives, at high particle densities, a negative expectation value for the potential energy varying quadratically with the number of particles. For certain functions $J(r)$ it can be shown then by an argument analogous to one previously used[4] that the same holds for every wave function independently of its extension in space. Since the expectation value of the kinetic energy is positive these conditions are also sufficient for the saturation of the total energy.

For wave functions with a small spatial extension the $J(r)$ in (1) may be replaced by $J(0)$. The problem of finding a trial wave function with the lowest expectation value for (1) is then reduced to that of finding the eigenfunction of

$$-MP^M-HP^H-BP^B-V\cdot 1$$

which corresponds to the lowest eigenvalue. Since the four operators in this sum commute, there is a complete set of eigenfunctions common to all four of them. The lowest eigenvalue is obtained for that eigenfunction for which the sum of the four eigenvalues is lowest.

It has been shown by Dirac[5] that the eigenfunctions of P^B correspond to definite values of the total spin S. Similarly, according to Feenberg and Phillips,[6] the eigenfunctions for P^H have definite isotopic spin[7] T and those for P^M are known[7] to have definite "multiplicity." The part of the potential energy which is proportional to the square of the total number of particles becomes

$$E=-A^2J(0)\{-\tfrac{1}{2}V+[\tfrac{1}{8}+\tfrac{1}{2}(P^2+P'^2+P''^2)]M+(\tfrac{1}{4}+\bar{T}^2)H-(\tfrac{1}{4}+\bar{S}^2)B\}. \quad (9)$$

Here[8] $A=N+Z=$atomic number, $\bar{S}=S/A$, $\bar{T}=T/A$, $S=$particle spin in units $\hbar$, $T=$isotopic spin, $P=$greatest $\bar{S}$ possible for the multiplet, $P'=$greatest $\bar{T}$ possible for this $\bar{S}$, $P''=$greatest Y/A possible for these $\bar{S}$, $\bar{T}$.

Since $M>0$ (see diagram), it will suffice to consider the following cases:

(1) $M>0$, $H>0$, $B<0$;
(2) $M>0$, $H>0$, $B>0$;
(3) $M>0$, $H<0$, $B>0$.

The case $M>0$, $H<0$, $B<0$ need not be considered because $B+H=\frac{1}{2}(1-q)>0$, which is impossible for $H<0$, $B<0$. For each of the

[4] E. Wigner, Proc. Nat. Acad. **22**, 662 (1936).

[5] Cf. P. A. M. Dirac, *The Principles of Quantum Mechanics*, second edition (Oxford, 1935) §61.

[6] E. Feenberg and M. Phillips, Phys. Rev. **51**, 597 (1937).

[7] E. Wigner, Phys. Rev. **51**, 947 (1937).

[8] E. Wigner, Phys. Rev. **51**, 106 (1937). The notation used in the present paper differs from that of this reference in referring to S, T, Y of Eqs. (11) of the latter as PA, $P'A$, $P''A$.

above cases the expression for the energy will be minimized by choosing suitably $\bar{S}$, $\bar{T}$, P, P', P''. It will then be required that E, as given by Eq. (9), be >0. For any other choice of $\bar{S}$, $\bar{T}$, P, P', P'' it follows that $E>0$. In this way one obtains, therefore, sufficient conditions for $E>0$ and it is necessary for nuclear stability that all such conditions be fulfilled. Since the actual energy may be lower than (9) these conditions may not be sufficient for stability but it appears likely that they are,[4] since this has been shown to be the case for a special class of functions $J(r)$.

For case (1) the minimum E is obtained for $P=P'=P''=\bar{T}=\bar{S}=0$ which leads on substitution into Eq. (9) to $c_1<0$ and is therefore contained in the preceding inequalities. For case (2) one may consider: (a) $M-2B>0$ and (b) $M-2B<0$. For (a) the combination

$$\tfrac{1}{2}P^2M-\bar{S}^2B=P^2(\tfrac{1}{2}M-B)+(P^2-\bar{S}^2)B$$

is a minimum when $P=\bar{S}=0$. The minimum of E corresponds, therefore, to $P=\bar{S}=P'=P''=\bar{T}=0$ which gives $c_1<0$ as in case (1). For (b) the combination $\frac{1}{2}P^2M-\bar{S}^2B$ is a minimum when P has its maximum and $P^2-\bar{S}^2$ has its minimum value. Since P is the largest possible $\bar{S}$, the minimum $P^2-\bar{S}^2=0$ and the maximum $P=1/2$ which corresponds to a parallel orientation of all the particle spins. The best values are thus $P=\bar{S}=1/2$. For these values the minimum E corresponds to $P'=P''=\bar{T}=0$. Substituting into Eq. (9) one finds then $c_3<0$ in agreement with the fact that in the inequality (4.3) all particle spins were taken to be parallel.

For case (3) it is convenient to rearrange the expression for E:

$$E=-A^2J(0)[\tfrac{5}{8}M+\tfrac{1}{2}H-\tfrac{1}{8}(q+3)]+E_v, \quad (9.1)$$

$$E_v=-A^2J(0)[\tfrac{1}{2}M(P^2+P'^2+P''^2)+H(\bar{T}^2+\bar{S}^2)-\tfrac{1}{2}(1-q)\bar{S}^2]. \quad (9.2)$$

The variable terms are contained in E_v. Here $H<0$, $-\frac{1}{2}(1-q)<0$. Hence, for fixed P, P', P'', a minimum is obtained for $\bar{T}=P'$, $\bar{S}=P''$. For these values Eq. (9.2) becomes

$$E_v=-A^2J(0)\{[H+\tfrac{1}{2}M-\tfrac{1}{2}(1-q)]P^2+(H+\tfrac{1}{2}M)P'^2+\tfrac{1}{2}MP''^2\}. \quad (9.3)$$

In this expression the coefficient of P'' is positive since $M>0$. The coefficient of P^2 is necessarily less than that of P'^2. Therefore, there are three possibilities: (a) $H+\frac{1}{2}M-\frac{1}{2}(1-q)>0$, $H+\frac{1}{2}M>0$; (b) $H+\frac{1}{2}M-\frac{1}{2}(1-q)<0$, $H+\frac{1}{2}M<0$; (c) $H+\frac{1}{2}M-\frac{1}{2}(1-q)<0$, $H+\frac{1}{2}M<0$. For (a) the minimum E is obtained if $P=P'=P''=0$. In this case, therefore, $\bar{S}=\bar{T}=0$ as well. The minimum E is the same as in case (1) and one obtains $c_1<0$. For (b) the minimum E is obtained by using maximum $P=\frac{1}{2}$ and minimum $P'=P''=0$ as in (2b). The condition $c_3<0$ is, accordingly, obtained again.

For (3b) the coefficients of P^2 and P'^2 are both negative. In order to obtain a low E it is now advantageous to use large values of P and P' and at the same time P'' must be made as small as possible. It is not possible, however, to vary P, P', P'' independently of each other as the minimum of E is approached. In fact the minimum for Eq. (9.3) with independent variations of P, P', P'' corresponds to $P=0$, $P'=1/2$, $P''=0$ which is an impossible set of these quantities since $P\geqq P'\geqq P''$. The way in which P, P', P'' may vary can be inferred[8] from their expression in terms of $\Lambda_4\geqq\Lambda_3\geqq\Lambda_2\geqq\Lambda_1\geqq 0$.

$$P=\frac{1}{2A}(\Lambda_4-\Lambda_3-\Lambda_2-\Lambda_1);$$

$$P'=\frac{1}{2A}(\Lambda_4-\Lambda_3+\Lambda_2-\Lambda_1)$$

$$P''=\frac{1}{2A}(\Lambda_4-\Lambda_3-\Lambda_2+\Lambda_1);$$

$$A=\Lambda_4+\Lambda_3+\Lambda_2+\Lambda_1.$$

If here $\Lambda_1>0$ one can decrease Λ_1 and increase Λ_4 by an equal amount. This leaves A, P'' unchanged and increases both P and P' which gives a lower energy. Thus $\Lambda_1=0$ will include the most favorable cases. With this restriction $P''=P+P'-\frac{1}{2}$ and

$$E_v=-A^2J(0)\left\{[H+M-\tfrac{1}{2}(1-q)]P^2+(M+H)P'^2+M(PP'+\tfrac{1}{8})-\frac{M}{2}(P+P')\right\}. \quad (9.4)$$

Further

$$\Lambda_4/A=P+P'>\Lambda_3/A=\tfrac{1}{2}-P'>\Lambda_2/A=\tfrac{1}{2}-P>0. \quad (9.5)$$

The above inequalities (9.5) confine the possible P, P' to a triangular region in the P, P' plane bounded by the lines $P=\frac{1}{2}$, $P=P'$, $2P'+P=\frac{1}{2}$. In this triangle the values of P, P' can be varied arbitrarily. If one uses the facts that in the present case $H<0$, $M+2H<0$ while according to conditions already derived $M+H>0$ one finds by means of Eq. (9.4), after a somewhat lengthy but quite elementary discussion, that the minimum E corresponds to $P=1/2$, $P'=0$, $P''=0$ which gives $c_3<0$ as in (3b). This exhausts the possibilities.

3. Final Remarks

It should be observed that the conditions (4) have been derived on the assumption of the absence of other nuclear forces than those given in Eq. (1). In particular forces of the "many body" type could bring about saturation in spite of the inequalities (4) not being fulfilled. Even if under ordinary circumstances these forces should be negligible they may possibly be of special importance in the state of high density considered for saturation.[9] A similar remark applies[2] to the influence of a velocity dependence of the potential.

It should also be pointed out that the inequalities (4) are obtained by a consideration of an idealized state of high density which would be the actual state, if the inequalities (4) were not satisfied. On the other hand, inequalities (5) follow from the consideration of actual nuclei and involve several approximations. One can derive them on the basis of the high density model also but this certainly is not the condition in actual nuclei. All other considerations on this question are based, apart from some, rather rough approximations, on the assumption that H and B are small compared[10] with M and should not be used, therefore, to establish the inequality $H<M$. It is rather the apparent agreement of these considerations with experiment that gives one confidence in the inequality $H<M$. The underlying experimental rule[11] holds without exception for[12] $A>14$. In fact, this seems to indicate that H is materially smaller than M, as otherwise accidental factors would be likely to make at least some of the heavier odd-odd nuclei stable.

On the other hand, information regarding the approximate symmetry of the nuclear Hamiltonian arises out of experimental material with ordinary rather than high nuclear densities. It is more closely related to the inequalities (5) than to (4) and one may be skeptical about the latter from this point of view.

Very little is known about the space dependence of the function $J(r)$ and still less about $J(0)$. It is possible that the coefficients M, H, B, V should be multiplied by different functions $J(r)$ and there is a chance that the four $J(r)$ are roughly the same for distances of the order 2×10^{-13} cm but that the $J(0)$ are widely different. If such should be the case the saturation inequalities (4) will have very little meaning.

One of us (E.W.), would like to express his indebtedness to the Wisconsin Alumni Research Foundation for its support of this work.

[9] J. A. Wheeler [Phys. Rev. **52**, 1083 (1937), especially p. 1106], has investigated the saturation properties of many particle forces.

[10] The following qualitative arguments suggest that H and B separately are small compared with M and hence neither of them has a large negative value. (1) The empirical mass differences $N^{13}-C^{13}+C^{14}-N^{14}=0.0026$, $C^{11}-B^{11}+Be^{10}-B^{10}=0.0027$, $He^3-H^3+He^6-Li^6=0.0039$ give approximate values of $-2(H+B)\bar{J}(r)$ in N^{14}, B^{10}, Li^6. The last value is not very reliable experimentally and can be expected to be great on account of the loose packing of He^6. The first two are seen to be practically the energy difference $^1S-{}^3S$ in H^2. If H and B were separately large such close agreement would not be expected for then the wave functions would be changed appreciably from the symmetry required by the preponderance of M. (2) Considerations of the kind as the one leading to Table II in footnote 7 and the apparent existence of S^{36} and Ca^{46} [A. O. Nier, Phys. Rev. **53**, 282 (1938)] may be considered as qualitative arguments supporting the above view. From this point of view (5.1) is a more restrictive assumption than (5.2) inasmuch as in the region of positive H and B a greater part of the plane is eliminated by (5.1). Small negative values of H or B cannot be excluded by the above arguments. Nevertheless, the set of values $M=14/12$, $H=-7/12$, $B=10/12$, $V=-5/12$ proposed by Volz, reference 2, contradicts the inequality $c_3<0$.

[11] W. D. Harkins, Phys. Rev. **19**, 135 (1922). J. Am. Chem. Soc. **39**, 856 (1917); **45**, 1426 (1923); J. Frank. Inst. **194**, 165, 329, 521, 645, 783 (1922); **195**, 67, 553 (1923); Phil. Mag. **42**, 305 (1921).

[12] For $A\leq14$, the conditions are different and odd-odd nuclei can be stable even if H is quite small.

The Thermal Conductivities of Mercury, Sodium, and Sodium Amalgams in the Liquid State

WAYNE C. HALL*
Department of Physics, University of Kansas, Lawrence, Kansas
(Received April 11, 1938)

A guard ring method for the measurement of the thermal conductivities of liquid metals in which the furnace automatically attains equilibrium is described. The design of the furnace permits frequent and easy replacement of specimens; a layer of paraffin over the liquid metal prevents oxidation by the air. The thermal conductivities of mercury, of sodium, and of sodium amalgams ranging in concentration from 70 to 94 atoms percent sodium are measured over these temperature ranges: mercury, 40°C–220°C; sodium 85°C–210°C; sodium amalgams, 100°C–150°C. Sodium behaves as a normal metal, but mercury and the sodium amalgams are abnormal. Some evidence for the existence of the intermetallic compounds Na_5Hg_2 and Na_3Hg in the liquid amalgams at 100°C is presented by breaks in the thermal conductivity-concentration curve. An eutectic at 86.5 atoms percent sodium is evident from the same curve. Calculations of Lorentz' number for sodium and for mercury are given.

MERCURY, sodium, and sodium amalgams are of particular interest when in the liquid state. The behavior of the electrical conductivity of mercury with temperature causes mercury to be classed with the abnormal metals; the same thing may be said of its thermal conductivity, though there is too much disagreement in the existing measurements to be certain of this fact. Sodium and mercury are known to form many intermetallic compounds in the solid state which may yet exist in the liquid state. The thermal conductivity of liquid sodium has never been investigated over any range of temperature. Hence, this investigation was carried out.

APPARATUS ARRANGEMENT

A method based on the use of a tall column of liquid for measuring the thermal conductivities of the liquid metals was developed. The major details of the furnace, including the significant dimensions, are shown by Fig. 1. The liquid metal was contained in a cylinder of sheet asbestos which had been formed about a bar of the proper diameter, and which had been coated thinly on both sides with Insalute cement. This cylinder rested on a bar of iron of the same diameter in the furnace. Two thermocouple tubes of Pyrex glass about 1.2 mm in diameter were set in the cylinder at right angles to the axis, with the aid of the cement. The tubes, which were approximately two centimeters apart, were set in from the ends of the liquid metal column by about one centimeter in order to insure a uniform flow of heat throughout the section of liquid metal whose temperature gradient was measured.

The heater which supplied the heat that was conducted down the column was wound uniformly of 38-gauge chromel wire on a sheet of mica. This was sealed in by the Insalute cement between two circular plates of stainless steel that were bolted together. After completion, the heater, which was only 5 mm thick, was allowed to float on the liquid metal. A layer of paraffin three or four millimeters in thickness above the heater protected the metal from oxidation or evaporation.

The details of the guard-ring arrangement are

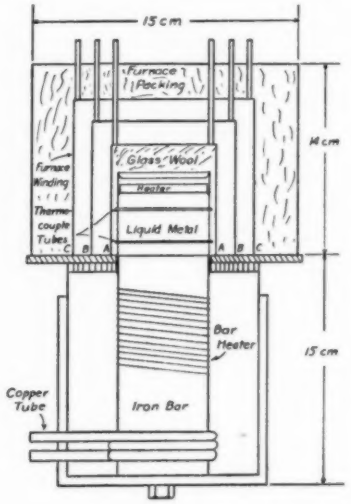

FIG. 1. The furnace.

* Now at Naval Research Laboratory, Washington, D. C.

of interest. About the asbestos cylinder were four, concentric, sheet metal cylinders which had the upper ends closed. Each one was held in position through bolts at the lower ends of the cylinders to a baseboard of pressed asbestos. The cylinder C was the guard ring proper, for it supported a uniform winding of nichrome wire around the wall and across the upper end which was used to maintain the average temperature of the cylinder C equal to that of the liquid metal column. A layer of sheet mica extended over each of the cylinders A and B; on each layer was wound nearly 25 feet of 30-gauge pure platinum wire which was uniformly spaced on the wall and across the top of the cylinder. Leads to the two resistance thermometers thus fashioned passed out of the top of the furnace through glass tubes.

Of course, the two sheet metal cylinders A and B reduced the lateral radiation from the liquid metal. But their main function was to support the two resistance thermometers which were used automatically to prevent heat transfer to or from the liquid metal. This was done simply by keeping the ratio of their resistances equal to the value which existed at room temperature; i.e., to the value at which the heat transfer was zero with all of the furnace at the same temperature. As long as the ratio had this value the two cylinders A and B were at equal temperatures, which meant that there was no heat transfer from the column of liquid metal.

It is true that the heat transfer by radiation or conduction between two surfaces whose average temperatures are equal will be zero only if Newton's law for the transfer of heat holds; i.e., $H=k(T_1-T_2)$. But at the operating temperatures of the furnace, which varied between 40°C and 220°C approximately, Newton's law would hold quite well for the small temperature differences which could have existed.

To facilitate changing one liquid metal for another, the construction of the furnace permitted the upper part which held the four cylinders to be raised away from the asbestos cylinder. The lower part of the furnace consisted essentially of the iron bar which held the asbestos cylinder and which served to adjust the mean temperature of the liquid metal to any desired value.

A voltage regulator was employed to regulate the voltage at the heater to within 0.3 percent while the furnace was in use. This was necessary because of the time required for the furnace to attain equilibrium.

The automatic apparatus for bringing the furnace to equilibrium functioned as follows: The short platinum leads of the two resistance thermometers were connected at a terminal board on the upper furnace to manganin resistances which made up the other two arms of a Wheatstone bridge. Connected across the bridge was a sensitive galvanometer. The mirror of this galvanometer reflected the light rays from a lamp filament to a lens which formed a bright image of the filament on a box housing a photoelectric cell. When the bridge circuit was balanced, the image of the lamp filament was just at the edge of an opening in the box before the photoelectric cell. But, when the bridge was unbalanced due to the passage of heat outward from the liquid metal, the galvanometer mirror reflected light into the photoelectric cell. After amplification, the resultant photoelectric current caused a relay to close, thus shunting part of the resistance in the power line to the furnace winding on the cylinder C. This increased the current to the furnace winding by about five or ten percent. As soon as the bridge circuit approached balance the galvanometer mirror started to rotate back to its first position, and by the time a very slight unbalance had been reached in the reverse direction caused by the passage of heat inward to the liquid metal, the galvanometer mirror had turned far enough so that light no longer passed through the opening to the photoelectric cell. Then the amplifier and relays operated in a reverse manner and removed the shunt from the previously mentioned resistance. A calculation indicated that a temperature difference of about one-hundredth of a degree centigrade between cylinder A and cylinder B was sufficient to cause the relays to operate.

A standard resistance of one ohm was included in one of the current leads to the heater for the measurement of the current. Leads to a high resistance voltage divider were connected directly to the heater terminals within the furnace eliminating the necessity for a correction to the voltage measurements caused by the resistance of the current leads.

The chromel-copel thermocouples which were used were calibrated at the boiling points[1] of water, napthalene and benzophenone. Six couples that were calibrated could be represented by the following equation to within 0.1 percent:

$$E=4.463\times10^{-2}t+5.017\times10^{-5}t^2-3.556\times10^{-8}t^3$$

millivolt, where the temperature is in degrees centigrade.

For the purpose of getting the distance between the thermocouples as accurately as possible a traveling microscope was bolted to a frame that was in turn bolted to the lower part of the furnace. The microscope was directed into the asbestos cylinder in line with the axis and just to one side of the two parallel thermocouple tubes. A very small mirror that had been attached a short distance from the objective end of the microscope turned the light rays from a thermocouple tube so that the microscope could bring them in focus. The microscope, without the mirror, was used to get the cross-sectional area of the asbestos cylinder simply by measuring the rise in the mercury level in the cylinder which resulted when a weighed quantity of pure mercury was poured in.

It is estimated that the maximum error in the absolute value of the thermal conductivity measurements which resulted from the neglected thermal expansion of the asbestos cylinder amounted to 0.15 percent.

Thermal Conductivity of Mercury

Many measurements of the thermal conductivity of mercury were made for the purpose of checking the operation of the furnace as well as to determine the true manner of variation of the thermal conductivity with temperature. The mercury used here and in the sodium amalgams came from the Mallinckrodt Chemical Company and was certified pure.

It is to be expected that if there were more than a negligible heat transfer laterally from the liquid metal it could be detected in a change in thermal conductivity which would result from a change in the temperature gradient down the liquid metal at a given mean temperature. Several of the measurements in which the temperature gradient varied by about a factor of two are given in Table I. The calculated value was arrived at by using the observed temperature coefficient from the data shown in Fig. 2. From the close agreement exhibited in this table and the other measurements it was decided that there was no heat transfer through the guard ring.

By taking the thermal conductivity of asbestos paper as 0.0006 cal./cm cube −°C, a calculation gave the ratio of the heat conducted by the asbestos cylinder to that conducted by the mercury at 0°C as 0.2 percent. This was the maximum value; hence it was neglected in all calculations.

The results of 51 observations of thermal conductivity fit the equation

$$K_t=0.0819(1+0.00314t-0.00000295t^2)$$

in watt/cm −°C, with an average deviation, regardless of sign, of 0.6 percent from the curve. These results are in agreement with the limited results of Nettleton[2] and of Berget,[3] but disagree with the results of Gehlhoff and Neumeier,[4] except as to the fact that mercury has a positive temperature coefficient of thermal conductivity.

Table I. *Effect of temperature gradient on the thermal conductivity of mercury (cross section of liquid metal = 18.70 cm²).*

Mean Temp. (°C)	Temp. Gradient (°C/cm)	Power (Watts)	Conductivity (Watt/cm°C) Measured	Conductivity (Watt/cm°C) Calculated
74.7	4.90	9.82	0.0999	0.0999
78.9	9.52	17.93	0.1007	0.1008
72.6	4.96	9.20	0.0991	0.0991
66.9	9.82	17.87	0.0973	0.0978

Thermal Conductivity of Sodium Amalgams

The sodium amalgams which lie between 70 and 94 atomic percent sodium were investigated. The sodium, which had been stored in benzene, was first freed from the scale that enclosed it by melting it under paraffin; then it was amalgamated with mercury under paraffin. A special

[1] Nat. Bur. Stand. Technologic Paper No. 170.

[2] H. R. Nettleton, Proc. Phys. Soc. **26**, 28 (1913); **27**, 129 (1915).

[3] Berget, 1900; Glazebrook, *Dictionary of Applied Physics*, Vol. 1 (1922).

[4] Gehlhoff and Neumeier, Verh. d. phys. Ges. **21**, 201 (1919); **15**, 876, 1069 (1913).

glass pipette was used to transport the various amalgams to the furnace so that the amalgams were never in contact with the air.

The ordinary method of analysis by titration of samples of the amalgams that had been added to beakers of distilled water was resorted to, using standardized hydrochloric acid with methyl orange as an indicator.

A condensed summary of the data over the amalgams is given in Table II.

A plot of the results for the first 12 alloys has been made in Fig. 3 to show that the points for a given alloy fall on a straight line over the temperature interval from 100°C to 150°C. From these lines the thermal conductivities, both at 100°C and at 150°C were obtained. The results are given by Table III.

The behavior of the thermal conductivity of the sodium amalgams with concentration changes at 100°C is indeed interesting, as Fig. 4 shows. For sodium amalgams which contain less than 80 atomic percent sodium by up to a considerable amount, the thermal conductivity lies below that of either component metal alone. Also, there are certain breaks in the curve which, if real, must throw some light upon the chemical structure of the amalgams. Two of these breaks, existing at 71.4 and 75.0 atomic percent sodium, respectively, may be caused by the presence of the intermetallic compounds Na_5Hg_2 and Na_3Hg.

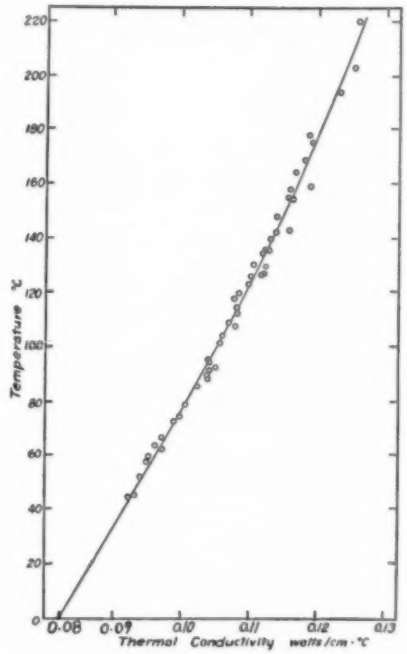

FIG. 2. The thermal conductivity of mercury.

TABLE II. *Thermal conductivity of sodium amalgams (thermocouple separation/cross section of liquid metal = 0.1103 cm^{-1}).*

Alloy	Mean Temp. (°C)	Difference (°C)	Power (Watts)	Thermal Conductivity (Watt/cm −°C)	Atomic Percent Sodium	Alloy	Mean Temp. (°C)	Difference (°C)	Power (Watts)	Thermal Conductivity (Watt/cm −°C)	Atomic Percent Sodium
1	147.6	20.55	19.02	0.1021	70.0	9	153.2	19.06	19.88	0.1150	80.0
	127.6	19.72	17.29	0.0967			126.3	17.82	17.35	0.1073	
	97.4	16.85	13.42	0.0879			101.2	15.82	14.34	0.0999	
2	148.6	20.21	18.84	0.1027	71.4	10	156.9	18.91	20.34	0.1186	80.4
	125.8	19.21	16.89	0.0972			125.9	17.43	17.39	0.1101	
	100.2	17.08	14.09	0.0910			103.7	15.79	14.75	0.1030	
	127.1	19.61	17.28	0.0972							
	150.5	20.23	18.98	0.1034		11	151.7	17.82	19.71	0.1219	82.1
							125.8	16.41	17.17	0.1154	
3	151.2	20.36	19.25	0.1042	73.1		102.2	15.01	14.65	0.1078	
	127.2	19.03	16.85	0.0977			102.3	15.02	14.64	0.1077	
	102.7	17.04	14.07	0.0911			136.1	18.82	20.17	0.1181	
4	149.4	19.44	18.56	0.1052	73.8	12	155.8	17.09	20.50	0.1323	83.9
	127.7	19.36	17.39	0.0990			128.5	16.16	18.09	0.1235	
	104.0	17.17	14.47	0.0929			103.2	14.43	15.15	0.1158	
5	154.1	20.35	19.82	0.1074	75.1	13	150.1	15.25	19.88	0.1437	86.4
	102.6	16.96	14.26	0.0928			124.0	14.05	17.18	0.1348	
	126.7	18.74	16.98	0.0998							
						14	151.6	14.73	20.52	0.1537	86.9
6	153.7	19.98	19.72	0.1088	76.1		131.8	14.51	19.39	0.1474	
	127.2	18.74	17.16	0.1010							
	101.6	16.50	14.07	0.0940		15	160.5	15.04	23.20	0.1701	88.4
							125.6	13.11	18.66	0.1569	
7	153.2	19.76	19.92	0.1112	77.6		107.2	12.41	16.77	0.1490	
	131.8	17.60	16.92	0.1060							
	105.5	17.06	15.08	0.0975		16	160.3	14.18	24.04	0.1870	90.6
	106.0	17.03	15.11	0.0978			131.4	13.23	21.00	0.1750	
8	152.0	19.24	19.65	0.1126	79.1	17	155.8	11.32	25.54	0.2486	93.7
	127.3	17.84	17.11	0.1058			126.6	10.95	23.01	0.2317	
	104.3	16.35	14.76	0.0995			100.2	13.92	26.93	0.2134	

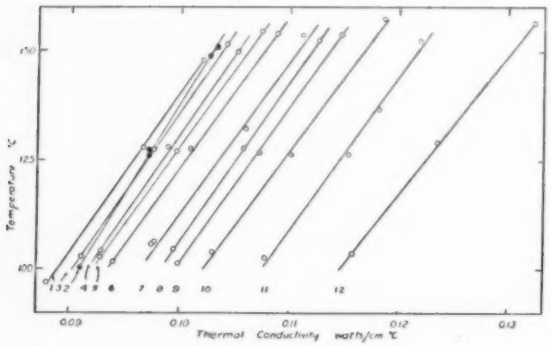

FIG. 3. The thermal conductivities of the sodium amalgams. The numbered curves are for the alloys listed in Table II.

Johnson and Fernelius[5] record the presence of these compounds in the solid sodium amalgams within the concentration range of Fig. 4. Several experimenters[6] have sought to detect the existence of these compounds, and others, in the liquid state but to no avail. The upper break in the curve occurs at 86.5 atomic percent sodium, which concentration agrees well with that of the eutectic which Vanstone[7] found at 85.5 atomic percent sodium in the thermal diagram.

Perhaps the most reasonable interpretation of the drops which may be found in the thermal conductivity concentration curve at 100°C at 71.4 and at 75.0 atomic percent sodium when the sodium content is increased, results by assuming that they are caused by decreases in the free electron concentrations when the compounds are formed. At the eutectic there is an increase in the number of free electrons.

With regard to the possibility of the liquid sodium amalgams being colloidal in nature as suggested by Paranjpe and Joshi,[8] it is evident that these data present nothing in favor of such a view. The breaks in Fig. 4 occur either at compounds or at an eutectic, and at no other points.

THERMAL CONDUCTIVITY OF SODIUM

The same procedure that was employed heretofore was used in the measurements on sodium. It was necessary, of course, to increase the buoyancy

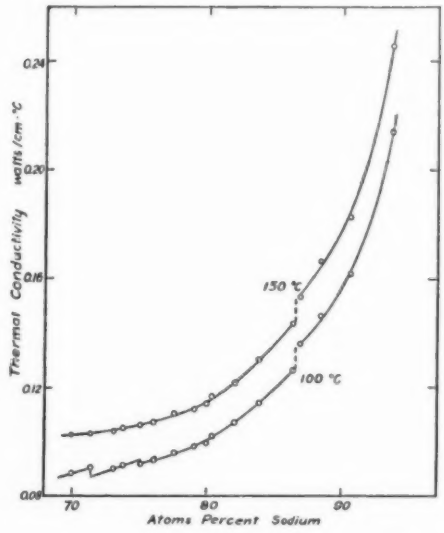

FIG. 4. The thermal conductivities of sodium amalgams.

of the heater on the molten sodium by means of a small support. Because of the high thermal conductivity of sodium the temperature gradient was quite small and varied from 1.15°C/cm to 3.45°C/cm at the extremes. Fig. 5 gives the results which were obtained.

The thermal conductivity of sodium in the range from 100°C to 210°C may be represented by the equation

$$K_t = 0.860[1 - 0.338\times10^{-3}(t-100) - 2.6\times10^{-6}(t-100)^2]$$

TABLE III. *Thermal conductivities of sodium amalgams at 100°C and 150°C.*

ALLOY	ATOMIC PERCENT SODIUM	THERMAL CONDUCTIVITY (WATT/CM −°C)	
		100°C	150°C
1	70.0	0.0887	0.1029
2	71.4	0.0907	0.1031
3	73.1	0.0903	0.1039
4	73.8	0.0916	0.1052
5	75.1	0.0921	0.1063
6	76.1	0.0934	0.1076
7	77.6	0.0960	0.1105
8	79.1	0.0983	0.1121
9	80.0	0.0996	0.1141
10	80.4	0.1022	0.1169
11	82.1	0.1073	0.1219
12	83.9	0.1146	0.1303
13	86.4	0.1266	0.1437
14	86.9	0.1362	0.1532
15	88.4	0.1463	0.1662
16	90.6	0.1619	0.1827
17	93.7	0.2140	0.2456

[5] W. C. Johnson and W. C. Fernelius, J. Chem. Ed. **7**, 981–99 (1930).
[6] Vanstone, J. Chem. Soc. London **105**, 2617 (1914); Bornemann and Müller, Métallurgie **7**, 396 (1909).
[7] Vanstone, Trans. Faraday Soc. **6**, 42 (1911).
[8] G. R. Paranjpe and R. M. Joshi, J. Phys. Chem. **36**, 2474 (1932).

where K_t is the thermal conductivity at t°C expressed in watt/cm −°C. The average deviation, regardless of sign, of the ten experimental points from this equation is slightly less than 0.4 percent.

Below the freezing point of sodium three measurements, which are included in Table IV, were made. As a check may be cited the value of thermal conductivity obtained by Bidwell[9] for sodium at 75°C of 1.13 watt/cm −°C. Extrapolation of the curve of Fig. 5 down to 75°C yields a value of 1.14 watt/cm −°C.

If one assumes that the experimentally determined curves for the solid and the liquid state can be extended exactly to the freezing point, which shall be taken at 97.5°C, one gets 0.861 watt/cm −°C for the thermal conductivity of liquid sodium at the freezing point, and 1.120 watt/cm −°C for solid sodium. The ratio of the thermal conductivity of the solid to the liquid state is thus 1.33. Porter and Simon[10] obtained 1.31 for the value of the same ratio.

Discussion

Table V presents the results of calculations of the Wiedemann and Frantz ratio and of Lorentz' number using the values of electrical conductivity obtained by Williams[11] for mercury, and listed in the International Critical Tables for sodium.

Table IV. *Thermal conductivity of solid sodium (cross section of sodium = 18.70 cm²).*

Mean Temp. (°C)	Temp. Gradient (°C/cm)	Power (Watts)	Thermal Conductivity (Watt/cm −°C)
84.7	1.15	24.47	1.133
88.2	1.27	26.78	1.128
91.5	1.37	28.92	1.127

Table V. *Wiedemann and Frantz ratio and Lorentz' number.*

Metal	Mercury			Sodium	
Temperature, °C	0	120	200	100	200
Thermal Conductivity, K (watt/cm −°C)	0.0819	0.1093	0.1237	0.860	0.808
Electrical Conductivity, σ (ohm^{-1} cm^{-1})	10630	9484	8726	102,000	73,600
Wiedemann and Frantz ratio, $(K/\sigma \times 10^6$ watt-ohm/°C)	7.70	11.53	14.17	8.43	11.0
Lorentz' number, $(K/\sigma T \times 10^9$ watt-ohm/$(°C)^2$)	2.82	2.93	2.99	2.26	2.32

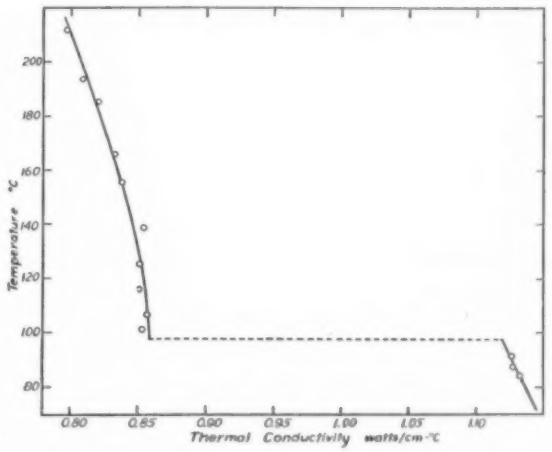

Fig. 5. The thermal conductivity of sodium.

Mercury is an exception to most metals, whether liquid or solid, in that its thermal conductivity increases with temperature. One can interpret this fact to mean that the effective number of free electrons increases with temperature. Mott[12] suggests that this would not be an unreasonable behavior for a divalent metal; however, many divalent metals exist which are normal in behavior. If one fails to take this interpretation, one must assume that the lattice conduction in mercury is large and that it increases with temperature. Such a view is inconsistent with the theory developed by Bloch,[13] and others.

The thermal conductivity of liquid sodium decreases in a normal manner as the temperature increases. But the liquid sodium amalgams are abnormal in their behavior, even when of high sodium content. In fact the conductivity increases with temperature at a more rapid rate as the sodium content increases.

In conclusion, the author wishes to express his thanks for the cooperation which was extended by the members of the department of physics at the University of Kansas, and to Dr. C. V. Kent in particular, who offered many useful suggestions.

[9] C. C. Bidwell, Phys. Rev. **28**, 584 (1926).
[10] Porter and Simon, Proc. Phys. Soc. **27**, 307 (1915).
[11] E. I. Williams, Phil. Mag. **50**, 589 (1925).
[12] N. T. Mott, Proc. Roy. Soc. **146**, 465 (1934).
[13] Bloch, Zeits. f. Physik **59**, 208 (1930).

Internal Friction in Solids

V. General Theory of Macroscopic Eddy Currents

CLARENCE ZENER
College of the City of New York

(Received April 30, 1938)

In vibrating ferromagnetic metals macroscopic eddy currents tend to shield the interior of the metal from changes in magnetic induction. The dissipation of energy by these eddy currents contributes to the internal friction of the metal. This internal friction has previously been investigated theoretically only for longitudinal vibrations, and only the asymptotic formulae for high and low frequencies have been found. In this paper this internal friction is calculated for all frequencies for both longitudinal and transverse vibrations. The theory of internal friction due to macroscopic eddy currents is shown to be formally identical with the theory of internal friction due to macroscopic thermal currents. The methods developed by the author for the study of thermoelastic internal friction are thus directly applicable to the study of the macroscopic electric eddy currents.

§1. INTRODUCTION

PART of the internal friction of ferromagnetic metals arises from the magnetic-elastic coupling. Under certain conditions this part is of a larger order of magnitude than the internal friction of nonferromagnetic origin. In spite of numerous experimental investigations,[1] only one source of ferromagnetic internal friction has been theoretically investigated[2] for small strains, namely that due to the macroscopic eddy currents. These eddy currents tend to shield the interior of the sample from changes in magnetic induction. Further, this effect has only been investigated for longitudinal vibrations, and only the asymptotic values for high and low frequencies have been obtained. In this paper the internal friction due to macroscopic eddy currents is calculated at all frequencies for the longitudinal and transverse vibrations of circular rods, and for the transverse vibrations of reeds.

It is found that the internal friction due to the eddy currents may be written in the form

$$Q^{-1}=[(E_B-E_H)/E_B]f(\nu). \tag{1}$$

Here Q^{-1} is $(1/2\pi)$ times the fraction of the vibrational energy dissipated per cycle. E_B and E_H are Young's moduli for constant magnetic induction and constant magnetic field, respectively. The first factor may be calculated by means of Eq. (14). The second factor is given in §3 for the three cases, and is plotted in Fig. 1. The asymptotic expressions for f at high and low frequencies are shown in Fig. 1 by broken lines, and are likewise given explicitly in §3. The frequency of maximum internal friction is determined by the magnetic diffusion constant D_H. This is given by

$$D_H=10^8/(0.4\pi\mu\sigma), \tag{2}$$

where μ is the differential magnetic permeability, and the electric conductivity σ is in ohm^{-1} cm^{-1}. The area beneath all three curves is the same, namely $\frac{1}{2}\pi \log_{10} e=0.682$. This is a direct consequence of the general formula

$$\int_0^\infty f(\nu)\nu^{-1}d\nu=\pi/2, \tag{3}$$

valid for a specimen of arbitrary cross section in which the only stress associated with the vibration is a tensile stress along the axis of the specimen.

The method used in the present investigation is that developed by the author for studying the internal friction due to macroscopic thermal currents.[3] The differential equations for the two problems become identical when T and S are replaced by H and $B/4\pi$, respectively. The two problems would be identical if the adiabatic boundary condition for thermal flow were replaced by an isothermal boundary condition.

[1] E. Giebe and E. Blechschmidt, Ann. d. Physik **11**, 905 (1931); O. v. Auwers, Ann. d. Physik **17**, 83 (1933); J. Zacharias, Phys. Rev. **44**, 116 (1933); W. T. Cooke, Phys. Rev. **50**, 1158 (1936); Mary D. Waller, Proc. Phys. Soc. **50**, 144 (1938).

[2] M. Kersten, Zeits. f. tech. Physik **15**, 463 (1934); W. F. Brown, Phys. Rev. **50**, 1165 (1936).

[3] C. Zener, Phys. Rev. **52**, 90 (1938).

Thus the thermoelastic internal friction due to macroscopic thermal currents would, if the surface were maintained at constant temperature, be given by Eq. (1) and Fig. 1, the subscripts H and B being replaced by T and S, respectively.

§2. General Theory

The theory for longitudinal and transverse vibrations is particularly simple when the wavelength of vibration is large compared with the transverse dimensions of the specimen. In the first place, all stresses are then negligible compared with the tensile stress parallel to the specimen's axis. If this axis is denoted as the z axis, the energy loss per cycle per unit volume is then

$$\Delta w = \nu^{-1} \text{ time average of } Z_z de_{zz}/dt. \quad (4)$$

In the second place, the transverse components of the oscillating part of the magnetic field and magnetic induction may then be neglected compared with the parallel components. Thus Z_z may be written as a linear function of only e_{zz} and ΔH_z, the fluctuation of H_z from its mean.

$$Z_z = (\partial Z_z/\partial e_{zz})_{H(z)} e_{zz} + (\partial Z_z/\partial H_z)_{e(zz)} \Delta H_z. \quad (5)$$

We are here neglecting a term proportional to the temperature fluctuation. The effect of this thermoelastic term has already been investigated by the author.

By substituting (5) into (4) we obtain

$$\Delta w = \nu^{-1} (\partial Z_z/\partial H_z)_{e(zz)} \text{ time average of } \Delta H_z de_{zz}/dt. \quad (6)$$

We must now find the differential equation which ΔH_z obeys. This is obtained of course from Maxwell's equations. Here the displacement current may be neglected compared with the real current, since their ratio is given by $\epsilon\sigma/(1.8\times 10^{12}\sigma)$, where σ is the electric conductivity in ohm^{-1} cm^{-1}. Elimination of the electric field from Maxwell's equations then gives

$$(d/dt)\mathbf{B} = -(10^8/0.4\pi\sigma) \text{ curl curl } \mathbf{H}.$$

If we take the z component of this vector equation, and use our previous approximation of neglecting H_y and H_x, we obtain

$$(d/dt)B_z = (10^8/0.4\pi\sigma)(\partial^2/\partial x^2 + \partial^2/\partial y^2) H_z.$$

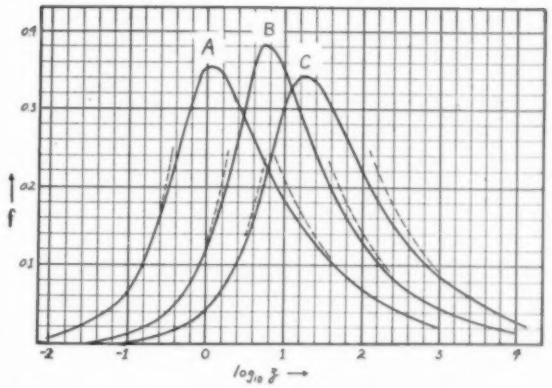

Fig. 1. f functions associated with macroscopic eddy currents. Curve A, transverse vibration of reed. $\zeta = D_H/2\pi d^2$, d = transverse width of reed. Curve B, longitudinal vibration of circular rod. $\zeta = D_H/2\pi a^2$, a = radius of rod. Curve C, transverse vibration of circular rod. $\zeta = D_H/2\pi a^2$, a = radius of rod.

On introducing the relation

$$\delta B_z = (\partial B_z/\partial H_z)_{e(zz)} \delta H_z + (\partial B_z/\partial e_{zz})_{H(z)} \delta e_{zz},$$

we obtain

$$(d/dt)\Delta H_z = D_H(\partial^2/\partial x^2 + \partial^2/\partial y^2)\Delta H_z + (\partial H_z/\partial e_{zz})_{B(z)} de_{zz}/dt. \quad (7)$$

Here D_H is defined by Eq. (2) with

$$\mu = (\partial B_z/\partial H_z)_{e(zz)}.$$

The first term on the right side represents the change in H_z arising from diffusion of the magnetic induction. The second term represents the change arising solely from the change in strain. This would be the only term in the absence of diffusion, i.e., if the electric conductivity were infinite.

The function de_{zz}/dt is affected only very slightly by the magnetic-elastic coupling. Hence very little error is introduced in Δw by regarding de_{zz}/dt in Eqs. (6) and (7) as specified by the elastic equations in the absence of this coupling. The function ΔH_z is then completely determined by Eq. (7) and by the appropriate boundary condition.

We have previously assumed the wave-length of the vibration to be long compared with the transverse dimensions of the sample, and also the transverse components of the oscillating part of H and B to be negligible compared with the parallel component. To this same approximation we may neglect ΔH_z outside the speci-

men. The appropriate boundary condition is thus

$$\Delta H_z = 0 \text{ at surface.} \tag{8}$$

Equations (6), (7), (8) contain the physics of our problem. The mathematics involved in the solution of Eq. (7) subject to the boundary condition (8), in taking the time average in Eq. (6), and finally in evaluating the integral

$$Q^{-1} = \frac{\int \Delta w dv}{2\pi \text{ energy of vibration}}$$

has been formally solved in the appendix of reference 3. The result is

$$Q^{-1} = [(E_B - E_H)/E_B] \sum f_k \nu_k \nu / (\nu_k^2 + \nu^2), \tag{9}$$

where f_k satisfies the condition

$$\sum f_k = 1. \tag{10}$$

The constants f_k and ν_k are interpreted in terms of the differential equation

$$\{D_H(\partial^2/\partial x^2 + \partial^2/\partial y^2) + 2\pi\nu_k\} U_k(x, y) = 0 \tag{11}$$

together with the boundary condition

$$U_k = 0 \text{ at surface.} \tag{12}$$

The ν_k are the eigenwert of this equation. The f_k are the squares of the coefficients of the expansion of the normalized function

$$e_{zz} \Big/ \left[\int e_{zz}^2 dx\, dy\right]^{\frac{1}{2}} \tag{13}$$

in terms of the normalized eigenfunctions U_k. Here e_{zz} is taken at an arbitrary z and t.

The ratio $(E_B - E_H)/E_B$ may be calculated in terms of the magnetostriction constant and the permeability by means of the equation[2]

$$(E_B - E_H)/E_B = 4\pi E_H (\partial e_{zz}/\partial H_{zz})_{z(z)}^2 / (\partial B_z/\partial H_z)_{z(z)}. \tag{14}$$

This equation may be derived in exactly the same way as the equation

$$(E_S - E_T)/E_S = E_T (\partial e_{zz}/\partial T)_{z(z)}^2 / (\partial S/\partial T)_{z(z)}.$$

§3. Application to Special Cases

In the previous section we found that the Q^{-1} of a rod of arbitrary cross section vibrating either longitudinally or transversely is given by $(E_B - E_H)/E_B$ times the function

$$f(\nu) = f_k \nu_k \nu / (\nu_k^2 + \nu^2). \tag{15}$$

In this section we describe in detail the evaluation of this function for one particular case, the transverse vibration of a circular rod, and then give the results for the longitudinal vibration of a circular rod, and for the transverse vibration of a reed.

Circular rod: transverse vibration

Let a be the radius of the circular rod. Then those eigenfunctions of Eq. (11) which satisfy the boundary condition (12), and whose associated coefficients in the expansion of

$$e_{zz} = \text{constant} \times r \cos\varphi$$

do not vanish, are given by

$$\cos\varphi J_1(q_k r/a).$$

Here q_k is the kth root of

$$J_1(q) = 0,$$

and determines the eigenwert ν_k by the equation

$$q_k = (2\pi\nu_k/D_H)^{\frac{1}{2}} a. \tag{16}$$

We may now write f_k explicitly as

$$f_k = \frac{\left(\int_0^a r^2 J_1(q_k r/a) dr\right)^2}{\int_0^a r^3 dr \int_0^a r J_1^2(q_k r/a) dr}.$$

With the aid of the integral formulae for Bessel functions[4] we obtain, as in reference 3, §2,

$$f_k = \frac{8 J_2^2(q_k)}{q_k^2 \{J_1^2(q_k) - J_0(q_k) J_2(q_k)\}}.$$

Since $J_1(q_k) = 0$, the recurrence formulae for Bessel functions[5] gives

$$J_2(q_k) = -J_0(q_k).$$

Hence

$$f_k = 8/q_k^2. \tag{17}$$

[4] See E. Jahnke and F. Emde, *Funktionentafeln* (Teubner, 1933), pp. 213–214.

[5] See G. N. Watson, *Theory of Bessel Functions* (Cambridge, 1922), p. 17.

As a check upon Eq. (10), we note that[6]

$$\sum q_k^{-2} = \tfrac{1}{8}.$$

On substituting Eqs. (16) and (17) into Eq. (15), we obtain

$$f(\nu) = 8z\sum (q_k^2 + z^2)^{-1}, \qquad (18)$$

where

$$z = (2\pi a^2/D_H)\nu.$$

The asymptotic expressions for small and large z may readily be obtained. From[6]

$$\sum q_k^{-4} = 1/192$$

we obtain

$$f(\nu) = z/24 \quad \text{when} \quad z \ll 1.$$

By observing that when k is large, successive k's differ by π, we obtain, for large z's,

$$f(\nu) = (8z/\pi)\int_0^\infty (q^4 + z^2)^{-1} dz.$$

Hence $$f(\nu) = 2^{\frac{1}{2}} z^{-\frac{1}{2}} \quad \text{when} \quad z \gg 1.$$

When z is of the order of magnitude of unity, $f(\nu)$ may be evaluated by means of the rapidly converging series (18). In plotting this function in Fig. 1, the values of q_k were taken from reference 5, p. 748.

Circular rod: longitudinal vibration

The constant f_k is given by

$$f_k = 4/q_k^2,$$

where q_k is the kth root of

$$J_0(q) = 0.$$

The constant ν_k is related to q_k by Eq. (16). The function f is given in terms of $z = (2\pi a^2/D_H)\nu$ by

$$4z \sum_{k=1}^{\infty} (q_k^4 + z^2)^{-1} \text{ exactly,}$$

by $z/8$ when $z \ll 2\pi$,

by $(2/z)^{\frac{1}{2}}$ when $z \gg 2\pi$.

These two asymptotic expressions have previously been obtained.[2]

Reed: transverse vibrations

Let d be the width of the reed in the plane of vibration. Then

$$f_k = 6/\pi^2 k^2,$$

$$\nu_k = k^2 D_H/2\pi d^2.$$

The function f is given in terms of $z = (2\pi d^2/D_H)\nu$ by

$$6\pi^{-2} z \sum_{k=1}^{\infty} (k^4 + z^2)^{-1} \text{ exactly,}$$

by $(\pi^2/15)z$ when $z \ll 4\pi$,

by $(3/\pi\sqrt{2})z^{-\frac{1}{2}}$ when $z \gg 4\pi$.

[6] Reference 5, p. 502.

LETTERS TO THE EDITOR

Prompt publication of brief reports of important discoveries in physics may be secured by addressing them to this department. Closing dates for this department are, for the first issue of the month, the eighteenth of the preceding month, for the second issue, the third of the month. Because of the late closing dates for the section no proof can be shown to authors. The Board of Editors does not hold itself responsible for the opinions expressed by the correspondents.

Communications should not in general exceed 600 words in length.

The Scattering of Neutrons by Deuterons

The angular distribution of 328 tracks of recoil deuterons has been studied. These tracks have been selected from one thousand tracks measured on 3000 photographs, which were taken with the aid of an expansion chamber. The chamber was filled with 54.3 percent deuterium, 37 percent argon, 6 percent nitrogen, and 2.7 percent heavy water vapor; this mixture was bombarded with neutrons of 2.6 Mev energy from the deuteron-deuteron reaction. The criterion for selecting the above tracks was established by using: (1) the calculated stopping power of the gas mixture, (2) the pressure variation within which tracks can form, (3) the energy-range relationship for deuterons,[1] and (4) the energy variation in the neutrons caused by (a) loss of energy of the incident deuteron beam in the thick heavy-ice target and (b) the angular aperture of the detector. To these selected tracks have been applied the necessary azimuthal, area, and random track corrections, in a manner similar to that used in the study of the scattering of neutrons by protons.[2]

The results are given in Table I and Fig. 1.

TABLE I. *Observations on the distribution and angle of the recoil deuterons bombarded with neutrons. $\Delta\phi$ is the scattering angle interval. N is the number of tracks observed in each $\Delta\phi$. C is the total correction factor. N_c is the number of tracks, corrected. $N_c/(\Delta\omega\cdot\Delta\phi)$ is the number of tracks per unit solid angle per unit $\Delta\phi$. $\%/(\Delta\omega\cdot\Delta\phi)$ is the relative number of tracks per unit solid angle per unit $\Delta\phi$.*

$\Delta\phi$	N	C	N_c	$N_c/(\Delta\omega\cdot\Delta\phi)$	$\%/(\Delta\omega\cdot\Delta\phi)$
0–9	17	3.2	55	7050	25
10–19	31	3.3	102	4600	16
20–29	38	3.5	132	3310	12
30–39	47	2.4	114	2280	8
40–49	53	3.0	158	2525	9
50–59	69	3.6	247	3470	12
60–69	54	5.2	281	3560	13
70–79	18	6.7	121	1447	5

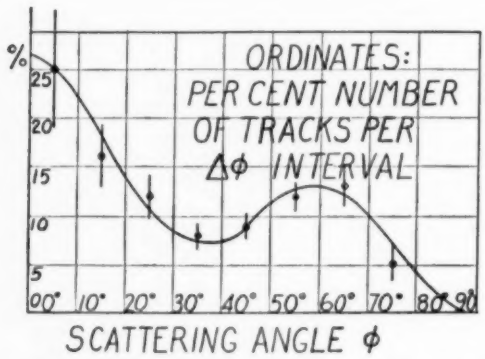

FIG. 1. Distribution and angle of deuterons recoiling from neutron collisions.

Although these results are based on a small number of tracks (328), the data indicate that there is present a marked deviation from spherically symmetrical scattering in the center of mass system. More data are needed before the precise shape and size of the peak in the curve (cf. Fig. 1) at scattering angle $\phi=60°$ can be determined.

The marked departure from S scattering in this experiment can possibly be explained in three ways. Massey and Mohr,[3] assuming a rectangular potential hole of radius 4×10^{-13} cm and one of 6×10^{-13} cm, obtained curves which are not far different in shape from our curve, except at small angles. Their calculations include 1 Mev and 6.25 Mev neutrons and take into account P scattering. It seems likely that the choice of a different potential hole with further regard for the structure of H^{3} [4] might allow agreement with this experiment. A second possibility,[5] to account for the marked difference from S scattering and the scattering predicted by Massey and Mohr at the small angles (0°–20°), would be to include the effect of a polarization of the deuteron by the incident neutron. A third possibility is to include higher orders of partial waves in the description of the scattered neutron wave.

From the stopping power of the gas in the chamber, the range-energy relation, and the maximum track length extrapolated in the usual way in the scattering angle intervals 0°–10°, 0°–20°, 0°–30°, the range of a recoil deuteron at 0° scattering angle has been calculated. This has been used to determine the disintegration energy Q for the reaction

$$ {}_1D^2+{}_1D^2\rightarrow{}_2He^3+{}_0n'+Q $$

and leads to a value of $Q=3.40\pm0.10$ Mev. This value, because it is based on deuteron recoil atoms, is an independent check on the value recently given by Bonner,[6] and agrees very well.

A more complete description of this experiment will be ready for publication shortly.

P. G. KRUGER
W. E. SHOUPP
R. E. WATSON
F. W. STALLMANN

Physics Department,
University of Illinois,
Urbana, Illinois,
May 17, 1938.

[1] H. Bethe, Phys. Rev. **53**, 313 (1938).
[2] P. Gerald Kruger, W. E. Shoupp, and F. W. Stallmann, Phys. Rev. **52**, 678 (1937).
[3] H. W. S. Massey and C. B. O. Mohr, Proc. Roy. Soc. **148A**, 206 (1935).
[4] L. I. Schiff, "Scattering of Neutrons by Deuterons," Phys. Rev. **52**, 149 (1937).
[5] This idea was suggested by Dr. J. H. Bartlett, Jr.
[6] T. W. Bonner, Phys. Rev. **53**, 711 (1938).

The Molecule of Sulphur and Its Raman Spectrum

Warren and Burwell[1] have recently shown that rhombic sulphur consists of S_8 molecules; the atoms in each molecule are located at the corners of a puckered octagon. We will now apply the methods based on group theory as developed by Wigner,[2] Tisza,[3] and others for investigating the normal modes of oscillation of such a molecule. There are sixteen symmetry operations which transform the model into itself and these operations form the point group S_{8u}. There are seven irreducible representations for this group and the character Table I obtained from the general tables given by Tisza is given.

The significance of h_j, x_j', n_i and n_i' is the same as that in a recent paper by Wilson.[4] The activity or otherwise of these oscillations is also given in the last two columns of the table. *P* indicates a strong and well-polarized Raman line. *D* indicates a completely depolarized Raman line and *f* stands for a forbidden line. The table shows that we should expect two strong and well polarized lines and five depolarized lines in the Raman spectrum of sulphur.

Venkateswaran[5] has recently obtained the complete Raman spectrum in which eight lines at 88, 114, 152, 185, 216, 243, 434 and 468 have been recorded. He has given good reasons to show that the lowest frequency is to be attributed to the lattice and not to the molecule. The molecular frequencies are therefore only seven and two amongst these, namely 216 and 468, have been found to be strong and well polarized in complete accord with our conclusions. These two represent the total symmetric vibrations A_1. All the other five, namely 114, 152, 185, 243 and 434 should be completely depolarized according to the theory. The stronger of these (152 and 434) have been found to be so but data in respect of others are not given by Venkateswaran presumably because they are weak. The Raman spectrum data so far as are available may thus be taken to be in complete accordance with the model proposed by Warren and Burwell. Interpretation of the infrared spectrum and a more detailed analysis of the vibrational modes and frequencies will be given elsewhere.

S. Bhagavantam

Department of Physics,
Andhra University, Waltair, India,
April 13, 1938.

[1] Warren and Burwell, J. Chem. Phys. **3**, 6 (1935).
[2] Wigner, Göttinger Nachrichten, 133 (1930).
[3] Tisza, Zeits. f. Physik. **82**, 48 (1933).
[4] Wilson, Phys. Rev. **45**, 706 (1934).
[5] Venkateswaran, Proc. Ind. Acad. Sci. **4**, 345 (1937).

Radioactive Iodine Isotopes

We have bombarded tellurium with 8 Mev deuterons and have found two new radioactive iodine isotopes, with half-lives of 13 hours and 8 days. The latter is created by two mechanisms: (1) by the decay of radio-tellurium and (2) by direct transmutation from stable tellurium. Process (1) is demonstrated by the fact that successive extractions of iodine, from the same solution of bombarded tellurium, show a growth of the 8-day period; this must therefore be associated with either I^{129} or I^{131}, as the second activity of a double decay: $Te^{128, 130}(d, p)Te^{129, 131}$; $Te^{129, 131} \rightarrow I^{129, 131} \rightarrow Xe^{129, 131}$. Process (2), which is known to occur on the basis of relative intensities, is the usual type of reaction: $Te^{128, 130}(d, n)I^{129, 131}$. Conclusive proof of this identification and interpretation has been furnished by the extraction of the 8-day iodine from tellurium which has been bombarded with neutrons. We cannot as yet state the period of the radio-tellurium from which this iodine grows.

Absorption measurements on the negative electrons emitted by the 8-day iodine indicate a maximum energy of 0.9 Mev; a gamma-ray is also present.

We have irradiated iodine with the fast neutrons from a lithium plus deuterons source and confirm the 13-day period reported for the same bombardment by Tape and Cork,[1] who surmised it to be due to I^{126}. We have chemically identified this activity as an iodine isotope, so that the assignment to I^{126} appears to be definite. (The antimony fraction of this same bombardment was inactive, while the tellurium precipitate exhibited a 10-hour half-life which can be ascribed definitely to Te^{127}. This tellurium period has been reported previously,[1] following neutron and deuteron bombardment of tellurium, but without definite isotopic identification.)

The yield of the 8-day iodine from $Te(d, n)I$ is very much larger than that of the strongest 13-day iodine that we have been able to produce by the reaction $I^{127}(n, 2n)I^{126}$.

This research has been aided by grants from the Research Corporation, The Chemical Foundation and the Josiah Macy Jr. Foundation.

J. J. Livingood
G. T. Seaborg

Radiation Laboratory, Physics Dept. (J. J. L.)
Chemistry Department (G. T. S.),
University of California,
Berkeley, California,
June 1, 1938.

[1] G. F. Tape and J. M. Cork, Phys. Rev. **53**, 676 (1938).

Table I.

	E	$2S^1$	$2C^2$	$2S^3$	C^4	$4\sigma_v$	$4C_2$	n_i	*R* & *T*	n_i'	Raman	Infra-red
A_1	1	1	1	1	1	1	1	2	—	2	*P*	*f*
A_2	1	1	1	1	1	−1	−1	1	R_z	0	—	—
B_1	1	−1	1	−1	1	1	−1	2	T_z	1	*f*	$M_\perp=0$
B_2	1	−1	1	−1	1	−1	1	1	—	1	*f*	*f*
E_1	2	$\sqrt{2}$	0	$-\sqrt{2}$	−2	0	0	3	$T_\perp$	2	*f*	$M_z=0$
E_2	2	0	−2	0	2	0	0	3	$R_\perp$	2	*D*	*f*
E_3	2	$-\sqrt{2}$	0	$\sqrt{2}$	−2	0	0	3	—	3	*D*	*f*
h_j	1	2	2	2	1	4	4					
x_j'	24	0	0	0	0	2	0					
$h_j x_j'$	24	0	0	0	0	8	0					

Radioactivity of Be^7

As reported at the Washington meeting of the American Physical Society[1] we have obtained evidence for the formation of Be^7 in the reaction $Li^6+H^2 \rightarrow Be^7+n$. At that time we had found that there was no radioactive emission of charged particles. We have since discovered a gamma-ray radioactivity with a 43-day half-life in lithium targets which have been bombarded by deuterons. Further experiments indicate that the gamma-ray activity originates in K electron capture by Be^7 which leaves the residual Li^7 nucleus in the 450-kv excited level.

The activity was first observed in a LiF target which had been bombarded a month previously with 35 microampere hours of 1000-kv deuterons. Similar activity was subsequently produced by bombarding a lithium metal target with 20 microampere hours of 1000-kv deuterons. The activity was followed for a month and showed a half-life of 43 ± 6 days. The absorption-coefficient in lead was 0.169 g cm^{-1}. No charged particles could be detected either by thin-walled counters, by ionization chambers, or by placing the sample in a cloud chamber, although the gamma-ray counting rate indicated the emission of more than 100 quanta per second.

The surface of the target (in which the activity was concentrated) was scraped off and subjected to a chemical separation, carried out by Dr. M. H. Van Horn of George Washington University. The activity was concentrated in the final precipitation of 100 micrograms of beryllium carbonate which had been added as a carrier. The separation would not, however, remove iron or aluminum. As iron also shows a 40-day period, we bombarded an iron target and looked for a similar gamma-ray. The iron impurity necessary to produce the observed gamma-rays from the lithium targets is greater than 100 percent.

Although we were not able to detect the alpha-particle group produced in the reaction[1] $B^{10}+H^1 \rightarrow Be^7+He^4$, we have since observed a long period gamma-ray activity from a B_4C target which had been bombarded with 11 microampere hours of 950-kv protons. The intensity of the radiation was 25 percent less than that produced in the lithium metal target. Its absorption-coefficient was also 0.169 g cm^{-1}. We therefore ascribe both this activity and that produced in the lithium targets to Be^7.

This unusual type of radioactivity could originate in two nuclear reactions. Either a positron is emitted with so little energy that it does not ionize appreciably and is detected only by the annihilation radiation, or a K electron is captured and the residual nucleus is left in an excited state. In the latter case the average number of quanta per disintegration is less than one because there exists the alternative process of capture in which the nucleus is left in the ground state. Assuming as usual that a neutrino is emitted, these reactions may be written:

$$Be^7 \rightarrow Li^7+e^++\eta$$
$$e^++e^- \rightarrow h\nu+h\nu \qquad h\nu=0.5 \text{ Mev}$$
$$Be^7+e_k^- \rightarrow Li^7+\eta \qquad \text{neutrino energy}=E \text{ Mev}$$
$$Be^7+e_k^- \rightarrow Li^{7*}+\eta \qquad \text{neutrino energy}=E-0.45 \text{ Mev}$$
$$Li^{7*} \rightarrow Li^7+h\nu \qquad h\nu=0.45 \text{ Mev}$$

The absorption-coefficient in lead of the gamma-rays from the lithium targets and of the annihilation radiation of the positrons from N^{13} were measured under idential conditions and were observed to be 0.169 ± 0.008 and 0.130 ± 0.002 g cm^{-1}, respectively. This indicates that the energy of the radiation is 425 ± 25 kv, which agrees well with the energy expected from K electron capture but differs from the energy of annihilation radiation.

A comparison of the numbers of quanta observed per neutron emitted from the carbon and lithium targets gives additional information about the process. Li^6 and Li^7 are (per atom) equally effective in producing neutrons at 800 kv and the yield curves for the two reactions are known.[2] The energy distribution of the neutrons from Li^6 shows that approximately one atom of Be^7 is formed for every two neutrons emitted. In carbon one neutron is emitted for each N^{13} atom formed. The comparison of the number of neutrons emitted by lithium and carbon has been made by Amaldi, Hafstad, and Tuve.[3] Thus the relative numbers of Be^7 and N^{13} atoms can be calculated. Assuming two quanta per N^{13} we find that, on the average, one quantum is emitted for each 10 Be^7 atoms produced. Positron-emission should lead to a gamma-ray intensity 20 times greater than that observed. On the other hand the data are consistent with the hypothesis of K electron capture, because in this case transitions to the ground state should be more probable than transitions to excited levels.

As a final check we have looked for double coincidence counts. No appreciable change in the background rate of 0.8 per minute was observed although the simultaneous emission of two quanta at 180°, which would be expected if positron annihilation occurred, should increase the rate by at least a factor of three.

R. B. Roberts
N. P. Heydenburg
G. L. Locher

Department of Terrestrial Magnetism (R. B. R. and N. P. H.), Carnegie Institution of Washington, Washington, D. C.,
Bartol Research Foundation of the Franklin Institute (G. L. L.), Swarthmore, Pennsylvania,
May 27, 1938.

[1] R. B. Roberts and N. P. Heydenburg, Abstract No. 78, 1938 Washington Meeting American Physical Society.
[2] L. H. Rumbaugh, R. B. Roberts, and L. R. Hafstad, to be published shortly in Phys. Rev.
[3] E. Amaldi, L. R. Hafstad, and M. A. Tuve, Phys. Rev. **51**, 896–912 (1937).

The Transmutations of the Cosmic-Ray Electrons and the Nuclear Forces

The "transmutations of mass" (i.e., the changes of the rest mass) of the electrons probably play an important role in the passage of cosmic rays through the atmosphere. Thus according to Blackett[1] the cosmic-ray particles at sea level are heavy when energetic, but change their mass suddenly when slowed down below a critical energy of about $2\text{–}3\cdot10^8$ ev and become ordinary electrons. According to Bowen, Millikan and Neher[2] the penetrating heavies are mainly secondaries produced in the atmosphere by incoming electrons and photons. However this conclusion, does not necessarily follow from the data of the authors mentioned;

these data are consistent also with the assumption of a primary character of the penetrating heavies.

No adequate mechanism has been suggested up to now for these transmutations of mass. The suggestions of Jauncey[3] and Bhabha[4] can be shown to be untenable. The creation of heavy pairs by photons does not account for the disappearance of the slowed down heavies. Youkawa's hypothesis of a spinless heavy electron seems to lead to difficulties[5] and will not be considered by us.

Considerations connected with the principle of detailed balance and also with the probable dependence of the cross section for transmutation on the atomic weight of the substance traversed, seem to indicate, that the heavies are stable in absence of atomic nuclei and that the transmutation of mass can be induced only by a nonelectromagnetic short range interaction of an electron with protons and neutrons.

Let us assume, that this interaction is of the δ-type and corresponds to terms of the form

$$\psi_k^* \psi_e \Psi^* \Psi \tag{1}$$

in the Hamiltonian, where ψ_k and ψ_e are the wave functions of electrons of mass km_0 and lm_0, respectively, and Ψ the wave function of a proton or a neutron.

Consider an electron of mass m_1 and energy E hitting a nucleus and scattered by it with a modified mass m_2. If the recoil of the nucleus is neglected

$$E = c(m_1^2c^2 + p_1^2)^{\frac{1}{2}} = c(m_2^2c^2 + p_2^2)^{\frac{1}{2}}, \tag{2}$$

where p_1 and p_2 are the momenta of the incident and the scattered electrons.[6]

The cross section σ for the transmutation $m_2 \rightarrow m_1$ differs from that for the transmutation $m_1 \rightarrow m_2$ by the factor

$$\frac{p_1^2}{p_2^2} = \frac{E^2 - m_1^2c^4}{E^2 - m_2^2c^4},$$

so that it is sufficient to consider only the case for which (for instance) $m_1 < m_2$. In this case σ vanishes for $E < m_2c^2$ and then increases with increasing E somewhat faster than E^2. But when the wave-length of the electron becomes comparable with the nuclear radius ($E \approx A^{-\frac{1}{3}} \cdot 7 \cdot 10^7$ ev, where A is the atomic weight) the interference of the partial waves scattered by different particles of the nucleus makes σ tend with increasing E to a constant "stationary" value σ_{st} and also ensures the preponderance of the forward scattering. σ_{st} is proportional to $A^{4/3}$. But if E exceeds about $2 \cdot 10^8$ ev the recoil of the nuclear particles can no longer be neglected, since the recoil energy exceeds their binding energy (if the angle of scattering is not very small). In consequence σ will again begin to increase in proportion to E^2. Hence, as long as σ has at $E = 10^{10}$ ev any reasonably moderate value, its value at $E \leqslant 5 \cdot 10^8$ ev must be quite negligible.

However, in the domain of very high energies the validity of the above calculations becomes questionable. It is known, that interactions of the type considered lead to divergent results even in such approximations, which can be satisfactorily treated by the present quantum electrodynamics. Thus the interaction under consideration implies the possibility for a neutron or a proton to create a pair, the electron and the positron of the pair having eventually different masses. Hence there must exist certain forces between neutrons and protons which correspond to the exchange of pairs between these particles. But if one tries to evaluate in the first approximation the energy $\vartheta(r)$ of this interaction one gets a divergent result, even if the separation r of the interacting particles is finite.[7]

In absence of any better theory let us introduce in the interaction operator (1) some "guillotine factor," e.g. the factor $e^{-\tau(p_k + p_l)}$; p_k and p_l are the momenta of the electrons of mass km_0 and lm_0, measured in that reference system, in which the nucleus is at rest. This factor makes the energy $\vartheta(r)$ finite: at large distances $\vartheta(r)$ varies as r^{-s}, but tends to a finite value $\vartheta(0)$ as r tends to zero.

But the guillotine factor will affect also the cross section for the scattering of electrons with transmutation of mass. No such factor is needed in the case of the Coulomb scattering since for the latter only distant encounters are essential, while the guillotine factor accounts in some very crude manner for the finite size of the interacting particles. On account of this factor the probability of transmutations of energetic electrons will become very small, but, if $\tau = 400\ m_0c$, it will rapidly increase as the electrons are slowed down to about $3 \cdot 10^8$ ev and at $E \approx 2 \cdot 10^8$ ev σ will reach the "stationary" value defined above. This is in accordance with Blackett's measurements.

With this value of τ one gets for the energy of interaction of nuclear particles a reasonable estimate $\vartheta(0) \approx -3N^2(\sigma_{st}^{\text{air}} \cdot 10^{25}) \times 10^6$ ev where σ_{st}^{air} is the "stationary" value of σ in air expressed in cm^2, and N the number of allowed values of the mass km_0 of an electron. The sign and the spin dependence (if any) of $\vartheta(0)$ are correct.

The possibility of explaining the nuclear forces by the exchange of pairs between neutrons and protons has already been suggested by Gamow and Teller[8] and by Wentzel,[9] who, however, considered only ordinary electrons ($m = m_0$) and were unable to establish any connection between the proposed explanation of nuclear forces and other physical phenomena. As pointed out by these authors, the forces due to the exchange of pairs do not depend on the electric charge of the nuclear particles and are consistent with Wick's explanation of the magnetic moment of the neutron. The only serious difficulty is that they apparently do not possess saturation properties.

A more detailed communication will appear in *Comptes Rendus Acad. Sci. U. S. S. R.*

IG. TAMM

Physical Institute of the Academy of Sciences of U. S. S. R.,
Moscow, U. S. S. R.,
May 3, 1938.

[1] Blackett, Proc. Roy. Soc. **164**, 1 (1938).
[2] Bowen, Millikan and Neher, Phys. Rev. **53**, 217 (1938).
[3] Jauncey, Phys. Rev. **52**, 1256 (1937).
[4] Bhabha, Proc. Roy. Soc. **164**, 257 (1938).
[5] Serber, Phys. Rev. **53**, 211 (1938).
[6] In lectures held in Moscow and Leningrad in February I suggested that some of the cloud chamber tracks which apparently violate the conservation of energy may be explained on the basis of Eq. (2). Afterwards I learned that Zwicky also suggested a similar explanation cf., Phys. Rev. **53**, 315 and 611 (1938).
[7] Although the integration may be arranged in such a way as to give a finite result at finite r's, still if one performs the integrations in a somewhat different succession the integrals do diverge even at finite r's. The reason at the bottom of this is that the interaction corresponds to the exchange of *pairs* of particles, and not of separate particles.
[8] Gamow and Teller, Phys. Rev. **51**, 289 (1937).
[9] Wentzel, Helv. Phys. Acta **10**, 107 (1937).

Excitation of Nuclei by Bombardment with Charged Particles

Charged particles are able to excite nuclei without penetrating into the nucleus by means of the action of their electric field upon the nucleus when they pass nearby. The cross section for such a process can be calculated and is surprisingly large. An approximate expression for the cross section for the excitation of a transition from a level A with the orbital momentum $l=0$ to another level B with $l=L\geqq 2$ is given by

$$\sigma_L \leqq \frac{16\pi^2}{(2L+1)}\frac{L}{(2L-1)(2L-2)} \cdot \frac{1}{Z^2}\frac{E'^2}{E^2}\left(\frac{\hbar v'}{2zZe^2}\right)^{2L-4}\frac{(Q_{AB})^{2L}}{\lambda\lambda'^{2L-3}}. \quad (1)$$

Here E and $2\pi\lambda$ are the energy and wave-length of the incident particle of charge ze; E', $2\pi\lambda'$, v' are its energy, wave-length and velocity after the nuclear excitation. Ze is the charge of the nucleus, and Q_{AB} is given by:

$$(Q_{AB})^L = \sum_i \int \phi_A^* r_i^L \phi_B d\tau,$$

where r_i are the radial coordinates of the nuclear protons and ϕ_A and ϕ_B are the eigenfunctions, respectively, of the nuclear states A and of one of the $2L+1$ degenerate states B.

The expression (1) is valid only so long as E is less than the potential barrier: $E<E_0=zZe^2/\rho$ (ρ nuclear radius). If E is greater than that limit, σ_L is to be multiplied by

$$\frac{(2L-1)}{(2L-2)}\left(\frac{E_0}{E}\right)^{2L-2}\left(1-\frac{E_0}{(2L-1)E}\right). \quad (2)$$

The exact formula for σ_L contains rather complicated expressions with E, E' and L and will be presented together with the derivation of (1) in a paper by M. S. Plesset and the present author which will appear shortly in the *Physical Review*.

The cross section σ_2 for the excitation of *one* quadrupole transition with an excitation energy of 1 Mev in a nucleus $Z=50$ by means of a proton of 6 Mev is according to (1): $\sigma_2=0.5\cdot 10^{-26}$ if one assumes $Q_{AB}=5\cdot 10^{-13}$. The cross sections for $L>2$ are much smaller. The dipole transitions which are not included in (1) are also very weak because of the smallness of nuclear dipole moments. The numerical values obtained by (1) are extremely sensitive to the value of Q_{AB}. The order of magnitude of Q_{AB} is deduced from γ-ray evidence.

It is possible to estimate the total excitation cross section; i.e., the sum of all cross sections for any possible excitation in a heavy nucleus. If the density of levels with $l=2$ is given by $\omega(E)$, the total cross section for excitation of a nucleus by means of a charged particle of an energy E is approximately (apart from the factor (2) if $E>E_0$)

$$\sigma_2^{\text{total}} = 5^{1/2}\pi^{5/2}\frac{1}{Z^2}\frac{E'^2}{E^2}\frac{Q^4}{\lambda\lambda'}T(E)\cdot\omega(E-E').$$

Here $E'=(5/2)T(E)$ and $2\pi\lambda'$ is the corresponding wave-length. The temperature $T(E)$ is given by $1/T=d\lg\omega/dE$ and $(E-E')$ is the average excitation energy of the nucleus after collision. Q is to be considered as the average value of the quadrupole moments corresponding to all possible transitions. One gets for the total excitation cross section of a nucleus with $Z=50$ with α-particles of 14 Mev: $\sigma_2^{\text{total}}\leqq 3\cdot 10^{-25}$ and a mean excitation energy of 10 Mev. An expression is used here for the level density given by Bethe[1] and Weisskopf,[2] and Q is taken equal to $0.4\cdot 10^{-13}$. This value of Q is computed from the radiation breadth of neutron capture levels. These results have to be considered as a rough estimate of the order of magnitude because of the uncertainty of the value of Q and $\omega(E)$.

The process described here may be of some interest for the investigations of nuclear excitation levels. Furthermore, after bombardment of nuclei with charged particles of high energy ($E>8$ Mev) one should expect that the excited nucleus emits a particle so that one gets processes of the kind $(p-p, n)$, or $(p-2p)$. This effect may be of some importance in bombardments of heavy nuclei; processes such as $(p-p, n)$, $(d-d, n)$, $(\alpha-\alpha, n)$ are not to be expected after penetration of the projectile into the nucleus since the re-emission of a charged particle by the compound nucleus is much less probable than the emission of neutrons.[2, 3] These reactions could, however, be produced in the way described here.

University of Rochester, Rochester, N. Y. V. F. WEISSKOPF
June 2, 1938

[1] H. A. Bethe, Phys. Rev. **50**, 332 (1936).
[2] V. F. Weisskopf, Phys. Rev. **52**, 295 (1937).
[3] E. J. Konopinski and H. A. Bethe, Phys. Rev. in press.

Heavy Electrons and β-Decay

Yukawa[1] has shown that nuclear forces of the correct magnitude and range can be accounted for by assuming the existence of new charged particles of mass about 137 times that of an electron and of zero spin. These heavy electrons have recently been observed[2] in expansion chamber photographs of cosmic rays and have consequently brought Yukawa's theory to general notice. If the heavy electron were formed from an electron and a mass-less neutrino it should be extremely unstable and should dissociate with the liberation of energy equal to 136 mc^2. It is difficult to see how it could ever exist long enough to be observed in cosmic rays. We can get over this difficulty by assuming the heavy electron to be formed from an electron and a "heavy neutrino" of mass 136 and spin $\frac{1}{2}$. It might now be possible to do away entirely with the conception of the mass-less neutrino, for it is evident that the emission of one of these heavy electrons obeying Bose statistics in β-disintegration would satisfy the statistical requirements of the nucleus. If this heavy electron then disintegrated into an electron and a heavy neutrino while still close enough to the nucleus to interact with it the continuous energy distribution of the β-rays would be qualitatively accounted for.

Bhabha[3] has pointed out that if the disintegration of the heavy electron is spontaneous it may be regarded as a "clock," and hence it follows merely from relativity considerations that the time of disintegration is longer the greater the velocity of the particle. A heavy electron of mass 137 formed as suggested above from an electron and a heavy neutrino of mass 136 would be just on the point

of instability since it would have no mass defect. It is of interest, therefore, to see if its much greater velocity in cosmic rays would increase its time of dissociation sufficiently to enable it to be observed.

If t_0 is the time of disintegration of the particle at rest and t the time when it is moving with velocity $v=\beta c$ we have

$$t=t_0/(1-\beta^2)^{\frac{1}{2}}.$$

From the relativistic energy equation

$$eV=300\ mc^2[(1-\beta^2)^{-\frac{1}{2}}-1],$$

it follows that the relative times of disintegration of two particles having energies V_1 and V_2 e-volts is given by

$$t_2=t_1\frac{V_2+300\ mc^2/e}{V_1+300\ mc^2/e},$$

where m is the mass of the particle, here equal to 137 times the mass of an electron, and $300\ mc^2/e=7\times10^7$. The relative distances traveled before disintegration is then given by $d_2=d_1v_2t_2/v_1t_1$.

Taking the mean energy of the end-points of β-decay spectra to be 10^6 e-volts I find that the ratio of the distance traveled by a cosmic heavy electron of 10^{12} e-volts energy to that traveled by a β-decay heavy electron before spontaneously disintegrating is 10^5. To account for the continuous energy distribution of β-rays the heavy electron would have to dissociate while still close enough to the nucleus to interact with it, so that this figure of 10^5 is hardly great enough to allow the heavy electron to be observed in cosmic rays, unless the interaction with the nucleus caused the slower β-ray heavy electron to be dissociated in a time much shorter than its time of spontaneous disintegration. Crane[4] has reported that in the course of some cloud chamber experiments a few β-particles appeared to behave in an anomalous way for which no satisfactory interpretation could be found. Zwicky[5] also has drawn attention to some peculiar cloud chamber tracks which, in his view, may be due to the electron suddenly changing its rest mass. This is just what would be observed if a β-decay heavy electron disintegrated spontaneously outside the atom, the probability of dissociation of the particle by interaction while it is still close to the nucleus is not quite unity.

Corben[6] has suggested that the heavy electron may be formed by the combination of an electron with one of Eddington's neutral particle ($\frac{1}{4}$ of a scalar particle) which has a mass 135.9. He considers this occurs with the emission of a neutrino. In Eddington's theory,[7] however, the neutral particles have no objective existence: they form a background consisting of the unspecified particles of the universe. The highest energy level of this background represents the ground level of the "object system" to which the vector wave functions of quantum theory apply: the scalars apply to the background which forms the reference frame. The neutral particles of the background, which are all below the ground level of the object system, are therefore in negative energy states. It is a *vacancy or hole* in the background that manifests itself as a particle in the object system.

If the neutron→proton transition in the nucleus interacts with the background as I have suggested,[8] and causes an electron to be created, the hole left in the background will represent the creation of a neutral particle with spin $\frac{1}{2}$, which could then combine with the electron to form a heavy electron which obeys Bose statistics, as is suggested above. The hole must represent an uncharged particle of spin $\frac{1}{2}$ for charge and spin to be conserved among the particles of the object system. On this view the heavy electron is created by the neutron→proton transition in the atom.

F. L. ARNOT

The University,
St. Andrews, Scotland,
May 14, 1938.

[1] Yukawa, Proc. Phys.-Math. Soc. Jap. **17**, 48 (1935).
[2] Neddermeyer and Anderson, Phys. Rev. **51**, 884 (1937) and others.
[3] Bhabha, Nature **141**, 117 (1938).
[4] Crane, Phys. Rev. **53**, 317 (1938).
[5] Zwicky, Phys. Rev. **53**, 611 (1938).
[6] Corben, Nature **141**, 747 (1938).
[7] Eddington, *Relativity Theory of Protons and Electrons*.
[8] Arnot, Nature **139**, 1065 (1937).

Some Results of the Search for Super-Novae

Some time ago Baade and I discussed the existence of a new class of novae which surpass the common novae in luminosity by a factor of one thousand.[1, 2] We proposed to call these new stars *super-novae*, a designation which is now in general use. It should be emphasized, however, that super-novae in some respects differ fundamentally from ordinary novae.

In our original communications[1, 2] we made a first tentative attempt to estimate how often super-novae appear in an average nebula. From a considerable, though very heterogeneous set of records from various sources extending over the past fifty years we concluded that the frequency of occurrence of super-novae in an average nebula is of the order of one per several centuries. We also suggested that the study of super-novae promises to throw new light on the problem of the generation of energy in stars and perhaps on the origin of the cosmic rays. In conjunction with considerations concerning the tremendous liberation of energy in super-novae we suggested the formation of *collapsed neutron stars*[1, 2] as the most powerful source of energy.

These suggestions clearly reveal the great potentialities of a study of super-novae. We decided that no effort should be spared to track down and to study in detail as many as possible of these rare objects. Several seasons of unsuccessful work with unsatisfactory telescopic equipment preceded a period in which the greatest advance was made with the aid of the 18-inch $f:2$ Schmidt telescope which had been built in the meantime with the authorization of the observatory council of the California Institute of Technology.

In the period from September 5, 1936 until January 31, 1938, about six hundred excellent photographs covering seventy square degrees each were obtained with the Schmidt telescope. The resulting search is equivalent to the continuous control during one year of about 1800 nebulae whose apparent brightness is greater than $m=15$. Since three super-novae were discovered in the period mentioned, the resulting frequency is one *super-nova per average nebula* of our collection *in a period of six hundred*

years, a result which confirms the correctness of our original estimate.

The two brightest of these super-novae, which appeared in N.G.C. 1003 and I.C. 4182, have now yielded a vast amount of information which will be presented in a series of papers to the *Astrophysical Journal*. Summarizing some of these results we may state:

1. For the first time excellent photographic light curves have been obtained for super-novae, including the maxima. A large number of photographs taken with yellow filters is also available from which red magnitudes may be derived.

2. Intensive spectroscopic studies by M. L. Humason, R. Minkowski and others have shown that super-nova spectra are totally different from the spectra of any other known stellar objects.

3. The most luminous super-novae may be brighter than the nebulae in which they appear by as many as five magnitudes, as the case of the super-nova in I.C. 4182 has shown. This brightest of all super-novae which is consequently the *brightest stellar object ever observed*, has, according to Baade, an absolute *photographic* magnitude close to $M=-16.6$, corresponding to about four hundred million times the luminosity of the sun. The total radiation of energy from a bright super-nova between the wave-lengths $\lambda=6800$A and $\lambda=3600$A over a period of one year after its appearance amounts to about 10^{49} ergs.

4. The frequency of occurrence of super-novae has been determined as already mentioned.

The most important conclusion which we may draw from these new observational results is, that the existence of *two classes of temporary stars*, super-novae and common novae, has been established beyond doubt. The new data have also furnished for the first time the necessary basis for a consistent statistical evaluation of the data available for previously observed super-novae. This evaluation has been carried out in detail by Dr. Baade and has resulted in significant results regarding the average absolute magnitudes of super-novae as well as the dispersion in magnitudes.

California Institute of Technology,
Pasadena, California,
May 18, 1938.

F. ZWICKY

[1] W. Baade and F. Zwicky, Phys. Rev. **45**, 138 (1934) and **46**, 67 (1934); Proc. Nat. Acad. Sci. **20**, 254 (1934) and **20**, 259 (1934). See also F. J. M. Stratton, *Handbuch der Astrophysik*, Vol. 7 (1936), p. 671.
[2] F. Zwicky, The Scientific Monthly **40**, 461 (1935); Proc. Nat. Acad. **22**, 457 (1936) and **22**, 557 (1936); Publ. Astro. Soc. Pac. **48**, 191 (1936) and **49**, 204 (1937).

Angular Distribution of Slow Neutrons from a Paraffin Surface

In experiments on the properties of slow neutrons and the induced radioactivities produced by slow neutrons it has been a common practice to use a Rn-Be neutron source embedded beneath the surface of a paraffin block and plane parallel layers of absorbers and detectors. The analysis of such experiments requires a knowledge of the angular distribution of neutrons coming from the surface. The expected distribution has been derived theoretically by Fermi[1] and found to be $f(\theta)\sim\cos\theta+\sqrt{3}\cos^2\theta$. The distribution has been studied experimentally and found to follow the Fermi distribution to within experimental errors.

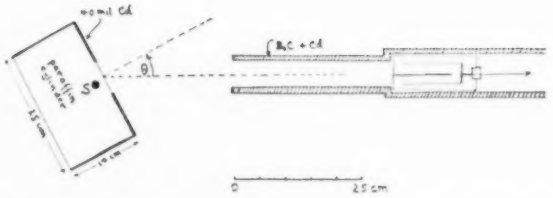

FIG. 1. Experimental arrangement for observing the angular distribution of slow neutrons emerging from a paraffin surface.

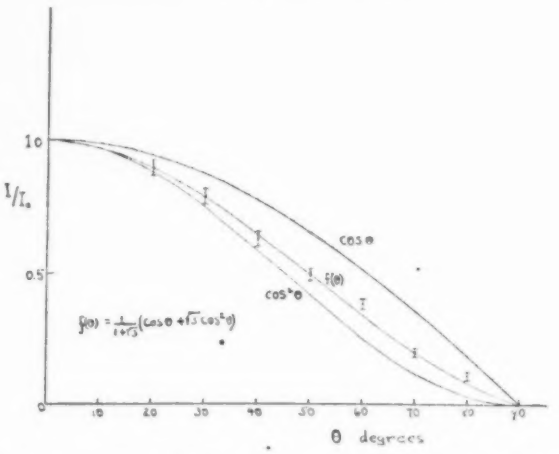

FIG. 2. Observed angular distribution of slow neutrons from a paraffin surface. The observations are shown with their standard errors and fit the Fermi distribution, $f(\theta)$, to within the accuracy of the experiments.

Figure 1 shows the experimental arrangement. A Rn-Be source of neutrons, S, was placed 3 cm beneath the surface of the end of a paraffin cylinder of the kind described by Amaldi and Fermi.[2] The neutrons emerging from the surface were detected in a BF_3 ionization chamber which was placed within cylindrical shields of B_4C and Cd forming a collimator for slow neutrons. The ionization pulses due to the slow neutron disintegration of B^{10} were observed with a pulse amplifier and counter. The variation of slow neutron intensity with angle was measured by rotating the BF_3 ionization chamber about a vertical axis in the plane of the paraffin surface.

The cylinder was covered entirely with Cd (0.88 g Cd/cm^2) with a hole 7 cm in diameter in the center of the end cover. This hole defined the area of the emitting surface, and was at the center of, and smaller than, the area "seen" by the detecting chamber. This insured having the same emitting surface effective at all angles. The BF_3 chamber subtended an angle of 6° 30′ from a point at the center of the emitting surface. The collimator tube absorbed possible stray slow neutrons from the walls and floor.

Counts were taken without and with Cd over the end of the collimator tube, the difference between these runs being taken as the slow neutron count. Fig. 2 shows I/I_0 plotted as a function of angle, θ. The observed points are shown with the fluctuations based on the standard errors of I and I_0. The solid lines give for purposes of comparison the functions $\cos\theta$, $\cos^2\theta$, and $f(\theta)$. The observed points tend to

follow the curve for $f(\theta)$. Runs taken with the neutron source 5 cm below the paraffin surface show the same trend.

Cornell University,
Ithaca, New York,
May 25, 1938.

J. G. HOFFMAN
M. S. LIVINGSTON

[1] E. Fermi, Ricerca Scient. **14**, 13 (1936). See also H. A. Bethe, Rev. Mod. Phys. **9**, 132 (1937).
[2] E. Amaldi and E. Fermi, Phys. Rev. **50**, 901 (1936).

Radial Lines in Laue Spot Photograms

Wadlund[1] recently published in these columns under the above title some Laue photographs showing sharp Laue spots together with faint radial striae. He found these radial lines with crystals of NaCl and KCl, but not with crystals of mica, Iceland spar, zinc blend, fluorite, or gypsum. Zachariasen,[2] in discussing these lines, considered it unreasonable to ascribe them to "strain," and suggested that they were cross-grating spectra from a two-dimensional array of atoms. He designated boundary layers of the mosaic blocks of the imperfect NaCl and KCl crystals as the cross gratings responsible for the lines.

Neither author has mentioned that the cross-grating explanation of "asterism" in Laue photograms has already received much discussion. Linnik[3] proposed it as an explanation of patterns in heated mica, but Bragg[4] showed that the ordinary conception of diffraction from a three-dimensional lattice was adequate to explain all features of Linnik's patterns, if a small gleviation of orientation about a mean orientation was assumed. He also offered experimental proof of this, reproducing Linnik's asterism by oscillating a normal mica crystal a few degrees in all directions from its mean position. Berg[5] has used the cross-grating conception, but merely as a convenient method of analyzing patterns rather than as a fundamental mechanism of diffraction. Bragg and Kirchner[6, 7] pointed out an obstacle to the theory as applied to equi-axed crystallites by showing that in order for atoms in a row parallel to the incident beam to scatter in phase and act as one point of a cross grating (for x-rays, not electrons) the crystallite containing the row could not be thicker than one or two atom layers in this direction, and an equi-axed crystallite of this size would be quite incapable of producing sharp cross-grating spectra.

Zachariasen's argument[2] avoids the above objection, since it applies to diffraction from a surface layer of atoms of considerable extent laterally, but of very few atoms thickness, a layer in which the periodicity in the direction of the beam is presumably abnormal because it is on the surface of a mosaic block. But the cross-grating theory cannot be tested by Wadlund's photographs, for these are fully explained by ordinary three-dimensional lattice diffraction.

If one interprets Fig. 1 of Wadlund's article in the conventional way, it may be stated that the crystal consists of regions of diverging orientations; and that a majority of the regions scatter less than 0.1° from the mean, but a few deviate up to 8° in all directions. The horizontal and vertical streaks near the center of the photograph are (200) reflections which form a spectrum from $\lambda_{min}=0.32$A up to $\lambda=0.63$A where the effective intensity of the general radiation and the amount of properly oriented material became small. The 45° streaks are (220) reflections which extend from $\lambda_{min}=0.32$A out to a reflecting angle of 8.0° corresponding to $\lambda=0.55$A, and are here terminated by the limit of scatter of orientations. It will be noted that both sets of streaks—as far as can be seen from the reproduction—have a tangential width and a shape consistent with this amount of scatter.

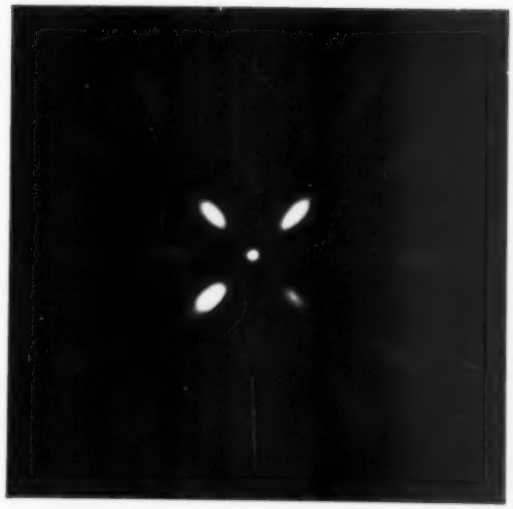

FIG. 1. Laue photograph of compressed iron crystal. Striae near center are from (110) and (200) planes and show a range of orientation up to 9° from the mean.

There is a striking similarity between the streaks in the rocksalt pattern discussed above and the Laue photograph which accompanies this note, Fig. 1. The specimen was a hydrogen-purified iron crystal that had been compressed in approximately the [100] direction to 1/20 of its original thickness, and set up in the camera with the compression axis parallel to the beam.[8] The position, length, intensity, and shape of every streak in the pattern are explicable, as above, by assuming a preferred orientation of the crystal axes such that they fill a solid angle around a mean position having two cube axes, one horizontal and one vertical in the figure, and the third parallel to the axis of compression (normal to the plane of the paper). The maximum deviation shown here is about 9°. The change in orientation was followed as deformation progressed by means of rotation photographs, and gradual changes in both the mean orientation and the range of scatter were observed. The equilibrium state is shown in Fig. 1.

The asterism in these cases is fully explained by the three-dimensional lattice orientations of the type to be expected in imperfect and deformed crystals and thus furnishes no evidence for a cross-grating effect.

Metals Research Laboratory,
Carnegie Institute of Technology,
Pittsburgh, Pennsylvania,
May 27, 1938.

CHARLES S. BARRETT

[1] Wadlund, Phys. Rev. **53**, 843 (1938).
[2] Zachariasen, Phys. Rev. **53**, 844 (1938).
[3] Linnik, Nature **123**, 604 (1929).
[4] W. L. Bragg, Nature **124**, 125 (1929).
[5] Berg, Zeits. f. Krist. **A83**, 318 (1932); **A89**, 587 (1934).
[6] Bragg and Kirchner, Nature **127**, 738 (1931).
[7] Bragg, *The Crystalline State*, Vol. I, p. 261.
[8] Barrett, Paper 59, Washington Meeting, American Physical Society 1938.

Magnetic Anisotropy of Ferromagnetic Crystals in Weak Fields and Reversible Susceptibility

The formula given for $\kappa_\perp$ in the previous letter[1] is a particular case of the general formula for the reversible susceptibility which may be obtained by calculation of the change in the magnetization dI caused by reversible displacement of the boundaries between domains when the field is changed by dH. In iron crystals there are six and in nickel crystals eight directions of easy magnetization. In weak fields the spins of domains are parallel to these directions. Therefore, in weak fields there are in iron crystals six and in nickel crystals eight different magnetic phases. The volume concentrations of these phases will be denoted by $n_1, \cdots n_i, \cdots \bar{n}_1, \cdots \bar{n}_i \cdots$ where $\bar{n}_i$ denotes the concentration of the phase whose spins are anti-parallel to those of the phase with concentration n_i.

The general formula obtained for the reversible susceptibility is of the following form:[2]

$$\kappa_r = \kappa_{r\perp} + \kappa_{r\parallel} \cdots, \tag{1a}$$

$$\kappa_{r\perp} = \kappa_{r2} \sum_{i \neq k} \{(n_i + \bar{n}_i)(n_k + \bar{n}_k)(h_i^2 + h_k^2) - 2(n_i - \bar{n}_i)(n_k - \bar{n}_k) h_i h_k\} \cdots, \tag{1b}$$

$$\kappa_{r\parallel} = \kappa_{r1} \sum_i \left\{1 - \left(\frac{n_i - \bar{n}_i}{n_i + \bar{n}_i}\right)^2\right\} (n_i + \bar{n}_i) h_i^2 \cdots, \tag{1c}$$

where h_i and h_k are the cosines of the angles between the directions of the spins of phases i and k and the direction of the field; κ_{r1} and κ_{r2} are constant coefficients which depend on the mechanical properties of the crystals. When $I=0$, i.e. when $n_i=\bar{n}_i$ formula (1b) turns into the formula for $\kappa_\perp$ of the previous letter.[1] Here, however, it should be noticed that the expression for κ_0 given in the previous letter represents the initial susceptibility while (1) for $n_i=\bar{n}_i$ represents only the initial reversible susceptibility κ_{r0}; which is defined as the limiting value of the reversible susceptibility at $I=0$ and $H=0$. Even though for $n_i=\bar{n}_i$ (1) coincides with the expression obtained previously for κ_0 except that the multiplying factor is different, experiment shows that in some cases $\kappa_0 > \kappa_{r0}$ may take place.

Formula (1) may be used to calculate the reversible susceptibility of iron crystals in different directions.

(1) The magnetic field $H \| [100]$. In this case $h_1=1$, $h_2=h_3=0$. The magnetization: $I=(n_1-\bar{n}_1)I_s$, whence

$$n_1 - \bar{n}_1 = j; \quad n_2 - \bar{n}_2 = n_3 - \bar{n}_3 = 0 \cdots, \tag{2}$$

where $j=I/I_s$.

(a) In the limiting case of the most advantageous orientation when all the spins are parallel or antiparallel to the direction [100],[3]

$$n_1 + \bar{n}_1 = 1, \quad n_2 = \bar{n}_2 = n_3 = \bar{n}_3 = 0 \cdots. \tag{3}$$

Substituting (2) and (3) in (1) we obtain

$$\kappa_{r\perp} = 0, \quad \kappa_{r\parallel} = \kappa_{r1}(1 - j^2) \cdots \tag{4}$$

whence if $\kappa_{r1} > 0$ it follows that

$$\kappa_r / \kappa_{r0} = 1 - j^2 \cdots. \tag{5}$$

(b) If in the initial state when $I=0$ the concentrations of the magnetic phases are equal, strict calculation of n_i, is very difficult if we exclude the particular case when $H \| [111]$. In the general case n_i may be determined as a function of j only from measurements of the magnetostriction. One may attempt to calculate κ_r for the case of equal concentrations in the initial state by using Heisenberg's[4] formula for n_i, obtained by statistical methods. The applicability of statistical methods to the calculation of n_i has as yet no theoretical basis, nevertheless experiment shows that values of n_i calculated by these methods are in quite good agreement with those determined from magnetostriction measurements in the case of not very soft crystals and polycrystals. When the magnetization is parallel to the axis [100] statistical calculation gives:

$$\left.\begin{aligned} n_1 + \bar{n}_1 &= -\tfrac{1}{3} + \tfrac{2}{3}(1 + 3j^2)^{\frac{1}{2}}; \\ n_2 + \bar{n}_2 = n_3 + \bar{n}_3 &= \tfrac{2}{3} - \tfrac{1}{3}(1 + 3j^2) \cdots. \end{aligned}\right\} \tag{6}$$

Substituting (2) and (6) in (1) we obtain:

$$\left.\begin{aligned} \kappa_{r\perp} &= (2/9)\kappa_{r2} \cdot [-4 - 6j^2 + 5(1 + 3j^2)^{\frac{1}{2}}]; \\ \kappa_{r\parallel} &= \frac{\kappa_{r1}}{3} \cdot \frac{5 + 3j^2 - 4(1 + 3j^2)^{\frac{1}{2}}}{-1 + 2(1 + 3j^2)^{\frac{1}{2}}} \end{aligned}\right\} \cdots. \tag{7}$$

From (4) and (7) it follows that when $H \| [100]$, the ratio κ_r / κ_{r0} depends on the relationship between κ_{r1} and κ_{r2}.

(2) The magnetic field $H \| [110]$. This calculation analogous to the above gives: (a) in the limiting case when $n_1 + \bar{n}_1 = n_2 + \bar{n}_2 = \frac{1}{2}$; $n_3 = \bar{n}_3 = 0$ the reversible susceptibilities

$$\left.\begin{aligned} \kappa_{r\perp} &= \tfrac{1}{4}\kappa_{r2}(1 - 2j^2); \\ \kappa_{r\parallel} &= \tfrac{1}{2}\kappa_{r1}(1 - 2j^2); \ \cdots, \end{aligned}\right\} \tag{8}$$

whence, *independently of the relationship between* κ_{r1} *and* κ_{r2} we have:

$$\kappa_r / \kappa_{r0} = 1 - 2j^2 \cdots. \tag{9}$$

(b) When the phase concentrations are equal in the initial state

$$\left.\begin{aligned} \kappa_{r\perp} &= (2/9)\kappa_{r2}[\tfrac{1}{2} - \tfrac{3}{2}j^2 + \tfrac{1}{2}(1 - \tfrac{3}{2}j^2)^{\frac{1}{2}}]; \\ \kappa_{r\parallel} &= \tfrac{1}{3}\kappa_{r1} \cdot \frac{5 - 6j^2 - 4(1 - \frac{3}{2}j^2)^{\frac{1}{2}}}{2 - (1 - \frac{3}{2}j^2)^{\frac{1}{2}}} \cdots \end{aligned}\right\} \tag{10}$$

as in the analogous case for $H \| [100]$ the ratio κ_r / κ_{r0} depends on the relationship between κ_{r1} and κ_{r2}. It should, however, be noticed that when $\kappa_{r1} \ll \kappa_{r2}$ the expression for κ_r / κ_{r0} obtained from formula (10) is practically very little different from expression (9).

(3) $H \| [111]$. If in this case the concentrations are equal in the initial state calculation gives:

$$\kappa_{r\perp} = (2/9)\kappa_{r2}(1 - 3j^2); \quad \kappa_{r\parallel} = \tfrac{1}{3}\kappa_{r1}(1 - 3j^2). \tag{11}$$

Hence again *independently of the relationship between* κ_{r1} *and* κ_{r2} we obtain:

$$\kappa_r / \kappa_{r0} = 1 - 3j^2. \tag{12}$$

There will be divergences from (12) if the section of the specimen perpendicular to the direction of the magnetic field deviates considerably from the circular form and if the demagnetizing factor becomes either less or greater along one of the axes of easy magnetization than along the others. The expression for κ_r may be obtained in an analogous manner for crystals of nickel.

Physical Institute of the State University,
Moscow, U. S. S. R.,
April 8, 1938.

E. KONDORSKY

[1] E. Kondorsky, Phys. Rev. **53**, 319 (1938).
[2] The deduction of formulae (1) will shortly be published in the Comptes Rendus Acad. Sci. U. S. S. R. Vol. 19, 4.
[3] It should be noticed that if the concentrations of the magnetic phases are unequal in the initial state, the directions of easy magnetization can no longer be considered as physically equal, and Eqs. (1) become inapplicable. However, in the limiting cases of unequal concentrations considered below, the concentrations of some of the phases are zero and those of the remainder are equal between themselves in the initial state. Therefore formulae (1) remain applicable to the limiting cases in question.
[4] W. Heisenberg, Zeits. f. Physik **62**, 287 (1931).

Author Index to Volume 53

References with (A) are to abstracts of papers presented at meetings of the American Physical Society. References with (L) are to Letters to the Editor; with (T) are title only.

Abelson, Philip. Neutron produced activities in uranium—211(A)

Acree, S. F. Oscillograph data on the electrode capacitance of conductivity cells—923(A)

Adams, Elliot Q. (see Barnes, Bentley T.)—545

——— **and Bentley T. Barnes.** Mechanism of the positive column in mercury vapor at intermediate pressures—556

Adams, Norman I., Jr. (see Kovarik, Alois F.)—928(A)

——— (see Page, Leigh)—819

Aird, R. B. (see Strait, L. A.)—213(A)

Alaoglu, Leon and Nicholas M. Smith, Jr. Statistical theory of a scaling circuit—832

Albertson, Walter. Extension of the analyses of the spectra of neutral osmium and iridium—940(A)

——— (see Harrison, George R.)—940(A)

——— **and George R. Harrison.** Preliminary report on the analysis of the spectrum of singly ionized cerium, Ce II—108(A)

Alichanian, A. I. and S. J. Nikitin. Shape of the β-spectrum of Th C and the mass of the neutrino—767(L)

———, **A. I. Alichanow and B. S. Dželepow.** On the form of the β-spectrum of Ra E in the vicinity of the upper limit and the mass of the neutrino—766(L)

Alichanow, A. I. (see Alichanian, A. I.)—766(L)

Allen, J. S. (see Haxby, R. O.)—921(A)

——— **and J. H. Williams.** Ion optics of a five section proton accelerating tube—928(A)

———, **Robert O. Haxby and John H. Williams.** Width of the resonance peaks in disintegration of boron by protons—325(A)

Allen, Mildred. Effect of tension on the electrical resistance of single tetragonal tin crystals—108(A)

Allison, S. K. (see Skaggs, L. S.)—946(A)

——— **and Nicholas M. Smith, Jr.** Energy spectra of particles from nuclear disintegrations—946(A)

———, **G. T. Hatch, L. S. Skaggs and N. M. Smith, Jr.** Operating characteristics of a voltage multiplying circuit for nuclear disintegration experiments—204(A)

Almy, G. M. and M. Rassweiler. Absorption spectrum of caesium hydride—890

Alvarez, Luis W. Electron capture and internal conversion in gallium 67—606(L)

——— Neutron yields from deuteron reactions at high energy—326(A)

——— Search for short-lived radioelements—215(A)

——— **and William M. Brobeck.** Cloud chamber studies in the cyclotron magnetic field—213(A)

Amaldi, E. (see Fermi, E.)—493(L)

Anderson, H. L. (see Dunning, J. R.)—334(A)

Andrews, C. L. Absorption of soft x-rays in beryllium, carbon, aluminum, copper, silver and gold—679(A)

Archibald, William J. Concentration of an ideal solution in a centrifugal field of force, as a function of the time—923(A)

——— Process of diffusion in a centrifugal field of force—746

Arenberg, David L. and Percy M. Roope. Stabilized a.c. operated ultramicrometer—687(A)

Arnot, F. L. Heavy electrons and β-decay—1018(L)

Aronson, C. J. (see O'Brien, Brian)—950(A)

Astin, A. V. Nature of energy losses in air capacitors—927(A)

——— (see Curtis, H. L.)—934(A)

——— (see Curtiss, L. F.)—23, 330(A)

——— (see Korff, S. A.)—14

Bacher, R. F. (see Tomboulian, D. H.)—678(A)

——— **and D. C. Swanson.** On the scattering of fast neutrons—922(A)

——— **and D. C. Swanson.** Scattering of fast neutrons—676(A)

Bainbridge, K. T. Isotopic weight of helium by direct comparison with oxygen—922(A)

Baker, Richard F. and John T. Tate. Ionization and dissociation by electron impact in CCl_2F_2 and in CCl_4 vapor—683(A)

——— **and John T. Tate.** Ionization and dissociation of normal and isobutane by electron impact—944(A)

Balamuth, Lewis. Thermal expansion of the alkalis—669(L)

Ballard, Stanley S. Spectrographic study of the distribution of mineral elements in sugar cane—689(A)

Bancroft, Dennison. Effect of hydrostatic pressure on the susceptibility of Rochelle salt—587

——— (see Jacobs, Robert B.)—687(A)

Bardeen, J. Compressibility of the alkali metals—683(A)

——— **and E. Feenberg.** Spacing of nuclear energy levels—938(A)

Barker, E. F. (see Borden, Avis)—932(A)

Barnes, Bentley T. (see Adams, Elliot Q.)—556

——— (see Forsythe, W. E.)—678(A)

——— **and Elliot Q. Adams.** Emission of radiation in the positive column of a mercury arc—545

Barnes, S. W. (see DuBridge, L. A.)—326(A), 447

——— **and George Valley.** Long period activity induced in Cu—946(A)

Barnóthy, J. and M. Forró. On the penetrating component of the cosmic radiation—848(L)

Barr, E. S. Design and calibration of an infra-red spectrometer with a fluorite prism—852(A)

Barrett, Charles S. Origin of deformation textures—925(A)

——— Radial lines in Laue spot photograms—1021(L)

Bartlett, J. H., Jr. Stopping-power for cosmic-ray electrons—915(A)

Bartlett, Russell S. and Alan T. Waterman. Colloquium on the college board examination in physics—109(T)

Bassoe, Else (see Cashman, R. J.)—919(A)

Beach, J. Y. and K. J. Palmer. Potential barrier in ethylene chloride—685(A)

Beams, J. W. Separation of solutions by the tubular centrifuge—850(A)
——— (see Black, Sheppard A.)—924(A)
——— (see Dietrich, J. R.)—923(A)
——— **and C. Skarstrom.** Air driven tubular vacuum type centrifuge—327(A)
Bearden, J. A. Determination of e/m from the refraction of x-rays in a diamond prism—917(A)
Bell, M. E., E. A. Coomes and W. B. Nottingham. Design and construction of an electron velocity analyzer for ionization probability measurements—328(A)
Bender, David. Refractive index of air in the visible and photographic infra-red—852(A)
Benford, Frank and A. G. Worthing. Important λT relation for black-body radiation—948(A)
Berkner, L. V. (see Booker, H. G.)—924(A)
Bernet, E. J. (see Parkinson, D. B.)—642
Beth, Richard A. Apparent discrepancy among the experimental measurements of the atomic constants—681(A)
Bethe, H. A. Binding energy of the deuteron—313
——— Barytron theory of nuclear forces—938(A)
——— Magnetic moment of Li^7 in the α-particle model—842(L)
——— Oppenheimer-Phillips mechanism of d-p reactions—205(A)
——— Oppenheimer-Phillips process—39
——— Possible deviations from the evaporation model of nuclear reactions—675(A)
——— (see Konopinski, E. J.)—679(A)
——— (see Marshak, R. E.)—677(A)
——— (see Rose, M. E.)—206(A)
——— **and E. J. Konopinski.** Alternative description of the compound nucleus—688(A)
Beyer, H. G. (see Carroll, H.)—680(A), 947(A)
——— (see Powers, P. N.)—947(A)
———, **H. Carroll, C. Witcher and J. R. Dunning.** Dependence of magnetic scattering of neutrons on magnetization of iron—947(A)
Bhagavantam, S. Molecule of sulphur and its raman spectra—1015(L)
Bikerman, J. J. and J. H. Schulman. On the structure of "built-up" films on metals—909(L)
Bitter, F. New magnetic laboratory at M.I.T.—933(A)
Black, Sheppard A., J. W. Beams and L. B. Snoddy. Electrically driven vacuum-type centrifuge—924(A)
Blake, F. C. Effect of lattice enlargement upon our ideas of order *versus* disorder in crystals, including mix-crystals—333(A)
Bleakney, Walker and John A. Hipple, Jr. New mass spectrometer with improved focusing properties—521
Bless, A. A. (see Byers, W. H.)—852(A)
Blewett, John P. Reduction of barium oxide by metals at high temperature—935(A)
Bol, C. High pressure capillary lamps—214(A)
Bonner, T. W. Energy of the neutrons from the disintegration of carbon by deuterons—496(L)
——— Formation of an excited He^3 in the disintegration of deuterium by deuterons—711, 928(A)
——— (see Hudspeth, Emmett)—928(A)
Booker, H. G. and L. V. Berkner. Decisive ionospheric investigation concerning the Lorentz polarization correction—924(A)
Borden, Avis and E. F. Barker. Infra-red absorption spectrum of methyl alcohol—932(A)
Bowen, I. S. Low terms in Co VI—889
———, **R. A. Millikan and H. V. Neher.** Distribution of energies among the incoming cosmic-ray electrons—328(A)
———, **R. A. Millikan and H. V. Neher.** Energy distribution of incident cosmic-ray electrons—915(A)
———, **R. A. Millikan and H. V. Neher.** New evidence as to the nature of the incoming cosmic rays, their absorbability in the atmosphere, and the secondary character of the penetrating rays found in such abundance at sea level and below—217
———, **R. A. Millikan and H. V. Neher.** New light on the nature and origin of the incoming cosmic rays—855
———, **R. A. Millikan and H. Victor Neher.** Secondary nature of cosmic-ray effects in the lower atmosphere—214(A)
Bowls, W. E. Effect of cathode material on the second Townsend coefficient for ionization by collision in pure and contaminated N_2 gas—210(A), 293
Bozorth, R. M. and F. E. Haworth. Focusing of an x-ray beam by rocksalt crystal—538
Bradbury, Norris E. Ionization, negative ion formation, and recombination in the ionosphere—210(A)
Bramley, Arthur. Estimates of age of the planet from isotope ratios—323(A)
——— Range of cosmic-ray particles—915(A)
——— **and A. Keith Brewer.** Radioactivity of potassium—502
Breit, G. Approximately relativistic equations—153
——— **and J. R. Stehn.** Fine structure of the nuclear ground level of Li^7—459, 684(A)
——— **and E. Wigner.** Saturation requirements for nuclear forces—998
Brewer, A. Keith (see Bramley, Arthur)—502
Brickwedde, F. G. (see Dunning, J. R.)—205(A)
Brobeck, William M. (see Alvarez, Luis W.)—213(A)
Brode, Robert B. (see Corson, Dale R.)—215(A), 773
——— **and Merle A. Starr.** Nuclear disintegrations produced by cosmic rays—3, 214(A)
Brown, B. W. (see Curtiss, L. F.)—23, 330(A)
Brown, Harrison. Note on the range of occurrence of stable isotopes—846(L)
——— (see Gibson, G. E.)—846(L)
Brown, Sanborn C. and Robley D. Evans. Coaxial tube counter—914(A)
Brown, S. Leroy. Mechanical harmonic synthesizer-analyzer—333(A)
Brown, William Fuller, Jr. Domain theory of ferromagnetics under stress. Part II. Magnetostriction of polycrystalline material—482
Brubaker, Gordon. Scattering of alpha-particles by argon, oxygen, and neon—921(A)
——— (see Pollard, Ernest)—351

Bruce, W. A. Experimental verification of the quantum-mechanical dispersion theory by reflection and diffuse scattering of x-rays from zinc—802
——— **and G. E. M. Jauncey.** Experimental verification of the quantum mechanical dispersion theory by reflections and diffuse scattering of x-rays from zinc—332(A)
Bruch-Willstätter, M. and H. Sponer. Calculation of transition energies of polymorphous molecular crystals—324(A)
Brunner, Eugene. Theory of the continuous x-ray spectrum near the Duane-Hunt limit—457
Buchwald, Charles E. and Caryl P. Haskins. Biological effects of low voltage electrons—920(A)
Buck, J. H. (see DuBridge, L. A.)—326(A), 447
——— (see Strain, C. V.)—942(A)
Byers, W. H. and A. A. Bless. Polar moment of cellosolves—852(A)

Cameron, Donald M. (see Sears, William C.)—330(A)
——— **and Harald H. Nielsen.** 4.3μ fundamental band in the spectrum of CO_2—246
Campbell, Edward C. Nuclear K electron capture and negative beta-emission—206(A)
——— (see Pool, M. L.)—272
Cannon, C. V. (see Wheeler, John A.)—684(A)
Carlson, J. F. Energy losses of Pauli-Weisskopf particles—330(A)
Carr, Emma P. and Hildegard Stücklen. Ultraviolet absorption of simple hydrocarbons. IV. Unsaturated cyclic hydrocarbons in the Schumann region—109(A)
Carroll, H. (see Beyer, H. G.)—947(A)
———, **H. G. Beyer, K. Wilhelm and J. R. Dunning.** Scattering of neutrons by gases—947(A)
———, **P. N. Powers, H. G. Beyer and J. R. Dunning.** Scattering of neutrons by gases—680(A)
Carroll, Kenneth G. Van der Waals forces between symmetrical rotators—310
——— **and Henry Margenau.** Note on the binding energy of Li^6—921(A)
Cartmel, W. B. New ether-drift interferometer of high efficiency—108(A)
——— Preliminary measurements with an oblique ether-drift interferometer—949(A)
——— Theory of the ether-drift interferometer in brief—949(A)
Carwile, Preston B. On the Trouton-Noble experiment—924(A)
——— Suggested explanation of the contradiction between the Rayleigh-Jeans formula and experiment—682(A)
Cashman, R. J. and Else Bassoe. Experimental and theoretical photoelectric spectral sensitivity of strontium and magnesium—919(A)
Chapman, Seville. Carrier mobility spectra of liquids electrified by bubbling—211(A)
Chipman, R. A. Absolute measurement of resistance and reactance at frequencies of the order 300 mC/second—672(L)
Chodorow, Marvin I. (see Manning, Millard F.)—937(A)
Clark, O. (see Halpern, O.)—173
Clearman, H. E., Jr. An extension of the Bi I spectrum—941(A)
Cleveland, Forrest F. and M. J. Murray. Raman spectra of disubstituted acetylenes—330(A)
——— **and M. J. Murray.** Raman spectra of disubstituted acetylenes in the region 2100–2300 cm^{-1}—931(A)
Cobine, J. D. Effect of oxides and impurities on metallic arc reignition—911(L)
Cohen, V. W. (see Zinn, W. H.)—921(A)
Colby, W. F. (see Spees, A. H.)—326(A)
Cole, Kenneth S. and Howard J. Curtis. Electric impedance of *Nitella* during excitation—687(A)
——— **and Howard J. Curtis.** Electric impedance of single arbacia eggs—333(A)
Collins, George B. and Victor G. Reiling. Asymmetric radiation produced by high velocity electrons—205(A)
——— **and Victor G. Reiling.** Čerenkov radiation—948(A)
Colwell, R. C. (see Friend, A. W.)—945(A)
——— **A. W. Friend and D. A. McGraw.** Velocity of sound in air—686(A)
Compton Arthur H. Alternative interpretation of Jauncey's "heavy electron" spectra—431(L)
Comstock G. C. Measurement at high frequencies of the diamagnetic Faraday effect in liquids—849(A)
Constant. F. W. and J. M. Formwalt. Ferromagnetic impurities—432(L)
——— **and J. M. Formwalt.** Sensitive method of detecting magnetic impurities—852(A)
——— **and J. M. Formwalt.** Some properties of ferromagnetic impurities—933(A)
Coolidge, Albert Sprague (see James, Hubert M.)—208(A)
Coomes, Edward A. Secondary electron emission from thorium-coated tungsten—936(A)
——— (see Bell, M. E.)—328(A)
Cooter, Irvin L. (see Wenner, Frank)—927(A)
Copeland, Paul L. Secondary emission of electrons from sodium films on tantalum—328(A)
Cork, J. M. (see Curtis, B. R.)—206(A), 681(A)
——— (see Tape, Gerald F.)—676(A)
——— (see Thornton, R. L.)—922(A)
——— **and B. R. Curtis.** Relative probability of the loss of neutron and alpha-particle in iron—946(A)
——— **and R. L. Thornton.** Loss of neutrons by neutron bombardment and the radioactive isotopes of scandium—866
Cornell, S. D. (see More, Kenneth R.)—678(A), 806, 931(A)
Corson, Dale R. and Robert B. Brode. Evidence for a cosmic-ray particle of intermediate mass—215(A)
——— **and Robert B. Brode.** Specific ionization and mass of cosmic-ray particles—773
Coy, Nettie H. and H. Sponer. Evidence for a band system of antimony nitride—495(L)
Crane, H. R. Note on the existence of heavy beta-rays—317(L)
——— (see Halpern, J.)—676(A)
——— (see Ruhlig, A. J.)—266(L), 618, 683(A)
——— **and J. Halpern.** New experimental evidence for the existence of a neutrino—789
Critchfield, C. and E. Teller. On the saturation of nuclear forces—684(A), 812
Crooker, S. J. Aerodynamics applied to the golf club—927(A)

Curtis, B. R. Energy loss of positive electrons in passing through aluminum—986
——— (see Cork, J. M.)—946(A)
——— **and J. M. Cork.** Beta-radiation from activated isotopes of arsenic—681(A)
——— **and J. M. Cork.** Energy loss of positrons passing through matter—206(A)
——— **and J. Reginald Richardson.** Gamma-radiation associated with indium—942(A)
Curtis, C. W. First spark spectrum of manganese—474
Curtis, H. L., A. V. Astin and C. Matilda Sparks. Alternating current method for measuring effective mutual inductance—934(A)
Curtis, Howard J. (see Cole, Kenneth S.)—333(A), 687(A)
Curtiss, L. F. (see Korff, S. A.)—14
———, **A. V. Astin, S. A. Korff, L. L. Stockmann and B. W. Brown.** Cosmic-ray observations in the stratosphere—330(A)
———, **A. V. Astin, L. L. Stockmann, B. W. Brown and S. A. Korff.** Cosmic-ray observations in the stratosphere—23

Dancoff. S. M. and P. Morrison. Relativistic spin-orbit coupling in nuclei—211(A)
Dart, F. E. and Eugene Guth. On the thermoelastic and structure of rubber—327(A)
Davidson, W. L., Jr. and Ernest Pollard. Transmutation of titanium by Th C′ alpha-particles—929(A)
Davis, Francis J. (see Winans, J. G.)—930(A)
Dean, George R. Solubility at the grain boundaries of solid solution—202(A)
Decherd. Loraine (see Williams, Dudley)—852(A)
Delfosse, J. M. and J. A. Hipple, Jr. Use of isotopes in the study of ionization processes of polyatomic molecules—683(A)
Delsasso, L. A. (see Ridenour, Louis N.)—770(L)
——— (see Sherr, R.)—946(A)
Dempster, A. J. Atomic masses of the heavy elements—64
——— Energy content of the heavy nuclei—869
——— Isotopic constitution of gadolinium, dysprosium, erbium and ytterbium—727
——— Packing fractions of titanium, iron, copper, silver, gold and platinum—202(A)
Dennison, David M. and Z. I. Slawsky. Potential functions of the methyl halides—930(A)
Dershem, Elmer. Radiography of thin microtome sections by means of fluorescence x-radiation—202(A)
Devaney, T. Edwin (see Pietenpol, W. B.)—325(A)
Dickerson, R. T. (see Hopkins, I. I.)—850(A)
Dieke, G. H. (see Wood, R. W.)—146
Dietrich, J. R., L. B. Snoddy and J. W. Beams. Impulse breakdown in long discharge tubes—923(A)
Digges, Thomas G. Effect of carbon on the critical cooling rate of iron-carbon alloys—925(A)
Doan, Richard L. (see Jesse, William P.)—691
——— **and William P. Jesse.** Rate of production of large cosmic-ray bursts as a function of lead shield thickness—203(A)
Dodson, H. (see Nielsen, J. Rud)—331(A)
Doermann, F. W. Nonideal Lloyd's mirror in wide-angle interference—420
Dorsey, N. Ernest. Supercooling and freezing of water—925(A)
Dow, R. B. (see Thomas, B. W.)—926(A)
Draper, C. S. Acoustics of the combustion chamber—108(A)
DuBridge, L. A., S. W. Barnes, J. H. Buck and C. V. Strain. Proton induced radioactivities—447
———, **S. W. Barnes, E. O. Wiig, J. H. Buck and C. V. Strain.** Radioactivities induced by high energy protons—326(A)
Duffendack, O. S. (see Lifschutz, Harold)—941(A)
Dunning, J. R. (see Beyer, H. G.)—947(A)
——— (see Carroll, H.)—680(A), 947(A)
——— (see Powers, P. N.)—947(A)
——— **and H. L. Anderson.** High frequency systems for the cyclotrons—334(A)
———, **H. J. Hoge, J. H. Manley and F. G. Brickwedde.** Interaction of neutrons with normal and parahydrogen—205(A)
Dwight, C. H. and H. Kersten. Viscosity of sols made from x-irradiated apple pectin—926(A)
Dwyer, Robert J. Persistence of molecular vibration in collisions—324(A)
Dželepow, B. S. (see Alichanian, A. I.)—766(L)

Eckart, Carl and Francis R. Shonka. Accidental coincidences in counter circuits—752
Ehrenkranz, Florence. Sparking potential measurements in nitrogen and argon for platinum and sodium cathodes—210(A)
Eichelberger, J. F. (see Green, J. B.)—934(A)
Ellis, J. W. and E. L. Kinsey. Rotational transitions associated with radiation in water molecules in nonpolar solvents—672(L)
Elmore, W. C. Magnetic structure of cobalt—757
——— Motion photomicrographs of magnetic colloid patterns which form on cobalt crystals—933(A)
——— Surface magnetization of cobalt—108(A)
Elsasser, W. M. Note on atmospheric absorption caused by the rotational water band—768(L)
Emo, Lorenzo (see Richardson, J. Reginald)—234
Emslie, A. G. Scattering of slow positive ions at very small angles—680(A)
Epstein, Paul S. Influence of the solar magnetic field upon cosmic rays—862
Estermann, I. O., O. C. Simpson and O. Stern. Free fall of molecules—947(A)
Evans, Robley D. (see Brown, Sanborn C.)—914(A)
——— (see Goodman, Clark)—916(A)
——— **and Clark Goodman.** Substandards of very feeble radioactivity—916(A)
Ewing, D. H. (see Plesset, M. S.)—943(A)

Failla, G. X-ray generator especially designed for biological experiments—916(A)
——— Wide range ionization current meter—687(A)
Fankuchen, I. Intense monochromatic beams of x-rays—910(L)
——— On the structure of "built-up" films on metals—909(L)

Farnsworth, H. E. (see Turnbull, John C.)—944(A)
——— **and Ralph P. Winch.** On methods of producing gas free surfaces—935(A)
Feenberg, E. (see Bardeen, J.)—938(A)
——— (see Horvay, G.)—938(A)
Ference, M. (see Stephenson, R. J.)—208(A)
Fermi, E., E. Amaldi and G. C. Wick. On the albedo of slow neutrons—493(L)
Fisher, Russell A. and Edson R. Peck. Analysis of hyperfine structure of Mn I and an indicated value for the nuclear magnetic moment—685(A)
———, **Arthur S. Fry and John R. Platt.** Hollow cathode discharge as a source for Zeeman effect—934(A)
Fisk, J. B. and I. A. Getting. Compact 750 kv Van de Graaff generator for high currents—916(A)
Focke, Alfred B. Segregation of polonium in bismuth crystals—324(A)
Folsom, T. R. 600 kv a.c. generator for the production of neutrons—687(A)
Forbush, S. E. On sidereal diurnal variation in cosmic-ray intensity—682(A)
——— On variations in cosmic-ray intensity associated with magnetic storms—914(A)
Formwalt, J. M. (see Constant, F. W.)—432(L), 852(A), 933(A)
Forró, M. (see Barnóthy, J.)—848(L)
Forsythe, W. E., B. T. Barnes and Ann L. Shrider. Relative luminosity of the yellow and green mercury lines—678(A)
Foster, Donald and H. W. Highriter. Comparison of intensities of spectral lines—673(L)
Fowler, W. A. (see Oppenheimer, Jacquenette)—928(A)
———, **E. R. Gaerttner and C. C. Lauritsen.** Gamma-radiation from boron bombarded by deuterons—942(A)
———, **E. R. Gaerttner and C. C. Lauritsen.** Gamma-radiation from boron bombarded by protons—212(A), 628
Fox, G. W. and J. R. Frederick. Further study of x-ray diffraction in quartz—135
Frederick, J. R. (see Fox, G. W.)—135
Freeman, Ira M. Red shift of the nebular spectrum lines—207(A)
——— Suggestion regarding the nature of the heavy electron—606(L)
Fried, B. (see Green, J. B.)—105(L), 934(A)
——— (see Shortley, George H.)—931(A)
Friend, A. W. (see Colwell, R. C.)—686(A)
———, **J. K. Stewart and R. C. Colwell.** Vibrations of the segments of a circular plate—945(A)
Friesen, A. P. Lorenz-Lorentz constant for paraffin oil between 30 and 115 degrees centigrade—688(A)
——— Optical constants of liquid thallium—678(A)
——— Optical constants and intermetallic compounds—688(A)
Frisch, O. R., H. von Halban, Jr. and Jørgen Koch. Some experiments on the magnetic properties of free neutrons—719
Fry, Arthur S. (see Fisher, Russell A.)—934(A)
Fryer, Oscar G. Radioactivity of air, water, cave and soil gases—325(A)
Furry, W. H. On the theory of the neutral particle—679(A)
Gaerttner, E. R. (see Fowler, W. A.)—212(A), 628, 942(A)
Gamertsfelder, Carl and Newell S. Gingrich. Use of intensifying screens in x-ray diffraction work—332(A)
Gamow, G. Nuclear energy sources and stellar evolution—595
——— Tracks of stellar evolution—908(L)
——— **and E. Teller.** On the neutron core of stars—929(A)
——— **and E. Teller.** Rate of selective thermonuclear reactions—608(L)
Gardner, Irvine C. Relation of camera error to photogrammetric mapping—945(A)
Gardner, Milton E. Recombination of ions in pure oxygen as a function of pressure and temperature—75
George, W. D. Phase shifts in controlled multivibrators from 200,000 to 1 cycle per second—924(A)
Germer, L. H. and K. H. Storks. Arrangement of molecules in unimolecular and multimolecular layers—322(A)
Getting, I. A. Galactic rotation and the variation of cosmic-ray intensity—914(A)
——— Multivibrator Geiger counter circuit—103(L)
——— (see Fisk, J. B.)—916(A)
Gibson, G. E. and Harrison Brown. Relation between atomic number and isotope number for stable isotopes—846(L)
Gingrich, Newell S. (see Gamertsfelder, Carl)—332(A)
——— (see Thomas, C. D.)—944(A)
——— (see Trimble, Frank H.)—203(A), 278
——— **and C. D. Thomas.** Atomic distribution in liquid white phosphorus and the amorphous forms of red and black phosphorus—943(A)
Gish, O. H. and K. L. Sherman. Cosmic radiation and electrical conductivity in the stratosphere—434(L)
Goeppert-Mayer, M. (see Sachs, R. G.)—991
Gold, Otto (see Guth, Eugene)—322(A)
Goldberg, Leo (see Manning, Millard F.)—662
Goldsmith, H. H. (see Powers, P. N.)—947(A)
——— **and Lloyd Motz.** Spin of the neutron—947(A)
Good, Wilfred M. Permanent electrets as a function of the method of preparation—323(A)
Goodman, Clark (see Evans, Robley D.)—916(A)
——— **and Robley D. Evans.** New physical method for the determination of geologic ages—916(A)
Goranson, Roy W. and W. A. Zisman. Demonstration of the existence of permanent volume polarization in certain types of multilayers—668(L)
Gordy, Walter. Spectroscopic study of deuterium bonds—851(A)
Gorham, John E. Signs of the nuclear magnetic moments of Li^6 and K^{41}—331(A), 563
——— (see Thode, H. G.)—920(A)
Goudsmit, S. (see Spees, A. H.)—326(A)
Grahame, D. C. and G. T. Seaborg. Elastic and inelastic scattering of fast neutrons—795
Granath, L. P. (see Williams, D. T.)—685(A)
Green, G. K. and P. Gerald Kruger. Energy variations in cyclotron ion beam—927(A)
Green, J. B. (see Maxwell, H. N.)—330(A)
——— (see Peoples, J. A., Jr.)—934(A)
——— **and R. A. Loring.** Zeeman effect of selenium II—330(A)

Green, J. B., B. Fried and J. F. Eichelberger. Zeeman effect in argon—934(A)
——, **J. A. Peoples, Jr. and B. Fried.** Zeeman effect of the $p^5 d$ configurations of neon and argon—105(L)
Gross, Bernhard. On the latitude effect of the soft component of cosmic rays—607(L)
Guth, Eugene. On the diffraction of electromagnetic waves by small obstacles—688(A)
—— On the theory of the emissivity of metals—682(A)
—— On the theory of the viscosity of suspensions of ellipsoidal particles—926(A)
—— (see Dart, F. E.)—327(A)
—— (see Haas, Arthur E.)—324(A)
—— **and Otto Gold.** On the hydrodynamical theory of the viscosity of suspensions—322(A)
—— **and Josef Mayerhöfer.** On the deviations from Ohm's law at high current densities—205(A)

Haas, Arthur E. Photon emission of the sun—681(A)
—— Relation between the gravitational constant and Hubble's factor—207(A)
—— **and Eugene Guth.** Relation between Stefan's radiation law and Nernst's heat theorem—324(A)
Hafstad, L. R., N. P. Heydenburg and M. A. Tuve. Scattering of protons by protons—239
Hall, Wayne C. Thermal conductivities of mercury, sodium, and sodium amalgams in the liquid state—1004
Halpern, J. (see Crane, H. R.)—789
—— **and H. R. Crane.** Method for measuring the nuclear recoil in beta-ray emission—676(A)
Halpern, Otto and M. H. Johnson, Jr. Remarks on resonance scattering of charged particles—939(A)
——, **R. Lueneburg and O. Clark.** On multiple scattering of neutrons. I. Theory of the albedo of a plane boundary —173
Ham, W. R. (see Thomas, B. W.)—926(A)
—— **and C. B. Post.** Diffusion of hydrogen through nickel—935(A)
Hardy, James D. and T. W. Oppel. Cold sensation by radiation—920(A)
Harkins, William D. and John G. Kirkwood. Viscosity of monolayers: Theory of the surface slit viscosimeter—322(A)
—— **and Richard W. Mattoon.** Contact potential of solid films formed by evaporation and by solidification and of built-up multilayers on metals—911(L)
Harrison, Goerge R. (see Albertson, Walter)—108(A)
—— **and Walter E. Albertson.** Further description and classification of the spectrum of single ionized cerium, Ce II—940(A)
Hartman, Paul L. and Lloyd P. Smith. Linear accelerator using a quarter wave-length transmission line—677(A)
Haskins, Caryl P. (see Buchwald, Charles E.)—920(A)
Hatch, G. T. (see Allison, S. K.)—204(A)
—— (see Skaggs, L. S.)—946(A)
Hawkes, John B. Variation of magnetic double refraction with temperature in acetone and certain acetic esters—84
Haworth, F. E. (see Bozorth, R. M.)—538
Haxby, Robert O. (see Allen, James S.)—325(A)
——, **J. S. Allen and J. H. Williams.** Angular distribution of the protons from the deuteron-deuteron reaction —921(A)
Heaps, C. W. Some observations of magnetic viscosity in iron—334(A)
Heilemann, John J. Intensity relations in the low voltage helium arc—977
Henderson, M. C. (see Sherr, R.)—946(A)
Herb, R. G. (see Parkinson, D. B.)—642
Herget, C. M. (see Hubbard, J. C.)—945(A)
Herman, R. C. and R. Hofstadter. Infra-red absorption spectra of light and heavy acetic acids—940(A)
Hersey, Mayo D. Physics of lubrication, III. Note on the theory of air-lubricated journal bearings—926(A)
Herzfeld, K. F. (see Lyddane, R. H.)—947(A)
—— Reflection of Sound—899
Heydenburg, N. P. (see Hafstad, L. R.)—239
—— (see Roberts, R. B.)—374, 929(A), 1016(L)
—— **and R. B. Roberts.** Scattering of protons and deuterons by deuterium and by helium—922(A)
Hickman, R. W. (see Hunt, F. V.)—913(A)
Hicks, Victor (see Sidhu, S. S.)—207(A)
—— **and S. S. Sidhu.** Space group of pyrrhotite—207(A)
Hidnert, Peter. Thermal expansion and effects of heat treatments on the growth, density and structure of some heat-resisting alloys—925(A)
Highriter, H. W. (see Foster, Donald)—673(L)
Hill, A. G. Energy distribution of photoelectrons from sodium—184
Hipple, John A., Jr. Dissociation of ethane by electron impact—530
—— (see Bleakney, Walker)—521
—— (see Delfosse, J. M.)—683(A)
Hire, Chas. Photographic measurements of the Brownian motion—205(A), 325(A)
Hocker, J. P. (see Suits, C. G.)—670(L)
Hoffman, J. G. (see Livingston, M. Stanley)—227
—— **and M. S. Livingston.** Angular distribution of slow neutrons from a paraffin surface—1020(L)
—— **and M. Stanley Livingston.** Collimation of slow neutrons—676(A)
—— **and M. Stanley Livingston.** Studies of the properties of slow neutrons—929(A)
Hofstadter, Robert. Absorption spectra of heavy formic acid—941(A)
—— (see Herman, R. C.)—940(A)
Hoge, H. J. (see Dunning, J. R.)—205(A)
Hole, W. L., R. Wright and H. B. Wahlin. Recalescence in uranium—768(L)
Holley, Clifford. X-ray and optical properties of barium-copper-stearate films—534
Holloway, M. G. (see Livingston, M. Stanley)—922(A)
—— **and M. Stanley Livingston.** Range and specific ionization of alpha-particles—676(A)
Hopfield, John J. New absorption bands of water vapor in the extreme ultraviolet—931(A)
Hopkins, I. I., R. T. Dickerson and W. M. Nielsen. Practical applications of electronic control principles to the operation of a Wilson cloud chamber—850(A)
Horvath, W. J. (see Salant, E. O.)—943(A)

Horvay, G. and E. Feenberg. Binding energy of O^{16}—938(A)
Houston, W. V. Resonance broadening of spectral lines—213(A)
How, T. G. and K. Lark-Horovitz. New Geiger counter—334(A)
Howard, Robert A. Atomic vibrations of a Zn-Cu alloy—966
——— Study of the anisotropy of the atomic vibrations of a Zn-Cu alloy—324(A)
Howe, J. D. and I. Walerstein. Effects of fringing flux in large magnets—334(A)
Hoyt, F. C. On the penetrability of a simple type of potential barrier—673(L)
Hubbard, Donald. Some notes on the effect of the solubility of glass on the behavior of glass electrodes—935(A)
Hubbard, J. C. (see Zartman, I. F.)—944(A)
——— **and C. M. Herget.** Ultrasonic study of CO_2 near its critical point—945(A)
Hudspeth, Emmett and T. W. Bonner. Passage of fast neutrons through lead—928(A)
Hughes, A. L. and Marvin M. Mann, Jr. New method for investigating atomic electron velocities—50
——— **and Marvin M. Mann, Jr.** Profile of the Compton modified band as determined by electron scattering measurements—204(A)
Hulburt, E. O. Density and temperature of the atmosphere to about 60 km from twilight sky brightness measurements—948(A)
——— Photoelectric ionization in the ionosphere—344
——— Seasonal variation in F_2 ionization—670(L)
Hull, Albert W. New type of thermionic cathode: The migration cathode—936(A)
Humphreys, C. J. Second spectrum of xenon—940(A)
Hunt, F. V. and R. W. Hickman. Effect of source resistance on electronic stabilizer performance—913(A)
Hurst, William. Sensitive differential barometer—850(A)
——— (see Sponer, Hertha)—851(A)

Infeld, L. Electromagnetic and gravitational radiation—836, 938(A)
Inglis, D. R. Heavy particle interactions—686(A)
——— Nuclear magnetic moment of Li^7 by perturbation theory—880
——— On nuclear magnetic moments—470
——— Perturbation theory of the nuclear magnetic moment of Li^7—939(A)
Irvine, John W., Jr. (see Roberts, Arthur)—609(L)
Ives, Herbert E. Light signals around a closed path—939(A)
Iwanenko, D. and A. Sokolow. On the mathematical formalism of the theory of showers—910(L)

Jacobs, C. W. and B. E. Warren. Crystal structure of uranium—108(A)
Jacobs, Robert Byron. Face-centered to body-centered transitions in the alkali-halides—930(A)
——— **and Dennison Bancroft.** New electrostatic method for the determination of Young's modulus—687(A)
Jaffe, Hans von R. Crystalline transitions and dielectric constant—917(A)
James. Hubert M. (see Johnson, Vivian A.)—327(A)
——— **and Albert Sprague Coolidge.** Quadrupole rotation-vibration spectrum of H_2—208(A)
Jauncey, G. E. M. Heavy beta-rays?—669(L)
——— Heavy beta-rays—More theory and experimental evidence—265(L)
——— Heavy beta-rays from RaE—197(L)
——— Heavy electrons from radium E—Discussion of the evidence—319(L)
——— Heavy particles and the neutrino—106(L)
——— Position of the center of the Compton modified band—332(A)
——— Variation of characteristic temperature with the temperature of zinc crystals—203(A)
——— (see Bruce, W. A.)—332(A)
Jenkins, F. A. (see Lyman, Elisabeth Reed)—214(A)
——— **and G. D. Rochester.** Absorption spectra of diatomic fluorides in the carbon-tube furnace—213(A)
——— **and Dean E. Wooldridge.** Mass ratio of the carbon isotopes from the spectrum of Cn—137
Jesse, William P. (see Doan, Richard L.)—203(A)
——— **and Richard L. Doan.** Rate of production of very large cosmic-ray bursts as a function of lead shielding thickness—691
Johnson, M. H. (see Halpern, Otto)—939(A)
Johnson, N. G. Effect of chemical combination of the $K\alpha_{1,2}$ line of sodium—434(L)
Johnson, R. P. Construction of filament surfaces—936(A)
——— Drift of adsorbed Th on W filaments heated with d.c.—766(L)
Johnson, Thomas H. Circuits for the control of Geiger counters and for scaling and recording their impulses—914(A)
——— Cosmic radiation and the earth's magnetism—329(A)
——— Intensity of the primary cosmic radiation and its energy distribution—499, 682(A)
Johnson, Vivian A. and Hubert M. James. Effect of valence electrons on intensities in electron scattering from zinc oxide—327(A)
Jones, Creighton C. (see Ruark, Arthur)—264(L), 454, 496(L), 679(A), 853(A)
——— **and Arthur Ruark.** Stereoscopic viewing and measuring instruments for cloud chamber photographs—677(A)

Kabakjian, D. H. Luminescence of pure crystals—919(A)
Kamen, Martin (see Kurie, Franz, N. D.)—212(A)
Karapetoff, Vladimir. Scale for predicting nuclear transformations—675(A)
Kaufman, A. R. Measurement of magnetic fields and susceptibilities in solenoids—933(A)
Kellogg, J. M. B. and Norman F. Ramsey. On the magnetic moments of neon and argon—331(A)
Kenty, Carl. Reversible clean-up effect in low pressure mercury vapor discharges—936(A)
Kersten, H. (see Dwight, C. H.)—926(A)
Kiess, C. C. Infra-red arc spectrum of germanium—931(A)
King, Allen. Photoelectric and thermionic investigations of thoriated tungsten surfaces—570

Kingdon, K. H. and H. E. Tanis, Jr. Experiments with a condenser discharge x-ray tube—128
Kinsey, E. L. (see Ellis, J. W.)—672(L)
Kip, Arthur F. Positive-point to plane discharge in air at atmospheric pressure—210(A)
Kirkwood, John G. (see Harkins, William D.)—322(A)
Kleis, J. D. Erratum: Ferromagnetic anisotropy of nickel-iron crystals at various temperatures—848(L)
Knauss, Harold P. (see Paul, Fred W.)—930(A)
Knipp, Julian K. Quadrupole-quadrupole interatomic forces—734
Knowlton, John W. and Frederick D. Rossini. Heat of combustion of tetramethylmethane—946(A)
Koch, Jørgen (see Frisch, O. R.)—719
Koch, W. R. Variation of contrast with wave-length in photographic materials—325(A)
Kolhörster, W. Cosmic rays; barometric effect, variations of second kind and disturbances produced by the earth's magnetic field—768(L)
Kondorsky, E. Magnetic anisotropy of ferromagnetic crystals in weak fields and reversible susceptibility—1022(L)
——— On magnetic anisotropy in ferromagnetic crystals in weak fields—319(L)
Konopinski, E. J. (see Bethe, H. A.)—688(A)
——— **and H. A. Bethe.** Mean life of rubidium 87—679(A)
Korff, S. A. Bursts in cosmic-ray ionization in the equatorial zone—914(A)
——— (see Curtiss, L. F.)—23, 330(A)
———, **L. F. Curtiss and A. V. Astin.** Latitude effect in cosmic radiation at high altitudes—14
Kovarik, Alois F. and Norman I. Adams, Jr. Disintegration constant of thorium—928(A)
Kruger, P. Gerald (see Green, G. K.)—927(A)
———, **W. E. Shoupp, R. E. Watson and F. W. Stallmann.** Scattering of neutrons by deuterons—1014(L)
Kuper, J. B. H. Electronic absorption photometer—920(A)
——— Scattering of fast electrons in gases—993
Kurie, Franz N. D. On some operating characteristics of a cloud chamber designed for use through a range of pressures—215(A)
——— **and Martin Kamen.** On the disintegration of nitrogen by neutrons; further experiments in a low pressure cloud chamber—212(A)
Kusch, P. (see Rabi, I. I.)—318(L), 495(L)

Lamb, W. E., Jr. and L. I. Schiff. On the electromagnetic properties of nuclear systems—651
——— **and R. Serber.** Theory of neutron-deuteron impacts—215(A)
——— **and A. J. F. Siegert.** Production of pairs by fast electrons—211(A)
Landshoff, Rolf. Theory of the x-ray absorption edges and their fine structure in ionic compounds—332(A)
Langer, Lawrence M. (see Mitchell, Allan C. G.)—505, 675(A)
Langer, R. M. Nature of the penetrating component of the cosmic radiation—494(L)
Lark-Horovitz, K. (see How, T. G.)—334(A)
Lauritsen, C. C. (see Fowler, W. A.)—212(A), 628, 942(A)
Lawson, J. L. (see Lifschutz, Harold)—204(A)
——— **and A. W. Tyler.** Improvement in Geiger-Müller tube design—605(L)
Leverenz, H. W. Relative emission spectra of zinc silicates and other cathodoluminescent materials—919(A)
Levy, Sam. (see Ramberg, Walter)—945(A)
Lewis, Arthur B. Effect of humidity and irradiation on the 2.0 cm sphere gap—850(A)
Lifschutz, Harold. Vacuum tube frequency meter—950(A)
——— **and O. S. Duffendack.** Simple method for determining counting losses of single scale recorders—941(A)
——— **and J. L. Lawson.** Vacuum tube scale of eight circuit—204(A)
Lindsay, R. B. Filtration of oblique plane compressional waves in a stratified medium—944(A)
Livingood, J. J. and G. T. Seaborg. Long lived radio cobalt isotopes—847(L)
——— **and G. T. Seaborg.** Radioactive iodine isotopes—1015(L)
——— **and G. T. Seaborg.** Radio isotopes of nickel—765(L)
Livingston, M. Stanley (see Hoffman, J. G.)—676(A), 929(A), 1020(L)
——— (see Holloway, M. G.)—676(A)
——— **and J. G. Hoffman.** Slow neutron disintegration of B^{10} and Li^6—227
——— **and M. G. Holloway.** Alpha-particle mean range standards—922(A)
Locher, Gordon L. Photoelectric Geiger-Müller counters with caesium cathodes—333(A)
——— (see Roberts, R. B.)—1016(L)
Loring, R. A. (see Green, J. B.)—330(A)
Lu, Hoff. Low temperature thermal source of Li ions—845(L)
Lueneburg, R. (see Halpern, O.)—173
Luyet, Basile J. Existence of a vitreous state in gelatin gels—323(A)
Lyddane, R. H. and K. F. Herzfeld. Lattice vibrations in polar crystals—948(A)
Lyman, Elisabeth Reed. Rotational energy distribution of OH molecules from the λ3064 band—379
——— **and F. A. Jenkins.** Rotational energy distribution of OH molecules from the λ3064 band—214(A)

Manley, J. H. (see Dunning, J. R.)—205(A)
Mann, Marvin M., Jr. (see Hughes, A. L.)—50, 204(A)
Mann, W. B. Nuclear transformations produced in zinc by alpha-particle bombardment—212(A)
Manning, Millard F. and Marvin I. Chodorow. Electronic energy bands in metallic tungsten—937(A)
——— **and Leo Goldberg.** Self-consistent field for iron—662
——— **and Jacob Millman.** Note on numerical integration—673(L)
Margenau, H. Excited states of the alpha-particles—198(L)
——— (see Carroll, K. G.)—921(A)
——— (see Tyrrell, W. A., Jr.)—939(A)
——— **and W. S. Wilson.** Pressure shifts of spectral lines—941(A)

Marshak, R. E. and H. A. Bethe. Electron pair theory of heavy particle interaction and the Rabi effect—677(A); Erratum 950(A)
Martin, S. T. Relative work functions and adsorptivities of the crystallographic planes of tungsten—937(A)
Mattoon, Richard W. (see Harkins, William D.)—911(L)
Maxfield, Frederick A. Characteristics of the glow-arc transition in mercury vapor—204(A)
Maxwell, H. N. and J. B. Green. Zeeman effect of gold—330(A)
Mayerhöfer, Josef. (see Guth, Eugene)—205(A)
McCarthy, John T. Collisions of alpha-particles with neon and deuterium nuclei—30
McGraw, D. A. (see Colwell, R. S.)—686(A)
McKeehan, L. W. Magnetic interaction in Heusler alloy—199(L)
——— Magnetic interaction in homogeneously strained ferromagnetic crystals—301
——— Magnetic interaction in pyrrhotite and in magnetite—307
McKibben, J. L. (see Parkinson, D. B.)—642
Meissner, K. W. Investigation of hyperfine structure of spectral lines from atomic beams—677(A)
——— Isotopic shift in the spectrum of magnesium MgI—931(A)
Menzel, D. H. (see O'Brien, Brian)—950(A)
Merritt, Ernest. Edward Leamington Nichols—1
Miller, Franklin, Jr. and Lyman G. Parratt. On the determination of single crystal x-ray diffraction patterns from two-crystal spectrometer rocking curves—200(L)
Miller, L. F. Factors affecting the measurement of solar radiation by pyrheliometers—948(A)
Millikan, R. A. (see Bowen, I. S.)—214(A), 217, 328(A), 855, 915(A)
Millman, Jacob (see Manning, Millard F.)—673(L)
Millman, S. (see Rabi, I. I.)—318(L), 495(L)
———, **I. I. Rabi and J. R. Zacharias.** Absolute nuclear moment of indium 115—331(A)
———, **I. I. Rabi and J. R. Zacharias.** On the nuclear moments of indium—384
Mitchell, Allan C. G. Long period activity of indium produced by slow neutrons—269
——— **and Lawrence M. Langer.** Nuclear isomers of In^{116}—505, 675(A)
Mitchell, F. H. Construction and use of Lissajous figures—850(A)
Mitchell, H. Rees. Electrical behavior of thin metallic films condensed at low temperatures—250
Mohler, Fred L. Cesium discharges under conditions of nearly complete ionization—683(A)
——— Resistivity and power input in a columnar discharge under conditions of nearly complete ionization—923(A)
Montgomery, C. G. (see Ramsey, W. E.)—196(L)
——— **and D. D. Montgomery.** Energy flux of the corpuscular cosmic radiation—193, 329(A)
——— **and D. D. Montgomery.** Multiplicative theory of showers as applied to large bursts of cosmic-ray ionization—682(A), 955
Montgomery, D. D. (see Montgomery, C. G.)—193, 329(A), 682(A), 955
——— (see Ramsey, W. E.)—196(L)
Mooney, Rose C. L. X-ray analysis of the structure of tetramethyl ammonium dichloriodide crystals—918(A)
——— X-ray crystal structure study of tetramethyl ammonium tri-iodide—851(A)
More, Kenneth R. and S. D. Cornell. Absorption spectra of SrH and SrCl—678(A)
——— **and S. D. Cornell.** Bands of the *D* system of SrH—931(A)
——— **and S. D. Cornell.** Band spectra of SrCl and SrH—806
Morgan, K. Z. (see Nielsen, W. M.)—915(A)
Morgan, Raymond, Sylvia Steckler and Edward B. Schwartz. X-ray diffraction study of grain boundaries in steel—918(A)
Morrison, P. (see Dancoff, S. M.)—211(A)
Morse, Philip M. (see Schecter, Harry)—107(A)
Motz, Lloyd. (see Goldsmith, H. H.)—947(A)
Murray, M. J. (see Cleveland, Forrest F.)—330(A), 931(A)
Myers, R. D. Angular distribution of resonance disintegration products—325(A)

Neddermeyer, Seth H. Penetrating cosmic-ray particles—102(L)
Neher, H. V. East-west effect in southern India—328(A)
——— (see Bowen, I. S.)—855, 214(A), 217, 328(A), 855, 915(A)
——— (see Pickering, W. H.)—329(A)
——— **and W. H. Pickering.** Latitude effect for cosmic-ray showers—111
——— **and W. H. Pickering.** Modified high speed Geiger counter circuit—316(L)
——— **and W. H. Pickering.** New techniques in the use of Geiger counters—214(A)
Nelson, Edward B. Optical activity of nickel sulfate α-hexahydrate—849(A)
Nielsen, Alvin H. Infra-red absorption by $C^{13}O_2^{16}$ at 4.375μ—983
Nielsen, Harald H. (see Cameron, Donald M.)—246
——— (see Sears, William C.)—330(A)
Nielsen, J. Rud, N. E. Ward and H. Dodson. Raman spectra of some inorganic compounds—331(A)
Nielsen, W. M. (see I. I. Hopkins)—850(A)
——— **and K. Z. Morgan.** Absorption of the penetrating component of the cosmic radiation—915(A)
Nier, Alfred O. Isotopic constitution of calcium, titanium, sulphur and argon—282
——— Isotopic constitution of uranium and the half-life of actino-uranium—922(A)
——— Isotopic constitution of Xe, Kr, As, Cs, I and Be—109(A)
——— Variations in the relative abundances of the lead isotopes—680(A)
Nikitin, S. J. (see Alichanian, A. I.)—767(L)
Nix, Foster C. Vacuum furnace for the production of single crystals of metals and alloys—917(A)
Nordheim, G. (see Sklar, A. L.)—932(A)
——— (see Sponer, H.)—932(A)
Nordheim, L. W. New analysis of cosmic radiation including the hard component—329(A), 694

Nordheim, L. W. and E. Teller. On the production of heavy electrons—937(A)
Nottingham, W. B. Ionization of mercury atoms as a function of the bombarding electron energy—328(A)
——— (see Bell, M. E.)—328(A)
Nuckolls, R. (see Zener, C.)—100
Nusbaum, C. Precision x-ray camera for high temperatures—918(A)

Obert, Leonard and C. H. Shaw. Study of the *K* fluorescent x-ray lines of chemical compounds—919(A)
O'Brien, Brian. (see Stewart, Harold S., Jr.)—949(A)
——— **and Harold S. Stewart, Jr.** Photochemical method for the determination of atmospheric ozone—949(A)
———, **D. H. Menzel, H. S. Stewart, Jr. and C. J. Aronson.** Isophot contours of polarized light photographs of the solar corona—950(A)
Oldenberg, O. Artificial radioactivity of tantalum—35, 109(A)
——— **and F. F. Rieke.** Absorption spectrum as a quantitative test for free hydroxyl—941(A)
Oppel, T. W. (see Hardy, James D.)—920(A)
Oppenheimer, Jacquenette and W. A. Fowler. Scattering and loss of energy of fast electrons and positrons in lead—928(A)
Oppenheimer, J. R. and R. Serber. Note on boron plus proton reactions—636
Otis, W. (see Zener, C.)—100

Page, Chester H. Van der Waals forces in helium—426
Page, Leigh and Norman I. Adams, Jr. Electrical oscillations of a prolate spheroid. Paper I—819
Palmer, K. J. (see Beach, J. Y.)—685(A)
Parkinson, D. B., R. B. Herb, E. J. Bernet and J. L. McKibben. Electrostatic generator operating under high air pressure—operational experience and accessory apparatus—642
Parratt, L. G. Widths of double-ionization x-ray energy states—679(A)
——— (see Miller, Franklin, Jr.)—200(L)
——— (see Richtmyer, F. K.)—678(A)
Paul, Fred W. and Harold P. Knauss. Rotational structure of the $^2\Sigma - {}^3\Pi$ bands of BF—930(A)
Peck, Edson R. (see Fisher, Russell A.)—685(A)
Peoples, J. A., Jr. (see Green, J. B.)—105(L)
——— **and J. B. Green.** Zeeman effect in neon—934(A)
Perrier, C., M. Santangelo and E. Segrè. Radioactive isotopes of zinc and cobalt—104(L)
Perry, Tom. Cyclotron magnet-current stabilizer—943(A)
Petersen, Max. Magnetic susceptibility variations of lead oxide—933(A)
Phillips, L. W. Seventh spectrum of chlorine (Cl VII)—248
Phillips, M. Multipole radiation probabilities in light nuclei—681(A)
Phipps, T. E. (see Seifert, R. L. E.)—493(L)
Pickering, W. H. Preliminary experiments with a cosmic-ray telescope—335(A)
——— Production of cosmic-ray showers at great depths—215(A)
——— (see Neher, H. V.)—111, 214(A), 316(L)
——— **and H. V. Neher.** Latitude effect for cosmic-ray showers—329(A)
Pidduck, F. B. Kinetic theory of the motion of ions in gases—197(L)
Pierce, John Alvin. Abnormal ionization in the *E* region of the ionosphere—942(A)
Pietenpol, W. B. and T. Edwin Devaney. Anodic properties of the aluminum cell—325(A)
Pike, E. W. Proposed new mechanism in excited neon—920(A)
Platt, John R. (see Fisher, Russell A.)—934(A)
Plesset, M. S. and D. H. Ewing. Nuclear excitation functions for high energy charged particles—943(A)
Plyler, E. K. (see Shearin, P. E.)—851(A)
——— (see White, J. W.)—932(A)
Podolsky, Boris. On Eddington's treatment of Dirac's equation—591
Pollard, Ernest. Transmutation of scandium by Th C′ alpha-particles—679(A)
——— (see Davidson, W. L., Jr.)—929(A)
———, **Howard L. Schultz and Gordon Brubaker.** Emission of neutrons from argon, chlorine, aluminum and some heavier elements under alpha-particle bombardment—351
Pool, M. L. Fast neutrons—707
——— Few related experiments with fast neutrons—334(A)
——— Induced radioactivity in silver by fast neutrons—206(A)
——— Isomers of radioindium—611(L)
——— Radioactivity induced in the rare earth elements by fast neutrons—326(A)
——— Radioactivity in silver induced by fast neutrons—116
——— **and Edward C. Campbell.** Note on *K* electron capture and isomerism in radiosilver—272
——— **and L. L. Quill.** Radioactivity induced in the rare earth elements by fast neutrons—437
Post, C. B. (see Ham, W. R.)—935(A)
Powell, Wilson M. Convenient light source for a ten inch Wilson cloud chamber—327(A)
Powers, P. N. (see Carroll, H.)—680(A)
———, **H. H. Goldsmith, H. G. Beyer and J. R. Dunning.** Dependence of neutron interaction with nuclei on neutron energy—947(A)
Primakoff, H. On the superposition of nuclear forces—938(A)

Quill, L. L. (see Pool, M. L.)—437

Rabi, I. I. (see Millman, S.)—331(A), 384
———, **S. Millman, P. Kusch and J. R. Zacharias.** Magnetic moments of $_3Li^6$, $_3Li^7$ and $_9F^{19}$—495(L)
———, **J. R. Zacharias, S. Millman and P. Kusch.** New method of measuring nuclear magnetic moment—318(L)
Ramberg, Walter and Sam Levy. Vibration of rotating propeller blades—945(A)
Ramsey, Norman F. (see Kellogg, J. M. B.)—331(A)

Ramsey, W. E., C. G. Montgomery and D. D. Montgomery. Artificial radioactivity produced by cosmic-rays —196(L)
Rassweiler, M. (see Almy, G. M.)—890
Razor, C. T. Hysteresis testing with cathode rays—851(A)
Reiling, Victor G. (see Collins, George B.)—205(A), 948(A)
Ribner, H. S. and F. O. Wollan. Determination of the characteristic temperature of MgO from x-ray measurements—332(A), 972
Richardson, J. Reginald. Gamma-radiations from Eu^{152} and Au^{198}—942(A)
——— Gamma-radiation from N^{12}—610(L)
——— Radiations emitted from artificially produced radioactive substances. IV. Further studies on the gamma-rays from several elements—124
——— (see Curtis, B. R.)—942(A)
——— **and Lorenzo Emo.** Photodisintegration of the deuteron by the gamma-radiation from Na^{24}—234
Richtmyer, F. K. and L. G. Parratt. Determination of widths of energy states: argon K absorption limit—678(A)
Ridenour, L. N. (see Sherr, R.)—946(A)
———, **L. A. Delsasso, M. G. White and Rubby Sherr.** Artificial radioactivity produced by protons—770(L)
Rieke, F. F. (see Oldenberg, O.)—941(A)
Roberts, Arthur and John W. Irvine, Jr. Concentration of radiohalides, and failure to observe gamma-rays from I^{128}—609(L)
Roberts, R. B. (see Heydenburg, N. P.)—922(A)
——— **and N. P. Heydenburg.** Formation of Be^{7}—929(A)
——— **and N. P. Heydenburg.** Further observations on the production of N^{13}—374
———, **N. P. Heydenburg and G. L. Locher.** Radioactivity of Be^{7}—1016(L)
Robertson, H. P. Invariant theory of isotropic turbulence —939(A)
Robertson, Randal M. Force on the cathode of a copper arc—578
Rochester, G. D. (see Jenkins, F. A.)—213(A)
Rodgers, Eric. Probable errors in counts from Geiger-Müller counters—850(A)
Rogers, F. T., Jr. and Marguerite M. Rogers. Energy-range relations for deuterons, protons and alpha-particles—713
Rogers, Marguerite M. (see Rogers, F. T., Jr.)—713
Roope, Percy M. (see Arenberg, David L.)—687(A)
Rose, M. E. Focusing and maximum energy of ions in the cyclotron—392
——— Gamma-radiation from proton bombardment of carbon—844(L)
——— Magnetic field corrections in the cyclotron—715
——— Maximum energy of ions from the cyclotron—675(A)
——— Multiple scattering of electrons—937(A)
——— **and H. A. Bethe.** On the theory of focusing in the cyclotron—206(A)
Rossini, Frederick D. (see Knowlton, John W.)—946(A)
Rostagni, Antonio. On the sensitivity of the balanced space charge method for detecting ionization of gases by collision of ions and atoms—729
Ruark, Arthur. Multivibrator Geiger counter circuit—316(L)
——— (see Jones, Creighton)—677(A)
——— **and Creighton C. Jones.** Cloud chamber evidence against the existence of heavy beta-particles—454
——— **and Creighton Jones.** Collision relations—853(A)
——— **and Creighton Jones.** Evidence against the existence of heavy beta-particles—264(L), 679(A)
——— **and Creighton C. Jones.** Further evidence against heavy beta-particles—496(L)
Ruhlig, A. J. and H. R. Crane. Absorption of high energy electrons. Part III—618
——— **and H. R. Crane.** Energy loss of electrons in lead—683(A)
——— **and H. R. Crane.** Evidence for a particle of intermediate mass—266(L)
Rumbaugh, L. H. (see Tate, John T.)—928(A)

Sachs, R. G. and M. Goeppert-Mayer. Calculations on a new neutron-proton interaction potential—991
Sagane, R. Minimum neutron energy to produce neutron loss process and its application to the measurement of Q values—492(L)
——— Radioactive isotopes of Cu, Zn, Ga and Ge—212(A)
Salant, E. O. and W. J. Horvath. Absorption of slow neutrons by chlorine—943(A)
Sambursky, S. and M. Schiffer. Static universe and nebular red shift. II—256
Santangelo, M. (see Perrier, C.)—104(L)
Schecter, Harry and Philip M. Morse. An acoustical study of the intake process in an internal-combustion engine—107(A)
Schiff, L. I. (see Lamb, W. E., Jr.)—651
Schiffer, M. (see Sambursky, S.)—256
Schneider, Edwin G. Cosmic-ray ionization in the neighborhood of a lead block—615
Schremp, E. J. Method of identifying the primary cosmic rays—915(A)
Schubauer, G. B. (see Skramstad, H. K.)—927(A)
Schulman, J. H. (see Bikerman, J. J.)—909(L)
Schultz, Howard L. Disintegration of Al by alpha-particles—929(A)
——— Disintegration of Be by alpha-particles—681(A)
——— Disintegration of the deuteron by alpha-particles—622
——— (see Pollard, Ernest)—351
Schwartz, Edward B. (see Morgan, Raymond)—918(A)
Schwarz, W. M. Effect of temperature on the reflection of x-rays from cadmium—919(A)
Scott, G. W., Jr. (see Smith, Lloyd P.)—677(A)
Seaborg, G. T. (see Grahame, D. C.)—795
——— (see Livingood, J. J.)—765(L), 847(L), 1015(L)
Sears, William C., Donald M. Cameron and Harald H. Nielsen. Infra-red absorption by the selenium hydrides —330(A)
Seeger, R. J. and E. Teller. On the electrical breakdown in alkali halides—923(A)
Seely, S. (see Zinn, W. H.)—921(A)
Segrè, E. (see Perrier, C.)—104(L)

Seifert, R. L. E. and T. E. Phipps. Evidence of a periodic deviation from the Schottky line for tungsten—493(L)
Seitz, Frederick. Alkali halide-thallium phosphors—685(A)
Serber, R. On the dynaton theory of nuclear forces—211(A)
——— (see Lamb, W. E., Jr.)—215(A)
——— (see Oppenheimer, J. R.)—636
Share, Simon S. Excited states of the H^3 and He^4 nuclei—875
Shaw, A. E. New method for the precision determination of e/m for electrons—208(A)
——— (see Stephenson, R. J.)—208(A)
Shaw, C. H. Widths and relative intensities of L series lines of the rare earth elements—940(A)
——— (see Obert, Leonard)—919(A)
Shearin, P. E. and E. K. Plyler. Calibration wave-lengths for infra-red spectrometers—851(A)
Shenstone, A. G. New continuum in the spectrum of helium—941(A)
Sherman, K. L. (see Gish, O. H.)—434(L)
Sherr, Rubby (see Ridenour, Louis N.)—770(L)
———, **M. C. Henderson, M. G. White, L. A. Delsasso and L. N. Ridenour.** Artificial radioactivity produced by proton bombardment—946(A)
Shonka, Francis R. (see Eckart, Carl)—752
Shortley, George H. and Bernard Fried. Theory of complex spectra—931(A)
——— **and R. Weller.** Numerical solution of Laplace's equation—207(A)
Shoupp, W. E. (see Kruger, P. G.)—1014(L)
Shrader, J. E. Three-component accelerometer—333(A)
Shrider, Ann L. (see Forsythe, W. E.)—678
Sidhu, S. S. X-ray investigation of the form of acetylsalicylic acid in certain sugars—918(A)
——— (see Hicks, Victor)—207(A)
——— **and Victor Hicks.** On the superstructure and magnetism of pyrrhotite—207(A)
Siegert, A. J. F. (see Lamb, W. E., Jr.)—211(A)
Simpson, O. C. (see Estermann, I.)—947(A)
Singer, George (see Taylor, Lauriston S.)—916(A)
Skaggs, L. S. (see Allison, S. K.)—204(A)
———, **G. T. Hatch and S. K. Allison.** Efficiency of disintegration of beryllium under proton bombardment—946(A)
Skarstrom, C. (see Beams, J. W.)—327(A)
Skinner, Selby M. Film lubrication of the journal bearing of finite width—927(A)
Sklar, A. L. (see Sponer, H.)—932(A)
———, **H. Sponer and G. Nordheim.** Comparison of the absorption spectra of gaseous and solid benzene—932(A)
Skramstad, H. K. and G. B. Schubauer. Application of thermal diffusion to the study of turbulent air flow—927(A)
Slater, J. C. Diamagnetism of small regions and the superconducting state—208(A)
Slawsky, Zaka I. Centrifugal distortion of axial molecules—924(A)
——— (see Dennison, David M.)—930(A)
Smith, Alpheus W. (see Walker, J. W.)—140
Smith, C. S. Capacity controlled magnetic suspension—933(A)
——— Vacuum type high speed electrostatic motor—688(A)
Smith, Lloyd P. (see Hartman, Paul L.)—677(A)
——— **and G. W. Scott, Jr.** Factors governing yield from ion sources using focused beams—677(A)
Smith, Nicholas M., Jr. (see Alaoglu, Leon)—832
——— (see Allison, S. K.)—204(A), 946(A)
Snoddy, L. B. (see Black, Sheppard A.)—924(A)
——— (see Dietrich, J. R.)—923(A)
Snow, Chester. Mutual inductance between two coaxial helical wires—934(A)
Snyder, H. Transition effects of cosmic rays in the atmosphere—960
Sokolow, A. (see Iwanenko, D.)—910(L)
Sparks. C. Matilda (see Curtis, H. L.)—934(A)
Spees, A. H. (see Zahn, C. T.)—357, 365, 511
———, **W. F. Colby and S. Goudsmit.** Capture cross section for thermal neutrons—326(A)
Sponer, H. (see Bruch-Willstätter, M.)—324(A)
——— (see Coy, Nettie H.)—495(L)
——— (see Sklar, A. L.)—932(A)
——— **and William Hurst.** Portable eagle mounting for a 3 m grating—851(A)
———, **G. Nordheim and A. L. Sklar.** On the analysis of the absorption spectrum of benzene at 2700–2200A—932(A)
Stallmann, F. W. (see Kruger, P. G.)—1014(L)
Starr, Merle A. Production of cosmic-ray showers in lead—6
——— (see Brode, Robert B.)—3, 214(A)
Staub, H. and W. E. Stephens. Neutrons from boron plus deuterons—212(A)
Steckler, Sylvia (see Morgan, Raymond)—918(A)
Stehn, J. R. (see Breit, G.)—459, 684(A)
Steigman, Joseph. Concentration of radioactive copper by use of a high speed rotating cathode—771(L)
Stephens, William E. Neutrons from lithium plus deuterons—212(A), 223
——— (see Staub, H.)—212(A)
Stephenson, R. J., M. Ference and A. E. Shaw. Production of uniform magnetic fields—208(A)
Stern, O. (see Estermann, I.)—947(A)
Stevenson, A. F. On the lower bounds of Weinstein and Romberg in quantum mechanics—199(L)
Stewart, G. W. Variation of apparent ionic volumes with concentration in aqueous solutions—323(A)
——— X-ray diffraction in ionic solutions—202(A)
Stewart, Harold S., Jr. (see O'Brien, Brian)—949(A), 950(A)
——— **and Brian O'Brien.** Automatic spectrograph and accessory equipment for solar spectrum photography—949(A)
Stewart, J. K. (see Friend, A. W.)—945(A)
Stockmann, L. L. (see Curtiss, L. F.)—23, 330(A)
Storks, K. H. (see Germer, L. H.)—322(A)
Strain, C. V. (see DuBridge, L. A.)—326(A), 447
——— **and J. H. Buck.** Additional radioactivities induced by high energy protons—943(A)
Strait, L. A. and R. B. Aird. Detection of cocaine-HCl in cerebrospinal fluid by spectroscopic analysis—213(A)

Straley, J. W. (see Walker, J. W.)—140
Stranathan, J. D. Electric moment of the methyl and ethyl alcohol molecules—323(A)
Street, J. C. Review of the evidence for the existence of a new particle—109(T)
Stücklen, Hildegard (see Carr, Emma P.)—109(A)
Suits, C. G. Multiple states in the high pressure discharge —609(L)
——— **and J. P. Hocker.** Role of oxidation in arc cathode —670(L)
Swanson, D. C. (see Bacher, R. F.)—676(A), 922(A)

Tamm, Ig. Transmutations of the cosmic-ray electrons and the nuclear forces—1016(L)
Tanis, H. E., Jr. (see Kingdon, K. H.)—128
Tape, Gerald F. and J. M. Cork. Induced radioactivity in tellurium—676(A)
Tarasov, L. P. Demagnetization coefficient of oblate spheroids—105(L)
Taschek, Richard (see Williams, Dudley)—851(A)
——— **and Dudley Williams.** Infra-red absorption spectrum of a liquid crystal—852(A)
Tate, John T. (see Baker, Richard F.)—683(A), 944(A)
———, **L. H. Rumbaugh and J. H. Williams.** Design and construction of the Minnesota pressure electrostatic generator—928(A)
Taylor, John K. (see Tilton, Leroy W.)—918(A)
Taylor, Lauriston S. and George Singer. Measurement of super-voltage radiation with the standard ionization chamber—916(A)
Teller, E. (see Critchfield, C.)—684(A), 812
——— (see Gamow, G.)—608(L), 929(A)
——— (see Nordheim, L. W.)—937(A)
——— (see Seeger, R. J.)—923(A)
——— **and J. A. Wheeler.** On the rotation of atomic nuclei—684(A)
——— **and J. A. Wheeler.** On the rotation of the atomic nucleus—778
Thein, Louis P. Photoelectric sensitization of aluminum—287
Thode, H. G., John E. Gorham and H. C. Urey. Further concentration of N^{15}—920(A)
Thomas, B. W., R. B. Dow and W. R. Ham. Absolute viscometer for lubricating oils at high pressure—926(A)
Thomas, C. D. (see Gingrich, Newell S.)—944(A)
——— **and Newell S. Gingrich.** Atomic distribution in liquid potassium at 70°C and at 395°C—943(A)
Thornton, R. L. Radioactive isotopes of zinc—326(A)
——— (see Cork, J. M.)—866
——— **and J. M. Cork.** Multiple ejection of neutrons from excited nuclei—922(A)
Tilton, Leroy W. and John K. Taylor. Refractive index and dispersion of distilled water for visible radiation, at temperatures 0 to 60°C—918(A)
Tomboulian, D. H. and R. F. Bacher. Interval rule in hyperfine structure—678(A)
Tonks, Lewi. Vaporization of mercury from anchored cathode spot—936(A)
Tool, A. Q. Heat effects of tridymite inversions—945(A)
Torrey, Henry C. Analysis of neutron absorption in boron —266(L)
Trichel, G. W. Mechanism of corona discharge—214(A)
Trimble, Frank H. and Newell S. Gingrich. Effect of temperature on the atomic distribution in liquid sodium —203(A), 278
Turnbull, John C. and H. E. Farnsworth. Inelastic scattering of electrons from a silver single crystal—944(A)
Tuve, M. A. (see Hafstad, L. R.)—239
Tyler, A. W. (see Lawson, J. L.)—605(L)
Tyrrell, W. A., Jr. and Henry Margenau. Variational theory of the alpha-particle—939(A)

Ufford, C. W. Term values in carbon—568
Underwood, Newton. Displacement polarimeter—853(A)
Urey, H. C. (see Thode, H. G.)—920(A)

Valasek, Joseph. X-ray spectroscopic data in regard to the electronic energy bands in potassium and sodium chlorides—274
Vallarta, M. S. Cosmic-rays and the earth's magnetic field —109(T)
Valley, George (see Barnes, S. W.)—946(A)
Van Dyke, K. S. Some unusual demonstrations with piezoelectric resonators—686(A)
——— Vibration modes of low decrement for a quartz ring—945(A)
Van Vleck, J. H. On the scattering of neutrons by paramagnetic media—680(A)
Varney, Robert N. Sensitivity of the balanced space charge positive ion detector—732
von Halban, H. (see Frisch, O. R.)—719

Wadlund, A. P. R. Radial lines in Laue spot photographs—843(L)
Wahlin, H. B. (see Hole, W. L.)—768(L)
Walerstein, I. (see Howe, J. D.)—334(A)
Walker, J. W., J. W. Straley and Alpheus W. Smith. Band spectra of PbSe, SnSe and PbTe in absorption—140
Wannier, G. Improved Wigner-Seitz method for the calculation of electronic energy bands—671(L)
Ward, N. E. (see Nielsen, J. Rud)—331(A)
Warren, B. E. (see Jacob, C. W.)—108(A)
Waterman, Alan T. (see Bartlett, Russell S.)—109(T)
Watson, R. E. (see Kruger, P. G.)—1014(L)
Watson, William W. Spectra of the monoxides of cerium and praseodymium—639
——— Spectra of rare earth oxides—678(A)
Way, Katharine. Nuclear quadrupole and magnetic moments—685(A)
Weber, Alfred H. Some photoelectric properties of evaporated bismuth films—895
Weber, Ernst. On the nature of the Hall effect—935(A)
Weisskopf, V. Excitation of nuclei by bombardment with charged particles—1018(L)
——— Note on the Hartree approximation method for calculating nuclear energies—680(A)
Weller, R. (see Shortley, G. H.)—207(A)

Wenner, Frank and Irvin L. Cooter. Precise control and measurements of the speed of a rotating shaft having a mechanical load of 200 watts—927(A)
Wheeler, J. A. (see Teller, E.)—684(A), 778
——— **and C. V. Cannon.** Rotational transition in solid methane—684(A)
White, A. B. Characteristics of the copper arc in air—935(A)
White, J. W. and E. K. Plyler. Infra-red absorption of mixtures of phenol and ethyl alcohol—932(A)
White, M. G. (see Ridenour, Louis N.)—770(L)
——— (see Sherr, R.)—946(A)
Wick, G. C. (see Fermi, E.)—493(L)
Wigner, E. (see Breit, G.)—998
Wiig, E. O. (see DuBridge, L. A.)—326(A)
Wilhelm, K. (see Carroll, H.)—947(A)
Williams, Dudley. Optical properties of fluorite in the 6μ region—930(A)
——— (see Taschek, Richard)—852(A)
——— **and Loraine Decherd.** Infra-red spectra of nitrate solutions—852(A)
——— **and Richard Taschek.** Device for controlling the temperature of absorption cells—851(A)
Williams, D. T. and L. P. Granath. Hyperfine structure of boron, yttrium, rhodium and palladium—685(A)
Williams, E. J. Scattering of cosmic-ray particles—433(L)
Williams, John H. (see Allen, James S.)—325(A), 928(A)
——— (see Haxby, R. O.)—921(A)
——— (see Tate, John T.)—928(A)
Wilson, Robert G. Vectorial photoelectric effect in barrier-layer cells—264(L)
Wilson, Robert R. Focusing actions in the cyclotron—213(A)
——— Magnetic and electrostatic focusing in the cyclotron—408
Wilson, Volney C. Cosmic-ray intensities at great depths—204(A), 337
——— On the nature of the penetrating cosmic rays—908(L)
Wilson, W. S. (see Margenau, Henry)—941(A)
Winans, J. G. and Francis J. Davis. Mercury-thallium molecular bands—930(A)
Winch, Ralph P. (see Farnsworth, H. E.)—935(A)
Witcher, C. (see Beyer, H. G.)—947(A)
Witmer, Enos E. Tabulation and study of the energy levels of the asymmetrical rotator—331(A)
Wollan, E. O. Simplified method of obtaining the integrated intensity from x-ray powder photographs—208(A)
——— X-ray investigation of the asymmetry of the atoms and of the atomic vibrations in a silver-cadmium alloy—203(A)
——— (see Ribner, H. S.)—332(A), 972
Wood, R. W. and G. H. Dieke. Spectrum of the arc in hydrogen—146
Wooldridge, Dean E. (see Jenkins, F. A.)—137
Worthing, A. G. (see Benford, Frank)—948(A)
Wright, R. (see Hole, W. L.)—768(L)

Yetter, E. W. Another circuit for use with Geiger-Müller counters—612(L)
Young, L. A. Rate of recrystallization in polycrystalline solids—686(A)

Zacharias, J. R. (see Millman, S.)—331(A), 384
——— (see Rabi, I. I.)—318(L), 495(L)
Zachariasen, W. H. Comments on the article by A. P. R. Wadlund: Radial lines in Laue spot photographs—844(L)
——— Crystal structure of potassium acid dihydronium pentaborate, $KH_3(H_3O)_2B_5O_{10}$—202(A)
——— Crystal structure of sodium formate, $NaHCO_2$—917(A)
Zahn, C. T. Heavy beta-particles?—431(L)
——— **and A. H. Spees.** Critical analysis of the classical experiments on the relativistic variation of electron mass—511
——— **and A. H. Spees.** Improved method for the determination of the specific charge of beta-particles—357
——— **and A. H. Spees.** Specific charge of disintegration electrons from radium E—365
Zartman, I. F. and J. C. Hubbard. Fixed path acoustic interferometer for the study of matter—944(A)
Zener, Clarence. Internal friction in solids. II. General theory of thermoelastic internal friction—90
——— Internal friction in solids. IV. Relation between cold work and internal friction—582
——— Internal friction in solids. V. General theory of macroscopic eddy currents—1010
——— Relationship between internal friction and cold work in metals—686(A)
———, **W. Otis and R. Nuckolls.** Internal friction in solids. III. Experimental demonstration of thermoelastic internal friction—100
Zinn, W. H., S. Seely and V. W. Cohen. Scattering cross sections of various elements for D-D neutrons—921(A)
Zisman, W. A. (see Goranson, Roy W.)—668(L)
Zwicky, F. Change and exchange of rest mass of elementary particles during collisions—611(L)
——— Intrinsic variability of the so-called fundamental physical constants—315(L)
——— Some results of the search for super-novae—1019(L)

Analytic Subject Index to Volume 53

References with (A) are to abstracts of papers presented at meetings of the American Physical Society. References with (L) are to Letters to the Editor.

Absorption
Of high energy electrons, A. J. Ruhlig, H. R. Crane—618; 683(A)
Of positive electrons in Al, B. R. Curtis—986
Acoustics
Fixed path acoustic interferometer, I. F. Zartman, J. C. Hubbard—944(A)
Persistence of molecular vibration in collisions, R. J. Dwyer—324(A)
Reflection of sound, K. F. Herzfeld—899
Ultrasonic study of CO_2 near critical point, J. C. Hubbard, C. M. Herget—945(A)
Velocity of sound in air, R. C. Colwell, A. W. Friend, D. A. McGraw—686(A)
Vibrations of a circular plate, A. W. Friend, J. K. Stewart, R. C. Colwell—945(A)
Of internal-combustion engine, H. Schecter, P. P. Morse—107(A); C. S. Draper—108(A)
Aerodynamics (see **Hydrodynamics**)
Alloys (see **Crystalline state**)
Arcs (see **Discharge of electricity in gases**)
Astrophysics
Electromagnetic and gravitational radiation, L. Infeld—938(A)
Gravitational constant and Hubble's factor, A. Haas—207(A)
Nebular red shift, S. Sambursky, M. Schiffer—256
Neutron core of stars, G. Gamow, E. Teller—929(A)
Nuclear energy sources and stellar evolution, G. Gamow—595; 608(L); 908(L)
Photographs of solar corona, B. O'Brien, D. H. Menzel, H. S. Stewart, Jr., C. J. Aronson—950(A)
Photon emission of sun, A. E. Haas—681(A)
Red shift, I. M. Freeman—207(A)
Solar spectrum photography, H. S. Stewart, Jr., B. O'Brien—949(A)
Super-novae; characteristics of, F. Zwicky—1019(L)
Atomic and molecular beams
Free fall of molecules, I. Estermann, O. C. Simpson, O. Stern—947(A)
Atomic and molecular radii (see **Scattering of electrons**)
Atomic mass (see **Isotopes**)

Biophysics
Barometer, for small volumes, W. Hurst—850(A)
Cold sensation by radiation, J. D. Hardy, T. W. Oppel—920(A)
Detection of cocain-HCl in cerebrospinal fluid, L. A. Strait, R. B. Aird—213(A)
Effects of low voltage electrons, C. E. Buchwald, C. P. Haskins—920(A)
Electronic absorption photometer, J. B. H. Kuper—920(A)
Impedance of *Nitella* during excitation, K. S. Cole, H. J. Curtis—687(A)
Impedance of single arbacia eggs, K. S. Cole, H. J. Curtis—333(A)
Measurement of super-voltage radiation, L. S. Taylor, G. Singer—916(A)
Radiography of thin microtome sections, E. Dershem—202(A)
Short exposure, high intensity x-rays, K. H. Kingdon, H. E. Tanis, Jr.—128
X-ray generator for biological experiments, G. Failla—916(A)
Brownian movement
Photographic measurements, C. Hire—205(A); 325(A)

Collision diameter (see **Atomic and molecular radii**)
Conductivity, electrical (see **Electrical conductivity; Discharge of electricity in gases**)
Constants, physical, standards
Discrepancy among experimental measurements, R. A. Beth—681(A)
Variability of constants, F. Zwicky—315(L)
Contact potentials
Of solid films on metals, W. D. Harkins, R. W. Mattoon—911(L)
Cosmic radiation
Absorption of penetrating component, W. M. Nielsen, K. Z. Morgan—915(A); V. C. Wilson—908(L)
Analysis including hard component, L. W. Nordheim—329(A); 694
Artificial radioactivity, W. E. Ramsey, C. G. Montgomery, D. D. Montgomery—196(L)
Bursts in equatorial zone, S. A. Korff—914(A)
Change of mass, Ig. Tamm—1016(L)
Cosmic-ray telescope, W. H. Pickering—335(A)
East-west effect in India, H. V. Neher—328(A)
Effect of earth's magnetism, T. H. Johnson—329(A)
Electrical conductivity in stratosphere, O. H. Gish, K. L. Sherman—434(L)
Energy and intensity of primary, T. H. Johnson—499; 682(A)
Energy distribution, I. S. Bowen, R. A. Millikan, H. V. Neher—328(A); 915(A)
Energy flux of corpuscular radiation, C. G. Montgomery, D. D. Montgomery—193; 329(A)
Galactic rotation, I. A. Getting—914(A)
Identification of primary rays, E. J. Schremp—915(A)
Influence of earth's field, W. Kolhörster—768(L)
Influence of solar magnetic field, P. S. Epstein—862
In stratosphere, L. F. Curtiss, A. V. Astin, L. L. Stockmann, B. W. Brown, S. A. Korff—23; 330(A)
Intensity and magnetic storms, S. E. Forbush—914(A)
Intensities at great depths, V. C. Wilson—204(A); 337
Ionization near a lead block, E. G. Schneider—615
Large bursts, function of Pb shielding, W. P. Jesse, R. L. Doan—203(A); 691

Cosmic radiation (continued)
Large bursts, theory of, C. G. Montgomery, D. D. Montgomery—682(A); 955
Latitude effect, high altitudes, S. A. Korff, L. F. Curtiss, A. V. Astin—14
Latitude effect, showers, H. V. Neher, W. H. Pickering—111; 329(A)
Latitude effect of soft rays, B. Gross—607(L)
Nature of penetrating component, R. M. Langer—494(L)
Nature of radiation, I. S. Bowen, R. A. Millikan, H. V. Neher—214(A); 217; 855
Nuclear disintegrations, R. B. Brode, M. A. Starr—3; 214(A)
Penetrating particles, S. H. Neddermeyer—102(L)
Range of particles, A. Bramley—915(A)
Scattering of particles, E. J. Williams—433(L)
Showers at great depths, W. H. Pickering—215(A)
Showers in lead, M. A. Starr—6
Sidereal diurnal variation, S. E. Forbush—682(A)
Specific ionization and mass of particles, D. R. Corson, R. B. Brode—215(A); 773
Stopping power of heavy elements, J. H. Bartlett, Jr.—915(A)
Theory of showers, D. Iwanenko, A. Sokolow—910(L)
Transition effects in atmosphere, H. Snyder—960
Cosmic rays
Penetrating component, J. Barnóthy, M. Forró—848(L)
Crystal structure
Form of acetylsalicylic acid in certain sugars, S. S. Sidhu—918(A)
Of $KH_2(H_3O)_2B_5O_{10}$, W. H. Zachariasen—202(A)
Of $N(CH_3)_4I_3$, R. C. L. Mooney—851(A)
Of $NaHCO_2$, W. H. Zachariasen—917(A)
Space group of pyrrhotite, V. Hicks, S. S. Sidhu—207(A)
Of $N(CH_3)_4I\,Cl_2$, R. C. L. Mooney—918(A)
Of uranium, C. W. Jacob, B. E. Warren—108(A)
Crystalline state
Alkali halide-thallium phosphors, F. Seitz—685(A)
Anisotropy of crystals, E. Kondorsky—1022(L)
Anisotropy of vibrations in a Zn-Cu alloy, R. A. Howard—324(A); 966
Asymmetry of atoms in Ag-Cd alloy, E. O. Wollan—203(A)
Barium-copper-stearate films, properties of, C. Holley—534; I. Fankuchen—909(L); J. J. Bikerman, J. H. Schulman—909(L)
Calculation of electronic energy bands, G. Wannier—671(L)
Characteristic temperature of MgO, H. S. Ribner, E. O. Wollan—332(A); 972
Characteristic temperature of Zn crystals, G. E. M. Jauncey—203(A)
Cold work and internal friction, C. Zener—582
Critical cooling rate of iron-carbon alloys, T. G. Digges—925(A)
Crystalline transitions and dielectric constant, H. v. R. Jaffe—917(A)
Deformation textures, C. S. Barrett—925(A)
Electrical breakdown in alkali halides, R. J. Seeger, E. Teller—923(A)
Electronic energy bands in W, M. F. Manning, M. I. Chodorow—937(A)
Electronic energy bands in KCl and NaCl, J. Valasek—274
Grain boundaries in steel, R. Morgan, S. Steckler, E. B. Schwartz—918(A)
Heat effects of tridymite inversions, A. Q. Tool—945(A)
Internal friction in solids, C. Zener—90; 100; 582; 686(A); 1010
Ions in surface structure, R. P. Johnson—766(L)
Lattice vibrations in polar crystals, R. H. Lyddane, K. F. Herzfeld—948(A)
Order *versus* disorder, lattice enlargement, F. C. Blake—333(A)
Oscillation in rhombic sulphur, S. Bhagavantam—1015(L)
Radial lines in Laue spots, A. P. R. Wadlund—843(L); W. H. Zachariasen, 844(L); C. S. Barrett—1021(L)
Rate of recrystallization, L. A. Young—686(A)
Recalescence in uranium, W. L. Hole, R. Wright, H. B. Wahlin—768(L)
Rotational transition in solid methane, J. A. Wheeler, C. V. Cannon—684(A)
Segregation of Po in Bi crystals, A. B. Focke—324(A)
Solubility at grain boundaries of solid solutions, G. R. Dean—202(A)
Supercooling and freezing of water, N. E. Dorsey—925(A)
Superstructure and magnetism of pyrrhotite, S. S. Sidhu, V. Hicks—207(A)
Transition energies of polymorphous molecular crystals, M. Bruch-Willstätter, H. Sponer—324(A)
Transitions in alkali-halides, R. B. Jacobs—930(A)
Vitreous state in gelatin gels, B. J. Luyet—323(A)

Dielectric constants (see **Dielectrics and dielectric properties**)
Dielectrics and dielectric properties
Crystalline transitions and dielectric constant, H. v. R. Jaffe—917(A)
Electric moment of methyl and ethyl alcohol, J. D. Stranathan—333(A)
Energy losses in air capacitors, A. V. Astin—927(A)
Permanent electrets, W. M. Good—323(A)
Permanent volume polarization, R. W. Goranson, W. A. Zisman—668(L)
Polar moment of cellosolves, W. H. Byers, A. A. Bless—852(A)
Susceptibility of Rochelle salt, D. Bancroft—587
Diffraction of electrons (see **Electron diffraction**)
Diffusion
In a centrifugal field of force, W. J. Archibald—746; 923(A)
Of hydrogen through Ni, W. R. Ham, C. B. Post—935(A)
Discharge of electricity in gases
Cathode material and Townsend coefficient, W. E. Bowls—210(A); 293

Clean-up effect in low pressure Hg vapor discharges, C. Kenty—936(A)
Cu arc in air, A. B. White—935(A)
Corona discharge, G. W. Trichel—214(A)
Discharges under nearly complete ionization, F. L. Mohler—683(A); 923(A)
Force on cathode of Cu arc, R. M. Robertson—578
Glow-arc transition in Hg vapor, F. A. Maxfield—204(A)
Impulse breakdown in long tubes, J. R. Dietrich, L. B. Snoddy, J. W. Beams—923(A)
Mechanism of positive column in Hg, E. Q. Adams, B. T. Barnes—556
New mechanism in excited neon, E. W. Pike—920(A)
Oxidation in arc cathode, C. G. Suits, J. P. Hocker—670(L); J. D. Cobine—911(L)
Positive-point to plane discharge, A. F. Kip—210(A)
Recombination in pure O_2, M. E. Gardner—75
Sparking potential, F. Ehrenkranz—210(A)
Sparking voltage of sphere gap, effect of humidity, A. B. Lewis—850(A)
States in high pressure discharge, C. G. Suits—609(L)
Vaporization of Hg from anchored cathode spot, L. Tonks—936(A)

Discharge of electricity in high vacuum (see **Thermionic emission; High voltage tubes and machines**)

Disintegration of nucleus (see also **Radioactivity**)
Of Al by He^4, H. L. Schultz—929(A)
Of C; γ-radiation, M. E. Rose—844(L)
Angular distribution of disintegration products, R. D. Myers—325(A)
Angular distribution of H^1 from H^2+H^2, R. O. Haxby, J. S. Allen, J. H. Williams—921(A)
Of Be by He^4, H. L. Schultz—681(A)
Of B^{10} and Li^6 by neutrons, M. S. Livingston, J. G. Hoffman—227
$B^{11}+H^1$ reactions, J. R. Oppenheimer, R. Serber—636
Cloud chamber studies, L. W. Alvarez, W. M. Brobeck—213(A)
Collision relations, A. E. Ruark, C. Jones—853(A)
Of H^2 by He^4, H. L. Schultz—622
Deuteron reactions at high energy, L. W. Alvarez—326(A)
Deviations from evaporation model of reactions, H. A. Bethe—675(A)
Efficiency of $Be+H^1$, L. S. Skaggs, G. T. Hatch, S. K. Allison—946(A)
Energy of neutrons from $C^{12}+H^2$, T. W. Bonner—496(L)
Energy-range relations, F. T. Rogers, Jr., M. M. Rogers—713
Energy spectra of particles, S. K. Allison, N. M. Smith, Jr.—946(A)
Formation of Be^7 and *K* electron capture, R. B. Roberts, N. P. Heydenburg—929(A)
Formation of excited He^3, T. W. Bonner—711
Gamma-radiation from $B+H^1$, W. A. Fowler, E. R. Gaerttner, C. C. Lauritsen—212(A); 628
Loss of neutron and alpha-particle in Fe, relative probability, J. M. Cork, B. R. Curtis—946(A)
Neutron-deuteron impacts, W. E. Lamb, Jr., R. Serber—215(A)
Neutron interaction with nuclei and neutron energy, P. N. Powers, H. H. Goldsmith, H. G. Beyer, J. R. Dunning—947(A)
Neutrons from A, Cl, Al and under He^4 bombardment, E. Pollard, H. L. Schultz, G. Brubaker—351
Neutrons from B, H. Staub, W. E. Stephens—212(A)
Neutrons from $Li+H^2$, W. E. Stephens—212(A); 223; M. L. Pool—707
Of N by neutrons, F. N. D. Kurie, M. Kamen—212(A)
Nuclear excitation functions, M. S. Plesset, D. H. Ewing—943(A)
Oppenheimer-Phillips process, H. A. Bethe—39; 205(A)
Photodisintegration of deuteron, J. R. Richardson, L. Emo—234
Production of N^{13}, R. B. Roberts, N. P. Heydenburg—374
Production of pairs, W. E. Lamb, Jr.—211(A)
Scale for predicting nuclear transformations, V. Karapetoff—675(A)
Of Sc by He^4, E. Pollard—679(A)
Of Sc by neutrons, J. M. Cork, R. L. Thornton—866
Thermonuclear reactions, G. Gamow, E. Teller—608(L)
Of Ti by He^4, W. L. Davidson, Jr., E. Pollard—929(A)
Width of resonance in $B+H^1$, J. S. Allen, R. O. Haxby, J. H. Williams—325(A)

Dispersion
Verification of the quantum mechanical theory, W. A. Bruce, G. E. M. Jauncey—332(A); W. A. Bruce—802

Dissociation
Of CCl_2F_2 and in CCl_4, R. F. Baker, J. T. Tate—683(A)
Of ethane by electron impact, J. A. Hipple, Jr.—530
Of normal and isobutane, R. F. Baker, J. T. Tate—944(A)

Elasticity
Determination of Young's modulus, R. R. Jacobs, D. Bancroft—687(A)
Filtration of compressional waves in stratified medium, R. B. Lindsay—944(A)
Fixed path acoustic interferometer, I. F. Zartman, J. C. Hubbard—944(A)
Internal friction in solids, C. Zener—90; 100; 582; 686(A); 1010
Thermoelastics and structure of rubber, F. E. Dart, E. Guth—327(A)
Vibration modes of low decrement, K. S. Van Dyke—945(A)
Vibration of rotating propeller blades, W. Ramberg, S. Levy—945(A)

Electrical conductivity and resistance
Deviations from Ohm's law, E. Guth, J. Mayerhöfer—205(A)
Drift of ions on filaments, R. P. Johnson—766(L)
Effect of tension; Sn crystals, M. Allen—108(A)
Electrical breakdown in alkali halides, R. J. Seeger, E. Teller—923(A)
At frequencies of the order 300 mC/second, R. A. Chipman—672(L)

Electrical conductivity and resistance (continued)
Of metallic films condensed at low temperatures, H. R. Mitchell—250
Electric moment (see **Dielectrics and dielectric properties**)
Electrolytic cells
Anodic properties of Al cell, W. B. Pietenpol, T. E. Devaney—325(A)
Electrode capacitance of conductivity cells, S. F. Acree —923(A)
Solubility of glass, behavior of glass electrodes, D. Hubbard—935(A)
Electromagnetic theory
Electromagnetic and gravitational radiation, L. Infeld—836
Light signals around a closed path, H. E. Ives—939(A)
Mutual inductance between two coaxial helical wires, C. Snow—934(A)
Oscillations of a prolate spheroid, L. Page, N. I. Adams, Jr.—819
Electron diffraction (see also **Electrons, scattering of**)
Molecules in unimolecular and multimolecular layers, L. H. Germer, K. H. Storks—322(A)
Electrons (see also **Positive electron and e/m**)
Energy loss in Pb, A. J. Ruhlig, H. R. Crane—618; 683(A)
Production of heavy electrons, L. W. Nordheim, E. Teller—937(A)
Electrons, secondary
From Na films on Ta, P. L. Copeland—328(A)
From thorium-coated tungsten, E. A. Coomes—936(A)
Electro-optical effects (see also **Photoelectric effect and properties**)
Optical activity of $NiSO_4$, E. B. Nelson—849(A)
E/m
Analysis of classical experiments, C. T. Zahn, A. H. Spees—511
Of β-rays from RaE, C. T. Zahn, A. H. Spees—365
Change of rest mass during collisions, F. Zwicky—611(L); Ig. Tamm—1016(L)
Determination for β-particles, C. T. Zahn, A. H. Spees—357
Energy losses of Pauli-Weisskopf particles, J. F. Carlson—330(A)
Heavy beta-rays, A. H. Compton—431(L); H. R. Crane —317(L); G. E. M. Jauncey—197(L); 265(L); 319(L); 669(L); A. Ruark, C. C. Jones—264(L); 454; 496(L); 679(A); C. T. Zahn—431(L); F. L. Arnot—1018(L).
Method for precision determination, A. E. Shaw—208(A)
Nature of heavy electron, I. M. Freeman—606(L)
Particle of intermediate mass, A. J. Ruhlig, H. R. Crane —266(L)
From refraction of x-rays, J. A. Bearden—917(A)
Energy states of atoms (see also **Spectra, atomic**)
Self-consistent field for Fe, M. F. Manning, L. Goldberg—662
Energy states of molecules (see also **Molecular structure and constants; Spectra, molecular**)
Energy levels of the asymmetrical rotator, E. E. Witmer —331(A)
Energy states of nucleus (see also **Nucleus**)
Of alpha-particles, excited states, H. Margenau—198(L)
Barytron theory of nuclear forces, H. A. Bethe—938(A)
Binding energy of H^2, H. A. Bethe—313
Binding energy of O^{16}, G. Horvay, E. Feenberg—938(A)
Compound nucleus, H. A. Bethe, E. J. Konopinski—688(A)
Dynaton theory of nuclear forces, R. Serber—211(A)
Energy of heavy nuclei, A. J. Dempster—869
Excitation of nuclei, V. Weisskopf—1018(L)
Excited He^3 in H^2+H^2, T. W. Bonner—928(A)
Fine structure of ground level of Li^7, G. Breit, J. R. Stehn—459; 684(A)
Ground state of deuteron, R. G. Sachs, M. Goeppert-Mayer—991
Hartree approximation, V. F. Weisskopf—680(A)
Heavy particle interactions, D. R. Inglis—686(A)
Of H^3 and He^4, S. S. Share—875
Of Li^6, K. G. Carroll, H. Margenau—921(A)
Multipole radiation probabilities, M. Phillips—681(A)
Rotation of atomic nuclei, E. Teller, J. A. Wheeler—684(A); 778
Saturation of nuclear forces, C. Critchfield, E. Teller—684(A); 812
Saturation requirements for forces, G. Breit, E. Wigner —998
Spacing of nuclear levels, J. Bardeen, E. Feenberg—938(A)
Superposition of nuclear forces, H. Primakoff—938(A)
Variational theory of alpha-particle, W. A. Tyrrell, Jr., H. Margenau—939(A)
Errata
Ferromagnetic anisotropy of nickel-iron crystals at various temperatures, J. D. Kleis—848(L)

Geophysics
Age of earth from isotope ratios, A. Bramley—323(A)
Determination of geologic ages, C. Goodman, R. D. Evans—916(A)
Substandards of feeble radioactivity, R. D. Evans, C. Goodman—916(A)
Gravitation
Electromagnetic and gravitational radiation, L. Infeld—836

Hall effect
Nature of the effect, E. Weber—935(A)
Heat of combustion
Of tetramethylmethane, J. W. Knowlton, F. D. Rossini —946(A)
High voltage tubes and machines
Accelerator using a quarter wave-length, P. L. Hartman, L. P. Smith—677(A)
Compact 750 kv Van de Graaff generator, J. B. Fisk, I. A. Getting—916(A)
Cyclotron magnet-current stabilizer, T. Perry—943(A)
Energy variations in a cyclotron ion beam, G. K. Green, P. G. Kruger—927(A)
Focusing and energy of ions in cyclotron, M. E. Rose, H. A. Bethe—206(A); M. E. Rose—392; 675(A); 715; R. R. Wilson—213(A); 408

Fringing flux in large magnets, J. D. Howe, I. Walerstein—334(A)
Generator for production of neutrons, T. R. Folsom—687(A)
High air pressure electrostatic generator, D. B. Parkinson, R. G. Herb, E. J. Bernet, J. L. McKibben—642
High frequency systems for cyclotron, J. R. Dunning, H. L. Anderson—334(A)
Ion optics of an accelerating tube, J. S. Allen, J. H. Williams—925(A)
Minnesota pressure electrostatic generator, J. T. Tate, L. H. Rumbaugh, J. H. Williams—928(A)
X-ray generator for biological experiments, G. Failla—916(A)

Hydrodynamics
Aerodynamics of golf club, S. J. Crooker—927(A)
Theory of isotropic turbulence, H. P. Robertson—939(A)

Hyperfine structure (see also **Nuclear moments and spin**)
Of B, Y, Rh and Pd, D. T. Williams, L. P. Granath—685(A)
Interval rule, D. H. Tomboulian, R. F. Bacher—678(A)
Of MnI, R. A. Fisher, E. R. Peck—685(A)
Of spectral lines from atomic beams, K. W. Meissner—677(A)

Instruments (see **Methods and instruments**)
Ionization by particles (see **Ionization potentials**)
Ionization potentials
Of CCl_2F_2 and in CCl_4, R. F. Baker, J. T. Tate—683(A)
And dissociation of ethane, J. A. Hipple, Jr.—530
Of Hg, W. B. Nottingham—328(A)
Of normal and isobutane, R. F. Baker, J. T. Tate—944(A)
Use of isotopes in study of ionization processes, J. M. Delfosse, J. A. Hipple, Jr.—683(A)

Ionosphere
Ionization in *E* region, J. A. Pierce—942(A)
Ionization and recombination, N. E. Bradbury—210(A)
Lorentz polarization correction, H. G. Booker, L. V. Berkner—924(A)
Photoelectric ionization, E. O. Hulburt—344
Variation in F_2 ionization, E. O. Hulburt—670(L)

Ions, mobility
Liquids electrified by bubbling, S. Chapman—211(A)

Isotopes
Abundances of Pb isotopes, A. O. Nier—680(A)
Of Ca, Ti, S and A, A. O. Nier—282
Of C from CN spectrum, F. A. Jenkins, D. E. Wooldridge—137
Concentration of N^{15}, H. G. Thode, J. E. Gorham, H. C. Urey—920(A)
Of Gd, Dy, Er and Yb, A. J. Dempster—727
Of heavy elements, A. J. Dempster—64
Of uranium, A. O. Nier—922(A)
Range of occurrence, H. Brown—846(L)
Stable isotopes and atomic numbers, G. E. Gibson, H. Brown—846(L)
Weight of He by direct comparison with O, K. T. Bainbridge—922(A)
Of Xe, Kr, As, Cs, I and Be, A. O. Nier—109(A)

Kinetic theory of gases
Air-lubricated journal bearings, M. D. Hersey—926(A)
Motion of ions in gases, F. B. Pidduck—197(L)
Persistence of molecular vibration in collisions, R. J. Dwyer—324(A)

Liquids (see also **Hydrodynamics**)
Atomic distribution in liquid K, C. D. Thomas, N. S. Gingrich—943(A)
Atomic distribution in liquid Na, F. H. Trimble, N. S. Gingrich—203(A); 278
Atomic distribution in liquid white P, N. S. Gingrich, C. D. Thomas—943(A)
Film lubrication of the journal bearings, S. M. Skinner—927(A)
Supercooling and freezing of water, N. E. Dorsey—925(A)
Variation of ionic volumes, G. W. Stewart—323(A)
Vitreous state in gelatin gels, B. J. Luyet—323(A)

Luminescence
Of pure crystals, D. H. Kabakjian—919(A)
Spectra of cathodoluminescent materials, H. W. Leverenz—919(A)

Magnetic fields
Demagnetization coefficient of oblate spheroids, L. P. Tarasov—105(L)
Production of uniform fields, R. J. Stephenson, M. Ference, A. E. Shaw—208(A)

Magnetic properties
Anisotropy in ferromagnetic crystals, E. Kondorsky—319(L)
Anisotropy of crystals, E. Kondorsky—1022(L)
Diamagnetism of small regions, J. C. Slater—208(A)
Ferromagnetic impurities, detection of, F. W. Constant, J. M. Formwalt—432(L); 852(A)
Hysteresis testing, C. T. Razor—851(A)
Interaction in Heusler alloy, L. W. McKeehan—199(L)
Interaction in pyrrhotite and in magnetite, L. W. McKeehan—307
Interaction in strained crystals, L. W. McKeehan—301
Magnetic viscosity in iron, C. W. Heaps—334(A)
Magnetostriction of polycrystalline material, W. F. Brown, Jr.—482
Photomicrographs of magnetic colloid patterns, W. C. Elmore—933(A)
Of pyrrhotite, S. S. Sidhu, V. Hicks—207(A)
Structure of Co, W. C. Elmore—757
Surface magnetization of Co, W. C. Elmore—108(A)
Susceptibility of lead oxide, M. Petersen—933(A)

Magneto-optical effects
Magnetic double refraction; acetone, esters, J. B. Hawkes—84
Verdet constants of CS_2, glycerine, isopropyl and amyl alcohols, G. C. Comstock—849(A)

Mass defects (see **Isotopes**)
Mass spectrography
Ion source (Li), Hoff Lu—845(L)

Mechanics, quantum—general
Lower bounds in quantum mechanics, A. F. Stevenson—199(L)
Neutral particle, Theory of, W. H. Furry—679(A)
Quadrupole-quadrupole interatomic forces, J. K. Knipp—734
Theory of neutral particle, W. H. Furry—679(A)
Mechanics, quantum—of solid bodies
Calculation of electronic energy bands, G. Wannier—671(L)
Compressibility of alkali metals, J. Bardeen—683(A)
Meteorology
Atmospheric absorption by water, W. M. Elsasser—768(L)
Density and temperature of the atmosphere to 60 km, E. O. Hulburt—948(A)
Determination of atmospheric ozone, B. O'Brien, H. S. Stewart, Jr.—949(A)
Factors affecting pyrheliometers, L. F. Miller—948(A)
Methods and instruments
Accelerator using a quarter wave-length transmission line, P. L. Hartman, L. P. Smith—677(A)
Atomic electron velocities; measuring of, A. L. Hughes, M. M. Mann, Jr.—50
Barometer, for small volumes, W. Hurst—850(A)
Capacity controlled magnetic suspension, C. S. Smith—933(A)
Capture cross section, A. H. Spees, W. F. Colby, S. Goudsmit—326(A)
Centrifuge, tubular, J. W. Beams—850(A)
Circuit for G-M counters, E. W. Yetter—612(L)
Cloud chamber technique, F. N. D. Kurie—215(A)
Coaxial tube counter, S. C. Brown, R. D. Evans—914(A)
Coincidences in counter circuits, C. Eckart, F. R. Shonka—752
Collimation of slow neutrons, J. G. Hoffman, M. S. Livingston—676(A)
Collision relations, A. E. Ruark, C. Jones—853(A)
Compact 750 kv Van de Graaff generator, J. B. Fisk, I. A. Getting—916(A)
Counting losses of single scale recorders, H. Lifschutz, O. S. Duffendack—941(A)
Cyclotron magnet-current stabilizer, T. Perry—943(A)
Deposition of Ra Cu on rotating cathode, J. Steigman—771(L)
Detection of cocain-HCl in cerebrospinal fluid, L. A. Strait, R. B. Aird—213(A)
Determination of e/m, A. E. Shaw—208(A)
Determination of geologic ages, C. Goodman, R. D. Evans—916(A)
Determination of specific charge of beta-particles, C. T. Zahn, A. H. Spees—357
Displacement polarimeter, N. Underwood—853(A)
Effective mutual inductance, alternating current method, H. L. Curtis, A. V. Astin, C. M. Sparks—934(A)
Electron velocity analyzer, M. E. Bell, E. A. Coomes, W. B. Nottingham—328(A)
Electronic stabilizer performance, F. V. Hunt, R. W. Hickman—913(A)
Energy variations in a cyclotron ion beam, G. K. Green, P. G. Kruger—927(A)
Errors in count from G-M tube, E. Rodgers—850(A)
Factors affecting pyrheliometers, L. F. Miller—948(A)
Ferromagnetic impurities, detection of, F. W. Constant, J. M. Formwalt—432(L); 933(A)
Filament surfaces, effects of a.c. and d.c., R. P. Johnson—936(A)
Fixed path acoustic interferometer, I. F. Zartman, J. C. Hubbard—944(A)
Focusing and energy of ions in cyclotron, M. E. Rose, H. A. Bethe—206(A); M. E. Rose—392; 675(A); 715; R. R. Wilson—213(A); 408
Focusing x-rays by rocksalt crystal, R. M. Bozorth, F. E. Haworth—538; I. Fankuchen—910(L)
Fringing flux in large magnets, J. D. Howe, I. Walerstein—334(A)
Gas free surfaces, H. E. Farnsworth, R. P. Winch—935(A)
Geiger counter, T. G. How, K. Lark-Horovitz—334(A)
Geiger counter circuit, I. A. Getting—103(L); H. V. Neher, W. H. Pickering—316(L); T. H. Johnson—914(A)
Geiger counters, use of, H. V. Neher, W. H. Pickering—214(A)
G-M tube design, J. L. Lawson, A. W. Tyler—605(L)
Generator for production of neutrons, T. R. Folsom—687(A)
Grating, mounting for, H. Sponer, W. Hurst—851(A)
High frequency systems for cyclotron, J. R. Dunning, H. L. Anderson—334(A)
High pressure capillary lamps, C. Bol—214(A)
High speed electrostatic motor, C. S. Smith—688(A)
Hollow cathode discharge source for Zeeman effect, R. A. Fisher, A. S. Fry, J. R. Platt—934(A)
Infra-red wave-lengths, for calibration, P. E. Shearin, E. K. Plyler—851(A)
Integrated intensity from x-ray powder photographs, E. O. Wollan—208(A)
Intensifying screens in x-ray diffraction work, C. Gamertsfelder, N. S. Gingrich—332(A)
Intensities of spectral lines, D. Foster, H. W. Highriter—673(L)
Ion source (Li), Hoff Lu—845(L)
Ion sources using focused beams, L. P. Smith, G. W. Scott, Jr.—677(A)
Ionization current meter, G. Failla—687(A)
Light source for cloud chamber, W. M. Powell—327(A)
Lissajous figures, F. H. Mitchell—850(A)
Magnetic fields and susceptibilities in solenoids, A. R. Kaufman—933(A)
Magnetic laboratory at M.I.T., F. Bitter—933(A)
Mass spectrometer, new, W. Bleakney, J. A. Hipple, Jr.—521
Measurement of the speed of a rotating shaft, F. Wenner, I. L. Cooter—927(A)
Measurement of super-voltage radiation, L. S. Taylor, G. Singer—916(A)
Measuring nuclear magnetic moment, I. I. Rabi, J. R. Zacharias, S. Millman, P. Kusch—318(L)

Mechanical harmonic synthesizer-analyzer, S. L. Brown —333(A)
Multivibrator counter circuit, A. Ruark—316(L)
Multivibrators from 200,000 to 1 cycle second, W. D. George—924(A)
New ether-drift interferometer, W. B. Cartmel—108(A)
New mass spectrometer, W. Bleakney, J. A. Hipple, Jr. —521
Nonideal Lloyd's mirror, F. W. Doermann—420
Nuclear recoil in β-ray emission, J. Halpern, H. R. Crane —676(A)
Numerical integration, M. F. Manning, J. Millman—673(L)
Numerical solution of Laplace's equation, G. H. Shortley, R. Weller—207(A)
With oscillograph, C. T. Razor—851(A)
Permanent electrets, W. M. Good—323(A)
Photoelectric counters with Cs cathodes, G. L. Locher—333(A)
Production of uniform magnetic fields, R. J. Stephenson, M. Ference, A. E. Shaw—208(A)
Radiography of thin microtome sections, E. Dershem—202(A)
Reduction of barium oxide, J. P. Blewett—935(A)
Scale of eight circuit, H. Lifschutz, J. L. Lawson—204(A)
Scale for predicting nuclear transformations, V. Karapetoff—675(A)
Sensitivity of balanced space charge method, A. Rostagni —729; R. N. Varney—732
Short exposure; high intensity x-rays, K. H. Kingdon, H. E. Tanis, Jr.—128
Single crystal diffraction patterns, F. Miller, Jr., L. G. Parratt—200(L)
Solar spectrum photography, H. S. Stewart, Jr., B. O'Brien—949(A)
Surface viscosimeter, W. D. Harkins, J. G. Kirkwood—322(A)
Temperature control for absorption cells, D. Williams, R. Taschek—851(A)
Theory of scaling circuit, L. Alaoglu, N. M. Smith, Jr.—832
Thermionic cathode, new type, A. W. Hull—936(A)
Three-component accelerometer, J. E. Shrader—333(A)
Ultramicrometer, D. L. Arenberg, P. M. Roope—687(A)
Unusual demonstrations with piezoelectric resonators, K. S. Van Dyke—686(A)
Vacuum furnace for production of single crystals, F. C. Nix—917(A)
Vacuum tube frequency meter, H. Lifschutz—950(A)
Vacuum-type centrifuge, S. A. Black, J. W. Beams, L. B. Snoddy—924(A); J. W. Beams, C. Skarstrom—327(A)
Velocity of sound in air, R. C. Colwell, A. W. Friend, D. A. McGraw—686(A)
Viewing and measuring instrument for cloud chamber, C. Jones, A. Ruark—677(A)
Viscometer for lubricating oils, B. W. Thomas, R. B. Dow, W. R. Ham—926(A)
Voltage multiplying circuit, S. K. Allison, G. T. Hatch, L. S. Skaggs, N. M. Smith, Jr.—204(A)
Wilson cloud chamber control, I. I. Hopkins, R. T. Dickerson, W. M. Nielsen—850(A)
X-ray camera for high temperatures, C. Nusbaum—918(A)
X-ray generator for biological experiments, G. Failla—916(A)
Young's modulus, determination of, R. R. Jacobs, D. Bancroft—687(A)

Mobility of ions (see **Ions, mobility**)

Molecular structure and constants (see also **Spectra, molecular and Raman spectra**)
Deuterium bonds, W. Gordy—851(A)
Potential barrier in ethylene chloride, J. Y. Beach, K. J. Palmer—685(A)
Potential functions of the methyl halides, D. M. Dennison, Z. I. Slawsky—930(A)

Neutrino (see also **Radioactivity**)
Evidence for neutrino, H. R. Crane, J. Halpern—789
Heavy neutrino, F. L. Arnot—1018(L)
Heavy particles; existence of, G. E. M. Jauncey—106(L)

Neutrons (see also **Scattering of electrons, neutrons and ions**)
Absorption in boron, H. C. Torrey—266(L)
Absorption by Cl, E. O. Salant, W. J. Horvath—943(A)
Albedo, slow neutrons, E. Fermi, E. Amaldi, G. C. Wick —493(L)
Angular distribution, M. L. Pool—334(A); J. G. Hoffman, M. S. Livingston—1020(L)
From B+H^2, H. Staub, W. E. Stephens—212(A)
From C^{12}+H^2, T. W. Bonner—496(L)
Collimation of slow neutrons, J. G. Hoffman, M. S. Livingston—676(A)
Distribution from Li+H^2, M. L. Pool—707
Emission from A, Cl, Al and under He^4 bombardment, E. Pollard, H. L. Schultz, G. Brubaker—351
Interaction with normal and parahydrogen, J. R. Dunning, H. J. Hoge, J. H. Manley, F. G. Brickwedde—205(A)
From Li+H^2, W. E. Stephens—212(A); 223
Magnetic properties of free neutrons, O. Frisch, H. von Halban, Jr., J. Koch—719
Magnetic scattering and magnetization of iron, H. G. Beyer, H. Carroll, C. Witcher, J. R. Dunning—947(A)
Minimum energy for disintegration, R. Sagane—492(L)
Multiple ejection from excited nuclei, R. L. Thornton, J. M. Cork—922(A)
Passage through lead, E. Hudspeth, T. W. Bonner—928(A)
Properties of slow neutrons, J. G. Hoffman, M. S. Livingston—929(A)
Scattering of fast neutrons, R. F. Bacher, D. C. Swanson —676(A); 922(A)
Scattering by gases, H. Carroll, H. G. Beyer, K. Wilhelm J. R. Dunning—947(A)
Spin, H. H. Goldsmith, L. Motz—947(A)

Nuclear moments and spin (see also **Hyperfine structure**)
Electron pair theory of particle interaction, R. E. Marshak, H. A. Bethe—677(A); Erratum 950(A)

Nuclear moments and spin (continued)
Hyperfine structure of spectral lines from atomic beams, K. W. Meissner—677(A)
Of In^{115}, S. Millman, I. I. Rabi, J. R. Zacharias—331(A); 384
Of Li^6 and K^{41}, J. E. Gorham—331(A)
Of Li^7; magnetic, H. A. Bethe—842(L)
Magnetic moment of Li^7, perturbation theory, D. R. Inglis—880; 939(A)
Magnetic moments of Li^6, Li^7 and F^{19}, I. I. Rabi, S. Millman, P. Kusch, J. R. Zacharias—495(L)
Magnetic moments of Li^6 and K^{41}, signs of, J. E. Gorham —563
Magnetic moments; theory, D. R. Inglis—470
Of Mn, R. A. Fisher, E. R. Peck—685(A)
Measuring nuclear magnetic moment, I. I. Rabi, J. R. Zacharias, S. Millman, P. Kusch—318(L)
Of Ne and A, J. M. B. Kellogg, N. F. Ramsey—331(A)
Quadrupole and magnetic moments, K. Way—685(A)
Relativistic spin-orbit coupling, S. M. Dancoff, P. Morrison—211(A)
Spin of neutron, H. H. Goldsmith, L. Motz—947(A)

Nucleus (see also **Disintegration of nucleus; Energy states of nucleus**)
Barytron theory of nuclear forces, H. A. Bethe—938(A)
Dynaton theory of nuclear forces, R. Serber—211(A)
Electromagnetic properties of nuclear systems, W. E. Lamb, Jr., L. I. Schiff—651
Excitation of nuclei, V. Weisskopf—1018(L)
Ground state of deuteron, R. G. Sachs, M. Goeppert-Mayer—991
Penetrability of potential barrier, F. C. Hoyt—673(L)
Relativistic equations, nuclear particles, G. Breit—153
Rotation of atomic nuclei, E. Teller, J. A. Wheeler—684(A); 778
Saturation of nuclear forces, C. Critchfield, E. Teller—684(A); 812
Saturation requirements for forces, G. Breit, E. Wigner —998

Optical constants and properties
Of fluorite in the 6μ region, D. Williams—930(A)
Intermetallic compounds, A. P. Friesen—688(A)
Of liquid thallium, A. P. Friesen—678(A)
Lorenz-Lorentz constant for paraffin oil, A. P. Friesen—688(A)
Refractive index and dispersion of distilled water, L. W. Tilton, J. K. Taylor—918(A)
Refractive index of air, D. Bender—852(A)

Optical instruments (see also **Methods and instruments**)
Oblique ether-drift interferometer, W. B. Cartmel—949(A)

Optical theory
Ether-drift interferometer, theory of, W. B. Cartmel—949(A)
Nonideal Lloyd's mirror, F. W. Doermann—420

Packing fraction (see also **Isotopes**)
Energy of heavy nuclei, A. J. Dempster—64; 869
Of Ti, Fe, Cu, Ag, Au and Pt, A. J. Dempster—202(A)

Photoelectric effect and properties; cells
Energy distribution of photoelectrons from Na, A. G. Hill—184
Sensitization of Al, L. P. Thein—287
Spectral sensitivity of Sr and Mg, R. J. Cashman, E. Bassoe—919(A)
Thoriated tungsten surfaces, A. King—570
Threshold and intensity from Bi film, A. H. Weber—895

Photography
Camera error and photogrammetric mapping, I. C. Gardner—945(A)
Variation of contrast with wave-length, W. R. Koch—325(A)

Photovoltaic effect
In polarized light, R. G. Wilson—264(L)

Piezoelectric effect
Unusual demonstrations with piezoelectric resonators, K. S. Van Dyke—686(A)
Vibration modes of low decrement, K. S. Van Dyke—945(A)

Positive electron
Energy loss in Al, B. R. Curtis—986

Quantum mechanics (see **Mechanics, quantum**)

Radiation (see also **Thermal radiation**)
Asymmetric radiation produced by β-rays, G. B. Collins, V. G. Reiling—205(A); 948(A)
Discharges under nearly complete ionization, F. L. Mohler—683(A); 923(A)
λT relation for black-body radiation, F. Benford, A. G. Worthing—948(A)
Luminosity of yellow and green Hg lines, W. E. Forsythe, B. T. Barnes, A. L. Shrider—678(A)

Radioactivity (see also **Disintegration of nucleus**)
Of air, water, cave and soil gases, O. G. Fryer—325(A)
Alpha-particle mean range standards, M. S. Livingston, M. G. Holloway—922(A)
Of As, B. R. Curtis, J. M. Cork—681(A)
β-emission, nuclear K-electron capture, E. C. Campbell —206(A)
β-spectrum of RaE, A. I. Alichanian, A. I. Alichanow, B. S. Dželepow—766(L)
β-spectrum of ThC, A. I. Alichanian, S. J. Nikitin—767(L)
Of Be^7, R. B. Roberts, N. P. Heydenburg, G. L. Locher—1016(L)
Of Co, J. J. Livingood, G. T. Seaborg—847(L)
In Cu, long period, S. W. Barnes, G. Valley—946(A)
Of Cu, Zn, Ga and Ge isotopes, R. Sagane—212(A)
Deposition of Ra Cu on rotating cathode, J. Steigman—771(L)
Disintegration constant of thorium, A. F. Kovarik, N. I. Adams, Jr.—928(A)
Energy of β-rays, G. E. M. Jauncey—106(L)
γ-radiation from $B+H^2$, W. A. Fowler, E. R. Gaerttner, C. C. Lauritsen—942(A)
γ-radiation from In, B. R. Curtis, J. R. Richardson—942(A)

γ-radiations from Eu^{152} and Au^{198}, J. R. Richardson—942(A)
Gamma-radiation from N^{13}, J. R. Richardson—610(L)
Gamma-rays from I^{128}, A. Roberts, J. W. Irvine, Jr.—609(L)
Gamma-rays from V^{48}, N^{13}, Cu^{64}, Mg^{27} and Na^{24}, J. R. Richardson—124
Of In, by slow neutrons, A. C. G. Mitchell—269
Induced by high energy protons, L. A. DuBridge, S. W. Barnes, E. O. Wiig, J. H. Buck, C. V. Strain—326(A); C. V. Strain, J. H. Buck—943(A); L. A. DuBridge, S. W. Barnes, J. H. Buck, C. V. Strain—447
Induced in Ni, Cu, Mg and Ag by H^1, L. N. Ridenour, L. A. Delsasso, M. G. White, R. Sherr—770(L)
Induced in the rare earths by neutrons, M. L. Pool, L. L. Quill—326(A); 437
Of I, J. J. Livingood, G. T. Seaborg—1015(L)
Isomerism in Ra Ag and *K* electron capture, M. L. Pool, E. C. Campbell—272
Isomers of In^{116}, A. C. G. Mitchell, L. M. Langer—505; 675(A); M. L. Pool—611(L)
Half-life of actino-uranium, A. O. Nier—922(A)
Mean life of Ru 87, E. J. Konopinski, H. A. Bethe—679(A)
Of Ni^{57} and Ni^{63}, J. J. Livingood, G. T. Seaborg—847(L)
Of K, A. Bramley, A. K. Brewer—502
K electron capture in gallium, L. W. Alvarez—606(L)
Produced by cosmic-rays, W. E. Ramsey, C. G. Montgomery, D. D. Montgomery—196(L)
Proton bombardment of various elements, R. Sherr, M. C. Henderson, M. G. White, L. A. Delsasso, L. N. Ridenour—946(A)
Range and specific ionization of α-particles, M. G. Holloway, M. S. Livingston—676(A)
Of Sc, J. M. Cork, R. L. Thornton—866
Short-lived radioelements, L. W. Alvarez—215(A)
In Ag, M. L. Pool—116; 206(A)
Substandards of feeble radioactivity, R. D. Evans, C. Goodman—916(A)
Of Ta, O. Oldenberg—35; 109(A)
Of Te, G. F. Tape, J. M. Cork—676(A)
In Ur, P. Abelson—211(A)
Of Zn, R. L. Thornton—326(A)
Of Zn by α-particle bombardment, W. B. Mann—212(A)
Of Zn and Co, C. Perrier, M. Santangelo, E. Segrè—104(L)

Raman spectra
Of disubstituted acetylenes, F. F. Cleveland, M. J. Murray—330(A); 931(A)
Of S, S. Bhagavantam—1015(L)

Reflecting power (see also **Absorption and reflection of light**)
Infra-red spectrometer with fluorite prisms, E. S. Barr—852(A)

Relativity
Eddington's treatment of Dirac's equation, B. Podolsky—591
New ether-drift interferometer, W. B. Cartmel—108(A)
Oblique ether-drift interferometer, W. B. Cartmel—949(A)
Relativistic equations; nuclear particles, G. Breit—153
Trouton-Nobel experiment, P. B. Carwile—924(A)

Resistance, electrical (see **Electrical conductivity and resistance**)

Scattering of atoms and molecules (see also **Atomic and molecular beams**)
α-particles by Ne and H^2, J. T. McCarthy—30
Scattering of H^1 by H^1, L. R. Hafstad, N. P. Heydenburg, M. A. Tuve—239

Scattering of electrons, neutrons, and ions (see also **Electrons, scattering of; Electron diffraction**)
Angular distribution, J. G. Hoffman, M. S. Livingston—1020(L)
Atomic electron velocities, A. L. Hughes, M. M. Mann, Jr.—50
Effect of valence electrons on intensities, V. A. Johnson, H. M. James—327(A)
Energy loss of positrons, B. R. Curtis, J. M. Cork—206(A)
Of fast electrons in gases, J. B. H. Kuper—993
Of fast electrons and positrons in Pb, J. Oppenheimer, W. A. Fowler—928(A)
Of fast neutrons, elastic and inelastic, D. C. Grahame, G. T. Seaborg—795
Of neutrons by deuterons, P. G. Kruger, W. E. Shoupp, R. E. Watson, F. W. Stallmann—1014(L)
Of He^4 by A, O, and Ne, G. Brubaker—921(A)
Inelastic scattering by Ag, J. C. Turnbull, H. E. Farnsworth—944(A)
Magnetic scattering and magnetization of iron, H. G. Beyer, H. Carroll, C. Witcher, J. R. Dunning—947(A)
Multiple scattering of electrons, M. E. Rose—937(A)
Multiple scattering of neutrons, O. Halpern, R. Luneburg, O. Clark—173
Of neutrons by gases, H. Carroll, H. G. Beyer, K. Wilhelm, J. R. Dunning—947(A)
Of neutrons by gases, H. Carroll, P. N. Powers, H. G. Beyer, J. R. Dunning—680(A)
Of neutrons by paramagnetic media, J. H. Van Vleck—680(A)
Of neutrons by protons, theory of, R. G. Sachs, M. Goeppert-Mayer—991
Of neutrons by various elements, W. H. Zinn, S. Seely, V. W. Cohen—921(A)
Of H^1 and H^2 by deuterium and by helium, N. P. Heydenburg, R. B. Roberts—922(A)
Profile of Compton band determined by electron scattering, A. L. Hughes, M. M. Mann, Jr.—204(A)
Resonance scattering of charged particles, O. Halpern, M. H. Johnson, Jr.—939(A)
Scattering of fast neutrons, R. F. Bacher, D. C. Swanson—676(A); 922(A)
Of slow positive ions, A. G. Emslie—680(A)

Scattering of light (see also **Raman spectra**)
Diffraction of electromagnetic waves, E. Guth—688(A)

Secondary electrons (see **Electrons, secondary**)

Spectra, absorption (see also **Absorption of light**)
Atmospheric absorption by water, W. M. Elsasser—768(L)

Spectra, absorption (continued)
Of benzene at 2700–2200A, H. Sponer, G. Nordheim A. Sklar—932(A)
Of $C^{13}O_2^{16}$ at 4.375μ, A. H. Nielsen—983
Of CsH, G. M. Almy, M. Rassweiler—890
Of diatomic fluorides in carbon-tube furnace, F. A. Jenkins, G. D. Rochester—213(A)
4.3μ band in CO_2, D. M. Cameron, H. H. Nielsen—246
Of gaseous and solid benzene, A. L. Sklar, H. Sponer, G. Nordheim—932(A)
Of heavy formic acid, R. Hofstadter—941(A)
Of PbSe, SnSe and PbTe, J. W. Walker, J. W. Straley, A. W. Smith—140
Of light and heavy acetic acids, R. C. Herman, R. Hofstadter—940(A)
Of liquid crystal, R. Taschek, D. Williams—852(A)
Of methyl alcohol, infra-red, A. Borden, E. F. Barker—932(A)
Of mixtures of phenol and ethyl alcohol, infra-red, J. W. White, E. K. Plyler—932(A)
Of nitrate solutions, D. Williams, L. Decherd—852(A)
Quadrupole rotation-vibration, of H_2, H. M. James, A. S. Coolidge—208(A)
Quantitative test for free hydroxyl, O. Oldenberg, F. F. Rieke—941(A)
Rotational transitions in water molecules in nonpolar solvents, J. W. Ellis, E. L. Kinsey—672(L)
Of SeH_2, infra-red, W. C. Sears, D. M. Cameron, H. H. Nielsen—330(A)
Of simple hydrocarbons, E. P. Carr, H. Stücklen—109(A)
Of SrH and SrCl, K. R. More, S. D. Cornell—678(A); 806
Of water vapor in extreme ultraviolet, J. J. Hopfield—931(A)

Spectra, atomic
Of Bi I, H. E. Clearman, Jr.—941(A)
Of Ce II, W. Albertson, G. Harrison—108(A); 940(A)
Of Cl VII, L. W. Phillips—248
Of Co VI, low terms, I. S. Bowen—889
Complex spectra, theory of, G. H. Shortley, B. Fried—931(A)
Of Ge, infra-red, C. C. Kiess—931(A)
Intensity relations in He arc, J. J. Heilemann—977
Of Mn II, C. W. Curtis—474
Of OsI and IrI, W. Albertson—940(A)
Pressure shifts, H. Margenau, W. S. Wilson—941(A)
Resonance broadening, W. V. Houston—213(A)
Self-consistent field for Fe, M. F. Manning, L. Goldberg—662
Term values in C, C. W. Ufford—568
Of Xe II, C. J. Humphreys—940(A)

Spectra continuous
Of He, A. G. Shenstone—941(A)

Spectra, general
Distribution of mineral elements in sugar cane, spectrographic study, S. S. Ballard—689(A)
Of H_2, arc, different conditions, R. W. Wood, G. H. Dieke—146
Intensity relations in He arc, J. J. Heilemann—977
Luminosity of yellow and green Hg lines, W. E. Forsythe, B. T. Barnes, A. L. Shrider—678(A)
Radiation in positive column of Hg arc, intensities, B. T. Barnes, E. Q. Adams—545

Spectra, molecular
Of SbN, N. H. Coy, H. Sponer—495(L)
Of CeO and PrO, W. W. Watson—639; 678(A)
Centrifugal distortion of axial molecules, Z. I. Slawsky—924(A)
D system of SrH analysis, K. R. More, S. D. Cornell—931(A)
Infra-red wave-lengths, for calibration, P. E. Shearin, E. K. Plyler—851(A)
Isotopic shift in MgI, K. W. Meissner—931(A)
Hg-Tl bands, J. G. Winans, F. J. Davis—930(A)
Rotational energy distribution of OH, E. R. Lyman, F. A. Jenkins—214(A); E. R. Lyman—379
$^2\Sigma - {}^3\Pi$ bands of BF, F. W. Paul, H. P. Knauss—930(A)

Spectroscopy, technique
Grating, mounting for, H. Sponer, W. Hurst—851(A)

Structure factor
In Zn-Cu alloy, R. A. Howard—324(A); 966

Thermal conductivity
Of Hg, Na and Na amalgams, W. C. Hall—1004

Thermal diffusivity
Thermal diffusion and turbulent air flow, H. K. Skramstad, G. B. Schubauer—927(A)

Thermal expansion
Of the alkalis, L. Balamuth—669(L)
Of some heat-resisting alloys, P. Hidnert—925(A)

Thermal radiation (see also **Radiation**)
Emissivity of metals, E. Guth—682(A)
Rayleigh-Jeans formula and experiment, P. B. Carwile—682(A)

Thermionic emission of electrons; Emitting surfaces
Deviation from Schottky line for W, R. L. E. Seifert, T. E. Phipps—493(L)
New type of cathode, A. W. Hull—936(A)
Thoriated tungsten surfaces, A. King—570
Work functions of crystallographic planes of tungsten, S. T. Martin—937(A)

Thermodynamics
Stefan's radiation law and Nernst's theorem, A. E. Haas, E. Guth—324(A)

Van der Waals forces
Between symmetrical rotators, K. G. Carroll—310
In He, C. H. Page—426

Viscosity
Air-lubricated journal bearings, M. D. Hersey—926(A)
Film lubrication of journal bearing, S. M. Skinner—927(A)
Of monolayers, W. D. Harkins, J. G. Kirkwood—322(A)
Of sols made from x-irradiated apple pectin, C. H. Dwight, H. Kersten—926(A)
Of suspensions, E. Guth, O. Gold—322(A); E. Guth—926(A)
Viscometer for lubricating oils, B. W. Thomas, R. B. Dow, W. R. Ham—926(A)

X-rays, absorption
Absorption in Be, C, Al, Cu, Ag and Au, C. L. Andrews—679(A)
Argon, *K* absorption limit, F. K. Richtmyer, L. G. Parratt—678(A)

X-rays, diffraction, scattering, reflection, refraction and polarization
In A, J. B. Green, B. Fried, J. F. Eichelberger—934(A)
Atomic distribution in liquid K, C. D. Thomas, N. S. Gingrich—934(A)
Atomic distribution in liquid Na, F. H. Trimble, N. S. Gingrich—203(A); 278
Atomic distribution in liquid white P, N. S. Gingrich, C. D. Thomas—943(A)
Barium-copper-stearate films, properties of, C. Holley—534
Characteristic temperature of MgO, H. S. Ribner, E. O. Wollan—332(A); 972
Characteristic temperature of Zn crystals, G. E. M. Jauncey—203(A)
Diffraction in ionic solutions, G. W. Stewart—202(A)
Effect of temperature on reflection, W. M. Schwarz—919(A)
Hollow cathode discharge as source for Zeeman effect, R. A. Fisher, A. S. Fry, J. R. Platt—934(A)
In Ne, J. A. Peoples, Jr., J. B. Green—934(A)
Position of Compton band, G. E. M. Jauncey—332(A)
In quartz, oscillating and non-oscillating, G. W. Fox, J. R. Frederick—135
Radial lines in Laue spots, A. P. R. Wadlund—843(L); W. H. Zachariasen—844(L); C. S. Barrett—1021(L)
Single crystal diffraction patterns, F. Miller, Jr., L. G. Parratt—200(L)
Verification of dispersion theory, W. A. Bruce, G. E. M. Jauncey—332(A); W. A. Bruce—802

X-rays, emission (see also **X-rays, spectra and spectroscopy, etc.**)
Absorption edges and their fine structure, theory of, R. Landshoff—332(A)
Continuous x-ray spectrum near Duane-Hunt limit, E. Brunner—457
$K\alpha_{1,2}$ line of Na, chemical combination, N. G. Johnson—434(L)
$K\beta$ group of NaCl and KCl, J. Valasek—274
K fluorescent lines of chemical compounds, L. Obert, C. H. Shaw—919(A)
Widths of energy states, L. G. Parratt—679(A)
Widths and intensities of *L* lines of rare earth elements, C. H. Shaw—940(A)

X-rays, spectra and spectroscopy, wave-length measurements (see also **X-rays, emission**)
Integrated intensity from x-ray powder photographs, E. O. Wollan—208(A)

X-rays, tubes, apparatus
Focusing by rocksalt crystal, R. M. Bozorth, F. E. Haworth—538; I. Fankuchen—910(L)
Intensifying screens in x-ray diffraction work, C. Gamertsfelder, N. S. Gingrich—332(A)
Short exposure; high intensity x-rays, K. H. Kingdon, H. E. Tanis, Jr.—128

Zeeman effect
Of Au, H. N. Maxwell, J. B. Green—330(A)
Of inorganic compounds, J. R. Nielsen, N. E. Ward, H. Dodson—331(A)
$p^5 d$ configurations of Ne and A, J. B. Green, J. A. Peoples, Jr., B. Fried—105(L)
Of Se II, J. B. Green, R. A. Loring—330(A)

Physics Lib.
DO NOT TAKE FROM LIBRARY
JUN 27 1938

THE PHYSICAL REVIEW

VOLUME 53 *Second Series* NUMBER 12

JUNE 15, 1938

DO NOT TAKE FROM LIBRARY

Published for the

AMERICAN PHYSICAL SOCIETY

by the

AMERICAN INSTITUTE OF PHYSICS
Incorporated

LANCASTER, PA., AND NEW YORK, N. Y.

CONTENTS

PHYS. REV. 53 (1938) JUNE 15

Multiplicative Theory of Showers as Applied to Large Bursts of Cosmic-Ray Ionization . . . . . C. G. MONTGOMERY AND D. D. MONTGOMERY 955

Transition Effects of Cosmic Rays in the Atmosphere . . . . . H. SNYDER 960

Atomic Vibrations of a Zn-Cu Alloy . . . . . ROBERT A. HOWARD 966

Determination of the Characteristic Temperature of MgO from X-Ray Measurements . . . . . H. S. RIBNER AND E. O. WOLLAN 972

Intensity Relations in the Low Voltage Helium Arc . . . . . JOHN J. HEILEMANN 977

Infra-Red Absorption by $C^{13}O_2^{16}$ at 4.375 μ . . . . . ALVIN H. NIELSEN 983

Energy Loss of Positive Electrons in Passing Through Aluminum . . . . . B. R. CURTIS 986

Calculations on a New Neutron-Proton Interaction Potential . . . . . R. G. SACHS AND M. GOEPPERT-MAYER 991

Scattering of Fast Electrons in Gases . . . . . J. B. HORNER KUPER 993

Saturation Requirements for Nuclear Forces . . . . . G. BREIT AND E. WIGNER 998

Thermal Conductivities of Mercury, Sodium, and Sodium Amalgams in the Liquid State . . . . . WAYNE C. HALL 1004

Internal Friction in Solids. V. General Theory of Macroscopic Eddy Currents . . . . . CLARENCE ZENER 1010

Letters to the Editor:

Scattering of Neutrons by Deuterons . . . . . P. G. KRUGER, W. E. SHOUPP, R. E. WATSON AND F. W. STALLMANN 1014

Molecule of Sulphur and Its Raman Spectrum . . . . . S. BHAGAVANTAM 1015

Radioactive Iodine Isotopes . . . . . J. J. LIVINGOOD AND G. T. SEABORG 1015

Radioactivity of Be^7 . . . . . R. B. ROBERTS, N. P. HEYDENBURG, G. L. LOCHER 1016

Transmutations of the Cosmic-Ray Electrons and the Nuclear Forces . . . . . IG. TAMM 1016

Excitation of Nuclei by Bombardment with Charged Particles . . . . . V. F. WEISSKOPF 1018

Heavy Electrons and β-Decay . . . . . F. L. ARNOT 1018

Some Results of the Search for Super-Novae . . . . . F. ZWICKY 1019

Angular Distribution of Slow Neutrons from a Paraffin Surface . . . . . J. G. HOFFMANN AND M. S. LIVINGSTON 1020

Radial Lines in Laue Spot Photograms . . . . . CHARLES S. BARRETT 1021

Magnetic Anisotropy of Ferromagnetic Crystals in Weak Fields and Reversible Susceptibility . . . . . E. KONDORSKY 1022

Author Index to Volume 53 1023

Analytic Subject Index to Volume 53 1037

LANCASTER PRESS, INC., LANCASTER, PA.